PHOSPHORYLATION SITE ANALYSIS OF THE CENTROSOMAL NEK2 KINASE AND ITS SUBSTRATES

Thesis submitted for the degree of
Doctor of Philosophy
at the
University of Leicester

By

Joanne Elizabeth Baxter BSc (Hons) (Manchester)
Department of Biochemistry
University of Leicester

July 2006

ProQuest LLC
789 East Eisenhower Parkway
P.O. Box 1346
Ann Arbor, MI 48106-1346

DECLARATION

The accompanying thesis submitted for the degree of Doctor of Philosophy, entitled *"Phosphorylation site analysis of the centrosomal Nek2 kinase and its substrates"* is based on work conducted by the author in the Department of Biochemistry at the University of Leicester mainly during the period between July 2001 and March 2006. All the work recorded in this thesis is original unless otherwise acknowledged in the text or by references. None of the work has been submitted for another degree in this or any other University.

Signed:

Date: 6th July 2006

Department of Biochemistry
University of Leicester
University Road
Leicester
LE1 7RH

PHOSPHORYLATION SITE ANALYSIS OF THE CENTROSOMAL NEK2 KINASE AND ITS SUBSTRATES

JOANNE ELIZABETH BAXTER

SUMMARY

The centrosome is the major microtubule organising centre of the cell. It undergoes timely duplication once every cell cycle in a semi-conservative manner. The duplicated centrosomes are then separated to opposite ends of the cell promoting formation of the bipolar mitotic spindle. Not surprisingly, the duplication and separation of centrosomes is controlled in large part by protein phosphorylation. Nek2 is a protein kinase that localises to the centrosome and has peak activity at the onset of mitosis. The aim of this thesis was to determine how the Nek2 protein is regulated and to identify phosphorylation sites both within the Nek2 kinase and its centrosomal substrates. Identification of a Nek2 phosphorylation consensus sequence would also facilitate the discovery of novel Nek2 substrates. Here, we have mapped eleven Nek2 autophosphorylation sites and identified those which are critical for Nek2 activity. These include sites within the activation loop of the catalytic domain and in the C-terminal non-catalytic domain. We have also identified a region within the Nek2 protein that may act as an auto-inhibitory domain. We also identify Nek2 phosphorylation sites within the centrosomal proteins, Nlp and C-Nap1. Nlp is localised to the mother centriole and may act as a novel microtubule anchoring protein. We have demonstrated that the localisation of Nlp is dependent upon the Nek2 protein kinase. Others have previously identified Plk1 as a kinase involved in Nlp regulation and we demonstrate here that Nek2 acts upstream of Plk1 and may be a Plk1 priming kinase. In addition, we identify Cdk1 as a possible Plk1 priming kinase on Nlp. C-Nap1 is a protein involved in centriole cohesion and phosphorylation by Nek2 may regulate its interaction with other centriole linker proteins. This work substantially increases our knowledge of Nek2 regulation by phosphorylation and also extends our understanding of how it regulates centrosome structure and function in a cell cycle dependent manner.

ACKNOWLEDGMENTS

I would like to thank all of my friends and family for their helpful support and encouragement throughout this work. All the members of lab 201 have been great friends and a very helpful source of knowledge throughout. I cannot thank enough Dr. Andrew Fry for all his help, guidance and time which has been very gratefully received. Thank you to my very supportive parents, grandmother and late grandfather who have always been there for me.

I would also like to thank Prof. Steve Smerdon and Frank Ivins for all their help with phosphosite mapping. Prof. Andrew Tobin and Dr. Raj Patel for offering very sound advice throughout this work. Millennium Pharmaceuticals for funding this work and the Department of Biochemistry for allowing me to study my PhD with them.

CONTENTS

ABBREVIATIONS

A_{260}	Absorbance at 260 nanometres
APC/C	Anaphase promoting complex / cyclosome
ATP	Adenosine triphosphate
BCA	Bicinchoninic acid
BCIP	5-bromo-4-chloro-3-indolyl phosphate
bp	base pairs
BSA	Bovine serum albumin
C-	Carboxy
CDK	Cyclin dependent kinase
cDNA	Complementary deoxyribonucleic acid
Ci	Curie
CKII	Casein kinase II
cm	Centimetre
C-Nap1	Centrosomal Nek2 associated protein 1
CSF	Cytostatic factor
DLBCL	Diffuse large B-cell lymphoma
DMEM	Dulbeccos modified eagle's medium
DMSO	Dimethylsufoxide
DNA	Deoxyribonucleic acid
DTT	Dithiothreitol
EDTA	Ethylene diamine tetra acetic acid
EGTA	Ethylene glycol-bis (β-aminoethylether) N, N, N' N' –tetraacetic acid
FCS	Foetal calf serum
G	Growth phase
g/l	Grams per litre
GCP	γ-tubulin complex proteins
GFP	Green fluorescent protein
GTBPs	γ-tubulin binding proteins
γ-TuRC	γ-tubulin ring complex

HEC	Highly expressed in cancer
HEPES	N-2-hydroxyethylpiperazine-N' -2-ethanesulphonic acid
hGCP-4	Human gamma-tubulin complex component 4
HMGA2	High mobility group AT-hook 2
IDC	Invasive ductal carcinoma
IF	Immunofluorescence
IgG	Immunoglobulin G
IMS	Industrial methylated spirit
IPTG	β-D-isopropyl-thiogalactopyranoside
IVT	*In vitro* translation
kDa	Kilo Dalton
l	Litre
LB	Luria-bertani
M	Molar
mA	Milliamp
MALD/I	Matrix assisted laser desorption/ionisation
MAPK	Mitogen activated protein kinase
mg	Milligram
min	Minutes
ml	Millilitre
mM	Millimolar
mRNA	Messenger ribonucleic acid
MTOC	Microtubule organising centre
N-	Amino-
NBT	Nitroblue tetrazolium
Nek2	NIMA-related kinase
ng	Nanogram
NIMA	Never in mitosis
Nlp	Ninein-like protein
OD	Optical density
O/N	Overnight

PAGE	Polyacrylamide gel electrophoresis
PBD	Polo box domain
PBS	Phosphate buffered saline
PCM	Pericentriolar matrix
PCR	Polymerase chain reaction
PKA	Protein kinase A
Plk	Polo-like kinase
Plx1	Polo-like kinase *Xenopus* 1
PMSF	Phenylmethylsulphonyl fluoride
PP1	Protein phosphatase 1
RNA	Ribonucleic acid
rpm	revolutions per minute
SCF	Skp1-cullin-F-box
SDS	Sodium dodecyl sulphate
SLIMB	Supernumerary limbs
SPB	Spindle pole body
TACC	Transforming acidic coiled coil
TEMED	N, N, N' N' –tetramethylethylenediamine
TOF	Time of flight
TRIS	Tris (hydroxymethyl) aminomethane
μg	Microgram
μl	Microliter
μM	Micromolar
V	Volts
(v/v)	Volume per volume ratio
(w/v)	Weight per volume ratio

TABLE OF FIGURES

Chapter One

Introduction

1.1 The eukaryotic cell division cycle

Eukaryotic cells reproduce by duplication of their genome and cellular contents followed by division into two daughter cells. Cells complete this task by performing a series of tightly controlled events involving cell growth, DNA replication, duplication of cytoplasmic organelles and cell division (Alberts et al., 1994). The cell cycle can be divided into two distinct phases, interphase and mitosis. Interphase can be further subdivided into G1, S and G2 phases. Specifically, the cell undergoes a first growth phase, G1, during which the cell monitors its environment and responds to extracellular signals to ensure that the environment is adequate to continue proliferation. Once the cell commits to DNA replication it enters the phase of DNA synthesis, S phase. Following completion of S phase, the cell enters a second growth phase, G2, which provides the cell with additional time to ensure that the DNA has replicated correctly and the cell has doubled in mass before entering into mitosis (Figure 1.1).

Mitosis can also be divided into a series of discrete stages: prophase, prometaphase, metaphase, anaphase and telophase (Figure 1.2). During prophase, the cell undertakes the process of chromosome condensation which involves the organisation of interphase chromatin into condensed sister chromatids. This organisation is required for efficient segregation of the chromosomes in the subsequent stages (Alberts et al., 1994). The nuclear envelope remains intact until prometaphase, when nuclear envelope breakdown occurs allowing the chromosomes to attach to the forming mitotic spindle. The mitotic spindle is a bipolar structure comprised of microtubules. The spindle poles contain the centrosomes whose function is to nucleate and anchor the microtubules (Figure 1.2). The sister chromatids are captured by the microtubules and aligned across the centre of the spindle - an event termed metaphase. Sister chromatids attach to the microtubules via their kinetochores and are moved towards opposite poles of the mitotic spindle during anaphase. Telophase begins by the reformation of the nuclear envelope and the decondensation of the chromosomes. The final stage to complete the cell division process is cytokinesis. Here, the cytoplasmic contents must be equally distributed into the two daughter cells. The process begins by the formation of an actomyosin contractile ring

which constricts to form the cleavage furrow (Alberts et al., 1994). Cellular movement and further constriction thins the furrow into a microtubule containing structure called the midbody which undergoes abscission forming the two separate daughter cells.

1.1.1 Cell cycle regulation by protein phosphorylation

The process of cell division is tightly controlled by both phosphorylation and degradation of proteins, which ensure that each stage is correctly executed. Reversible protein phosphorylation is a common post-translational modification that plays a key role in regulating molecules within the cell. Phosphorylation of a protein can alter its conformation or charge which in turn can stimulate or inhibit enzymatic activity, alter binding partners or complex formation and affect the subcellular localisation of the protein. In this way, phosphorylation events are responsible for regulating many if not all of the critical processes within the cell, including control of the cell division cycle. The cell division cycle is responsible for regulating the correct timing of DNA synthesis, chromosome segregation and cytokinesis and relies on phosphorylation to ensure that each event is carried out in the correct temporal and spatial manner (Nigg, 2001). Any mishaps could ultimately lead to abnormal cells and cancer. The cell division cycle is controlled in large part by a number of heterodimeric protein kinases called cyclin dependent kinases (Cdks) which when associated with the correct cyclin partner are activated and go forth to trigger key cell cycle events. The cyclin partners accumulate at various stages of the cell cycle when they are required to activate their Cdk partners.

Cdk-cyclins are essential to ensure that cell cycle events take place in the correct order. For instance, DNA replication is triggered by Cdk2-cyclin E while the onset of mitosis is activated by Cdk1/cyclin B. However, Cdks are not the only kinases that are important for cell cycle control. Others include Polo-like kinases (Plks), Aurora kinases and NIMA-related kinases, or Neks. The aim of this project is to understand how the Nek2 serine/threonine kinase is regulated by autophosphorylation and how it regulates downstream substrates by phosphorylation at the centrosome.

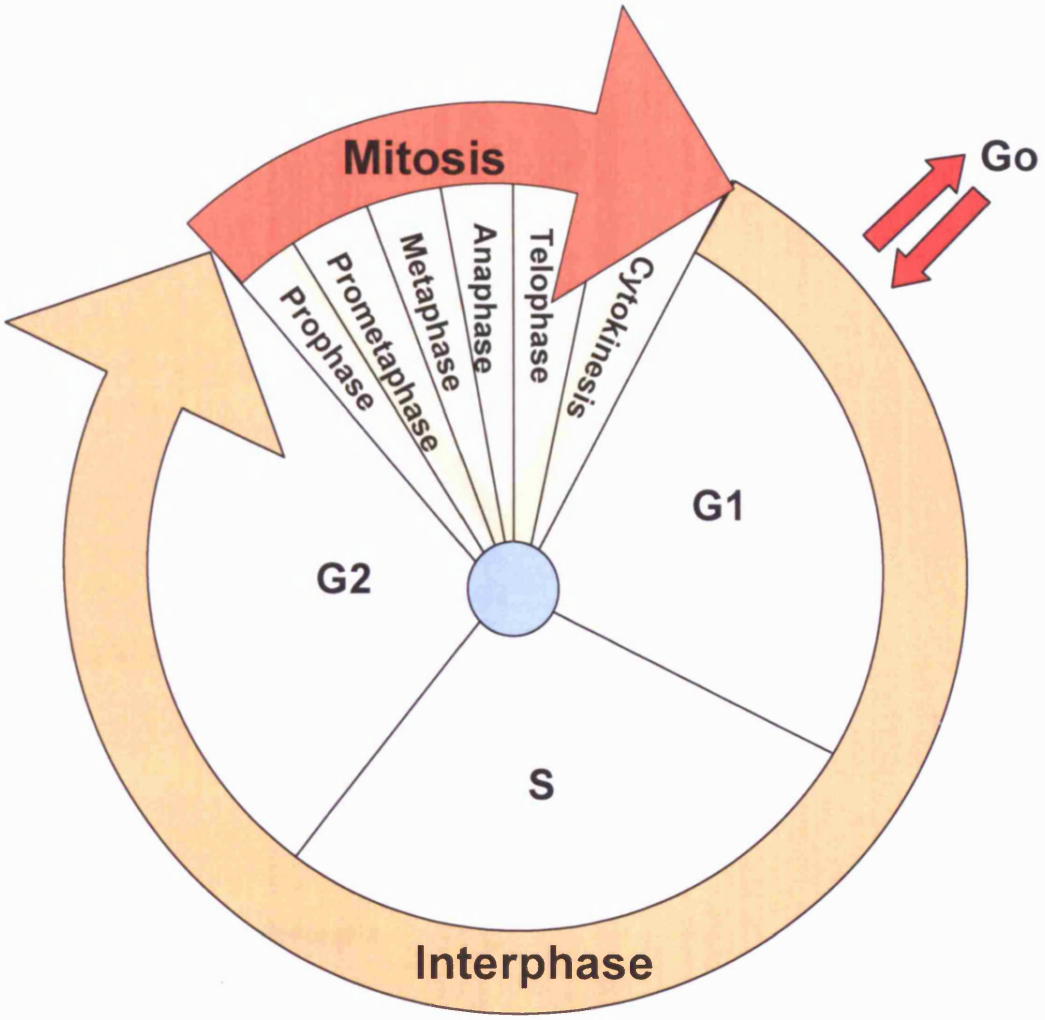

Figure 1.1 The eukaryotic cell cycle

Diagramatic representation of the eukaryotic cell cycle. The cell cycle comprises of interphase (G1, S and G2) and mitosis. Mitosis can be further divided into the stages indicated within the circle. Cells with no growth signals are quiescent (Go).

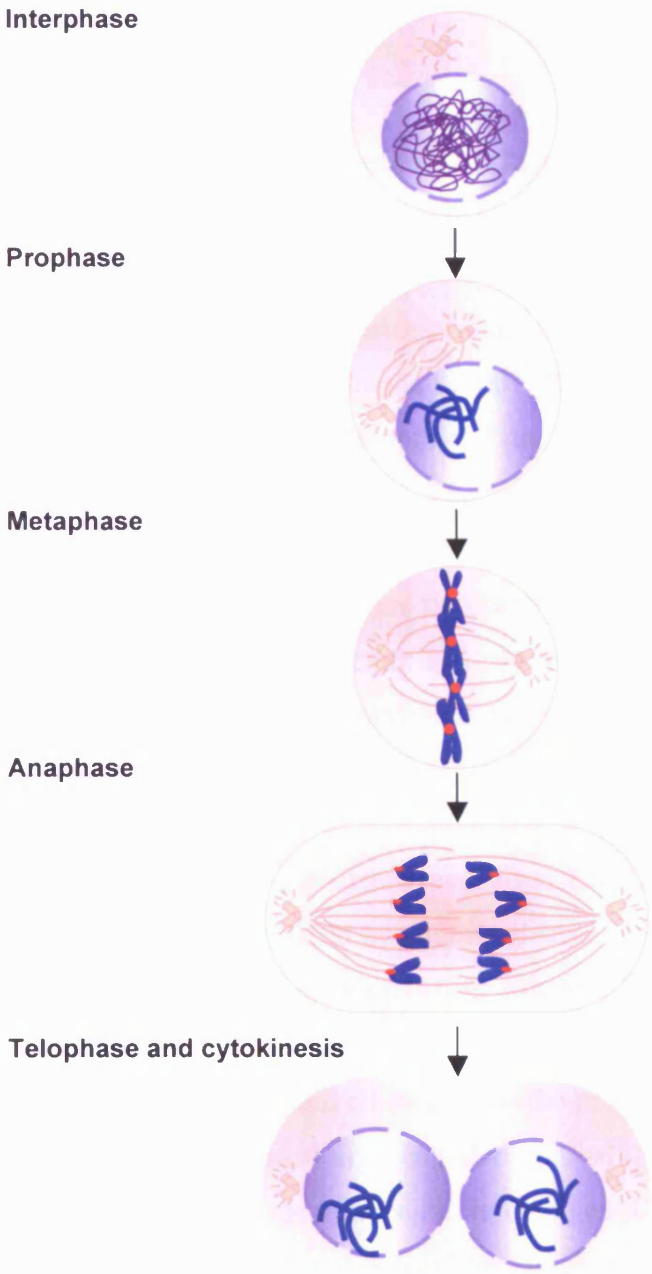

Figure 1.2 Mitosis
Stages within mitosis are represented by schematic diagrams of the cell. Structures shown include the centrosome, nucleus, DNA and the microtubule network. During interphase the chromosomes are decondensed within the nuclear envelope. Prophase marks the point at which chromosome condensation occurs and prometaphase (not shown) the breakdown of the nuclear envelope and attachment of chromosomes to the mitotic spindle. Metaphase marks the alignment of chromosomes at the equator of the mitotic spindle followed by movement of the chromosomes to the poles during anapahase. Telophase and cytokinesis mark the end of mitosis with decondensation of chromosomes, formation of the cleavage furrow and separation into two daughter cells.

1.2 The mammalian centrosome

1.2.1 Centrosome structure

The centrosome is a non-membranous organelle of 1-2 μm^3 volume usually located near the centre of the cell. Using light microscopy, it was first described by Theodor Boveri in 1901 as a densely packed organelle lying close to the nucleus. The centrosome consists of two substructures, the centrioles and the pericentriolar material (PCM) (Doxsey, 2001; Doxsey et al., 2005; Mack et al., 2000; Marshall, 2001, Karsenti, 1999). Centrioles are barrel-shaped structures that are 0.5 μm in length, 0.2 μm in diameter and made up from nine sets of triplet microtubules (Doxsey, 2001). The centrioles act as a scaffold on which to assemble the PCM which comprise 12-15 nm filaments to which other components associate (Urbani and Stearns, 1999). There are two centrioles per centrosome that differ in age: the older centriole is named the mother and can be distinguished by appendages towards its distal tip, while the younger centriole is called the daughter (Figure 1.3 see page 11).

Centrioles are polar structures with a proximal and distal end. The proximal and distal ends of each centriole can be distinguished by additional structures located on and within the lumen of the centrioles. For instance, a cartwheel structure is located at the proximal end which comprises of a set of nine spokes connected to a central axis (Marshall, 2001) (Figure 1.3). Nek2, C-Nap1 and γ-tubulin all localise to the proximal end of the centriole (Mack et al., 2000). Centriole proximal ends can also be distinguished during centriole duplication as the end at which the new procentriole emerges. Distal ends of centrioles can be distinguished as they are the site of a disc-type structure, and have, in the case of the mother centriole, sub-distal and distal appendages which are thought to anchor microtubules (Marshall, 2001).

The two centrioles are held in close proximity by a fibrous link called the intercentriolar linkage. The composition of the linkage is not well characterised, but the proteins C-Nap1 and rootletin have been proposed to be part of the structure (Bahe et al., 2005; Fry et al., 1998a; Mayor et al., 2000). Centriolar satellites are present around the PCM and

are possibly involved in microtubule anchoring or trafficking to the centrosome (Marshall, 2001).

The PCM surrounds the centrioles but is preferentially associated with the mother (Mack et al., 2000). The PCM consists of a meshwork of salt-insoluble fibres, protein aggregates, and coiled-coil proteins, which form a lattice or matrix (Dictenberg et al., 1998). This matrix may provide a framework for anchoring proteins involved in microtubule nucleation but other functions of the PCM still remain unclear. The integrity of the centrosome structure is dependent upon the two centrioles which are required to organise all the centrosome components into a single stable structure (Bobinnec et al., 1998).

1.2.2 Centrosome duplication

The centrosome undergoes duplication once per cell cycle. Initial insights into the process of centrosome duplication were based upon electron microscope images of cells taken during the cell cycle (Anderson, 1999) (Figure 1.3). These clearly identified a series of stages of duplication that can be summarized as follows. Initially, the loss of an orthogonal relationship between the mother-daughter centriole pair occurs early in G1 (centriole disorientation). At the beginning of S-phase, two short pro-centrioles are formed at right angles to the original centrioles (centriole duplication). These elongate through S-G2 reaching a mature length in mitosis. Disjunction of the two mother-daughter centriole pairs follows forming two new centrosomes (centrosome disjunction). Finally, centrosome separation occurs and the newly formed centrioles reach maturity (Hinchcliffe and Sluder, 2001) (Figure 1.4). These events will be discussed in detail in the following sections.

1.2.2.1 Centriole disorientation

The majority of cultured animal cells enter G1 with a single centrosome made up of two orthogonally arranged centrioles surrounded by a single cloud of PCM. However, at some point in G1 (which may be dependent upon cell type) the two centrioles move slightly apart and acquire their own distinct region of PCM. The process of centriole

disorientation is not well understood. Centrioles have been observed to separate from one another, with the mother present in a stationary position located in the centre of the cell and the daughter moving through the cytoplasm (Piel et al., 2000). However, before the duplication process begins, the centrioles regain their close proximity in the centre of the cell. It has been proposed that the Skp1-cullin-F-box (SCF) ubiquitin ligase may play a role in centriole disorientation. Degradation of proteins by the SCF may trigger these events. Proteasome inhibitors and antibody-mediated interference of the SCF block centriole disorientation and duplication in *Xenopus* embryos (Freed et al., 1999). One target of the SCF, Slimb, when mutated, causes the appearance of multiple centrosomes and mitotic defects. This supports a role for this complex in the initiation of centrosome duplication (Wojcik et al., 2000).

1.2.2.2 Centriole duplication

The process of centriole duplication is complex and essential for the formation of a bipolar mitotic spindle and correct distribution of chromosomes and cell fate determinants into the two daughter cells (Doxsey, 2002). It is also essential for the stable inheritance of centrosomes themselves. Centrosome duplication is dependent upon factors intrinsic to the centrosome itself as well as to cytoplasmic factors (Wong and Stearns, 2003). To establish how the duplication process occurs, biotinylated tubulin was microinjected into early G1 cells. Using this method, it was found that during each cell cycle tubulin was incorporated into the newly-forming daughter centrioles. After cytokinesis, each daughter cell therefore contained a newly formed centriole and an older centriole from the previous cell (Kochanski and Borisy, 1990). Centriole duplication, like that of DNA replication, is therefore semi-conservative. This suggests a templated model of centriole formation, where the new centriole is formed from a structure residing on the parent centriole.

In addition to the templated mechanism of centrosome duplication, there appears to be a second mechanism for centrosome duplication, the *de novo* pathway, that occurs in the absence of a parent centriole. The *de novo* formation of centrioles only occurs during S phase in HeLa cells. This was shown by laser ablation of both centrosomes (Khodjakov

et al., 2002; La Terra et al., 2005). In S-phase cells lacking intact centrosomes numerous centriolar structures are formed which upon entry into the next cell cycle mature and gain the ability to organise microtubules and replicate (La Terra et al., 2005). Re-duplication after *de novo* formation does not occur until the following cell cycle suggesting a time period is required for centriole maturation, possibly to create the new site for templated centriole formation.

A block to centrosome re-duplication normally exists in cells and this block is not dependent on the ratio of centrosomes to nuclei (Wong and Stearns, 2003). However, in $p53^{-/-}$ cancer cells this intrinsic block to re-duplication is overcome when in prolonged S-phase arrest (Wong and Stearns, 2003). The *de novo* assembly pathway is suppressed in the presence of a single centriole (La Terra et al., 2005). Indeed, *de novo* formation does not occur after certain defects in the centrosome duplication pathway. For instance, after siRNA depletion of centrin-2, centrioles fail to duplicate. However, the unduplicated centrioles are still capable of forming a functional mitotic spindle and completing at least one cell division (Salisbury et al., 2002). A control pathway to re-duplication must therefore exist to prevent *de novo* formation occurring when a functional centrosome is present. This would be necessary to prevent multiple centrosomes assembling leading to multipolar spindle formation. Furthermore, the *de novo* formation of centrioles occurs much more slowly than templated assembly (Marshall et al., 2001). The *de novo* pathway creates numerous centrosome structures all capable of microtubule nucleation and spindle assembly. The number of centrioles formed during the *de novo* pathway does not correlate with the doubling time of the cell and therefore their production probably does not rely upon the templated mode of duplication (Wong and Stearns, 2003). This has huge implications in human cancers where an initial mutation in p53 may trigger onset of the *de novo* pathway. Centrosome duplication pathways are therefore critical for the integrity of the genome.

1.2.2.3 Centrosome disjunction

By the G2/M transition, centrioles have more or less completed duplication and the process of separating the two newly-formed centrosomes begins. The centrosomes are

thought to be linked by a poorly characterised "inter-centriolar linkage", a connecting structure which exists between the two parental centrioles. This fibrous link has been observed by isolating centrosomes and examining them using electron microscopy (Paintrand et al., 1992). The existence of a linkage between the parental centrioles is also supported by the appearance of isolated centrosomes as paired dots under the microscope (Bornens, 2002). The fact that centrosome pairs are found together is strongly suggestive of a physical link which cannot be microtubule-mediated as isolated centrosomes are prepared in the presence of nocadozole. Time-lapse imaging of L929 cells stably expressing GFP-centrin has also shown that mother and daughter centrioles make correlated movements as if held together by a piece of string (Piel et al., 2000). The linkage must be broken to allow disjunction to occur. This is thought to be under the control of protein phosphorylation (see later).

1.2.2.4 Centrosome separation

Disjunction of the centriole pairs occurs prior to the physical separation of centrosomes to the two spindle poles. This depends upon the action of motor proteins, especially the kinesin Eg5 (Blangy et al., 1995; Sawin and Mitchison, 1995). Microinjection of antibodies directed toward Eg5 blocks centrosome separation leading to an arrest in mitosis and monoastral microtubule arrays (Blangy et al., 1995). The localisation of Eg5 to the centrosomes is regulated by its phosphorylation by Cdk1 (Sawin and Mitchison, 1995). Once again this highlights the role of protein phosphorylation in control of the centrosome duplication cycle.

1.2.3 Centrosome functions

The vertebrate centrosome was initially anticipated to be 'the organ of cell division *par excellence*' (Wilson, 1925). Clearly, its main function is to act as a microtubule organising centre, MTOC, responsible for the control of microtubule events such as microtubule nucleation, anchoring and release (Anderson, 1999). However, the range of functions associated with centrosomes is growing rapidly, it is now thought to play major roles in mitotic spindle assembly, positioning of the mitotic spindle, G2/M entry, mitotic progression, cytokinesis and possibly G1/S control (Nigg, 2004).

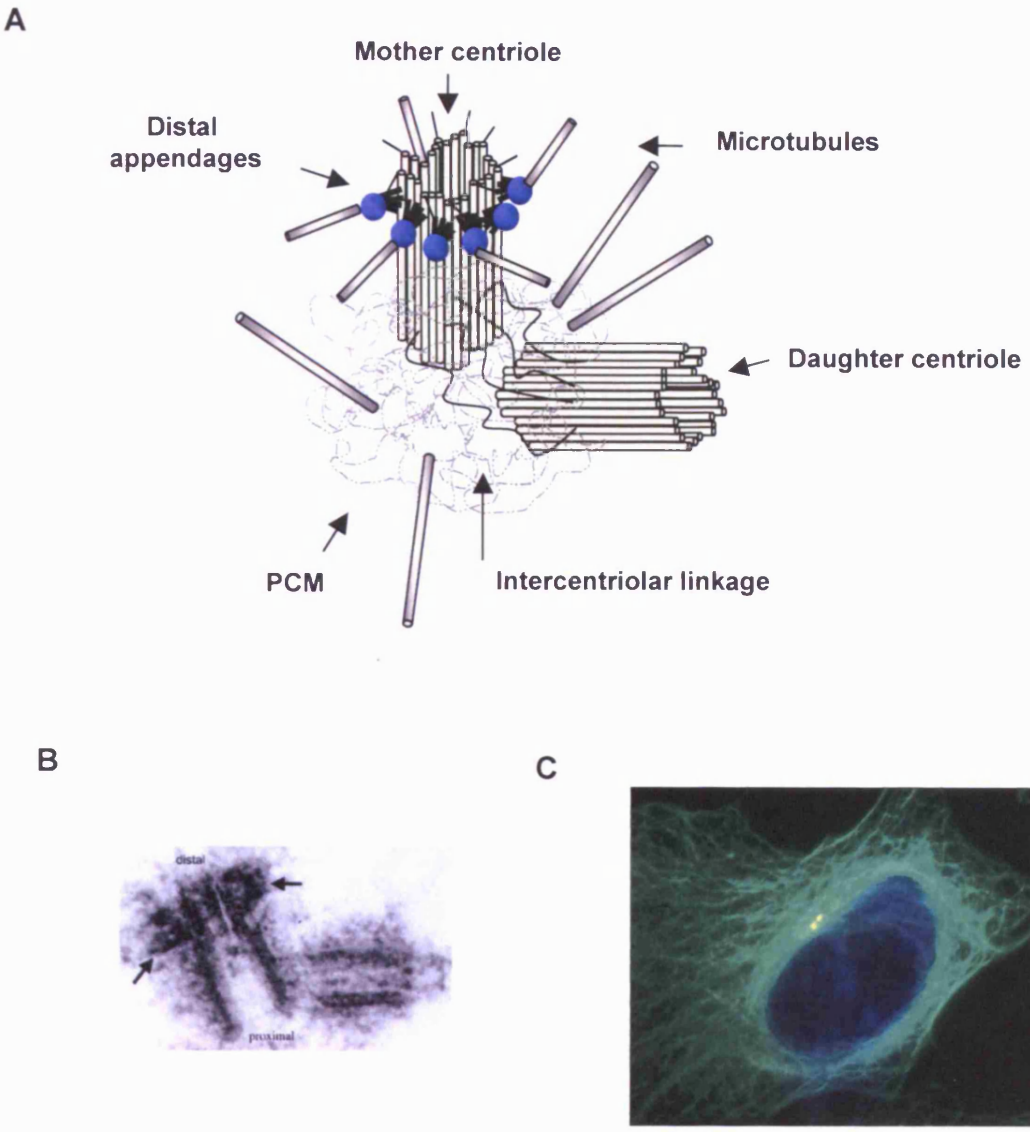

Figure 1.3 The mammalian centrosome

A. Diagramatic representation of the mammalian centrosome. Substructures are indicated by small arrows. **B.** Electron micrograph image of the centriole structure. Arrows point to mother centriole distal appendages. Picture taken from Delattre and Gonczy (2004). **C.** Immunofluorescence image of a typical human cell. The centrosome (yellow) is located at the heart of the microtubule network (green) close to the nucleus (blue). Picture courtesy of Dr. Andrew Fry.

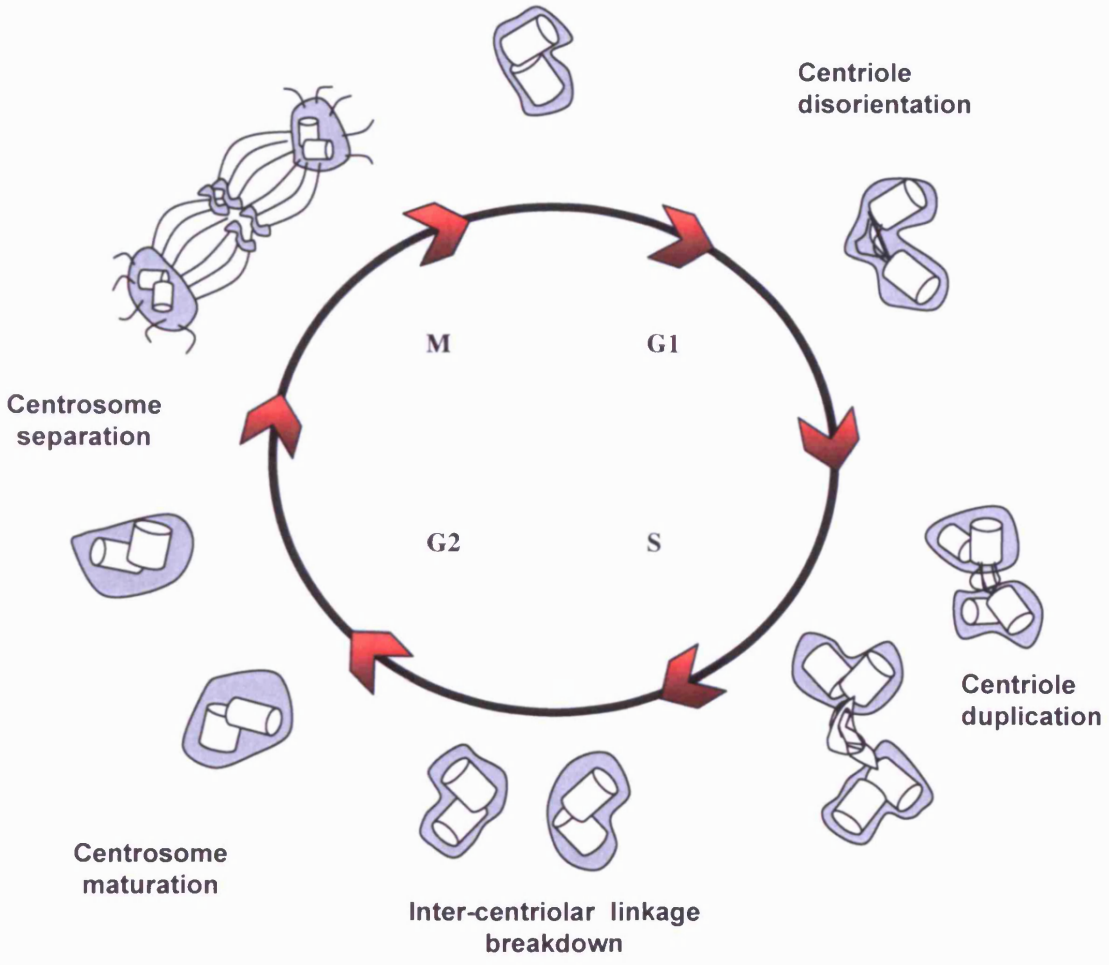

Figure 1.4 The centrosome duplication cycle
The centrosome duplication cycle is directly co-ordinated with the cell cycle. Centriole disorientation occurs during G1 followed by duplication through S and G2. Inter-centriolar linkage breakdown follows during G2 and the centrosome matures during G2-M. Coinciding with mitotic spindle formation, the centrosomes separate to the poles of the mitotic spindle until they are separated into the two newly formed daughter cells.

Centrosomes, when present, act dominantly to regulate mitotic spindle assembly through organisation of the spindle poles (Heald et al., 1997). This pathway may ensure the high fidelity of chromosome segregation and ensure centrosomes are inherited equally during each cell division cycle. The involvement of centrosomes in this process is highly important and mistakes may be causative in the initiation or progression of human cancers. For example, the presence of more than two centrosomes can result in the formation of multipolar spindles and abnormal chromosome segregation, which in turn may result in aneuploidy (Brinkley, 2001; Nigg, 2002). Positioning of the mitotic spindle is essential for accurate segregation of chromosomes, asymmetric distribution of cell fate determinants, normal and asymmetric cell divisions and in defining the plane of cytokinesis. Centrosomes and associated astral microtubules are important for spindle positioning in mammalian cells. In cells lacking centrosomes, no astral microtubules are produced and spindles may become mispositioned causing problems in cytokinesis (Khodjakov and Rieder, 2001).

The contribution of centrosomes to cytokinesis is mechanistically unclear with some studies indicating that centrosomes might be involved in activating cytokinesis, while others suggest a role in the release of cells from a checkpoint that monitors the completion of mitosis. There may be a specific role for the mother centriole in cytokinesis as the mother centriole moves into the midbody just prior to cell abscission (Piel et al., 2000). In the absence of centrosomes some cells fail to complete cytokinesis. Those that successfully divide then appear to arrest in G1 and do not initiate DNA replication (Hinchcliffe et al., 2001; Khodjakov and Rieder, 2001). It was postulated that cells may be activating a checkpoint that monitors centrosome number or excess DNA. Alternatively, centrosomes might be required to activate DNA replication (Hinchcliffe et al., 2001). It is unclear whether the centrosome directly mediates these events or centrosomal defects trigger checkpoints, which monitor the completion of mitosis. One consequence of these checkpoints may be to ensure that dividing animal cells receive the correct number of centrosomes after each cell division.

1.3 Microtubule organisation

Microtubules are involved in a wide range of functions within the cell. During interphase, they form the cytoskeleton upon which proteins and organelles can be transported throughout the cell. In mitosis, they form the bipolar mitotic spindle. Microtubules are made up from α- and β-tubulin dimeric subunits arranged in a tubular conformation (Dammermann et al., 2003; Moritz and Agard, 2001). The tube consists of thirteen parallel protofilaments made up from individual α- and β-tubulin dimers. Microtubules are intrinsically polar due to the arrangement of α-tubulin next to a β-tubulin molecule. The polarity gives rise to a rapidly growing (plus end) and a slower growing (minus end) end. The dynamic nature of microtubules allows movement and directionality of the microtubule units (Dammermann et al., 2003). The growth and shrinkage of microtubules happens constantly and as such their relative length will vary at any one time. Microtubules are often anchored at their minus ends at the centrosome.

1.3.1 Microtubule nucleation

A number of centrosomal proteins not surprisingly play critical roles in microtubule nucleation. Indeed, it is the concentration of these proteins at the centrosome that confers on it the status of a microtubule organising centre. Microtubule nucleation occurs from within the PCM at 25S complexes known as γ-tubulin ring complexes, or γ-TuRCs (Job et al., 2003). These are open rings of roughly 25 nm in diameter, which localise directly at the centrosome (Moritz et al., 1995). The complex is thought to act as a direct template for the assembly of α- and β-tubulin dimers and is absolutely required for microtubule nucleation *in vivo* (Zheng et al., 1995). In *Xenopus,* the complex was identified as an open ring structure which in addition to microtubule nucleation, may also cap the minus ends of microtubules (Zheng et al., 1995). Microtubule capping is required to prevent rapid depolymerisation of the minus ends of microtubules after they are released. Microtubules polymerised spontaneously have an irregular number of protofilaments whereas those formed from γ-TuRCs have a regular 13 protofilament structure suggesting that the γ-TuRC is acting as a template to directly influence the structure of the microtubule (Urbani and Stearns, 1999). The γ-TuRC consists of γ-tubulin and at least another five proteins which include Spc97p (GCP2), Spc98p (GCP3) and GCP4, -5 and –

6 (Stearns and Winey, 1997). These proteins form a stable complex, which localises to the the centrosome in mammalian cells.

γ-tubulin is absolutely required for microtubule nucleation. It is present at the centrosome at all cell cycle stages but there is a rapid increase during mitosis (Khodjakov and Rieder, 1999). Presumably, this coincides with the increase in microtubule nucleation required for mitotic spindle formation. Fluorescence recovery after photobleaching (FRAP) analysis of cells expressing GFP-γ-tubulin reveals that γ-tubulin is present at the centrosome in two populations: one in rapid exchange with the cytoplasm and one in slow exchange (Khodjakov and Rieder, 1999). The study also reported that recruitment of γ-tubulin is not dependent on microtubules. In contrast, others have reported that recruitment of γ-tubulin is dependent upon dynactin (Quintyne et al., 1999). Dynactin is a component of the dyein/dynactin complex and is comprised of subunits including an actin-like backbone and a sidearm $p150^{GLUED}$. The sidearm binds to dynein, which is a minus-end directed motor. Together, the complex is responsible for the transport of some proteins to the centrosome via the microtubule network. Overexpression of parts of the sidearm subunits result in a dominant-negative effect on the endogenous protein. As such microtubule arrays become unfocused and disorganised and γ-tubulin recruitment is lost (Quintyne et al., 1999). Microinjection of dynein antibodies into *Xenopus* cells also inhibits γ-tubulin recruitment to the centrosome (Young et al., 2000). The authors note that both pericentrin and γ-tubulin assembly are inhibited in the absence of microtubules. Together, the data strongly argue that γ-tubulin recruitment to the centrosome is dependent on microtubules after all.

Although both γ-tubulin and the γ-TuRC can be found in the cytoplasm, microtubule nucleation only occurs at the centrosome suggesting that γ-TuRC activators are present at the centrosome. In plant cells that lack centrosomes, microtubule nucleation occurs at the nuclear surface from a focused array of microtubules docked by their minus ends (Canaday et al., 2000). It is not yet clear exactly how γ-TuRCs are held within the PCM. A number of candidate γ-tubulin binding proteins (GTBPs) have been identified

including pericentrin/kendrin, CG-Nap, CP309, Nlp and Asp (Bornens, 2002; Canaday et al., 2000; Casenghi et al., 2003; Delgehyr et al., 2005; Doxsey et al., 1994).

Within the pericentriolar material, the protein pericentrin is localised and is ordered into a lattice structure to which γ-tubulin co-localises (Doxsey et al., 1998). Pericentrin is required for microtubule nucleation from *Xenopus* sperm centrosomes and therefore the binding of pericentrin to γ-tubulin may represent another mechanism for γ-TuRC anchoring at the centrosome (Anderson, 1999). Indeed, pericentrin complexes with γ-tubulin to recruit γ-tubulin to the centrosome and is also required for the assembly of the γTuRC (Young et al., 2000). GFP-pericentrin and GFP-γ-tubulin move along microtubules at a similar speed to dynein (1 μm/s) and their assembly at the centrosome is inhibited in the absence of microtubules. Pericentrin binds to microtubules in a dynein-dependent manner as the disruption of dynein by antibody microinjection inhibits recruitment of both γ-tubulin and pericentrin (Young et al., 2000). It is highly plausible therefore that pericentrin plays a critical role in organising γ-TuRCs to promote microtubule nucleation at the centrosome.

1.3.2 Microtubule anchoring and release

Microtubule nucleation occurs within PCM associated with both the mother and the daughter centrioles. However, once nucleation has occurred, microtubules are often released or severed from their site of nucleation. Free microtubules may be released into the cytoplasm or become anchored at centrosomal or non-centrosomal sites. The centrosomal sites of microtubule anchoring are concentrated at the distal appendages of the mother centriole. The processes of microtubule nucleation and anchorage therefore involve distinct groups of proteins.

One protein involved in microtubule anchorage is ninein. Ninein was originally cloned from mouse and identified as having two splice variants, 245 kDa and 249 kDa, containing 2 EF hand domains, a GTP-binding site and 4 leucine zipper domains (Bouckson-Castaing et al., 1996). Human ninein has since been cloned as a 239 kDa protein similar to mouse ninein but containing no EF hands (Hong et al., 2000). Ninein

was proposed to be involved in microtubule anchoring due to its specific localisation to the mother centriole distal appendages (Mogensen et al., 2000; Young et al., 2000). Depletion or overexpression of ninein affects the ability of the centrosome to organise microtubules without affecting its ability to nucleate them (Dammermann et al., 2003). Ninein has also been reported to localise to the proximal end of the daughter centriole along with centriolin and C-Nap1. This localisation only occurs at the telophase-G1 transition when the daughter centriole matures into the mother (Ou et al., 2002). This suggests that ninein localisation to the daughter centriole may be required for centriole maturation. Indeed ninein or an additional centriolar protein may be required for centrosome integrity. Microinjection of centriolin or ninein antibodies disrupts centrosome function and causes the dispersal of centrosomal material (Young et al., 2000). Ninein may contribute to centrosome stability by anchoring γ-tubulin via its N-terminal domain and anchoring to the centriole by its C-terminal domain (Delgehyr et al., 2005). Thus, two separate roles of ninein in microtubule anchoring and nucleation have been proposed (Delgehyr et al., 2005).

A recently identified protein, ninein-like protein (Nlp) (Casenghi et al., 2003), is also localised to the mother centriole and could possibly have a role in microtubule nucleation and anchorage as will be discussed in later chapters. As mentioned previously, dynactin overexpression leads to unfocused arrays of microtubules and a loss of microtubule binding to the centrosome (Quintyne et al., 1999). Dynactin is also concentrated at the mother centriole and therefore may be involved in microtubule anchorage to the centrosome.

Microtubule anchorage is not limited to the centrosome. In mouse epithelial cells, microtubules dock with their minus ends to the apical cell surface; antibodies to γ-tubulin and pericentrin do not detect these proteins at these sites (Mogensen et al., 1997). This suggests that these sites are not additional nucleation sites. Ninein localises to the minus ends of microtubules while in transit and also to the apical non-centrosomal sites where microtubule minus ends are anchored (Mogensen et al., 2000). Pericentrin is also found located in these non-centrosomal regions (Doxsey, 2001). It would be interesting to

determine whether Nlp and other candidate anchoring proteins are involved in non-centrosomal anchorage.

1.4 Centrosomes and Cancer

A cancerous or malignant growth contains cells that have broken free of normal cell cycle limits and controls (Alberts et al., 1994). Tumour progression occurs via a distinct series of transformation events. Initially there is an increase in cell number which is termed hyperplasia. Here the cell cycle has undoubtedly been disrupted to the extent that the cell continuously divides. One consequence of the uncontrolled division is a potential increase in further mutations which carry a selective advantage over normal cells and allow the cancer to progress. Dysplasia/metaplasia marks a change in cell morphology followed by invasion of the tumour cells into secondary tissues. Ultimately, metastasis occurs in which there is a total transformation of cellular characteristics including a loss of cellular features, loss of normal cytoplasmic organisation and tissue architecture and invasion of distant sites.

Cancer is usually the accumulation of multiple processes which may include activation of one or more oncogenes, loss of tumour suppressor genes, a deregulated cell cycle or possibly a deregulated centrosome cycle (Brinkley and Goepfert, 1998). The implications of a deregulated centrosome cycle and mutation of centrosome associated proteins will be discussed.

1.4.1 Centrosomal defects: cause or consequence of cancer?

Solid tumours often display aneuploidy and abnormal centrosome numbers. The centrosome plays a major role in the correct distribution of chromosomes and other cell fate determinants into daughter cells during mitosis. Incorrect centrosome numbers can result in abnormal spindle formation, for example if centrosome duplication fails or occurs more than once per cell cycle (Nigg, 2002). Monopolar spindles lead to a complete failure of chromosome segregation and tetraploidization whereas multipolar spindles can lead to uneven segregation or chromosome breakage. Tumour suppressor

genes may be lost or oncogenic alleles accumulate as a result of this mis-segregation and hence cancer may occur. Abnormal centrosome numbers are found in many cancer types and are thought to be a key event in tumour progression in breast, prostate and colon cancer (Saavedra et al., 2003). The loss of tumour suppressors such as p53, p21, GADD45, BRCA1, BRCA2 and APC or the expression of oncogenes Aurora A, Ras, MAPKK and Mos, can all lead to abnormal centrosome numbers and anueploidy (Saavedra et al., 2003). There is a strong correlation between increased centrosome numbers and chromosome number aberrations but, like the chicken and egg, it is hard to determine which one comes first (Nigg, 2002). Mouse mammary tumour models suggest that centrosomal abnormalities occur at a pre-malignant stage of cell transformation and are followed by clonal selection of viable tumour progenitor cells (Brinkley and Goepfert, 1998; Saunders, 2005). However, others have observed that centrosomal abnormalities are only associated with chromosomal abnormalities and therefore suggest that the changes only occur late in tumour progression (Saunders, 2005).

Centrosome abnormalities in cancer cells do not merely comprise abnormal numbers. The centrosomes may also have an increased size, with an accumulation of excess pericentriolar material and exhibit inappropriate phosphorylation of centrosomal proteins (Salisbury et al., 2002). However, much focus has been on abnormal centrosome numbers leading to multiple MTOCs and as such multipolar spindles and aneuploidy (Saunders, 2005). There is no doubt that abnormal centrosomes are associated with tumour progression but which proteins may be involved in the deregulation of the centrosome cycle to cause such a catastrophic event is still to be determined.

1.5 Protein kinases in control of the centrosome duplication cycle

As previously described, the centrosome undergoes a series of morphological changes throughout the cell cycle, which allow a dynamic change in structure and function (Mayor et al., 1999). Protein kinases and reversible phosphorylation are key to the organisation and control of these cell cycle dependent changes within the centrosome (Fry et al., 2000b). Many protein kinases have been localised to the centrosome and

these are likely to be activated at the centrosome to contribute to global and localised cell cycle events (Figure 1.5). Four major groups of protein kinases appear to localise and function at the centrosome, these include the cyclin dependent kinases (CDKs), polo-like kinases (Plks), Aurora kinases and NIMA kinases (Fry and Faragher, 2001). Some of these will be discussed in the following sections. Although other kinases do localise to the centrosome (e.g PKA (Matyakhina et al., 2002)) they are less relevant to this thesis and will not be discussed.

1.5.1 Cdk2

Centriole duplication, as well as DNA replication, is triggered by the Cdk2-cyclin E/A complex (Mussman et al., 2000). Inhibition of Cdk2 in *Xenopus* egg extracts blocks the initiation of centrosome duplication, showing that the kinase activity of Cdk2-cyclin E is required for initiation of centrosome duplication (Lacey et al., 1999). It is proposed that the Cdk2-cyclin E complex phosphorylates centrosomal proteins and that this phosphorylation event triggers the initiation of centrosome duplication. One such protein is nucleophosmin/B23, (NPM/B23) a target for the Cdk2-cyclin E complex (Okuda et al., 2000). The NPM/B23 protein associates specifically with unduplicated centrosomes and dissociates when phosphorylated by the Cdk2-cyclin E complex, an event that triggers the disorientation of the two centrioles (Okuda et al., 2000). An anti-NPM/B23 antibody which prevents Cdk2-cyclinE mediated phosphorylation of NPM/B23 inhibits centrosome duplication as does the expression of a non-phosphorylatable mutant (Okuda et al., 2000). The phosphorylation site has been identified as threonine 199 and expression of a T199A non-phosphorylatable mutant blocks duplication and results in aberrant mitosis with monopolar spindles (Tokuyama et al., 2001).

In addition, it has been suggested that Cdk2 phosphorylation of BRCA1 the breast cancer tumour suppressor inactivates the protein and allows centrosome duplication to occur (Deng, 2002). BRCA1 involvement in centrosome duplication may not be so clear-cut. The protein localises to the centrosome and it's disruption leads to centrosome amplification but its involvement in amplification may be secondary to other more global changes within the cell such as p53 deregulation.

1.5.2 Mps1 and Zyg-1

Another kinase implicated in centrosome duplication is the Mps1 protein. In yeast Mps1p is essential for spindle pole duplication and may also function in the spindle assembly checkpoint. Mouse Mps1 localises to centrosomes and its kinase activity is required for centrosome re-duplication in S-phase arrested cells (Fisk and Winey, 2001). The murine Mps1 protein is phosphorylated by Cdk2 *in vitro* and GFP-Mps1 stimulates centrosome re-duplication in S-phase arrested cells (Fisk and Winey, 2001). It is proposed that a Cdk2 dependent de-stabilization of Mps1 is part of a mechanism restricting centrosome duplication in S-phase (Fisk and Winey, 2001). The human Mps1 kinase is cell cycle regulated with maximal levels in mitosis. However, unlike the mouse Mps1, human Mps1p does not localise to the centrosome and siRNA interference does not inhibit centrosome duplication but does activate the spindle checkpoint (Stucke et al., 2002).

The *C. elegans* Zyg-1 protein localises to centrosomes late in mitosis and mutations in Zyg-1 cause monopolar spindle formation. This suggests Zyg-1 kinase may play a role in centrosome duplication (O'Connell, 2002). Possible substrates of Zyg-1 include the Spd-2, Sas-4, Sas-5 and Sas-6 proteins, all of which are essential for centrosome duplication in *C. elegans* (Leidel and Gonczy, 2005).

1.5.3 Aurora A

Overexpression of Aurora A results in centrosome amplification and has been associated with chromosomal instability and transformation of mammalian cells (Zhou et al., 1998). However, the role of Aurora A in centrosome regulation is complex as the kinase is involved in many aspects of centrosome regulation including assembly, maturation, maintaining centrosome separation, spindle assembly and promotion of microtubule organisation.

First of all, there is evidence that Aurora A is involved in centrosome maturation. At late G2, Aurora A is activated by autophosphorylation on threonine-288 (T288) (Walter et al., 2000). Evidence from studies on the *C. elegans* homologue AIR1 suggests that

Aurora A is required for recruitment of γ-tubulin to the centrosome and therefore in centrosome maturation. RNAi of AIR1 causes spindle assembly failure after nuclear envelope breakdown. Separated centrosomes collapse back together resulting in monopolar spindle formation due to a lack of γ-tubulin recruitment and centrosome maturation (Hannak et al., 2001). This study links the role of centrosome maturation with the overall progress of the centrosome and cell division cycles.

Aurora A is also required for mitotic entry as RNAi of Aurora A impairs the cell's ability to enter mitosis (Hirota et al., 2003). Depletion of Aurora A reduces the levels of γ-tubulin at the centrosome thus preventing centrosome maturation. In addition, Aurora A is required to recruit the Cyclin B1-Cdk1 complex (a key activator of mitosis) to the centrosome and this may account for the block. A similar phenotype is observed when an activating partner of Aurora A, Ajuba, is absent (Hirota et al., 2003). In the absence of Ajuba, Aurora A is recruited to the centrosome but remains inactive. It is therefore possible that Aurora A is activated by Ajuba and this is a key event in mitotic entry.

The involvement of Aurora A in centrosome duplication is not obvious as excess levels of Aurora A, either wild-type or kinase-inactive, induce centrosome amplification and multinucleation. In fact overexpression of other mitotic kinases such as Plk1 and Aurora B also result in centrosome overduplication, multinucleation and tetraploidization. An identical phenotype arises from the addition of cytochalasin D, an inhibitor of cytokinesis (Meraldi et al., 2002). Taken together, these data suggest that overexpression of the protein causes a failure of cells to complete cytokinesis, due to a variety of mitotic defects which results in cells with abnormal DNA content and amplified centrosomes (Meraldi et al., 2002).

Microtubule organisation and nucleation occurs primarily at the centrosome during mitosis. This is mediated in part by transforming acidic coiled-coil proteins (TACCs), which help to stabilize microtubules during mitosis by recruiting minispindles (Msps/XMAP215/TOG) proteins to the centrosome. It has recently been demonstrated using *D. melanogaster* mutants and *Xenopus* egg extracts that Aurora A phosphorylates

TACC proteins *in vivo* (Barros et al., 2005; Peset et al., 2005). This phosphorylation occurs exclusively at mitosis and is absolutely required for TACC protein complexes, including Maskin and Msps, to localise at the centrosome (Barros et al., 2005; Kinoshita et al., 2005; Peset et al., 2005). This stabilisation of microtubules at the centrosome during mitosis is therefore in part under the regulation of Aurora A activity and may explain why centrosomes are such dominant sites of microtubule assembly during mitosis.

Aurora A is also implicated in spindle assembly through a Ran mediated signalling pathway (Tsai et al., 2003). Ran-GTP is a nuclear factor believed to regulate spindle assembly (Di Fiore et al., 2003). Ran-GTP serves to release spindle assembly factors such as TPX2 and NuMA from the inhibitor importin-α to promote spindle assembly (Gruss et al., 2001). The release of TPX2 allows it to interact with Aurora A stimulating Aurora A activity (Tsai et al., 2003). Aurora A activity is then directed toward TPX2, PP1 and Eg5 (kinesins) to contribute to spindle assembly.

An additional binding partner of Aurora A as identified by co-immunoprecipitation experiments is the promyelocyte leukaemia gene splice variant, PLM3 (Xu et al., 2005). PLM3 is localised to centrosomes and its deficiency results in centrosome amplification. The presence of PLM3 is thought to reduce the level of Aurora A phosphorylation on T288 and as such this repression has been suggested as a mechanism to prevent centrosome re-duplication, again highlighting the importance of the Aurora A kinase in the centrosome duplication cycle. This provides a mechanism for the activity of Aurora A to be repressed after entry into mitosis (Xu et al., 2005). A second mechanism is through targeted degradation of Aurora A by the proteasome (Walter et al., 2000).

1.6 Polo-like kinases

Polo-like kinases represent a highly conserved family of serine/threonine kinases implicated in cell division and centrosome regulation (Barr et al., 2004). The first member, polo, was identified in *Drosophilia melanogaster* as a protein which when

mutated led to abnormal mitosis (Llamazares et al., 1991). Llamazares (1991) reported that mutations in *polo* lead to overcondensed chromosomes, bipolar spindles with extra chromosomes, monopolar spindles and bipolar spindles with one spindle pole being extra broad. These abnormal phenotypes associated with *polo* mutations all point to a function in organising mitosis.

Since then homologues of polo have been identified in many species including Plo1 of *Schizosaccharomyces pombe*, Cdc5p of *Saccharomyces cerevisiae*, murine homologues Snk, Fnk and Sak, and human Plk1, Plk2, Plk3 and Plk4 (Donohue et al., 1995; Fode et al., 1994; Golsteyn et al., 1994; Hamanaka et al., 1994; Holtrich et al., 1994; Kitada et al., 1993; Llamazares et al., 1991; Ohkura et al., 1995; Simmons et al., 1992). Lower eukaryotes have one polo-like kinase, whereas mammals have at least four. The family of kinases can be identified by structural features, a conserved N-terminal catalytic domain and a conserved region in the carboxy-terminal region named the polo-box domain (PBD). This PBD is structurally important for targeting polo-like kinases to their substrates and will be discussed in detail later (Lee et al., 1998). The *S. cerevisiae* Cdc5p protein kinase accumulates at the G2/M transition and cells with *cdc5* mutants have a dumbbell shaped morphology. This is characteristic of a defect in completion of sister chromatid separation (Kitada et al., 1993). The dumbbell morphology is also observed in HeLa cells depleted of Plk1 by RNAi (Liu and Erikson, 2003).

Plx1 (*Xenopus* homologue of human Plk1) and mammalian Plk1 have direct roles in mitotic entry and exit. Plx1 phosphorylates and activates Cdc25 which leads to the dephosphorylation and subsequent activation of Cdk1 and as such has a direct role in mitotic entry (Cogswell et al., 2000). Plk1 on the other hand may play a direct role in mitotic exit by the phosphorylation of Cdc27 and other APC components thereby activating the APC for degradation of cyclin B and other proteins (Kotani et al., 1999).

The murine Snk (Plk2), Fnk (Plk3) and Sak (Plk4) polo kinases were identified due to their high sequence similarity with the Polo kinase domain (Barr et al., 2004). These are all highly expressed in dividing tissues and are thought to play a role in meiotic and

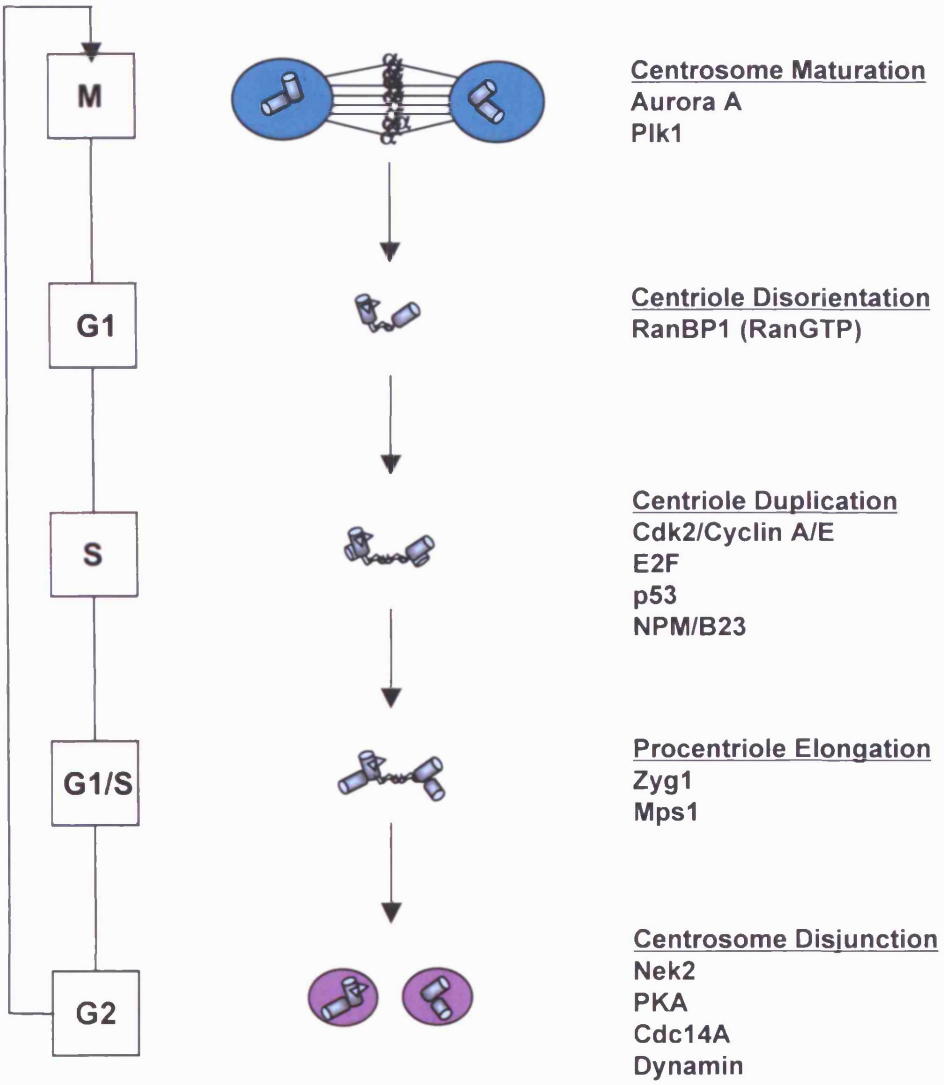

Figure 1.5 Proteins implicated in the regulation of the centrosome duplication cycle

Regulators of the centrosome cycle and the timing of their activity in relation to centrosome duplication and the cell cycle.

mitotic divisions (Donohue et al., 1995; Fode et al., 1994; Simmons et al., 1992). These will be discussed in more detail in later sections.

1.6.1 Polo-like kinase 1 (Plk1)

Plk1 has been implicated in a wide range of functions during mitosis. Plk1 was identified as a protein kinase by homology of its protein sequence to polo and cdc5 (Golsteyn et al., 1994). The specific activity of Plk1 increases in mitosis as does its expression levels (Mundt et al., 1997) Plk1 binds to the mitotic spindle poles and is redistributed to the midzone at anaphase (Golsteyn et al., 1995). In line with an increased expression at mitosis the kinase activity of Plk1 is low during interphase and high during mitosis (Golsteyn et al., 1995). However, the increase in activity is more than can be explained simply through increased protein levels suggesting specific activation of the kinase during mitosis (Mundt et al., 1997). Indeed, autophosphorylation of Plk1 occurs during mitosis and phospho-amino acid analysis reveals phosphate incorporation on serine and threonine residues in Plk1 (Golsteyn et al., 1995). Mutation of the activation loop threonine residue T210 to aspartate increases the kinase activity of Plk1 supporting evidence for autoactivation (Lee and Erikson, 1997). The kinase activity of Plk1 is lost when the protein is degraded at the completion of mitosis through an ubiquitin-proteasome mediated pathway (Ferris et al., 1998). The degradation of Plk1 is required for exit from mitosis as, when a non-degradable form of Plk1 is present, cells are prevented from exiting mitosis (Lindon and Pines, 2004). High levels of hyperactive Plk1-T210D also delay mitotic exit suggesting that Plk1 activity must be subdued before mitotic exit can occur (Lindon and Pines, 2004). Plk1 is thought to have an additional function in regulating cytokinesis before it is destroyed (van Vugt and Medema, 2005).

1.6.2 Plk1 substrates and functions

The Plk1 kinase plays multiple roles during the course of mitosis. It has been implicated in the control of centrosome maturation, mitotic entry, regulation of the APC/C, chromosome segregation and cytokinesis. A role for Plk1 in early mitosis was identified by purification of Plx1 from *Xenopus* egg extracts as a kinase that phosphorylated the nuclear export sequence Ser147 of cyclin B (Toyoshima-Morimoto et al., 2001). S147

phosphorylation does not occur in Plk1-depleted HeLa cells and mutation of this site and S133 to alanine prevents the nuclear localisation of cyclin B. Plk1 when co-expressed stimulates the entry of Cdk1/cyclin B into the nucleus (Toyoshima-Morimoto et al., 2001). Therefore, this highlights an important role for Plk1 in recruitment of mitosis promoting factors into the nucleus during prophase. The peptidyl-prolyl *cis/trans* isomerase, Pin1, is also phosphorylated by Plk1 increasing its stability by regulating its ubiquitination (Eckerdt et al., 2005). Pin1 is thought to regulate mitotic entry and as such this represents another mechanism by which Plk1 regulates this stage of the cell cycle.

Plk1's role in centrosome maturation was first highlighted by antibody microinjection assays. Inhibition of Plk1 resulted in monoastral spindles and a decrease in γ-tubulin recruitment to the centrosome (Lane and Nigg, 1996). This suggests an involvement of Plk1 in the maturation of the centrosome at the G2/M transition. However, how Plk1 contributes to centrosome maturation is not clear. It could be either through displacement of Nlp, or through recruitment of proteins such as Asp and RanBPM (Jang et al., 2004). Nlp is a novel substrate of Plk1 that binds the γ-TuRC (Casenghi et al., 2003). Nlp localises to the mother centriole and thus may be involved in microtubule anchoring (Rapley et al., 2005). Phosphorylation of Nlp by Plk1 displaces it from the centrosomes and this may be an essential step in centrosome maturation. Nlp will be discussed in more detail in later sections.

Abnormal spindle protein (Asp) is required for normal bipolar spindle formation in *Drosophila* with *asp* mutations resulting in broad unfocused spindles (Avides and Glover, 1999). Asp is a microtubule associated protein (MAP) that localises to the polar regions of the spindle in early mitosis and the midbody at telophase (Saunders et al., 1997). Asp is phosphorylated by *polo in vitro* (Avides et al., 2001). Mutations of *asp* and *polo* have similar mutant phenotypes with defects in spindle pole assembly. Extracts depleted of Asp or Polo lack the ability to nucleate microtubules from the MTOC. Addition of Asp alone does not restore the ability of depleted centrosomes to nucleate and organise a focused mitotic spindle (Avides and Glover, 1999). However, phosphorylated Asp or the re-addition of Polo restores nucleation and a focused spindle pole (Avides et al., 2001).

Asp and Polo co-immunoprecipitate demonstrating an association between Asp and Polo. These data suggests that, at early mitosis (prophase), Asp and Polo form a complex in which Asp is phosphorylated and stimulated to organise microtubule asters. This organisation of focused asters is later required for the correct formation of the mitotic spindle at metaphase.

An additional role of Plk1 at the centrosome may include the recruitment and activation of RanBPM to the centrosome (Jang et al., 2004). RanBPM is involved in microtubule assembly and co-localises with Plk1 at the centrosome. This interaction may play an important role in centrosome maturation and spindle integrity.

Chromosome condensation occurs during prophase in preparation for sister chromatid separation. Cohesin and condensin are two proteins involved in this process mediating cohesion and condensation of chromosomes, respectively. Cohesin release from the chromosomes is essential for sister chromatid separation; cohesin is released as a result of cleavage by separase which is normally inhibited by securin until securin is degraded by the APC/C. However, there are additional controls regulating the dissociation of cohesin including phosphorylation by Polo/Cdc5 (Alexandru et al., 2001). In Plx1 depleted *Xenopus* egg extracts, the release of cohesin from prophase chromosomes is blocked (Losada et al., 2002). Cohesin release from the chromatin can also occur in the absence of cleavage. Plk1 has been implicated in this process by phosphorylation of cohesin (Sumara et al., 2002). Plk1 phosphorylation of cohesin is, therefore, a major regulation event in release of cohesin from chromatin and the onset of sister chromatid separation.

Depletion of Plx1 from mitotic egg extracts also prevents mitotic exit suggesting that Plx1 might regulate the APC/C (Descombes et al., 1998). Plk1's role in regulating the APC/C and as such regulating mitotic progression was shown in kinase assays and immunoprecipitations of APC/C components. Cdk1/cyclin B-activated Plk1 can phosphorylate the APC/C components Cdc16, Cdc27 and Tsg24. This phosphorylation activates the APC/C (Kotani et al., 1999). In addition, Plx1 phosphorylates the APC/C inhibitor XErp1 targeting it for degradation (Schmidt et al., 2005). Thus, the Plk1 protein

plays a direct role in mitotic exit through activation of the APC/C and degradation of specific targets required for cell cycle progression.

The motor mitotic kinesin-like protein 2 (Mklp2) is a late mitotic substrate of Plk1. Mklp2 binds the polo-box-domain (PBD) of Plk1 and is phosphorylated by Plk1 on Serine 528 (Neef et al., 2003). Blocking the phosphorylation of Mklp2 by Plk1 leads to a cytokinesis defect. It has been demonstrated that phosphorylation of Mklp2 by Plk1 targets Plk1 complex to the central spindle. Plk1 localisation is thus controlled by the phosphorylation of Mklp2. Plk1 function and targeting is blocked in Mklp2-S528A mutants (Neef et al., 2003). Therefore, Plk1 can direct its own targeting to the central spindle by phosphorylating the Mklp2 protein. Plk1 can then contribute to further cell cycle events by the spatial activation of targets at the central spindle.

Depleting Plk1 by RNAi leads to an inhibition of cell proliferation, decreased cell viability and the activation of apoptosis as seen by caspase 3 activation. In addition, cells arrest at G2/M with 4N DNA content and dumbbell-shaped DNA (Liu and Erikson, 2003). This highlights the importance of Plk1 at all stages of mitosis. Increased Cdk1 activity is also observed when either an inactive Plk1-K82M kinase or a truncated Plk1ΔN is expressed (Seong et al., 2002). The expression leads to a pre-anaphase arrest with an increase in both Cdk1 and Plk1 activity. These mutants are most probably having a dominant-negative effect on the endogenous Plk1 protein and as such give a phenotype in line with that of RNAi depletion.

1.6.3 Polo-like kinases: structure and activation

The polo-like kinases are characterised by their structure, which contains not only a characteristic kinase domain but also a region within the non-catalytic domain termed the PBD. Within the catalytic activation loop of Plk1 lie two conserved residues E206 and T210, both of which are equally important for Plk1 activity. T210, when mutated to aspartate, increases kinase activity and E206 when mutated to a non-acidic group decreases kinase activity (Lee and Erikson, 1997). The kinase activity of Plk1 is therefore dependent on either autophosphorylation on T210 or activation by an upstream kinase.

Also there is a requirement for a negative residue at position –4 from the phosphorylation site. It is also interesting to note that a Plk1-ΔC mutant was three-fold more active than the wild type kinase (Lee and Erikson, 1997; Mundt et al., 1997). This may represent an auto-inhibitory action of the C-terminal domain, which could be relieved in a cell cycle-dependent manner by conformational changes in Plk1.

The PBD of Plk1 comprises of two polo boxes, PB1 from amino acids 405-494 and PB2 from 505-598. These come together in three dimensions to form the PBD. The main functions of the PBD are thought to be in substrate binding and subcellular localisation of Plk1. Overexpression of the PBD alone leads to mitotic defects including spindle abnormalities and micronucleated cells. These occur in the absence of centrosome duplication suggesting that the abnormalities are not a result of cytokinesis failure (Seong et al., 2002). Mutation of the PBD (W414F) disrupts localisation of Plk1 to spindle poles without affecting the kinase activity of the protein (Lee et al., 1998).

Crystal structure determination of the polo motif revealed it to comprise of a six-stranded β-sheet and an α-helix,each PBD has two of these (Cheng et al., 2003; Elia et al., 2003b). Importantly, structural analysis revealed that the PBD is a phospho Ser/Thr binding motif. Co-crystallisation with a phospho-peptide bound to the PBD revealed that binding occurs via a positively-charged cleft. Mutation of residues within this cleft led to the loss of centrosome localisation and a block in mitotic progression (Elia et al., 2003a). Phospho-peptide binding to the PBD also stimulates the kinase activity of Plk1 (Elia et al., 2003a). Using peptide libraries, it was found that the PBD preferentially binds the consensus sequence SS/T where the second serine or the threonine is phosphorylated (Elia et al., 2003b). Hence, the auto-inhibitory effect of the C-terminal domain most likely occurs via binding of the catalytic domain to the PBD.

Plk1 possibly remains in this inactive state and becomes active only when phosphorylated and pre-activated substrates bind to the PBD, which targets and directs Plk1 activity towards them at the correct time and place in the cell cycle. For example, the Chk2 tumour suppressor protein binds to the PBD and is thought to link Plk1 function in

mitosis with DNA damage checkpoints (Tsvetkov et al., 2005). In addition, Cdc25C contains a phospho Ser/Thr motif capable of binding the PBD (Elia et al., 2003a). Targeting of Plk1 via the PBD thus provides a mechanism by which proteins can be "primed" for phosphorylation at different times of mitosis.

1.6.4 Polo-like kinases 2, 3 and 4

In mammalian cells four polo-like kinase proteins have been identified whereas in yeast and *Drosophila* only one has been identified. Polo-like kinase 2 (Plk2/Snk) is expressed in G1 with kinase activity peaking near the G1-S transition (Ma et al., 2003a; Warnke et al., 2004). Plk2 shares the conserved basic structure of the polo-like kinase family with an N-terminal kinase domain and the characteristic C-terminal PBD. The PBD of Plk2 is required for its centrosomal localisation presumably by binding substrates that reside at the centrosome (Ma et al., 2003b). One such binding partner of Plk2 is calcium and integrin-binding protein (CIB). CIB negatively regulates the activity of Plk2 (Ma et al., 2003b). Plk2 is also negatively regulated by its C-terminal domain and gene expression by the p53 transcription factor (Burns et al., 2003). Both Plk2 and Plk3 may have a role outside of the cell cycle as induced Plk2 and Plk3 are targeted to dendrites of activated neurons (Kauselmann et al., 1999) and are consistently expressed in mitotic neurons.

Plk2 localises to the centrosome and down regulation by RNAi as well as overexpression of inactive Plk2 in S-phase arrested cells blocks centriole duplication (Warnke et al., 2004). However, unlike Plk1, Plk2 is not an essential gene as gene targeting of Plk2 demonstrated that Plk2 is not required for embryonic or post-natal growth (Ma et al., 2003a). Cultured $Plk2^{-/-}$ embryonic fibroblasts do grow more slowly and have a delayed S-phase, but cells continue to divide (Ma et al., 2003a). However, it may be possible that in this situation Plk3 is compensating for the loss of Plk2.

Plk3 (Prk/Fnk) expression is activated by growth factors and is restricted to a limited number of tissues (placenta, ovaries and lung) (Li et al., 1996). Its kinase activity is low in G1 and G1/S and peaks during late S and G2 (Ouyang et al., 1997). Plk3 and Plk1 share 50% sequence identity and both proteins can rescue *cdc5* temperature sensitive

mutants in *S. cerevisiae* suggesting a conserved function (Ouyang et al., 1997). Plk3 undergoes autophosphorylation and can phosphorylate both casein and Cdc25C *in vitro* (Ouyang et al., 1997). Cdc25C is a positive regulator of the G2/M transition and therefore it is possible that Plk3 may regulate the onset of mitotic progression by phosphorylation of Cdc25C. Plk3 has also been implicated in the DNA damage response pathway as ectopic expression of Plk3 induces apoptosis (Xie et al., 2001). This response is mediated through the phosphorylation of p53 by Plk3 (Bahassi et al., 2002; Xie et al., 2001). Chromatin condensation, G2/M arrest and apoptosis are a common feature of Plk3 overexpression in mammalian cells (Conn et al., 2000; Wang et al., 2002). It is also proposed that the kinase has a role in cytokinesis as it is localised to the midbody during telophase (Wang et al., 2002). Constitutively active Plk3 results in cells with elongated and unsevered midbodies (Wang et al., 2002). Plk3 is localised to the centrosome but a centrosomal function for Plk3 is yet to be identified.

Plk4 (Sak) was isolated as two isoforms encoding a serine/threonine protein kinase in mice (Fode et al., 1994). Northern Blot analysis of the Plk4 mRNA in mouse embryos and adult tissues implicated Plk4 expression with mitotic and meiotic cell division (Fode et al., 1994). Plk4 has recently been identified as being down regulated by p53 (Li et al., 2005). RNAi mediated interference of Plk4 induced apoptosis supporting a role previously identified in cell proliferation (Fode et al., 1994; Li et al., 2005). Gain- and loss-of function experiments have demonstrated that Plk4 is a key regulator of centrosome duplication (Habedanck et al., 2005). Overexpression of the active kinase leads to centrosome amplification and antibody-mediated interference or depletion using RNAi of endogenous Plk4 prevents centrosome overduplication. Depletion of the Plk4 protein by RNAi over 48 hours led to the appearance of monopolar spindles and a loss in correct centriole numbers. The Plk4 protein is therefore essential for centrosome duplication in mammalian cells. As discussed previously, Cdk2 activity is also required for centrosome duplication. However, Cdk2 requires Plk4 to cause centrosome duplication as does Plk4 require Cdk2. It is therefore plausible to assume that these two major regulators of centrosome duplication are integrated in a pathway which links the cell cycle and centrosome duplication.

1.7 NIMA-related kinases

The NIMA-related kinase or 'Nek' family of protein kinases was first identified by structural similarity with the serine/threonine protein kinase *never in mitosis A* (NIMA) of *Aspergillus nidulans* (Fry and Nigg, 1997). In *Aspergillus nidulans,* entry into mitosis requires the activation of NIMA. Overexpression of the wild type nimA allele drives cells into a premature mitotic state but expression of inactive NIMA or the C-terminal non-catalytic domain of NIMA causes a G2 arrest (O'Connell et al., 2003). The structural features of the NIMA protein kinases include a catalytic N-terminal region containing a characteristic activation loop present in all protein kinases (Hanks and Hunter, 1995). The C-terminal domains of the NIMA kinases vary but most contain coiled-coil motifs (Fry et al., 1999). The NIMA kinases are serine/threonine protein kinases and the consensus site of NIMA, as identified by the use of synthetic peptides, is FRx**S/T** with the phenylalanine within the sequence essential (Lu et al., 1994).

Nek kinases have been identified in many eukaryotes including fungi, *Dictyostelium*, *Drosophilia*, mammals and unicellular algae (Figure 1.6). The yeast *S. cerevisiae* contains a single NIMA homologue, Kin3 (Barton et al., 1992; Jones and Rosamond, 1990). This protein is actively expressed in mitotic cells but mutation or overexpression of Kin3 causes no obvious growth defects and as such its function remains unclear (Barton et al., 1992; Jones and Rosamond, 1990; Schweitzer and Philippsen, 1992). *S. pombe* also contains one homologue to NIMA called Fin1. Fin1 is implicated in chromosome condensation as overexpression at any point in the cell cycle promotes premature chromatin condensation. Like NIMA, its levels fluctuate throughout the cell cycle peaking at mitosis (Krien et al., 1998). Fin1 localises to the spindle pole body (SPB) and may be involved in spindle function (Krien et al., 2002). *Fin1Δ* cells show defects in mitotic spindles and disrupted nuclear envelopes (Krien et al., 2002). However, its role in chromosome condensation is now disputed as the kinase activity peaks at the metaphase-anaphase transition after chromosome condensation has occurred (Krien et al., 2002). A role in spindle pole formation is supported by a temperature sensitive mutant of *Fin1,* which failed to form a mitotic spindle (Grallert and Hagan, 2002). Fin1 has recently

been linked with SIN (septum initiation network) pathway activation on anaphase B SPBs (Grallert et al., 2004). The SIN pathway is located asymmetrically on the two SPBs of fission yeast, however, the yeast divide symmetrically. Only one of the SPBs activates the SIN pathway and this is achieved by specific recruitment of Fin1 to the mature SPB. Fin1 then inhibits the SIN pathway at this SPB and the SIN is activated on the less mature SPB and as such asymmetric activation is achieved.

Other NIMA homologues include Nim-1 of *Neurospora crassa* which shares 75% identity to the NIMA catalytic domain and can functionally complement a *nimA* mutant (Pu et al., 1995). TpNrk of *Tetrahymena pyriformis* shares 37% identity to NIMA over the catalytic domain and its mRNA levels may be under cell cycle control (Wang et al., 1998). Pf-Nek-1 identified in *Plasmodium falciparum* may be involved in MAPK signalling cascades and shares 42% identity to the Nek2 kinase (Dorin et al., 2001). The functions of these kinases are not understood. However, the Fa2 protein of *Chlamydomonas reinhardtii* is localised to the basal body and may play a role in centriole associated microtubule severing (Mahjoub et al., 2002). *Fa2* mutants have a delay in cell cycle progression at the G2/M transition and in the assembly of flagella structures after exit from mitosis (Mahjoub et al., 2002). Fa2 shares 40% identity to NIMA over the catalytic domain but has an unrelated C-terminal domain.

These studies in lower eukaryotes suggest that many members of the NIMA family of kinases play roles within the cell cycle and specifically mitosis. The general conservation of cell cycle control proteins in eukaryotes made it likely that a homologue of NIMA would also be present in man. By sequence comparison, the human genome contains eleven Nek proteins, Nek1 to Nek11 (Hayashi et al., 1999; Holland et al., 2002; Kandli et al., 2000; Letwin et al., 1992; Noguchi et al., 2002; Schultz et al., 1994; Tanaka and Nigg, 1999). I will firstly discuss the Nek2 protein followed by some of the other Nek mammalian kinases.

1.7.1 Nek2

Nek2 is the most closely related mammalian relative of NIMA not only structurally but also in its expression during the cell cycle. Nek2 is almost undetectable during G1 but accumulates abruptly at the G1/S transition remaining high until late in G2 (Schultz et al., 1994). This evidence led to the belief that Nek2, like NIMA, may function at the onset of mitosis, at the G2/M transition. The Nek2 protein kinase and NIMA share 47% sequence identity over their catalytic domains (Fry et al., 1995). The Nek2 gene is located on chromosome 1 and Nek2 mRNA is encoded on eight exons. The initiation codon is located in exon 1 and the UAG stop codon on exon 8. The seventh intron contains a termination codon starting 43 nucleotides after the splice site and an alternative polyadenylation signal after a further 625 nucleotides.

The positioning of the alternative polyadenylation signal results in the generation of the human Nek2B protein of 384 amino acids and a M.wt of 44.9 kDa whereas Nek2A protein is 445 amino acids in length and has a M. wt of 48 kDa (Hames and Fry, 2002) (Figure 1.6). Both Nek2 splice variants consist of an N-terminal catalytic domain containing the characteristic features of a Ser/Thr protein kinase (discussed in detail later). This is followed by a C-terminal novel leucine zipper motif required for Nek2 homodimerisation and activity (Fry et al., 1999).

Xenopus also expresses two structural variants, Nek2A and Nek2B (Uto et al., 1999). Nek2B is present in immature and mature oocytes and early embryos whereas the longer Nek2A is expressed after the gastrula/neurula transition. This suggests that the two variants of Nek2 might play both meiotic and mitotic roles in a temporal manner during *Xenopus* development (Uto et al., 1999). The human kinase Nek2 splice variants, exhibit distinct patterns of expression in mitosis (Hames and Fry, 2002). Nek2A was found to match the expression of the previously studied Nek2 whereas Nek2B levels remained high in cells arrested at mitosis (Hames and Fry, 2002). The decrease in Nek2A upon entry into mitosis is due to the presence of destruction motifs in the C-terminal region, which are not present in the Nek2B protein (Hames et al., 2001).

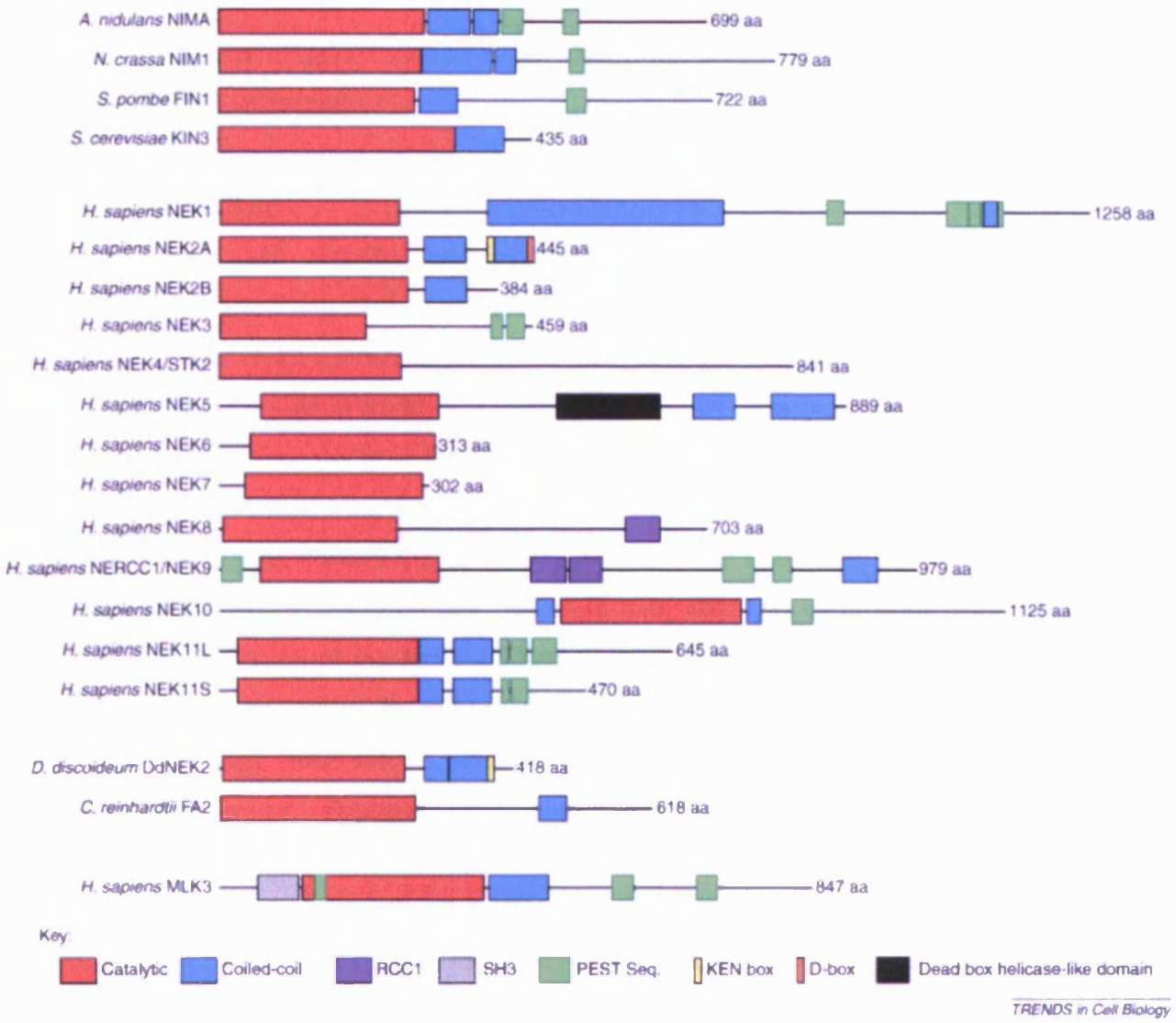

Figure1.6 NIMA kinases

Structures of NIMA related kinases. Figure taken from O'Connell et al. (2003). The NIMA kinases share a characteristic catalytic domain (red) but have divergent C-termini. Many of the NIMA kinases also contain coiled coiled motifs (blue).

It is possible that a third alternately spliced variant of Nek2 exists in testis, Nek2A-T (Fardilha et al., 2004). The alternate splicing results in a protein of 437 amino acids that differs from Nek2A in that it is missing residues 371-378 of the C-terminal domain (Fardilha et al., 2004) (Figure 1.7). The splice variant was identified by yeast two hybrid analysis with PP1γ as the bait.

1.7.2 Nek2 regulation

Nek2 expression and activity are regulated via transcription, post-translational modifications, targeted degradation and protein-protein interactions (Hayward and Fry, 2005). Analysis of Nek2 mRNA levels by RT-PCR revealed that Nek2 transcription is low in M and G1 and high in S and G2 (Twomey et al., 2004). This correlates with Nek2 protein levels which increase from G1/S and reach a peak in S and G2 (Fry et al., 1995). Two transcription factors have been implicated in the regulation of Nek2 expression. These are E2F4 and the Forkhead transcription factor, FoxM1 (Ren et al., 2002; Wonsey and Follettie, 2005). E2F4 represses genes in G0 and G1 correlating with the transcriptional repression of the Nek2 mRNA. Further evidence for E2F4 regulation of Nek2 transcription was shown by the fact that loss of the Rb family proteins p107 and p130 led to elevated Nek2 mRNA levels (Ren et al., 2002). The role of E2F4 as a transcriptional repressor is facilitated by the binding of Rb family proteins.

Nek2 protein levels are also regulated by degradation (Hames et al., 2001). As mentioned previously, Nek2 exists in two splice variants. Nek2A contains motifs responsible for the destruction of Nek2A including a cyclin A type D-box and a KEN box both present in the extreme C-terminus of Nek2A (Hames et al., 2001). Nek2B is also a relatively short-lived protein but the mechanism of its degradation has yet to be determined. Other post-translational mechanisms also play a major role in the regulation of Nek2, including autophosphorylation (Fry et al., 1995). The regulation of Nek2 by autophosphorylation will be the subject of later chapters within this thesis.

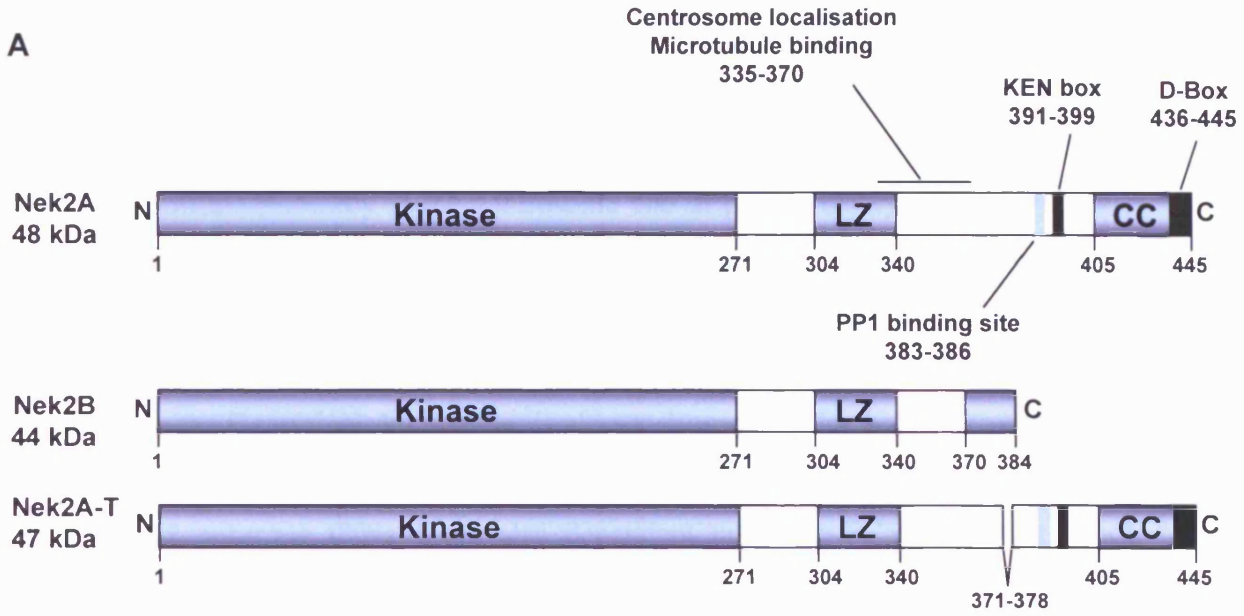

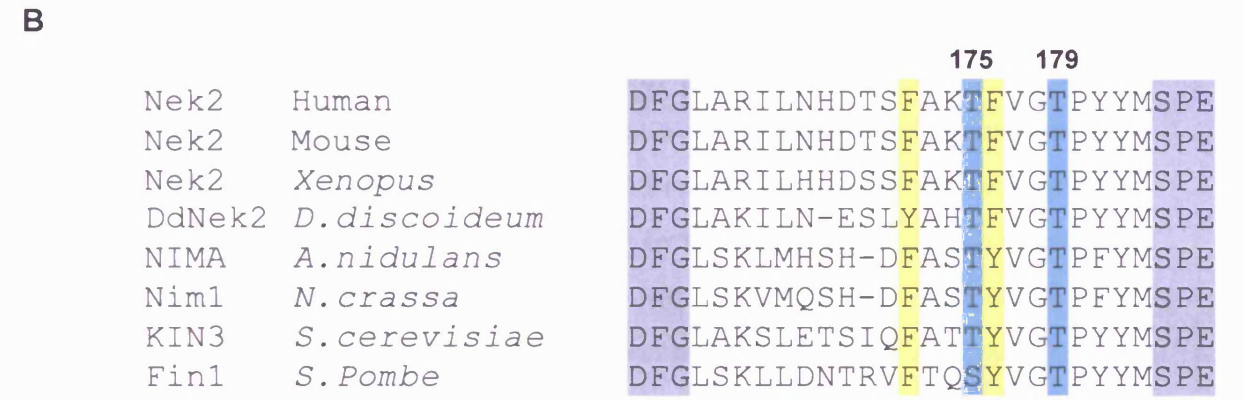

Figure 1.7 Nek2 kinases

A. Schematic diagram representing the Nek2 protein kinase splice variants. Kinase indicates the kinase domain, LZ the leucine zipper and CC the coiled coil domain. Diagram was adapted from Hayward and Fry (2005). **B.** The conserved amino acids in the Nek2 kinase activation loop. Grey shading represents highly conserved residues of the activation loop in all serine/threonine kinases. Yellow shading shows conserved residues that may contribute to the specificity of the kinase. Threonine 175 and possibly Threonine 179 (blue), are thought to be the sites of autophosphorylation in Nek2 (see chapter 3).

1.7.3 Nek2 localisation

Nek2 is highly enriched at the centrosome (Fry et al., 1998b). The localisation of Nek2 to the centrosome occurs in 90% of exponentially growing U2OS cells and is therefore assumed to localise at the centrosome throughout the cell cycle (Fry et al., 1998b). GFP-Nek2 also localises primarily at the centrosome and in part to the cytoplasm (Faragher and Fry, 2003). The cytoplasmic Nek2 portion co-localises with microtubules (Hames et al., 2005). Cytoplasmic Nek2 particles are highly dynamic moving over long distances to and from the centrosome via the microtubule network. This localisation is dependent on a region within the C-terminal domain that is absolutely required for both microtubule and centrosomal localisation (Hames et al., 2005). The recruitment of Nek2 to the centrosome and the Nek2 substrate C-Nap1 are also dependent upon the PCM-1 protein which colocalises in part with Nek2 in the cytoplasmic particles (Hames et al., 2005).

Nek2, although primarily known as a centrosomal kinase, has been detected at the nucleus, chromatin and the kinetochores (Kim et al., 2002). Localisation of Nek2 at the nucleus was suggested by its co-localisation with nucleophosmin (Yao et al., 2004). Indeed the localisation of Nek2 with chromatin in spermatocytes correlates with localisation of a Nek2 substrate, HMGA2. HMGA2 is released from chromatin during the G2/M transition possibly after its phosphorylation by the Nek2 kinase (Di Agostino et al., 2004). Nek2 localisation at the chromosomes is further supported by the protein being exclusively localised to chromosomes during porcine oocyte maturation (Fujioka et al., 2000). The localisation of Nek2 to the kinetochores (where it may be involved in spindle checkpoint signalling) has been identified using one specific antibody (Lou et al., 2004b). This localisation remains to be confirmed either with other antibodies or recombinant protein.

1.7.4 Nek2 interactions

Nek2 exists in cells as a stable homodimer, dependent on a leucine zipper coiled-coil motif in its C-terminal domain (Fry et al., 1999) (Figure 1.7). As a result Nek2 undergoes trans-autophosphorylation predominantly on serine residues (Fry et al., 1995). The removal of the leucine zipper results in a reduction in the kinase activity of Nek2 (Fry et

al., 1999). This reduction in kinase activity could be due to the loss of trans-autophosphorylation of Nek2 or just the result of a loss in dimerisation. In addition to homodimerisation the Nek2A and Nek2B proteins can heterodimerise (Hames and Fry, 2002).

The Nek2A and Nek2B proteins diverge in sequence after amino acid 370 causing Nek2B to lack important regulatory motifs that are present in the extreme C-terminus of Nek2A. One of these important motifs is a binding site for protein phosphatase 1 (PP1). This site, KVHF, is present at amino acids 383-386 in the C-terminus of Nek2A (Helps et al., 2000). The phenylalanine in this sequence is highly important for Nek2A binding to PP1 as no interaction occurs when the residue is mutated to alanine (Helps et al., 2000) (Figure 1.7).

PP1 is a major protein phosphatase that regulates a range of cellular processes by dephosphorylation of serine and threonine residues. As well as binding Nek2A, PP1 also forms complexes with Aurora A demonstrating another PP1-kinase complex involved in cell cycle control. Nek2A and PP1 form a kinase-phosphatase complex which maintains Nek2A in a dephosphorylated state (Hames and Fry, 2002). When bacterially expressed PP1 is added to GST-Nek2A a 65% inhibition of Nek2 activity is seen (Helps et al., 2000).

Nek2 substrates can only be efficiently phosphorylated when PP1 activity is reduced at the G2/M transition. Nek2 itself may inhibit the phosphatase activity of PP1. PP1γ is phosphorylated by Nek2 on threonines 307 and 318 *in vitro* within the consensus R/Kxx(A/I)**T**R/K (Helps et al., 2000). However, PP1 phosphorylation by Nek2 can be reduced as PP1 can auto-dephosphorylate itself (Helps et al., 2000).

The kinase-phosphatase complex of PP1 and Nek2 may be further regulated by an additional protein, named inhibitor-2 (Inh2), a physiological inhibitor of PP1. Inh2 binds to a site on PP1 that is distinct from the Nek2 binding site (Eto et al., 2002). The binding site of Inh2 has the conserved residues IKGI and lies next to the binding site of Nek2 on

PP1. Competition between Inh2 and Nek2 exists as when one protein is bound to PP1 allosteric movements may prevent the other binding, suggesting that when Inh2 is present Nek2 can no longer bind PP1 (Egloff et al., 1997; Eto et al., 2002). Inh2 could then enhance the kinase activity of Nek2 by displacing Nek2 from PP1. In fibroblasts expressing Inh2, increased centrosome splitting is observed which is an indicator of enhanced Nek2 kinase activity (Eto et al., 2002). The expression level of Inh2 peaks at S phase and during mitosis and its activation may be regulated by phosphorylation as it is phosphorylated by MAPK at Thr72. This may provide a mechanism for the cell cycle regulation of the kinase-phosphatase complexes. When MAPK inhibitors were added to cells, the Nek2 activity was blocked supporting the notion that such a pathway might exist (Di Agostino et al., 2002). Although lacking the PP1 binding site, Nek2B may be regulated by PP1 through heterodimerisation with Nek2A via the leucine zipper motif (Hames and Fry, 2002).

Extracellular signal-regulated kinase 2 (ERK2), a MAP kinase member, has also been demonstrated as a binding partner of Nek2 and RNAi of Nek2 prevented ERK2 from localising to the centrosome (Lou et al., 2004a). These authors also identified an interaction of Nek2 with Mad1. The interaction of Nek2 with Mad1 may be via binding the Telomere repeat binding factor 1 (Trf1) as this too has recently been shown to bind Nek2 and in turn can bind Mad1 (Prime and Markie, 2005). Trf1 plays a role in telomere length and therefore the interaction between Trf1 and Nek2 may provide a link between telomere length and mitotic progression.

Nek2 interacting protein (NIP1) was identified in a yeast two hybrid screen as a binding partner of Nek2 and is phosphorylated by Nek2 *in vivo* (Yoo et al., 2004). NIP1 is a Golgi protein, opening opportunities that Nek2 may be involved in regulation of the Golgi complex at mitosis (Yoo et al., 2004).

1.7.5 Nek2 substrates

The C-Nap1 protein was identified as a substrate of Nek2 when it was isolated in a yeast two-hybrid screen using Nek2A as the bait (Fry et al., 1998a) (Figure 1.8). C-Nap1 is a

281 kDa protein consisting largely of coiled-coil structure. It has globular N- and C-termini and a central proline rich region that could act as a hinge. The C-terminal globular domain of C-Nap1 has been shown to be an excellent substrate for Nek2. *In vitro* phosphorylation assays showed that approximately 13 moles of phosphate were incorporated per mole of C-Nap1 by Nek2 (Helps et al., 2000). This suggests there may be 13 different phosphorylation sites present on the C-terminus of C-Nap1 which Nek2 could phosphorylate.

C-Nap1 co-localises with Nek2 at the centrosome and immunochemical and biochemical studies demonstrate that it is part of the core centrosome (Fry et al., 1998a). In fact C-Nap1 specifically localises to the proximal ends of mother and daughter centrioles in interphase but dissociates from centrosomes at the onset of mitosis (Mayor et al., 2000). Evidence for a role for C-Nap1 in centrosome cohesion comes from antibody interference of C-Nap1, which induces centrosome splitting regardless of the cell cycle phase (Mayor et al., 2000). Aggregates of C-Nap1 are formed throughout the cell when C-Nap1 is overexpressed but these patches do not affect entry into mitosis suggesting C-Nap1 is still correctly dismantled from the centrosome allowing centrosome separation and spindle formation to be achieved (Mayor et al., 2002). The patches of C-Nap1 formed from overexpression are significantly smaller when Nek2 is co-expressed but not when kinase-inactive Nek2 is co-expressed. This provides supporting evidence that phosphorylation by Nek2 dismantles the C-Nap1 higher structure (Mayor et al., 2002). Initially, C-Nap1 was thought to span the distance between the two centrioles to form part of a linker structure. However, staining using antibodies raised against different parts of C-Nap1 always revealed two distinct dots at the centrosomes and no spanning regions in between (Mayor et al., 2000). Hence, additional proteins to C-Nap1 are likely to be involved in the intercentriolar linkage. Moreover, C-Nap1 is still detected on centrioles when premature centrosome splitting is induced by Nek2 overexpression (Faragher and Fry, 2003).

Therefore, C-Nap1 probably binds other, as yet unidentified centrosomal proteins. Perhaps phosphorylation of C-Nap1 by Nek2 triggers the dissociation of this complex, in turn resulting in centrosome separation (Mayor et al., 2002). Additional evidence that C-

Nap1 is a substrate of Nek2 comes from evidence that C-Nap1 protein is hyper-phosphorylated in mitosis (Mayor et al., 2002). Recently, a structural homologue of C-Nap1 called Rootletin has been identified as a 220 kDa protein localised to the cilary rootlet and basal body (Yang et al., 2002). Centrioles and basal bodies share essentially the same structure. Rootletin is structurally required for the formation of the rootlet and is an *in vitro* substrate for Nek2 (Bahe et al., 2005). Rootletin akin to C-Nap1 may be part of a linker structure between the two centrioles. Immunoelectron microscopy of endogenous rootletin reveals fibres emanating from the proximal ends of centrioles (Bahe et al., 2005). Rootletin interacts with C-Nap1 and is displaced from centrosomes at the onset of mitosis. RNAi depletion of either rootletin or C-Nap1 causes centrosome splitting (Bahe et al., 2005). This evidence suggests that both rootletin and C-Nap1 are targets of the Nek2 kinase and may be involved in centrosome cohesion as a fibrous linker structure which is dismantled at mitosis possibly initiated by the activity of Nek2.

We have recently identified ninein like protein (Nlp) as a novel target of the Nek2 protein kinase (Rapley et al., 2005). Nlp was identified via a yeast two hybrid screen using Plx1 as the bait (Casenghi et al., 2003). The protein shares a high degree of homology with ninein, a protein localised to the mother centriole appendages and involved in microtubule anchoring at the centrosome. Nlp is a novel substrate for Plk1 and Nek2 with phosphorylation of Nlp causing its displacement from centrosomes at the G2/M transition (Casenghi et al., 2003; Rapley et al., 2005). Overexpression of Nlp causes aberrant spindle formation presumably because it cannot be fully removed from the centrosomes upon mitotic entry (Casenghi et al., 2003). Hence, Nlp is implicated in MT nucleation and anchoring on interphase, but not mitotic centrosomes. Nlp will be discussed in more detail in later chapters.

Recent research has identified another possible substrate of Nek2 named Hec1 (highly expressed in cancer) (Chen et al., 2002). Hec1 is thought to be involved in chromosomal segregation and is found to localise at the kinetochores. Hec1 is phosphorylated during the G2/M phase of the cell cycle (Chen et al., 2002). A Hec1-Nuf2 complex is localised to centrosomes at G1-S phase and photobleaching experiments show its interaction with

the centrosome is highly dynamic (Hori et al., 2003). During the G2 and M phases of the cell cycle it has been proposed that Hec1 is phosphorylated by Nek2 (Chen et al., 2002). The phosphorylation of Hec1 by Nek2 kinase is vital for Hec1 to coordinate faithful chromosome segregation although the mechanism is unclear (Chen et al., 2002). Phospho-amino acid analysis of ^{32}P-orthophosphate-labelled Hec1 revealed that Hec1 is phosphorylated specifically on serine residues (Chen et al., 2002). An antibody raised to serine 165 of Hec1 when added into *in vitro* kinase assays abolished Nek2 phosphorylation of Hec1 in T24 cell lysates (Chen et al., 2002). Nek2 phosphorylation of Hec1 was also abolished when serine 165 was mutated to an alanine residue and kinase assays were performed *in vitro* (Chen et al., 2002). Serine 165 lies in the consensus FALSKSS and mutational analysis of Hec1 in yeast has shown that this site is important for the function of Hec1 (Chen et al., 2002).

Numatrin/nucleophosmin/B23, as previously discussed, is a substrate of the Cdk2/cyclin E complex involved in the initial stages of centrosome duplication. Nucleophosmin has been identified by pull down experiments from HeLa cells as a binding partner of Nek2 (Yao et al., 2004). Nek2 phosphorylates nucleophosmin *in vitro* and depletion of Nek2 by RNAi caused not only centrosomal segregation defects but a dispersed level of nucleophosmin (Yao et al., 2004). Hence numatrin, could possibly be a novel target of the Nek2 kinase.

1.7.6 Nek2 functions

It has long been established that Nek2 is a major kinase involved in centrosome assembly and separation. Recently, new roles for Nek2 have been postulated in chromosome segregation (Sonn et al., 2004), chromosome condensation (Chen et al., 2002), cytokinesis (Prigent et al., 2005), tubulin polyglutamylation (Westermann and Weber, 2002), spindle checkpoint signalling (Lou et al., 2004b), targeting to the nucleolus (Noguchi et al., 2004), DNA damage response pathways (Fletcher et al., 2004) and mitotic progression (Nek2B) (Fletcher et al., 2005).

The best studied function for Nek2 is in the separation of the two centrosomes at the onset of mitosis. This stage in the centrosome duplication cycle is fundamental in ensuring that the centrosomes separate and take their places at the poles of the mitotic spindle ensuring correct segregation of chromosomes. Overexpression of the active, but not inactive, kinase causes premature centrosome separation probably through the phosphorylation of the centrosomal protein C-Nap1. Nek2 has also been implicated in the DNA damage response pathway as the activity of Nek2 is decreased 50% in response to radiation and Nek2 induced centrosome splitting is reduced after irradiation (Fletcher et al., 2004).

Besides causing centrosome splitting, overexpression of Nek2 also causes the centrosome to disperse. This is not dependent upon kinase activity suggesting that Nek2 plays a structural role in maintaining centrosome integrity. Studies in lower eukaryotes support a role for Nek2 in centrosome assembly and maintenance. *Dictyostelium* Nek2 (DdNek2) shares 54% identity to the catalytic domain of human Nek2 (Graf, 2002). DdNek2 also shares similar structural features containing a leucine zipper that leads to autophosphorylation in its C-terminus. Overexpression of active or inactive GFP-DdNek2 kinase caused 40% of cells to exhibit supernumerary MTOCs, misshapen centrosomes, multiple GFP foci and nuclear size and shape abnormalities (Graf, 2002). Although kinase activity is not required for these abnormalities, they are dependent on the C-terminal domain.

Studies in *Xenopus* egg extracts and embryos provide further evidence of a role for Nek2 in centrosome assembly. Immune depletion of X-Nek2B from egg cytoplasm delayed the conversion of the sperm basal body into a functional centrosome. It also interfered with the recruitment of γ-tubulin to the basal body (Fry et al., 2000a). These defects could be rescued by adding back active or inactive Nek2B (Twomey et al., 2004). In separate experiments, inhibition of Nek2B caused centrosome fragmentation, abnormal spindle formation and abortive cleavage of early embryos (Uto and Sagata, 2000). X-Nek2B is therefore required for both the assembly and maintenance of the centrosome structure in *Xenopus* embryos.

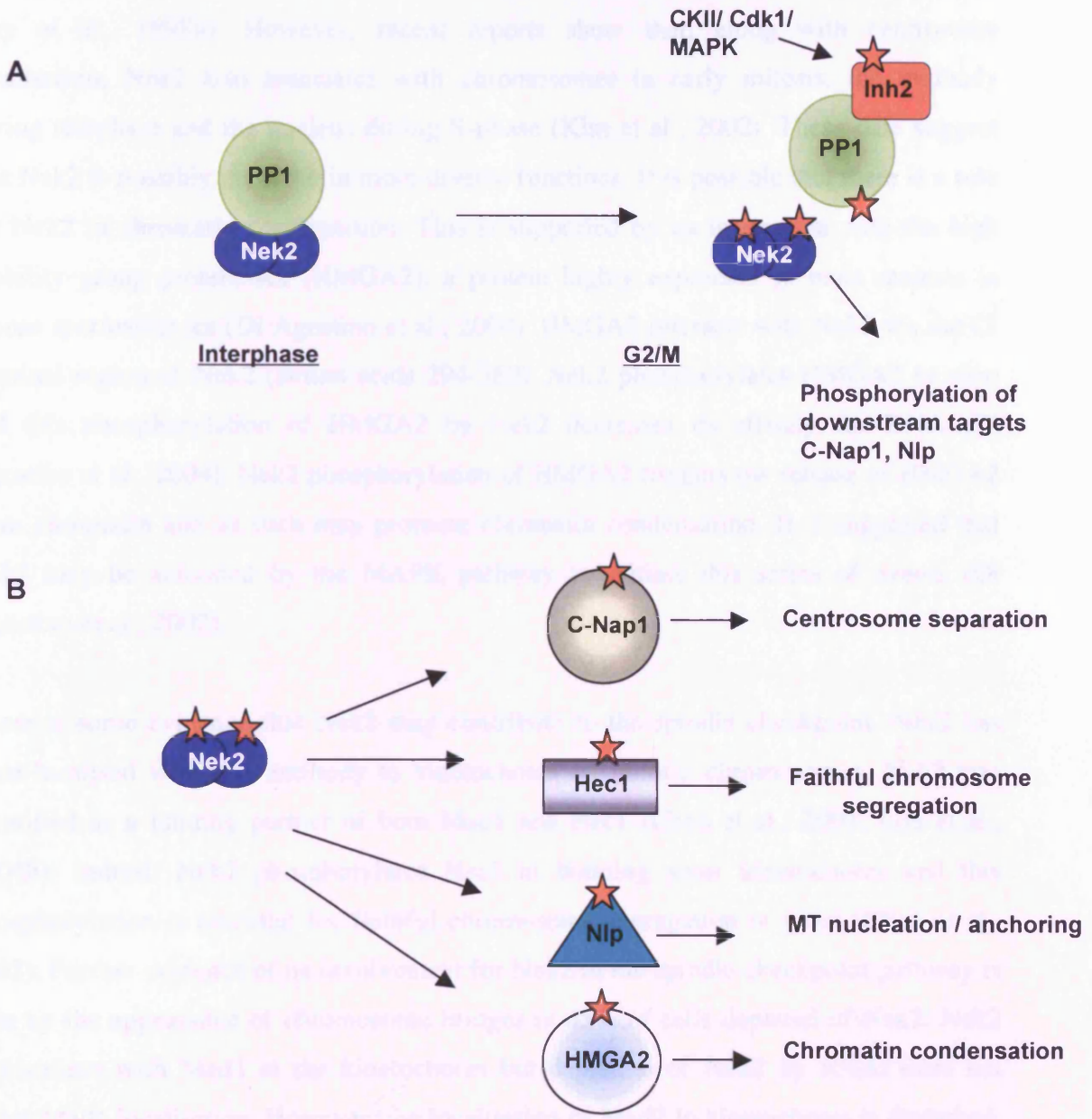

Figure 1.8 Nek2 substrates

A. Nek2 exists in cells as a dimer and is repressed by protein phosphatase one (PP1). At the G2/M transition, Inh2 protein binds and inhibits PP1 allowing Nek2 to become active and target downstream substrates. **B.** Active Nek2 phosphorylates substrates including C-Nap1, Hec1, Nlp and HMGA2 which initiate downstream events in control of the cell and centrosome division cycles. Stars represent phosphorylation.

The role of Nek2 at the centrosome is consistent with its localisation to the centrosome (Fry et al., 1998b). However, recent reports show that, along with centrosome localisation, Nek2 also associates with chromosomes in early mitosis, the midbody during telophase and the nucleus during S-phase (Kim et al., 2002). These data suggest that Nek2 is possibly involved in more diverse functions. It is possible that there is a role for Nek2 in chromatin condensation. This is supported by its interaction with the high mobility group protein A2 (HMGA2), a protein highly expressed in male meiosis in mouse spermatocytes (Di Agostino et al., 2004). HMGA2 interacts with Nek2 via the C-terminal region of Nek2 (amino acids 294-369). Nek2 phosphorylates HMGA2 *in vitro* and this phosphorylation of HMGA2 by Nek2 decreases its affinity for DNA (Di Agostino et al., 2004). Nek2 phosphorylation of HMGA2 triggers the release of HMGA2 from chromatin and as such may promote chromatin condensation. It is suggested that Nek2 may be activated by the MAPK pathway to initiate this series of events (Di Agostino et al., 2002).

There is some evidence that Nek2 may contribute to the spindle checkpoint. Nek2 has been localised with one antibody to kinetochores on mitotic chromosomes. Nek2 was identified as a binding partner of both Mad1 and Hec1 (Chen et al., 2002; Lou et al., 2004b). Indeed, Nek2 phosphorylates Hec1 at budding yeast kinetochores and this phosphorylation is essential for faithful chromosome segregation in yeast (Chen et al., 2002). Further evidence of an involvement for Nek2 in the spindle checkpoint pathway is seen by the appearance of chromosome bridges in 45% of cells depleted of Nek2. Nek2 co-localises with Mad1 at the kinetochores but depletion of Nek2 by RNAi does not affect Mad1 localisation. However, the localisation of Mad2 to kinetochores is disturbed, suggesting Nek2 may be required for the interaction between Mad1 and Mad2 (Lou et al., 2004b). Nek2 may therefore have a direct impact on Mad1 but, it is also possible that Mad2 is a target of Nek2.

A role for Nek2B in mitotic exit has been demonstrated by specific depletion of Nek2B by RNAi. Cells depleted of Nek2B spend significantly longer in mitosis and a higher percentage of these fail to complete cytokinesis (Fletcher et al., 2005). Cleavage furrow

formation and cytokinesis failure has also been observed upon the overexpression of *Drosophilia* Nek2 (Prigent et al., 2005).

1.7.7 Other Nek kinases

Nek1 is structurally related to NIMA with 42% sequence identity within their catalytic domains (Letwin et al., 1992). Nek1 contains the typical kinase motifs as described by Hanks and Hunter but unlike NIMA and all other Nek kinases identified to date the Nek1 kinase was originally claimed to display dual specificity, that is it is capable of phosphorylating tyrosine as well as serine and threonine residues (Hanks and Hunter, 1995). The protein itself is 85.4 kDa in size and its preferred *in vitro* substrates include β-casein, like NIMA and Nek2 (Letwin et al., 1992). Nek1 is expressed highly in testis, which supports a role for Nek1 in spermatogenesis. Mutations of the Nek1 gene also called *kat* mutations lead to male sterility (Upadhya et al., 2000). *Kat* mutations can also lead to polycystic kidney disease and facial dysmorphism suggesting the Nek1 protein may be involved in diverse signalling pathways which when disrupted lead to different abnormalities. A second Nek kinase Nek8, has been implicated in cilia related diseases. Nek8 was identified through a mutation that leads to polycystic kidney disease (Liu et al., 2002). Nek8 shares the highest homology to Nek9 with both sequences containing an RCC1 domain. Expression of kinase-inactive Nek8 in mice leads to multinucleated cells and an abnormal actin cytoskeleton (Liu et al., 2002). The protein is normally located in the apical cytoplasm of collecting duct epithelial cells but the mutated protein localises diffusely throughout the cytoplasm. The function of Nek8 is thought to be involved in regulating the local cytoskeleton structure in kidney tubule epithelial cells (Liu et al., 2002). It has also been shown that Nek8 protein is overexpressed in primary human breast tumours (Bowers and Boylan, 2004).

Nek3 shows 42% identity with NIMA, it is a 56 kDa protein expressed mainly in the cytoplasm with no changes of expression or evidence of post-translational modifications during the cell cycle (Tanaka and Nigg, 1999). Northern blot analysis revealed Nek3 to be preferentially expressed in mitotically active tissue although no function has yet been assigned to this kinase (Chen et al., 1999). Murine Nek4 protein is the direct homologue

to human STK2 protein with 96.5% homology over their kinase domains. The protein, like Nek3, does not contain coiled-coil motifs and mNek4 is abundant in testis (Chen et al., 1999). Human Nek4 (STK4) exists as two forms, a long and a short form, which both contain a nuclear localisation sequence but only the long version of mouse contains this sequence (Hayashi et al., 1999). However, both forms are cytoplasmic throughout the cell cycle and neither show expression or localisation that is cell cycle dependent and as such no function has been assigned to Nek4.

The murine Nek6 and Nek7 kinases were identified along with F196H.1 of *C. elegans* as representing a novel branch of the NIMA kinases (Kandli et al., 2000). These are the shortest of all the Neks and encode little more than a kinase domain. They share 37-40% identity to other mammalian Nek kinases and 87% identity across the kinase domains to one another. They share the characteristic subdomains of protein kinases and are expressed in a complementary manner to one another. Nek6 expression is high in the placenta and intestine whilst expression of Nek7 is low. However, expression of Nek6 is low and expression of Nek7 high in the kidney (Kandli et al., 2000). They both localise to the cytoplasm throughout the cell cycle. Due to their similarity in structure they are thought to perform similar functions.

Initially, Nek6 and Nek7 were isolated as kinases that lay upstream of the $p70^{S6K}$ kinase (Belham et al., 2001). The evidence for phosphorylation of $p70^{S6K}$ by the Nek6 kinase was persuasive as Nek6 could phosphorylate T412 thereby activating the kinase *in vitro* and *in vivo* (Belham et al., 2001). Identification of substrate specific target sites for Nek6 by the Jerini pepSTAR method revealed a requirement for leucine three amino acids upstream of the phosphorylated residue (Lizcano et al., 2002). However, mutation of leucine to alanine in the $p70^{S6K}$ target site abolished phosphorylation by Nek6 *in vitro,* but not *in vivo* suggesting that $p70^{S6K}$ is not a genuine *in vivo* target of Nek6 (Lizcano et al., 2002). More recently, it has been demonstrated that Nek6, along with Nek7 and Nek9, are involved in mitotic progression (Belham et al., 2003; Yin et al., 2003). Nek6 activity is cell cycle regulated with peak activity at the G2/M transition. Overexpression or RNAi depletion of Nek6 results in apoptosis and an accumulation of cells at the G2/M transition

suggesting that Nek6 is required for progression through mitosis (Yin et al., 2003). Similar phenotypes are observed upon inhibition of Nek9 by antibody microinjection (Roig et al., 2002).

Nek9, originally named Nerrc1 and Nek8, was identified as a binding partner of Nek6 (Holland et al., 2002; Roig et al., 2002). The catalytic domain shares 49% identity to NIMA and the C-terminal domain contains RCC1-like repeats, a coiled-coil domain and a putative NLS. However, localisation studies indicate that Nek9 is cytoplasmic (Roig et al., 2002). Nek6 is phosphorylated by Nek9 in mitosis on Ser 206 which is located within the activation loop of Nek6. Mutation of Ser 206 to Ala results in a 98% drop in Nek6 activity and 2D ^{32}P tryptic mapping demonstrates that phosphorylation at Ser 206 is required for further phosphorylation of Nek6 and thus probably activation (Roig et al., 2002). A possible signalling cascade between Nek9 and Nek6/7 may exist to control mitotic progression. Nek9 may also be involved in DNA replication and transcription as Nek9 was found in a 600 kDa complex with FACT (a chromatin specific transcription elongation factor) in the interphase nucleus (Tan and Lee, 2004). This association is cell-cycle dependent and phosphorylation and activation of Nek9 occurs when bound to FACT (Tan and Lee, 2004). As such Nek9, complexed with different partners, may have distinct functions in the cell cycle.

Nek11 may be involved in regulating DNA replication in response to genotoxic stress or DNA damage pathways. Evidence for this is that the kinase activity of Nek11 is increased in response to DNA replication inhibitors. Nek11 exists as a long and short form with a catalytic domain more similar to Nek3 than Nek2 or NIMA. Nek11L mRNA levels increase from S to G2/M. Nek11 is nuclear in interphase and on polar microtubules during prometaphase and metaphase (Noguchi et al., 2002).

MLK3 (mixed lineage kinase 3) shares 22% similarity to the C-terminal domain of NIMA. Only the Nim1 homologue of *Neurosopra crassa* shares more homology to NIMA in this region. MLK3 also contains coiled-coil domains, a leucine zipper, PEST motifs and a CRIB domain. MLK3 is involved in MAP kinase signalling cascades.

However, activity increases at the G2/M transition and, although the kinase is phosphorylated throughout the cell cycle, it is hyperphosphorylated at G2/M (Swenson et al., 2003). A fraction of the protein is located at the centrosome and this localisation is dependent upon microtubules. RNAi depletion of MLK3 increases the stability of microtubules suggesting that MLK3 acts to destabilize microtubules (Swenson et al., 2003). Therefore, it is proposed that MLK3 functions at the centrosome to destabilise microtubules at the onset of mitosis.

1.7.8 Nek2 and cancer

There are numerous target genes which could lead to an abnormal centrosome duplication event. For example, Plk1 and Aurora A are both centrosomal kinases which exhibit elevated expression in a wide range of tumours and cancer cell lines. Altered expression of Nek2 was first shown in human cancer when microarray analysis revealed it to be up-regulated in Ewing tumour derived cell lines (Wai et al., 2002). The Nek2 mRNA also exhibits increased levels in abnormal diffuse large B-cell lymphomas (DLBCL) (Vos et al., 2003). Elevated Nek2 mRNA expression may be a result of gene amplification (Loo et al., 2004, Weiss et al., 2004). However, it may also be the result of uncontrolled transcription.

The E2F4 transcription factor binds p107 and p130 to repress target genes including Nek2. Mutations in p107 or p130 could result in a de-repression in Nek2 transcription (Ren et al., 2002). Nek2 elevation in human breast cancers could also be due to elevation of the FoxM1 transcription factor. FoxM1 expression is elevated in primary human breast cancer and Nek2 is a gene regulated by FoxM1 (Wonsey and Follettie, 2005). Therefore, deregulation of either E2F4 or FoxM1 may provide one mechanism for the altered expression of Nek2 in tumour progression. However, Nek2 is also regulated by post-transcriptional and translational mechanisms and as such the involvement of Nek2 in cancer may be due to the de-regulation of these processes (Hayward and Fry, 2005).

Nek2 protein levels also show a 2-5 fold elevation in cell lines derived from breast, cervical and prostate carcinomas (Hayward and Fry, 2005). Immunohistochemistry

analysis of high-grade invasive ductal carcinomas (IDC) of the breast demonstrated elevated Nek2 expression in 16 out of 20 samples and no elevation in normal tissues (Hayward and Fry, 2005). Whether this increased expression of Nek2 was associated with abnormal centrosomes or abnormal spindle formation is yet to be seen. However, the overexpression of Nek2 in HBL100 non-transformed breast cells does induce aneuploidy (Hayward et al., 2004).

1.8 Structural features of protein kinases

Protein kinase domains are found in 2% of eukaryotic genes. Their function is to transfer the γ-phosphate of ATP to the hydroxyl group of Ser/Thr or Tyr residues. Protein kinases consist of a number of evolutionary conserved sequences (Hanks and Hunter, 1995; Johnson et al., 1996; Krupa et al., 2004; Nolen et al., 2004). The three-dimensional structures of different kinase domains share a high degree of similarity with a number of absolutely conserved residues responsible for the catalytic mechanism of the kinase. In addition there is sequence variation within these conserved regions that confer the substrate specificity of the individual kinases although the catalytic phospho-transfer method remains the same (Figure 1.9). There are twelve sequences which are highly conserved within the kinase domain and within these there are 12 conserved residues found in 95% of kinase sequences (Hanks and Hunter, 1995) (Figure 1.9B). The Nek2 protein contains each of these twelve residues confirming that it is a functional kinase.

There are distinct groups of protein kinases including Ser/Thr, Tyr and His kinases. Here, I will focus upon the structural features of the Ser/Thr kinases. Ser/Thr kinases fall into two categories, those activated by phosphorylation of the activation loop (also called the T-loop) and those activated by other means (Johnson et al., 1996). All those regulated by phosphorylation contain a conserved motif (RD) within their catalytic loop. Nek2 contains these residues at position 140/141 placing Nek2 into the category of kinases that require phosphorylation of their activation loop for activity (Figure 1.9C). PKA was the first kinase shown to be activated by phosphorylation of the activation loop at Thr 197 (Johnson et al., 1996). Since then many protein kinases have been shown to require

activation loop phosphorylation including Pak1 and Plk1 (Banerjee et al., 2002; Lee and Erikson, 1997). Phosphorylation of the activation loop stabilizes it into an open and extended conformation to allow efficient substrate binding (Huse and Kuriyan, 2002). In addition to the RD motif, a residue at the N-terminal end of the activation loop (R/K) is an indicator of the requirement of activation loop phosphorylation (Johnson et al., 1996). Within Nek2 this residue, an arginine is located at position 164. It is therefore safe to assume based upon the structural criteria, that Nek2 is a Ser/Thr protein kinase that requires phosphorylation upon its activation loop for activity (Figure 1.9C). Kinases usually undergo phosphorylation at a primary site within the activation loop but sometimes multiple phosphorylation events may be required to achieve full activity.

The activation loop itself is structured such that it is anchored at its N- and C-terminal ends (Johnson et al., 1996; Nolen et al., 2004). The N-terminal anchor located at the start of the activation loop contains the residues DFG. The Asp serves to chelate a Mg^{2+} ion such that it orientates the phosphate group for phospho-transfer (Hanks and Hunter, 1995 ; Johnson et al., 1996; Nolen et al., 2004) (Figure 1.9). The C-terminal anchor mediates interactions at the binding interface; it hydrogen bonds with a lysine residue and mutation of the anchor seriously disrupts kinase activity (Nolen et al., 2004). Within Cdk2, the C-terminal anchor residue is T165 which interacts with K129 and D127. Based on the relative positions of the N-terminal anchor sequence (DFG) and the end of the activation domain (APE) the corresponding residues within Nek2 are T179, K143 and D141.

The non-catalytic regions of kinases are varied and do not share a conserved structure. The C-terminal domains are probably involved in substrate specificity, targeting and localisation of protein kinases. The C-terminal domain of Nek2 contains a leucine zipper domain for homodimerisation in addition to other coiled coil motifs. It contains the KEN and D-box involved in Nek2A degradation and recently a region has been mapped for targeting of Nek2 to the centrosome (amino acids 335-370). Therefore, protein kinases share conserved features which maintain the catalytic mechanism but their specificity and unique features allow them to target different substrates and perform diverse functions.

A

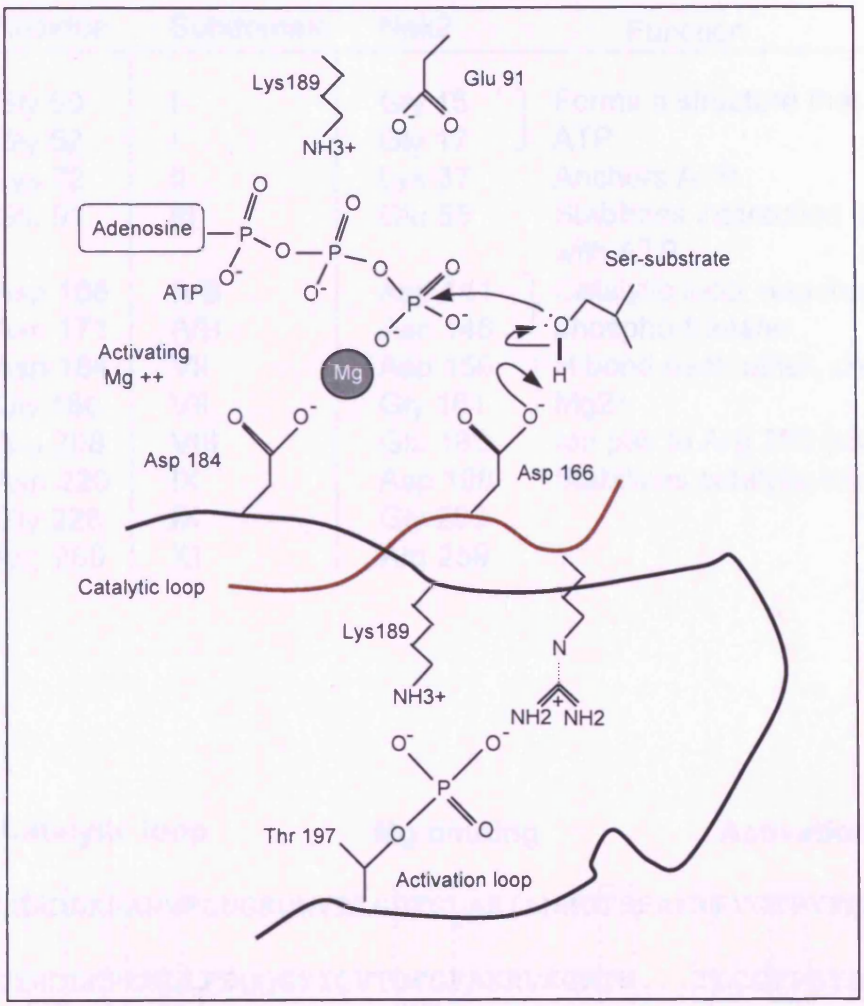
Lys189
Glu 91
NH3+
Adenosine
ATP
Ser-substrate
Activating
Mg ++
Mg
H
Asp 184
Asp 166
Catalytic loop
Lys189
N
NH3+
NH2 NH2
Thr 197
Activation loop

B

Residue	Subdomain	Nek2	Function
Gly 50	I	Gly 15	Forms a structure that anchors
Gly 52	I	Gly 17	ATP
Lys 72	II	Lys 37	Anchors ATP
Glu 91	III	Glu 55	Stabilizes interaction of Lys37 with ATP
Asp 166	IVB	Asp 141	Catalytic loop, required for
Asn 171	IVB	Asn 146	phospho-transfer
Asp 184	VII	Asp 159	H bond each other, chelates
Gly 186	VII	Gly 161	Mg2+
Glu 208	VIII	Glu 186	Ion pair to Arg 280 (stabilizes)
Asp 220	IX	Asp 198	Stabilizes catalytic loop
Gly 225	IX	Gly 203	
Arg 280	XI	Arg 259	

C

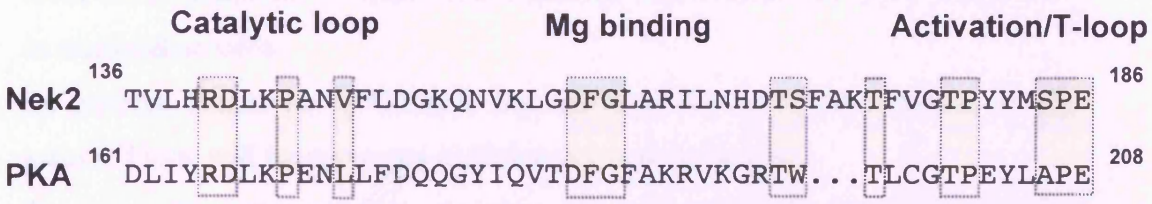

Figure 1.9 Structural comparison of the Nek2 kinase domain to PKA

A. The activation loop of protein kinases based upon the structure of PKA. The catalytic loop is highlighted in red and important residues named. The ATP molecule is positioned such that the phosphate group is transferred to the Ser substrate efficiently. **B.** The table lists essential amino acids required for PKA activity. The subdomains and corresponding residues within the Nek2 kinase are listed alongside. **C.** The amino acid sequence of part of the Nek2 kinase domain. This is aligned with that of PKA to demonstrate the conserved residues which play a major role in kinase activity (square yellow boxes).

1.9 Aims and Objectives

Nek2 is a cell cycle-regulated protein kinase that localises to the centrosome. C-Nap1, PP1, Hec1, Nlp and Nek2 have all been identified as Nek2 substrates. However, only a very few Nek2 substrate phosphorylation sites have been identified using *in vitro* phosphorylation approaches. Thus the function of Nek2 phosphorylation upon these proteins remains obscure. Moreover, the consensus sites where Nek2 phosphorylation takes place are yet to be identified. Early work on the Nek2 kinase with a series of peptides suggested a requirement for basic residues N- and C-terminal to the phosphorylation site. Identifying a consensus site of substrate recognition would be highly advantageous in identifying other potential substrates of Nek2. The aim of this project is to use a combination of biological approaches to identify phosphorylation sites for Nek2 within Nek2 itself, C-Nap1 and Nlp. The role of these proteins and their regulation by Nek2 will also be investigated.

Experimental objectives

A. To generate purified human and *Xenopus* Nek2 kinases for *in vitro* phosphorylation studies. These will be isolated from expression in insect cells from recombinant baculovirus, from expression in bacteria and from transfection in mammalian cells.
B. To generate fragments of C-Nap1, Nlp and Nek2 for use as substrates in kinase assays. These will be expressed as fusion proteins in bacteria.
C. To assess the kinase activity *in vitro* and *vivo* of Nek2 constructs carrying mutations that alter its phosphorylation state.
D. To establish techniques through collaboration for phosphosite identification.
E. To perform functional analysis of phosphosites identified by a mutational approach.

Chapter Two

Materials and methods

2.1 Materials

2.1.1 Chemical suppliers

All reagents and chemicals were purchased from Sigma (Poole, UK) or Roche (Lewes, UK) apart from those indicated in the table below.

Reagent	Supplier
DNA nucleotides dATP, dGTP, dCTP, dTTP Glutathione Sepharose™	Amersham Pharmacia Biotech (Bucks, UK)
Maltose monohydrate	BDH (Poole UK)
Poly-prep columns Protein A Beads	Bio-Rad (Herts, UK)
Super RX X-Ray film	Fuji photo film Ltd (Germany)
Acetic acid glacial Sodium Chloride EDTA EGTA NaH_2PO_4	Fischer Scientific (Loughborough, UK)
Protogel	Flowgen (Ashby de-la Zouch, UK)
Bovine Serum Albumin	Fluka Biochemika (Gillingham, UK)
Dulbeccos-MEM Feotal Calf Serum (FCS) Opti-MEM TC100 Gene Tailor™ Site Directed mutagenesis system DH5α-T1 max efficiency bacteria Lipofectamine 2000 LR clonase BP clonase	Invitrogen (Paisley, UK)

Ethidium Bromide solution	
DNA ladder 100 bp DNA ladder 1 kb Restriction endonucleases Amylose resin	New England Biolabs (Herts, UK)
Agar Yeast Extract Tryptone	Oxoid (Basingstoke, UK)
Slide-A-Lyzer Dialysis Cassettes	Pierce (Rockford, USA)
TnT T7 Quick Coupled Transcription/Translation kit T4 DNA ligase	Promega (Southampton, UK)
QIA Filter Plasmid Maxi Kit QIA Filter Plasmid Miniprep Kit QIAquick PCR purification kit QIAquick gel extraction kit	Qiagen (Sussex UK)
Nitrocellulose Transfer membrane	Schleicher and Schuell (Dassel, Germany)
Oligonucleotides	Thermohybaid (Egelsbach, Germany)

2.1.2 Radioisotopes

Isotope	**Specific Activity**	**Supplier**
^{32}P-γ-[ATP]	167 Tbq/mmol	ICN
[^{35}S] methionine	43.5 Tbq/mmol	NEN Life Science products

2.1.3 Vectors and constructs

Vector	Application	Supplier
pET32	Bacterial protein expression	Novagen
pMAL-p2X	Bacterial protein expression	New England Biolabs
pRcCMV-Myc-Nek2A	Eukaryotic protein expression	Fry *et al.*, 1998a
pGEX-4T-1	Bacterial protein expression	Phamacia
pGEX-6P2-Nlp-NTD	Bacterial protein expression	Casenghi *et al.*, 2003
pGEM-Nek2	In vitro translation (T7)	Fry et al., 1998a
GST-PBD	Far Western Blotting	Gift from Dr. F. Barr
PP1α (P94)	Bacterial expression	Gift from Dr. F. Barr
PP1γ cDNA (bluescript)	Bacterial expression	Gift from Prof. P. Cohen
Inhibitor-2 cDNA (bluescript)	Bacterial expression	Gift from Prof. P. Cohen
His-Plk1-210D	Kinase	Gift from Prof. E.Nigg
His-Plk1-	Kinase	Gift from Prof. E.Nigg
pEGFP-C1-Aurora2K162R (RHO13)	Eukaryotic protein expression	Gift from Prof. E.Nigg
pEGFP-C1-Aurora2 (RHO10)	Eukaryotic protein expression	Gift from Prof. E.Nigg

2.1.4 Antibodies

Primary Antibodies	Working Conc. / dilution	Application	Supplier
Anti-C-Nap1 polyclonal	1 μg/ml	Immunofluorescence	Fry et al., 1998a
Anti-GFP polyclonal	0.1 μg/ml	Immunofluorescence	Abcam
Anti-Myc monoclonal	1/1000	Immunoprecipitation Western Blotting Immunofluorescence	Cell signalling technology

Anti-GST polyclonal	1/1000 (2 μg/ml)	Western Blotting Immunoprecipitaion	Santa Cruz
Nek2 R671 polyclonal	1/200 (1 μg/ml)	Wesern blotting	Fry lab
Nek2 (human) monoclonal	1.0 μg/ml	Immunofluoresence Immunoprecipitation Western Blotting	Transduction Laboratories
Anti-Nlp (human) polyclonal	1.0 μg/ml	Western Blotting Immunofluorescence	Casenghi et al., 2003
Anti-γ-tubulin monoclonal	1/2000 (6.5 μg/ml)	Immunofluorescence	Sigma
Anti-α-tubulin monoclonal	1/2000	Immunofluorescence	Sigma
Hoechst 33258	1/8000 (0.1μg/ml)	Immunofluorescence	Calbiochem

Secondary Antibodies	**Working Concentration**	**Application**	**Supplier**
Anti-mouse alkaline phosphatase conjugate	1/7500 (0.1 μg/ml)	Western Blot	Promega
Anti-rabbit alkaline phosphatase conjugate	1/7500 (0.1 μg/ml)	Western Blot	Promega
Anti-rabbit Alexa 488 nm Goat	1/200 (10 μg/ml)	Immunofluorescence	Invitrogen
Anti-rabbit Alexa 594 nm Goat	1/200 (10 μg/ml)	Immunofluorescence	Invitrogen
Anti-mouse Alexa 488 nm Goat	1/200 (10 μg/ml)	Immunofluorescence	Invitrogen
Anti-mouse Alexa 594 nm Goat	1/200 (10 μg/ml)	Immunofluorescence	Invitrogen

2.1.5 Bacterial strains

Strain	Supplier
DH5α-library efficient competent cells	Invitrogen
DH5α-T1 competent cells max efficiency	Invitrogen
One shot BL21 star (DE3) chemically competent *E. coli*	Invitrogen
Rosetta (DE3) *E. coli*	Invitrogen

2.1.6 Buffers and solutions

Buffer	Composition
3 x Laemmli	62.5 mM Tris-HCl pH 6.8, 2% (w/v) SDS, 5% (v/v) β-mercaptoethanol, 10% (v/v) glycerol, 0.01% (v/v) bromophenol blue
10 x PBS	137 mM NaCl, 26.8 mM KCl, 2.7 mM Na_2HPO_4, 1.4 mM KH_2PO_4
TBE	89 mM Tris, 89 mM boric acid, 1 mM EDTA pH 8.0
TE	10 mM Tris pH 8.0, 1 mM EDTA
Transfer Buffer	25 mM Tris, 192 mM Glycine, 10% (v/v) methanol (optional)
Alkaline Phosphatase	100 mM NaCl, 5 mM $MgCl_2$, 100 mM Tris-HCl pH 9.5
BCIP	50 mg/ml in DMF
NBT	50 mg/ml in 70% (v/v) DMF
Kinase Assay	50 mM Hepes KOH pH 7.4, 5 mM $MnCl_2$, 5 mM β-glycerophosphate, 5 mM NaF, 4 μM ATP, 1 mM DTT, 10 μCi $-\gamma-^{32}P$ [ATP], d H_2O

2.2 Molecular biological techniques

2.2.1 Growth and maintenance of bacterial strains

One colony of bacteria was selected and streaked for growth on Luria Bertani (LB) agar plates (NaCl 10 g/l, tryptone 10 g/l, yeast extract 5 g/l and agar at 2% (w/v) adjusted to pH 7.0 and autoclaved) and grown at 37°C overnight (O/N). For O/N cultures in liquid media, one colony was selected and grown in 5 ml of LB omitting the agar at 37°C in a shaking incubator. Bacterial stocks were prepared from 200 µl of the O/N culture mixed with 800 µl sterile glycerol and stored at -80°C. Selective media was prepared where appropriate by the addition of antibiotic (ampicillin 100 µg/ml, chloramphenical 34 µg/ml, kanamycin 50 µg/ml, tetracycline 12.5 µg/ml).

2.2.2 Transformation of competent bacteria

Competent cells were defrosted on ice and 200 µl added to 100 ng of ice cold DNA. The slurry was mixed by gentle tapping and stored under ice for 10 min. The sample was then heat shocked at 42°C for 45 secs and returned to ice for 1 min. 200 µl of LB was added to the sample and the sample incubated at 37°C for 45 min in a shaking incubator. 200 µl of the sample was directly spread on an agar plate containing the appropriate antibiotic for selection and incubated O/N at 37°C.

2.2.3 Plasmid preparation (small scale)

One bacterial colony was selected and grown O/N in 5 ml of LB containing the appropriate antibiotic in a shaking incubator. The culture was spun down at 2000 rpm for 10 mins and the supernatant aspirated. The pellet was then subjected to the Qiagen Mini Prep Spin Kit for plasmid isolation. Typically, the plasmid was eluted into 50 µl of distilled purified sterilised water yielding between 5-10 ng of DNA.

2.2.4 Plasmid preparation (large scale)

One bacterial colony was selected and grown for 8 hours in 5 ml LB containing the appropriate antibiotic. 2 ml of the starter culture was diluted into 100 ml of LB containing the appropriate antibiotic and grown in a shaking incubator at 37°C O/N. The culture was

then spun down at 6000 g for 20 min at 4°C and the supernatant removed. The remaining pellet was subjected to the Qiagen Maxi Prep Kit for plasmid isolation. Typically, the plasmid was resuspended in 500 µl of distilled purified sterilised water and diluted to a concentration of 1 mg/ml.

2.2.5 Quantification of DNA concentration

DNA concentrations were measured either by comparison to known DNA concentrations on a DNA agarose gel or by UV light at OD_{260}. Concentration determination was calculated by the following calculation,

$$A_{260} \text{ x Dilution factor x } 40 = \text{DNA concentration } (\mu g/ml)$$

2.2.6 Restriction digestion

Restriction digestion of plasmid DNA was performed using 10 units (U) restriction endonuclease to approximately 5 µg DNA. The appropriate 10 x buffer according to the manufacturer's instructions and appropriate amount of water were added. The reaction was incubated from 2 to 5 hours. Double digestions were performed by the addition of a second enzyme to the reaction or a separate experiment performed after removal of the first enzyme using the DNA nucleotide removal kit (Qiagen).

2.2.7 DNA gel electrophoresis

DNA was analysed on 1% agarose gels. 0.5 g of agarose powder was added to 50 mls 1 x TBE in a conical flask. The mixture was heated for 45 seconds at full power and allowed to cool. Following a brief cooling period 0.5 µl of ethidium bromide was added and the mixture poured into a pre-made gel tank. The gel was allowed to set for 20 mins before removal of a comb which creates the loading wells. DNA samples were mixed with DNA loading dye (50% (v/v) glycerol, 0.1 M EDTA, 0.3% (w/v) bromophenol blue) at a ratio of 5:1 before loading on the gel. 2 µl of either 1 Kb or 100 bp markers were added to a separate well and the gel was run at 80 V for 45 minutes.

2.2.8 Isolation of DNA from agarose gels

DNA was purified from agarose gels by placing the gel upon a UV transilluminator and removing the DNA band using a scalpel. The excised band was placed into an eppendorf tube and the weight determined. The Gel Extraction Kit (Qiagen) was used to isolate the DNA and the DNA eluted into 20 µl of sterilised water.

2.2.9 DNA Ligation

Ligation of purified DNA fragments was carried out using 1 µl T4-ligase, 10 x ligase buffer and water. The restricted DNA was added at ratios of 1:1, 1:3, 1:5 vector:insert. The mixture was mixed and left on ice O/N.

2.2.10 DNA sequencing

DNA samples were sent at 10 μM to Lark Technologies (Takely, Essex UK) for sequencing. The appropriate oligonucleotide primer was also sent with the DNA to be sequenced. Sequencing data was analysed using Gene Jockey computer software.

2.2.11 Oligonucleotide design

Oligonucleotides designed for PCR-based cloning were between 20-25 bp in length with a GC:AT ratio of 50% to ensure an annealing temperature of 55-60°C. Additional bases were added to the 5' ends of oligonucleotides to incorporate restriction digest sequences. Additional base pairs were also added when required to ensure the reading frame was in line with that of the vector. Oligonucleotides for site directed mutagenesis were approximately 30 bp in length and contained the various features outlined below:

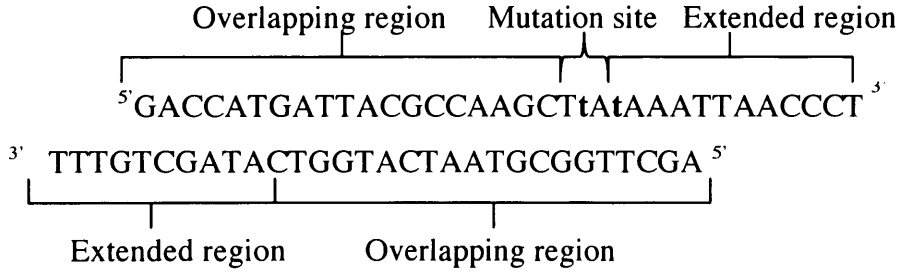

Oligonucleotides were synthesised by Thermohybaid (Germany) and upon arrival diluted in the stated volume of water to a concentration of 100 μM. A working solution was then made at 20 μM.

2.2.12 Site-directed mutagenesis

Site-directed mutagenesis was performed using the Invitrogen Gene Tailor™ Site-directed mutagenesis system. 100 ng of target plasmid was methylated by incubation with 1.6 μl methylation buffer, 1.6 μl 10 x SAM, 4 U/μl DNA methylase, 16 μl water for 1 hour at 37°C. The methylated plasmid was then PCR amplified using 10 μM of forward/reverse primers, 10 mM dNTPs, 12 ng methylated plasmid, 10 x expand buffer and 2.5 U of Expand enzyme to 50 μl with dH_2O. The PCR mix was thermocycled at the following temperatures, 94°C (2 mins) for 1 cycle, 94°C (30 secs), 60°C (30 secs), 68°C (1 min/kb) for 25 cycles and 68°C for 10 minutes for 1 cycle. The reaction was maintained at 4°C until transformation into DH5α-T1 cells. Transformants were selected, grown up and plasmids prepared by QIAgen miniprep kits for analysis by DNA sequencing.

2.2.13 Polymerase chain reaction (PCR)

Each reaction consisted of 0.1-1 μg DNA or bacterial colony, 1 mM of each primer, 10 x reaction buffer, 0.4 mM dNTPs, 1 U of Expand high fidelity Taq polymerase and water to a final volume of 50 μl. Generally, the PCR cycle was as follows:

Cycles	Time (secs)	Temperature (°C)
1	30	94
25	30 30 60 (per kb)	94 55 68
1	600	68
1	∞	4

2.3 Protein techniques

2.3.1 SDS-PAGE gel production

SDS-PAGE protein gels were prepared with varying levels of acrylamide dependent on the protein size to be analysed. The different recipes for these percentages are as follows:

Separating gel	5%	10%	12%	15%
Protogel (acrylamide)	1.0 ml	2.0 ml	2.4 ml	3.0 ml
Water	3.5 ml	2.5 ml	2.1 ml	1.5 ml
Lower Tris (1.5 M Tris pH 8.8, 0.4% SDS)	1.5 ml	1.5 ml	1.5 ml	1.5 ml
10 % Ammonium Persulphate	75 μl	75 μl	75 μl	75 μl
TEMED	5 μl	5 μl	5 μl	5 μl
Protein size for analysis (kDa)	120-250	40-100	20-70	15-40

Gel casting apparatus provided by Biorad was assembled and 3.5 ml of separating gel was added. 100 μl of water-saturated butanol was pipetted onto the surface of the solution to ensure even setting. The gel was allowed to set, the butanol removed and 2 ml of resolving gel pipetted over the separating gel (0.65 ml Protogel, 3 ml water, 1.25 ml upper Tris (0.5 M Tris pH 6.8, 0.4% SDS), 75 μl 10% (w/v) ammonium persulphate, 5 μl TEMED). A teflon comb to create the loading wells was inserted and removed after the gel was set. Samples were boiled with 5 x or 3 x Laemmli sample buffer for 2-10 mins and the appropriate quantity loaded into the wells. Sigma Dalton marker proteins were added to one well for indication of protein size. Wells were filled and the gel submerged in running buffer (0.1% SDS (w/v), 0.3% Tris (w/v), 1.44% Glycine (w/v)). Proteins were separated by the application of 180 V for 45 mins.

2.3.2 Analysis of SDS-PAGE gels

The separating gel was removed from the apparatus and the resolving gel discarded. The gel was soaked in Coomassie Brilliant Blue (0.25% (w/v) Coomassie Brilliant Blue, 40% (v/v) IMS, 10% (v/v) acetic acid) for 10-20 mins followed by washing in destain (25% (v/v) IMS, 7.5% (v/v) acetic acid) until proteins were visible and background reduced.

Gels were dried onto 3MM Whatmann paper under vacuum at 80°C for storage. For analysis of radioactive gels the dried gel is placed into a cassette and exposed to X-ray film for the appropriate time period.

2.3.3 Western Blotting

SDS-PAGE gels were soaked in Western blotting buffer (25 mM Tris, 192 mM glycine, 10% (v/v) methanol) for 5 mins, as were nitrocellulose transfer membrane (Schleiser and Schuell) and Whatmann 3MM chromatography paper cut to 10 cm by 7cm. The gel was placed on the membrane sandwiched between filter paper and placed in the Hoeffe Semi-phor blotting apparatus at 70 mAmps for 1 hour. The blotting paper was removed and stained with Ponceau red solution in order to visualise markers and lanes which were marked with a pencil. The membrane was blocked in 1 x PBS / 1% (v/v) Tween-20 and 5% (w/v) Marvel for 30 mins gently shaking. 1° antibody was added to 3 mls blocking solution and incubated on a roller for 1 hour. The membrane was washed 3-6 times for 30 mins in washing buffer (1 x PBS, 1% (v/v) Tween-20) followed by incubation for 1 hr in alkaline phosphate conjugated 2° antibody in 3 mls blocking solution. The membrane was washed and developed in AP buffer (100 mM NaCl, 5 mM $MgCl_2$, 100 mM Tris-HCl pH 9.5 containing 33% (v/v) NBT (50 mg/ml in DMF) and 66% (v/v) BCIP (50 mg/ml in DMF)).

2.3.4 Far-Western blotting

Proteins were transferred to the nitrocellulose as indicated above. The membrane was incubated with 1 μg/ml GST-Polo box domain (amino acids 300-603) in 3 mls blocking solution O/N at 4°C. The nitrocellulose membrane was washed in washing buffer 3-6 times for 30 mins. The membrane was subsequently analysed using standard Western blotting procedures using the anti-GST 1° antibody as described in 2.3.3.

2.3.5 *In vitro* translation (IVT)

1 μg of a plasmid DNA, 1 μl of ^{35}S-methionine or unlabelled methionine was added to 8 μl of T7 Quickmix (Promega) and incubated at 30°C for 1.5 hours. 1 μl of reaction mix was added to 9 μl of sample buffer for analysis on an SDS-PAGE gel.

2.3.6 *In vitro* pull-down assays

In vitro protein-protein interactions were tested using purified tagged protein constructs and proteins generated by IVT. 100 µl of glutathione beads were washed three times with 1 x PBS. The beads were split and to each half 1 mg of either GST or GST-PP1 purified protein was added. Protein was allowed to bind for 1 hour rotating at 4°C. Beads were subsequently washed in NETN buffer (1 mM EDTA pH 8, 20 mM Tris HCl pH 8, 100mM NaCl, 0.5% (v/v) Nonidet) three times. 18 µl of protein translated *in vitro* (see 2.3.5) was added to either GST-PP1 or GST bound beads and allowed to bind for 2 hours rotating at 4°C. Beads were washed three times in NETN buffer followed by re-suspension in 20 µl SDS sample buffer. Binding was determined by SDS-PAGE, autoradiography and detection by X-ray film.

2.3.7 Immunoprecipitation

Immunoprecipitations were performed using either protein G sepharose beads for use with monoclonal antibodies or protein A beads for use with polyclonal antibodies. 50 µl of beads were washed with 1 x PBS three times to remove excess storage buffer. 10 µl of IVT mix or 20 µl of cell lysate was added to 490 µl NEB buffer (NEB: 50 mM HEPES-KOH, pH 7.4, 5 mM $MnCl_2$, 10 mM $MgCl_2$, 5 mM EGTA, 2 mM EDTA, 100 mM NaCl, 5 mM KCl, 0.1% (v/v) Nonidet P-40, 30 µg/ml Rnase A, 30 µg/ml Dnase I, 10 µg/ml leupeptin, 10 µg/ml bestatin, 10 µg/ml pepstatin, 1 mM PMSF, 20 mM β-glycerophosphate and 20 mM NaF) and 10 µl of beads and rotated at 4°C for 30 minutes to pre-clear the sample. The supernatant was taken and incubated under ice with appropriate antibody for 1 hour (for myc-Nek2A constructs the anti-myc antibody was commonly used). The remaining beads were blocked with rabbit reticulocyte lysate or a control cell extract by rotating at 4°C for 45 minutes followed by washing in NEB buffer 3 times and re-suspending in 50 µl of NEB buffer. 40 µl of the blocked bead slurry was taken and added to the antibody/protein mix and rotated at 4°C for 1 hour followed by three washes of the beads in NEB buffer. Beads were then stored at -80°C or used immediately in a kinase assay after washing two times in kinase buffer.

2.4 Protein expression and purification

2.4.1 Expression of protein in bacteria

DNA fragments were cloned into suitable protein expression vectors and transformed into *E. coli* (Rosetta DE3, BL21). A single colony was selected and a starter culture of 20 ml LB containing the appropriate antibiotic was grown O/N shaking at 37°C. The starter culture was diluted into 1 litre of pre-warmed LB and grown at 30°C until the OD_{600} reached 0.2 (typically 45 mins). IPTG was added to a final concentration of 1 mM to induce protein expression. Cultures expressing Nlp constructs were grown for a further 12 hours O/N at room temperature; all other protein constructs were grown for a further 5 hours at 30°C shaking.

2.4.2 Purification of GST-Nlp fusion proteins

Bacterial cultures were spun at 6000 G for 20 mins and the supernatant discarded. The pellet from a 1 litre culture was re-suspended in 20 ml lysis buffer (50 mM NaH_2PO_4 pH 8.0, 300 mM NaCl, 1 mg/ml lysozyme), incubated on ice for 10 mins followed by crushing using a French press. Lysed bacteria was centrifuged at 10,000 G for 45 mins at 4°C. The supernatant (soluble fraction) was stored at -80°C or immediately mixed with 2 mls of pre-washed glutathione-Sepharose beads (Amersham) washed in 1 x PBS three times) and rotated at 4°C for 2 hours in a 50 ml universal tube. The insoluble pellet was discarded.

The supernatant bead slurry was centrifuged at 2000 rpm for 30 secs and the supernatant discarded (unbound protein fraction). Beads were washed with 3 ml of wash buffer (20 mM Tris HCl pH 7.5, 100 mM NaCl) 3 times by rotation in wash buffer for 5 minutes followed by centrifugation and removal of the supernatant. 20 µl samples of supernatant were collected at all stages for analysis by SDS-PAGE. The protein was eluted by rotation in 2 mls elution buffer (20 mM Tris HCl pH 7.5, 100 mM NaCl, 20 mM Glutathione) for 45 minutes followed by collection of the supernatant by centrifugation at 2000 rpm for 2 minutes. This was repeated five times to gain a total of 10 mls eluted protein. The elutions were analysed by SDS-PAGE and the most concentrated elution

dialysed against 50 mM Hepes pH 7.4, overnight using Slide-A-Lyzer® Dialysis Cassette 10,000 MWCO (Pierce).

2.4.3 Purification of MBP, His, and GST tagged fusion proteins

Bacterial cultures were spun at 6000 g for 20 mins and the supernatant discarded. The pellet from a 1 litre culture was re-suspended in 20 ml lysis buffer (50 mM NaH_2PO_4 pH 8.0, 300 mM NaCl (for His tagged proteins add 10 mM imidazole)) on ice. Typically the pellet from a 1 litre culture was resuspended in 100 ml lysis buffer containing 1 mg/ml lysozyme. The sample was incubated on ice for 30 minutes before sonication on ice (MSE Soniprep 150, 10 mm probe, amplitude 12 μm) with six 10 second bursts at 200-300 W with a 10 second cooling period between bursts. The sample was then centrifuged at 11,000 rpm for 45 minutes at 4°C to remove cell debris. Supernatant was stored at minus 80°C as soluble protein. Purification was achieved using either 1 ml of Ni-NTA beads (His), amylose beads (MBP) or glutathione beads (GST) to 4 ml cleared lysate. Two column volumes of wash buffer (20 mM Tris HCl pH 7.5, 100 mM NaCl (for His tagged proteins add 20mM Imidazole)) was passed through the column followed by four 1 ml volumes of elution buffer consisting of wash buffer containing either, 250 mM imidazole (His) 15 mM maltose (MBP) or 20 mM reduced glutathione (GST) to elute the protein. 5 μl samples were taken throughout the procedure for SDS-PAGE analysis to determine protein elution solubility and purity. The most concentrated elution was dialysed against 50 mM Hepes pH 7.4. overnight using Slide-A-Lyzer® Dialysis Cassette 10,000 MWCO (Pierce).

2.4.4 Quantification of protein concentration

Protein concentration was determined by SDS-PAGE analysis against known quantities of BSA. Alternatively, by Bicinchoninic acid (BCA) assay following the manufacturer's instructions (Pierce). Protein concentrations were estimated from a standard curve of BSA concentrations.

2.5 Cell biology techniques

2.5.1 Maintenance and storage of human cell lines

HeLa and U2OS cells were grown in DMEM containing 10% (v/v) FCS and 1% (v/v) penicillin-streptamycin. Cells were grown to approximately 80% confluency, split and re-plated in new media. Long-term storage of human cells was achieved by freezing in liquid nitrogen. Cells were grown to 90-95% confluency, lifted from the plate and spun down at 2000 rpm for 5 minutes. The supernatant was removed and cells washed with 1 X PBS before a second spin at 2000 rpm for 5 minutes. Cells were re-suspended in DMEM containing 10% (v/v) DMSO and 20% (v/v) FCS and transferred to a cryo-tube. Cells were slowly frozen first at -20°C O/N then at -80°C O/N and finally into liquid nitrogen.

2.5.2 Maintenance and storage of insect cell lines

Sf9 cells were grown in TC100 media containing 10 FCS and 1% (v/v) penicillin-streptomycin at 27°C and split when reaching 80% confluency. Cell splitting required removal of all media from the flask, cells were removed by washing the surface with fresh media followed by transfer to 2 new flasks. Cells for long-term storage were prepared as in section 2.5.1 with the exception of using TC100 media instead of DMEM as the freezing media.

2.5.3 Transfection of human cells

Transfections were carried out using the Lipofectamine plus reagent (Invitrogen). Cells were plated on 10 cm or 6 cm dishes to reach 80% confluency on the day of transfection. 5 μg (10 cm plate) or 2 μg (6 cm plate) of plasmid DNA was added dropwise to the lipofectamine reagent in 500 μl or 250 μl OPTI-MEM, and left at room temperature for 20 mins. Cells were re-plated in OPTI-MEM media with no serum added (4 mls for a 10 cm dish and 2 mls for a 6 cm dish) the lipofectamine/DNA mix was added directly to each plate. The media was replaced with D-MEM containing 10% (v/v) FCS and 1% (v/v) penicillin streptomycin, 5 hrs post transfection and cells either lysed or fixed at 24 hrs post transfection.

2.5.4 Preparation of cell extracts

HeLa cells were washed once with 1 x PBS followed by incubation at 37°C for 5 min in 4 mls of 1 x PBS 0.5 mM EDTA. Resuspended HeLa cells were pipetted into a sterile falcon tube and centrifuged at 4000 rpm for 5 minutes. The supernatant was removed and the pellet resuspended in approximately 100 µl of NEB lysis buffer per 3 cm area of cell growth and stored under ice for 30 minutes. Lysates were passed through a 27 G needle 10 times. Lysates were centrifuged at 13000 rpm for 10 minutes at 4°C and the supernatants transferred to an eppendorf and stored at -80°C until required. The same procedure was used to prepare extract from Sf9 insect cell, except cells were harvested direct from 20 cm flasks and centrifuged at 2500 rpm for 5 minutes. The cell pellet was washed with 1 ml ice cold 1 x PBS, 1 mM PMSF and cells transferred to an eppendorf tube. Lysates were centrifuged at 1,500 rpm for 5 minutes at 4°C and the supernatant resuspended in Neb buffer containing 1 µM okadaic acid and 100 mM sodium orthovanadate.

2.5.5 Infection and maintenance of baculoviruses

TC100 media supernatants containing recombinant baculovirus were stored at 4°C protected from light and stocks retained in liquid nitrogen. 1 ml of baculovirus supernatant was used to infect a 25 cm^3 flask containing 90% confluent Sf9 cells. For amplication of the virus titre, the infected cells were allowed to grow for a further 5 days at 27°C. The supernatant was collected as a fresh viral stock. For collection and purification of proteins, infected cells were maintained at 27°C for three days and the cells collected by centrifugation at 4000 rpm for 5 minutes. Lysis of infected insect cells was carried out as in 2.5.4.

2.5.6 Microtubule depolymerisation / re-growth

Microtubule depolymerisation was achieved by placing cell culture dishes on ice for 30-45 mins. Regrowth was achieved by the addition of 37°C media to the dishes for approximately 30 seconds.

2.6 Immunofluorescence microscopy

For all microscopy experiments, HeLa or U2OS cells were plated into 6 well dishes containing glass coverslips and transfected as described in section 2.5.3. 24 or 48 hours post transfection, all media was removed from the wells and approximately 2 mls -20°C methanol added to each well and the coverslips stored at -20°C for a minimum period of 30 minutes. Coverslips were subsequently washed in 1 x PBS three times for 5 minute periods to re-hydrate the cells. Coverslips were blocked by the addition of 1.5 mls of 1% (w/v) BSA in 1 x PBS solution for 10 minutes at room temperature followed by washing in 1 x PBS as previously described. 100 µl of primary antibody solution containing the appropriate 1° antibodies (see 2.1.4) in 3% (w/v) BSA in 1 x PBS was incubated with the cover slip in a humid environment for 45 mins. Coverslips were washed three times in 1 x PBS. The appropriate 2° antibodies were diluted into 100 µl of 3% (w/v) BSA, 1 x PBS and incubated with the coverslip in a humid environment for 45 mins followed by washing three times with 1 x PBS. Finally, 2 mls of Hoechst 33258 solution at 1/10000 in 1 x PBS was added to each coverslip for two minutes followed by three 5 minute washes in 1 x PBS. The coverslips were mounted onto glass slides using 7.5 µl of 80% (v/v) glycerol, 3% (w/v) n-propylgallate solution and sealed using nail varnish. Slides were viewed using a 100 x oil objective on a Nikon TE300 immunofluorescence microscope using the Openlab (Improvision) imaging package.

2.7 Antibody generation and purification

2.7.1 Phosphospecific antibody generation

A synthetic phosphorylated peptide DTSFAKpTFVGTPYYMSPEQMNR representing the activation loop amino acids 169-190 of human Nek2 was synthesized by Millennium Pharmaceuticals and used to immunise two rabbits. The reactivity of test bleeds against both the endogenous Nek2 protein and overexpressed myc-Nek2A was determined by Western blotting and immunofluorescence microscopy.

2.7.2 Preparation of affinity purification columns

0.2 g of CH Sepharose was swelled in 15 mls 1 mM HCl for 15 mins in a column (Bio-Rad) and the excess liquid allowed to elute. The column was then washed in 4 ml of coupling buffer (0.1 M $NaHCO_3$, 0.5 M NaCl, pH 8.0). Peptides were dissolved in coupling buffer to approximately 2 mg/ml added to the column and allowed to rotate at room temperature for 4 hours. The flow through was collected and the column blocked with blocking buffer (0.1 M Tris/HCl pH 8.0 for 1 hr end over end) followed by washing with 10 column volumes of wash buffer 1 (50 mM Tris/HCl pH 8.0, 0.5 M NaCl) followed by 10 column volumes in wash buffer 2 (50 mM acetic acid, 0.5 M NaCl) to remove any excess ligand. This was repeated five times. The column was equilibrated with 20% (v/v) EtOH and stored at 4 °C. Two columns were prepared, one with the phosphorylated-peptide (phospho column) and a second with a non phosphorylated version of the same peptide (non-phospho column).

2.7.3 Affinity-purification of Nek2 phosphospecific antibodies

The phospho column was washed in two column volumes of wash buffer 1 followed by two column volumes of 50 mM Tris HCl pH 7.5. If used previously then the column was washed in 1% (w/v) SDS followed by ten column volumes of the wash buffer 1. 2 mls of antibody serum was added to 2 mls of 50 mM Tris HCl pH 7.5 containing 2% (v/v) Triton X100. The mixture was filter sterilised using a 0.45 μm filter and loaded onto the column. The column was rotated for four hours end to end at room temperature. Subsequently the column was washed with wash buffer 1 until the elutions measured 0.003 at OD_{595}. Antibodies were eluted in 200 µl 50 mM glycine pH 2.5 into eppendorfs containing 40 µl 1 M Tris HCl pH 8.0. The presence of antibody was detected by Ponceau staining. The fractions containing the highest visible protein were stored at 4°C overnight and BSA assay performed to determine the protein concentration in each elution. The column was washed with two column volumes of wash buffer 1 followed by two column volumes of 50 mM Tris HCl pH 7.5 and the process repeated three times. The column was then washed with two column volumes of 1% (w/v) SDS followed by five column volumes of 20% (v/v) EtOH and stored in 20% EtOH at 4°C.

The non-phospho column was washed and prepared as above and loaded with the individual fractions collected from the phospho column. The flow through was collected and stored as the phosphospecific Nek2 antibody. The non-phosphospecific Nek2 antibody was eluted as above using glycine and the column washed and stored as outlined above. BSA protein assay was performed on all the eluted antibodies and the most concentrated fractions stored at 4°C.

2.8 Miscellaneous techniques

2.8.1 *In vitro* kinase assays

Kinase assays were performed using 40 µl of kinase buffer (50 mM Hepes.KOH, 5 mM $MnCl_2$, 5 mM β-glycerophosphate, 5 mM NaF, 4 µM ATP, 1 mM DTT, 10 µCi [^{32}P]-γ-ATP, dH_2O to 500 µl) per reaction mixed with 5 µl of substrate protein (typically at 5 mg/ml). 45 µl of this mixture was then added to 5 µl purified Nek2 kinase (10 ng) or 5-10 µl of washed immune complex beads and incubated at 30°C for 30 minutes. 50 µl of sample buffer was added to stop the reaction and samples heated to 95°C for 3 mins before separating on an SDS-PAGE gel and exposing to X-ray film.

2.8.2 RNAi

HeLa cells were seeded into a 24 well dish so as to reach a confluency of 20% for the day of transfection. Cells were seeded in MEM containing no serum or antibiotics. Cells were transfected with pooled RNA duplexes directed against Nek2 (Dharmacon) at a final concentration of 50 nM. Transfections were performed as in section 2.5.3 using Oligofectamine (Invitrogen) and Optimem (Invitrogen) with 1 µl Oligofectamine added per 125 pmol RNAi. Antibiotic free MEM containing 30% (v/v) FCS was added 4 hours post transfection and cells fixed at 48 hours post transfection.

2.8.3 Scintillation counting

Bands of radioactive sample were cut from dried SDS-PAGE Coomassie stained gels. These were submerged in 3 ml of scintillation fluid in a scintillation vial. Samples were analysed for 1 min (Beckman coulter tricarb). Counts per minute were used to calculate the relative radioactivity incorporation into substrate.

2.8.4 Quantification of centrosome splitting

Centrosome splitting was assessed in cells by the distance between the two centrosomes. If the distance was greater than 2 μm the centrosomes were classed as split and if the distance was smaller than this the centrosomes were classed as unsplit. Initial counts were made using cells transfected with the myc-Nek2A-WT protein, the myc-Nek2A-KR protein and cells transfected with myc-pRcCMV vector alone. Transfected cells were identified by the anti-myc antibody staining at the centrosome. Approximately 100 cells per coverslip were counted and the level of splitting shown as a percentage of this number. For accuracy three coverslips per protein were counted and the final figure shown as an average of these counts. Error bars represent standard error.

2.8.5 Quantification of centrosome intensities

To measure the relative abundance of protein at the centrosome the Openlab imaging package was used. Pictures were taken using the same exposure time and gain settings and preferably on the same day (to limit discrepancies caused by the mercury bulb usage). Intensity measurements were taken by selecting a region of interest box. This box remained the same size for each set of data. The region of interest covered the average size of one centrosome. Pixel intensity was measured within the region of interest for each centrosome. This generated a series of data which included the mean pixel intensity for each centrosome. Approximately 20-100 regions of interest were taken per experiment and the mean pixel intensity of these taken as the average. A background measurement was taken for each condition and deducted from the total intensity. For each

condition the average intensity was compared in a histogram to identify abundance changes of the protein in question.

2.8.6 Quantification of kinase activity

The kinase activities of the *in vitro* kinase assays were assessed using two approaches, (i) by NIH image software and (ii) by scintillation counting. For quantification using NIH image software the autoradiograph was scanned using an Epson 2600 scanner into the Adobe Photoshop software program. The data was transferred to NIH image and a region of interest selected. Pixel intensities were measured for each sample using the same region of interest and a background measurement taken. The background value was subtracted from each of the other values. The Nek2A-WT protein measurement was taken as 100% and the remaining values calculated as a percentage of this value. For scintillation counts the counts per minute of the Nek2A-WT kinase were again converted to 100% and the remaining values calculated as a percentage of this value. Error bars represent standard error unless otherwise stated.

2.8.7 Preparation of samples for mass spectrometry analysis

Kinase assays were performed using the Nek2-NTD-KR protein fragment and 5 μg GST-Nlp-NTD as a substrate in kinase buffer containing 100 mM ATP for 40 minutes at 30°C. 0.2 μg of trypsin was added to the reaction and the sample incubated at room temperature overnight. Enrichment of phosphopeptides was achieved by the use of IMAC resin and HPLC.

Chapter Three

Autophosphorylation of the Nek2 protein kinase

3.1 Introduction

The activity of most, if not all, protein kinases is itself regulated by protein phosphorylation. Frequently this can be within a particular loop of the catalytic domain known as the activation loop (also called the T-loop). Phosphorylation of the activation loop can lead to activation of the kinase by either stabilising the active conformation or destabilising the inactive conformation. Only the active conformation is properly positioned for substrate binding and phosphate transfer. The activation loop consists of a region of approximately 20-25 amino acids residing between the conserved DFG and APE protein sequences (Johnson et al., 1996). First described in protein kinase A (PKA), this region spans from 184 to 208 and includes Thr-197 which serves as an autophosphorylation site. Since then other kinases including the microtubule associated protein kinase (MAPK) and the fission yeast cdc2 cell division control kinase have been found to be activated by activation loop phosphorylation. Phosphorylation of T210 in the activation loop of Plk1 and T212 within Pak1 are further examples where activation loop phosphorylation contributes to the cell cycle regulation of a kinase (Banerjee et al., 2002; Jang et al., 2002).

The Nek6 protein requires activation loop phosphorylation at serine 206 for activation in mitosis (Belham et al., 2003). This phosphorylation and activation is increased by co-expression with activated Nek9. Nek6 is also phosphorylated at threonine 202. Phosphorylation at threonine 202 may be stimulated by prior phosphorylation at serine 206. This represents a mechanism of sequential phosphorylation and autophosphorylation which allows the kinase to reach maximum activity in mitosis. The Nek2 protein kinase also contains a conserved activation loop. It is known that Nek2 undergoes autophosphorylation and is predominantly phosphorylated upon serine and threonine residues (Fry et al., 1995). Autophosphorylation of recombinant Nek2 protein is also demonstrated by the presence of higher molecular weight bands on Western blots (Twomey et al., 2004). Nek2 may undergo autophosphorylation to achieve full activity at the G2/M transition. However, Nek2 may also be phosphorylated by an upstream kinase. For example the $p90^{Rsk2}$ protein kinase has been shown to phosphorylate the Nek2 kinase domain *in vitro* (Di Agostino et al., 2002). In addition, incubation of mouse spermatocyte

cell extracts with activated $p90^{Rsk2}$ causes stimulation of Nek2 kinase activity (Di Agostino et al., 2002). It is therefore possible that Nek2 activation at the G2/M transition is jointly controlled by autophosphorylation and activation by upstream kinases.

The aim of this chapter is to understand how the Nek2 serine/threonine kinase is regulated by phosphorylation. I have studied this by mutation and measurement of Nek2 activity *in vitro* and *in vivo* by using three standard experiments: (i) *in vitro* translation of Nek2A constructs followed by immunoprecipitation and *in vitro* kinase assay using β-casein as the substrate, (ii) transfection of myc epitope tagged Nek2A constructs into either HeLa or U2OS cell lines followed by counts of centrosome splitting, and, in some cases, (iii) transfection of myc-epitope-tagged Nek2A constructs into HeLa or U2OS cells followed by lysis, immunoprecipitation and *in vitro* kinase assays using β-casein as the substrate.

Autophosphorylation site identification was achieved by two approaches: (i) by a candidate approach where sites are mutated and the effects of the mutations studied, and (ii) a direct approach to identify sites by mass spectrometry followed by mutation to ascertain their function. In collaboration with Prof. S. Smerdon and Mr. F. Ivins of the NIMR (London), the autophosphorylation of Nek2A has been studied by mass spectrometry. Using mass spectrometry, a number of phosphorylation sites were identified within both the kinase domain and the non-catalytic domain which may play a role in the regulation of Nek2 activity.

3.2 Results

3.2.1 The Nek2A protein kinase undergoes autophosphorylation

In order to study sites of Nek2 autophosphorylaiton, it was first necessary to identify potential sources of active Nek2A kinase. Active Nek2A kinases were generated by (i) transient transfection of myc-Nek2A into mammalian cells followed by immunoprecipitation; (ii) infection of Sf9 insect cells with a his-Nek2A baculovirus followed by lysis and purification on nickel beads; and (iii) *in vitro* translation of Nek2A followed by immunoprecipitation. Each method provides Nek2A kinases of which the wild type kinase (Nek2A-WT) is capable of phosphorylating the *in vitro* substrate β-casein (Figure 3.1 and 3.5). Nek2A also undergoes autophosphorylation, although this is somewhat reduced in the presence of the substrate β-casein (Figure 3.1B). A kinase-inactive version of Nek2A (Nek2A-KR) containing a mutation of Lys-37 to Arg in the ATP binding site does not phosphorylate β-casein or undergo autophosphorylation demonstrating the purity of the kinase preparations. Wild-type Nek2A undergoes autophosphorylation demonstrating that the protein is behaving in a predicted manner and is probably folded correctly. Kinases used within this thesis were generated from one of these methods.

3.2.2 Mass spectrometry of Nek2A reveals eleven putative autophosphorylation sites

The quantities of Nek2A kinase generated using the methods outlined in section 3.2.1 are not sufficient for mass spectrometry. Unfortunately, active Nek2 kinase is toxic to bacteria and therefore it is not possible to purify wild-type Nek2A kinase through bacterial expression. It is possible though to express mutants of Nek2A with reduced activity. The Nek2A-KR mutant, although essentially inactive in human cells, retains sufficient activity to undergo autophosphorylation when expressed in *E. coli*. Mass spectrometry was therefore performed on tryptic fragments of the Nek2A-KR kinase expressed in *E. coli* and purified using a C-terminal His tag. All fragments used for mass spectrometry analysis were produced by Mr. F Ivins and Prof. S. Smerdon (London). Bacteria do not contain serine/threonine protein kinases (Hanks and Hunter, 1995) and thus all sites identified by mass spectrometry can be classified as autophosphorylation sites.

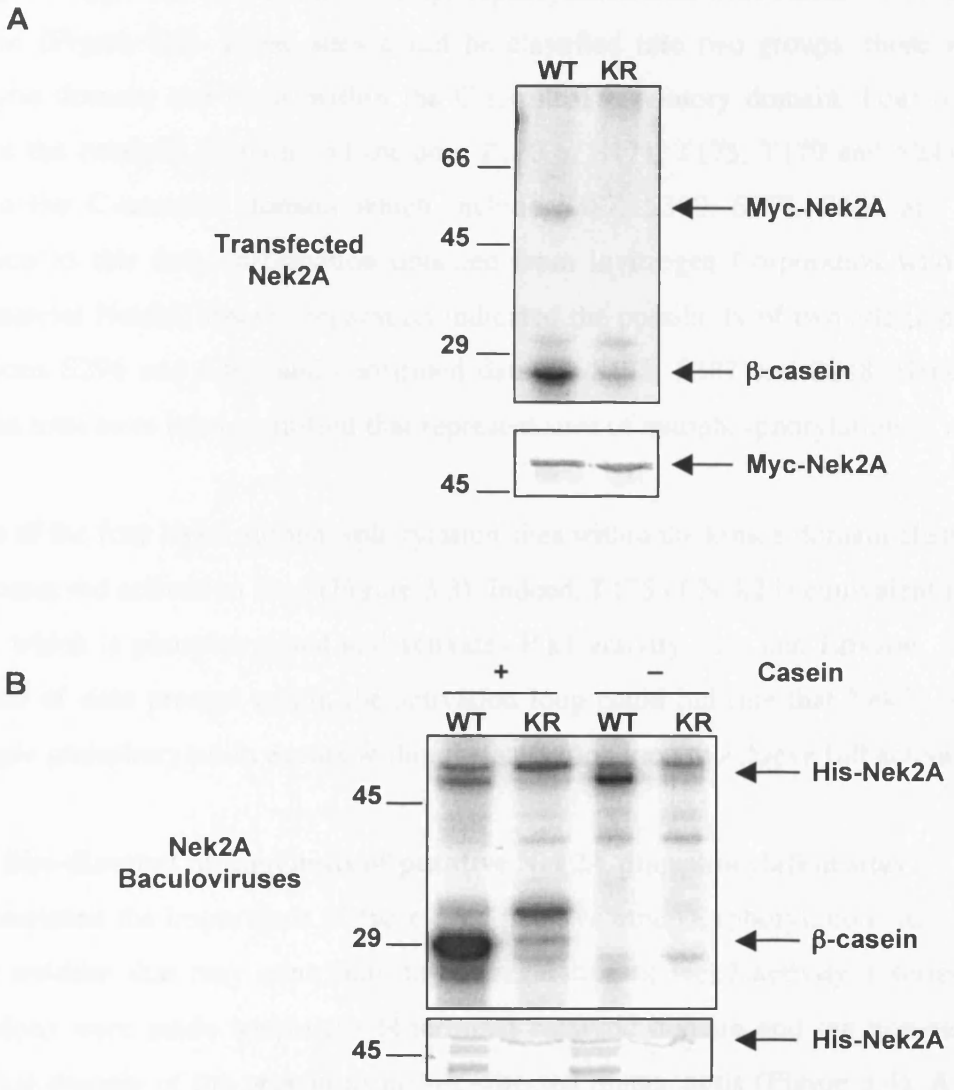

Figure 3.1 The Nek2A protein kinase undergoes autophosphorylation

A. U2OS cells were transiently transfected with myc-Nek2A-WT and myc-Nek2A-KR for 24 hours. The Nek2A proteins were harvested via cell lysis and immunoprecipitation using the anti-Myc antibody before incubation with ^{32}P-γ-[ATP] in kinase buffer with the substrate β-casein. Kinase reactions were separated on a 12% SDS-PAGE gel, dried and subjected to autoradiography (upper panel). A Western blot of the immunoprecipitated kinases was also performed with an anti-Nek2 antibody to confirm equal amounts of Nek2 protein were present (lower panel). **B.** Sf9 cells were infected with His-Nek2A-WT and His-Nek2A-KR baculoviruses for 48 hrs followed by cell lysis and purification by nickel affinity chromotography. Purified kinases were incubated with ^{32}P-γ-[ATP] in kinase buffer with the substrate β-casein. Kinase reactions were separated on a 12% SDS-PAGE gel, dried and subjected to autoradiography (upper panel). A Western blot of the purified kinases using an anti-Nek2 antibody (lower panel). M.wt. markers (kDa) are indicated on the left. Representation of at least 3 experiments.

Using this approach nine putative autophosphorylation sites were identified in the Nek2A protein (Figure 3.2). These sites could be classified into two groups: those within the catalytic domain and those within the C-terminal regulatory domain. Four are located within the catalytic domain and include, T170 or S171, T175, T179 and S241 and five within the C-terminal domain which include S387, S390, S397, S403 and S428. In addition to this data, information obtained from Invitrogen Corporation who supply a commercial Nek2A kinase preparation indicated the possibility of two additional sites at positions S296 and S368 and confirmed data for S171, S387 and S248. Hence, eleven sites in total have been identified that represent sites of autophosphorylation *in vitro*.

Three of the four Nek2 autophosphorylation sites within the kinase domain cluster around the conserved activation loop (Figure 3.3). Indeed, T175 of Nek2 is equivalent to T210 of Plk1, which is phosphorylated and activates Plk1 activity (Lee and Erikson, 1997). The number of sites present within the activation loop could indicate that Nek2A undergoes multiple phosphorylation events within the activation loop to achieve full activation.

3.2.3 Site-directed mutagenesis of putative Nek2A phosphorylation sites

To determine the importance of the eleven putative autophosphorylation sites as well as other residues that may contribute to the regulation of Nek2 activity a series of point mutations were made within the N-terminal catalytic domain and the non-catalytic C-terminal domain of the protein using site-directed mutagenesis (Figure 3.4). A summary of all the mutations made in the Nek2 protein is shown in Fig 3.4C. Firstly, serines or threonines which were possible phosphorylation sites were mutated to aspartate or glutamate, respectively. This should mimic the shape and charge of the phosphorylated residue. Secondly, serines and threonines were mutated to alanine, which prevents phosphorylation and mimics the unphosphorylated state. If phosphorylation of a particular serine leads to Nek2 activation, then the mutation to aspartate may render it constitutively active whereas mutation to alanine would render it constitutively inactive.

3.2.4 Validating the activity assays with wild-type and inactive Nek2A

To test the consequence of these mutations on the activity of Nek2A *in vitro* and *in vivo*

A

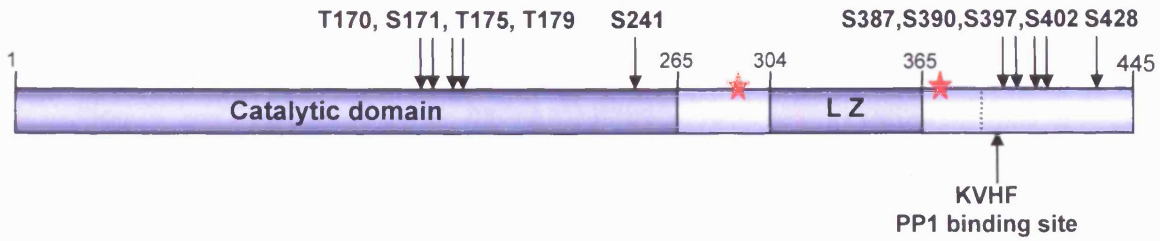

B

1 MPSRAEDYEVLYTIGTGSYGRCQKIRRKSD
GKILVWKELDYGSMTEAEKQMLVSEVNLLR
ELKHPNIVRYYDRIIDRTNTTLYIVMEYCE
GGDLASVITKGTKERQYLDEEFVLRVMTQL
TLALKECHRRSDGGHTVLHRDLKPANVFLD
GKQNVKLGDFGLARILNHDTSFAKTFVGTP
YYMSPEQMNRMSYNEKSDIWSLGCLLYELC
ALMPPFTAFSQKELAGKIREGKFRRIPYRY
SDELNEIITRMLNLKDYHRPSVEEILENPL
IADLVADEQRRNLERRGRQLGEPEKSQDSS
PVLSELKLKEIQLQERERALKAREERLEQK
EQELCVRERLAEDKLARAENLLKNYSLLKE
RKFLSLASNPELLNLPSSVIKKKVHFSGES
KENIMRSENSESQLTSKSKCKDLKKRLHAA
QLRAQALSDIEKNYQLKSRQILGMR 445

Figure 3.2 Mass spectrometry reveals nine possible Nek2A autophosphorylation sites

A. A schematic diagram of the human Nek2A protein kinase with the positions of the putative autophosphorylation sites as identified by mass spectrometry highlighted. Additional sites identified by Invitrogen are marked by a star at position S296 and S368. **B.** The Nek2A amino acid sequence is indicated and the autophosphorylation sites highlighted in red. The PP1 binding site is highlighted in blue. It is not yet clear which of T170 or S171 is the correct site of autophosphorylation.

A

T-Loop conservation	170 171 175 179
Human	DFGLARILNHDT SFAKTFVGTP YYMSPE
Rat	DFGLARILNHDT SFAKTFVGTP YYMSPE
Chicken	DFGLARILHHDT SFAKTFVGTP YYMSPE
Dog	DFGLARILNHDT SFAKTFVGTP YYMSPE
Frog X.tropicalis	DFGLARILHHDS SFAKTFVGTP YYMSPE
Frog X.laevis	DFGLARILHHDS SFAKTFVGTP YYMSPE
Mouse	DFGLARILNHDT SFAKTFVGTP YYMSPE

Serine 241	241
Human	GKFRRIPYRY SDELNEIITR MLNLKDYH
Rat	GRFRRIPYRY SDGLNDLITR MLNLKDYH
Chicken	GKFRRIPYRY SEQLNELLKE MLNLKDYC
Dog	GKFRRIPYRY SDELNDIITR MLNLKDYH
Frog X.tropicalis	GRFRRIPYRY SEELNQVITN MLHLKDYL
Frog X.laevis	GRFRRIPYRY SEELNQVITN MLHLKDYL
Mouse	GRFRRIPYRY SDGLNDLITR MLFLKDYH

B

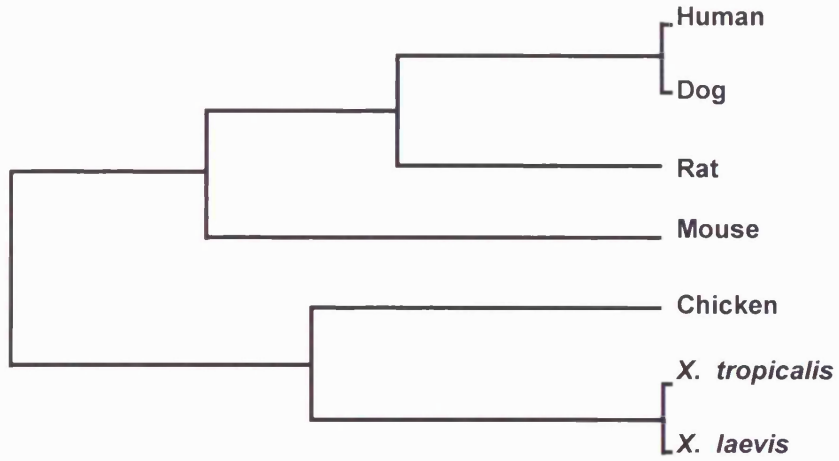

Figure 3.3 The putative autophosphorylation sites in the Nek2 catalytic domain are highly conserved in vertebrates

A. The activation loop residues of Nek2 and the residues surrounding S241 within different species are aligned to demonstrate the conserved nature of these regions within the Nek2 kinase family. Residues highlighted in red represent phosphorylation sites. **B.** Phylogenetic analysis of the Nek2 activation loop domain across species (generated using ClustalW software).

A

B

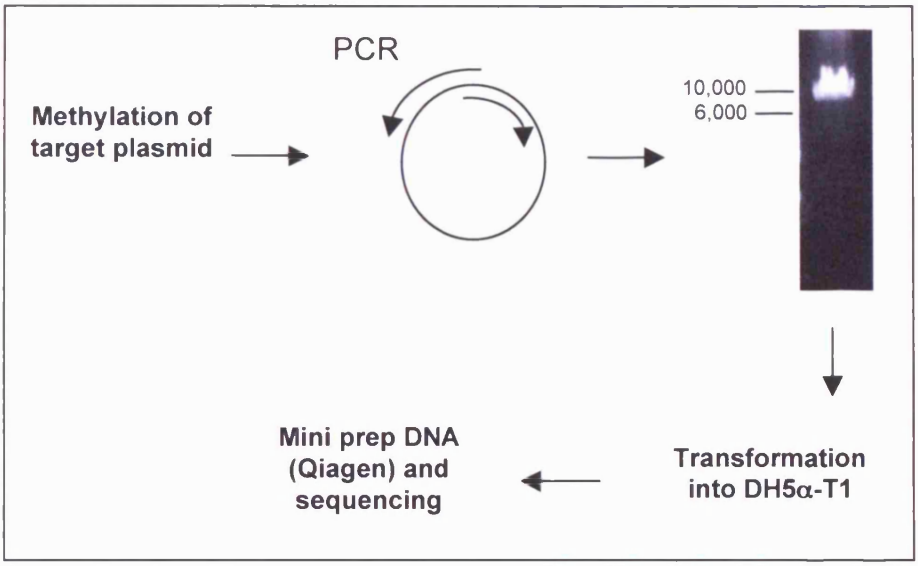

C

Region	Mutation
Activation loop	T170A, T170E, S171A, S171D, T175A, T175E, T179A, T179E F172A, F176A
Kinase domain	S241A, S241D
C-terminus	F386A, S387/390/397/403A, S387/390/397/403D, S428A

Figure 3.4 Site-directed mutagenesis protocol and summary of mutants generated

A. An example of a typical set of primers for site-directed mutagenesis, approximately 30 nucleotides in length. They contain an overlapping region, an extended region for accurate annealing and the forward primer contains the mutation site (green). **B.** Schematic representing the stages of the mutagenesis procedure. **C.** Table listing the specific mutations made within the Nek2A kinase. Note that two of the C-terminal domain mutants were not single point mutations but contained four mutations within the same construct.

three assays were performed as previously described (see section 3.1). These assays were first tested using wild-type Nek2A and Nek2A-KR. The Nek2A-KR mutant (Figure 3.5A) has a mutation at residue lysine 37 in the ATP binding site of the kinase. Mutation of this lysine to arginine (K37R) prevents ATP binding and causes a major reduction in kinase activity. For the first assay, myc-Nek2A-WT and myc-Nek2A-KR, were translated *in vitro* and immunoprecipitated using an anti-myc antibody; the immune complexes were then incubated in kinase buffer containing ^{32}P-γ-[ATP] and casein as a substrate for 30 minutes at 30°C. The kinase activities of the mutants were assessed by autoradiography (Figure 3.5B) and quantified using the software package NIH image (Figure 3.5C). For future comparisons, the amount of ^{32}P incorporated into the substrate β-casein during this assay is set at 100%. Based on this analysis, the non-ATP binding mutant Nek2A-KR had less than 10% activity.

Previously, it has been shown that transfection of HeLa or U2OS cells with wild-type Nek2A induces the premature splitting of centrosomes by >2μm in 40-60% of cells after 24 hours. In contrast, untransfected cells have only approximately 10% split centrosomes (Fry et al., 1998b; Meraldi and Nigg, 2001). Kinase-inactive Nek2A does not induce centrosome splitting. The induction of centrosome splitting may be a direct result of the Nek2A kinase phosphorylating its substrates C-Nap1 and rootletin at the centrosome (Bahe et al., 2005; Fry et al., 1998a). The proteins are thought to form part of the intercentriolar linkage and, when phosphorylated by Nek2, cause the linkage to be disrupted and the centrosomes move apart. Therefore, we decided to determine whether the mutant kinases generated in this study (a) localized to the centrosome, and (b) induced centrosome splitting. This latter observation would give an indication of the activity of the mutants in cells.

U2OS cells transfected with myc-tagged Nek2A constructs were fixed in methanol after 24 hours and stained with antibodies to the Myc-tag, C-Nap1 or γ-tubulin. DNA was stained with Hoechst 33258 to highlight the nucleus. C-Nap1 and γ-tubulin identify the position of the centrosomes and are used to determine the extent of centrosome splitting. Transfected cells were identified as having ten-fold brighter Myc stain (red) than surrounding cells. One hundred transfected cells were counted for each mutant in three

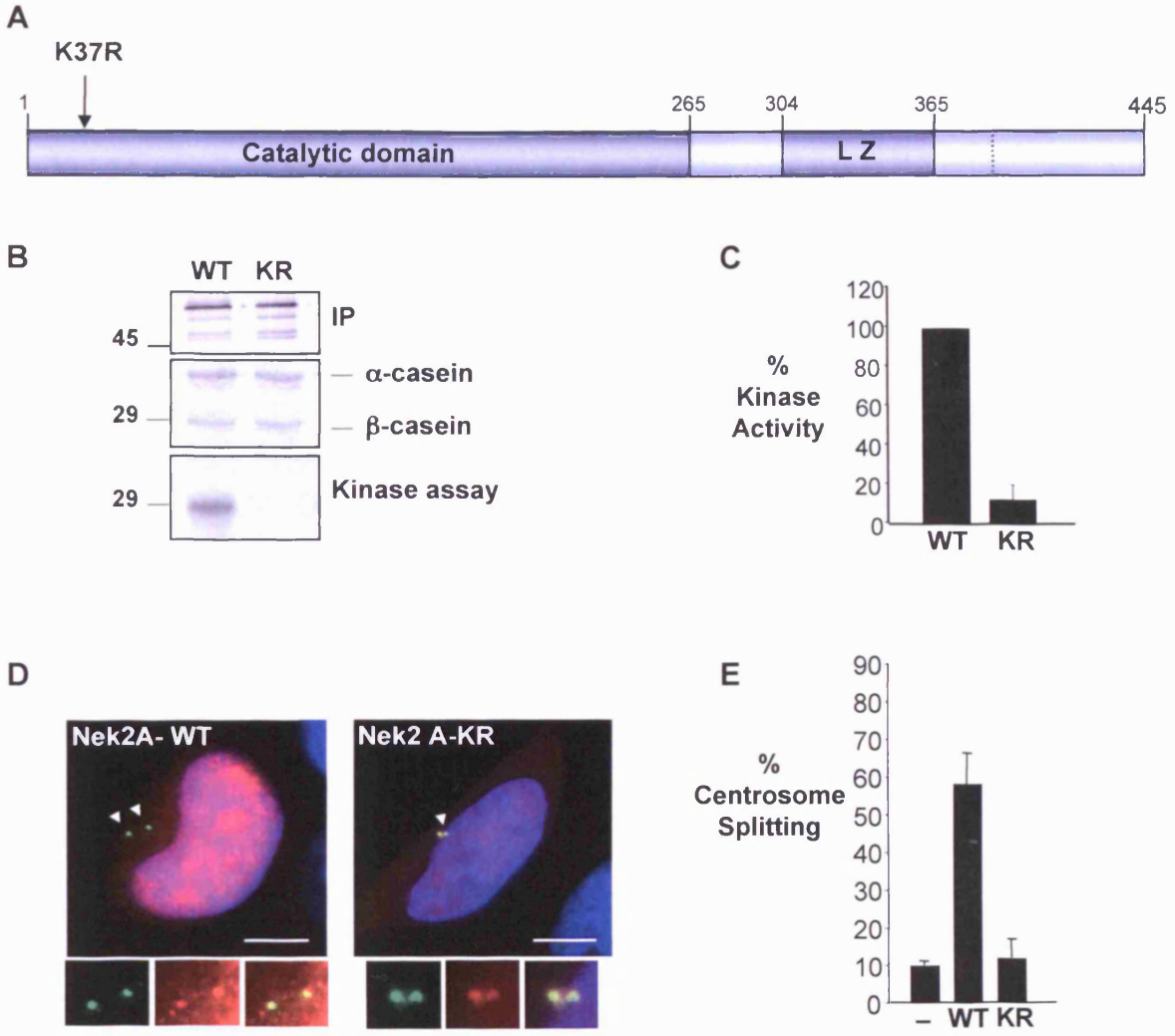

Figure 3.5 Nek2A kinase activity induces premature centrosome splitting in interphase cells

A. A schematic diagram of the Nek2A protein indicating the position of the K37R mutation within the catalytic domain. **B.** The pGEM:Nek2A-WT and Nek2A-KR constructs were translated (*in vitro)*, immunoprecipitated using the Zymed Nek2 antibody and either Western blotted to confirm equal precipitation (upper panel) or incubated with kinase buffer containing ^{32}P-[γ-ATP] and the substrate casein for 30 minutes at 30°C. Proteins were separated by SDS-PAGE, stained with Coomassie Blue (middle panel) and subjected to autoradiography (lower panel). Radioactivity is incorporated into the substrate β-casein specifically by the Nek2A-WT kinase. **C.** *In vitro* kinase assays were performed three times and the activity relative to WT (100%) calculated by NIH image. **D.** U2OS cells were transfected with the myc-Nek2A-WT and myc-Nek2A-KR constructs for 24 hours. Cells were fixed with methanol and stained with a myc antibody (red), a C-Nap1 antibody to reveal the centrosome (green) and Hoechst 33258 to highlight the DNA (blue). Scale bar, 10 μm. White arrowheads point to centrosomes. Inserts are enlargements of the centrosome region. **E.** Approximately 100 transfected cells were scored in three independent experiments as either having split or non-split centrosomes. Similar results were obtained for transfected HeLa cells (not shown). Untransfected cells were scored as a control (–).

separate experiments (Figure 3.5D). As previously shown, wild-type Nek2A localised to the centrosome and induced centrosome splitting in 58.2% of transfected cells confirming that the Nek2A protein is active. The Nek2A-KR protein also localised to the centrosome but induced very little centrosome splitting (12%) confirming that this protein has no activity (Figure 3.5E).

3.2.5 T175 is essential for Nek2A kinase activity *in vitro* and *in vivo*

Three putative autophosphorylation sites were identified by mass spectrometry in the activation loop of Nek2A. One of these, T175, is equivalent in position to T197 of PKA, T160 of Cdk2 and T210 of Plk1. All of these sites require phosphorylation for kinase activity. We therefore first looked at the consequences of mutating T175 in Nek2A. The T175A and T175E mutations were made in a pGEM:Nek2A construct for *in vitro* translation and a pRcCMV:myc-Nek2A construct for transfection studies. Initially, the pGEM constructs were translated *in vitro* and their migration analysed by SDS-PAGE confirming the correct protein sizes. The proteins were then immunoprecipitated and *in vitro* kinase assays performed using β-casein as a substrate (Figure 3.6B). The activity of the Nek2A-T175A construct was considerably reduced compared to that of the wild-type kinase, whereas the Nek2A-T175E mutant had increased activity (Figure 3.6C). Upon transfection into U2OS cells both Nek2A-T175A and Nek2A-T175E localised to the centrosome demonstrating that the mutations did not affect Nek2 localisation (Figure 3.6D). Importantly, the level of centrosome splitting in cells expressing Nek2A-T175A was reduced to 21.25% supporting the notion that this mutant has reduced kinase activity (Figure 3.6E). Expression of Nek2A-T175E protein triggered centrosome splitting to a similar level to that of the wild-type protein. This may be due to the fact that the kinase activity of Nek2 on its targets can induce centrosome splitting to a certain extent but other mechanisms may be in place to prevent further splitting. This could involve microtubules or protein cascades which are involved in the timing of centrosome splitting. Hence, the T175 residue in the Nek2 activation loop is very important for the activity of the Nek2 protein kinase. When mutated to alanine, it leads to loss of kinase activity and when mutated to glutamate it increases kinase activity, at least *in vitro*. This

suggests that phosphorylation of T175 helps to position the kinase into an active conformation or promote further autophosphorylation events which fully activate the kinase.

3.2.6 T179 is required for Nek2 kinase activity *in vivo*

The next site we analysed was T179. This lies in the heart of the activation loop of Nek2 and is absolutely conserved within the Nek2 kinases (Figure 3.3A). Again T179 was mutated to both alanine and glutamate to determine the effects upon Nek2 activity. The proteins were translated *in vitro*, immunoprecipitated and *in vitro* kinase assays performed using β-casein as a substrate (Figure 3.7B, top panel). In addition, U2OS cells were transiently transfected with Nek2A-T179A and Nek2A-T179E, lysed, immunoprecipitated and subjected to kinase assays (Figure 3.7B, lower panel). These assays revealed that the kinase activity of both Nek2A-T179A or Nek2A-T179E to be significantly reduced compared to wild-type Nek2A (Figure 3.7B/C). Nek2A-T179A and Nek2A-T179E proteins still localised to the centrosome suggesting that there was no major misfolding of the kinases (Figure 3.7D). However, centrosome splitting activity was also reduced compared to the Nek2A-WT kinase (Figure 3.7E). These results suggest that threonine 179 is absolutely required for Nek2 activity *in vitro* but that mutation to glutamate does not generate a hyperactive kinase.

3.2.7 Mutation of the conserved activation domain phenylalanine residues increases Nek2A activity

Studies on the *Aspergillus* NIMA kinase had identified the consensus sequence, FxxS/T, as the preferred substrate recognition site (Lu et al., 1994). It is therefore intriguing to note that both T175 and T179 lie in an FxxT motif. In order to test the relevance of these phenylalanines in Nek2A, F172A and F176A mutants were generated in the pRcCMV:mycNek2A construct (Figure 3.8A). These proteins were translated *in vitro* and immunoprecipitated with the Myc antibody. The beads were subsequently mixed with the substrate β-casein and kinase buffer containing $^{32}P\gamma$-[ATP] and incubated at 30°C for 30 minutes. Surprisingly, the results indicated that both Nek2A-F172A and Nek2A-F176A were four-fold more active than the Nek2A-WT kinase *in vitro* (Figure 3.8B/C).

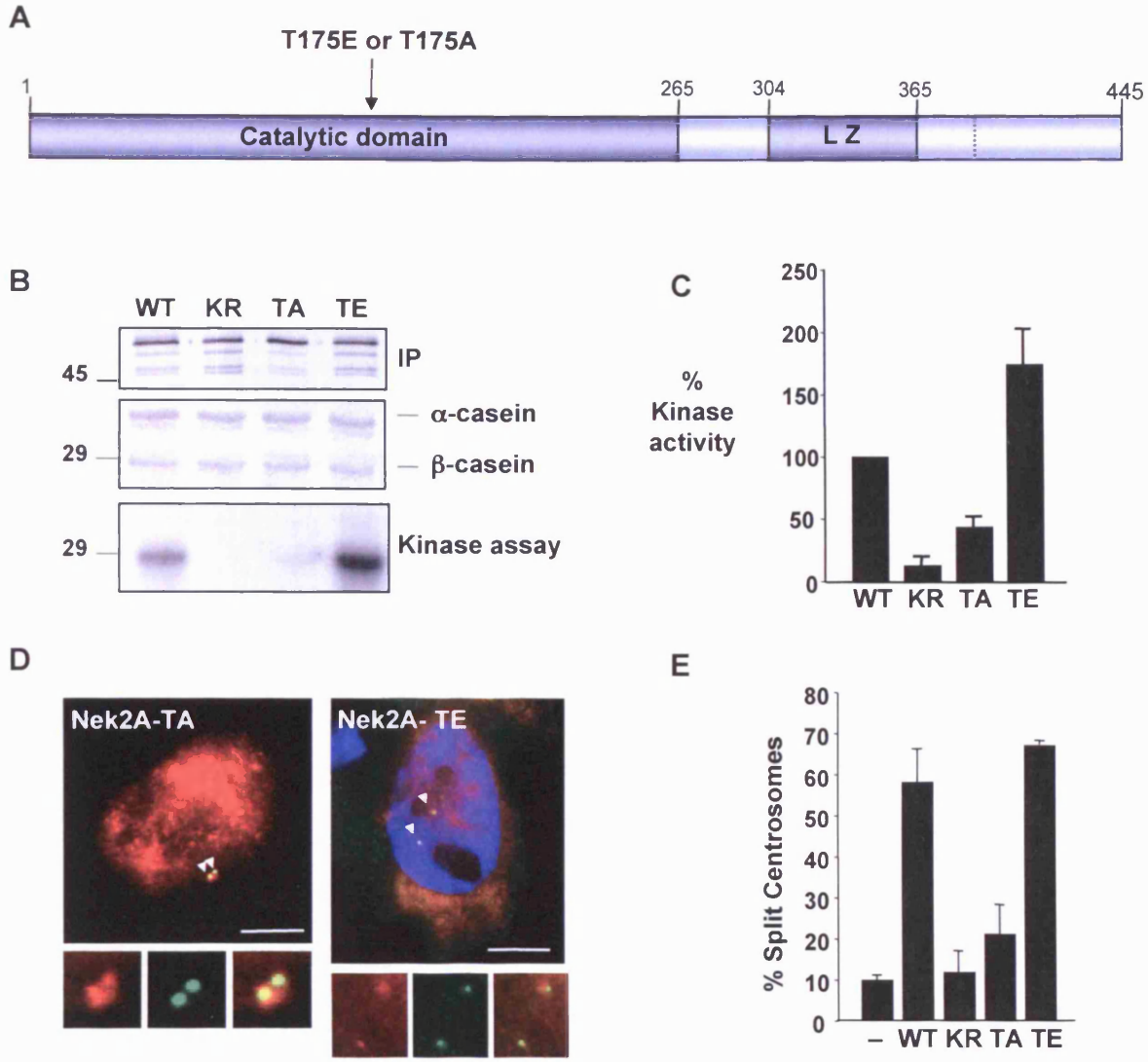

Figure 3.6 Mutation of T175 alters Nek2A kinase activity

A. A schematic diagram of Nek2A indicating the position of T175 within the catalytic domain of Nek2A-TA and Nek2A-TE. **B.** The pGEM Nek2A-WT, Nek2A-KR, Nek2A-TA and Nek2A-TE constructs were translated (*in vitro)*, immunoprecipitated and incubated with kinase buffer containing ^{32}P-γ-[ATP] as described in Figure 3.5B. **C.** Histogram representing the kinase activity of each mutant as measured by NIH image in three separate experiments. **D.** U2OS cells were transfected with the myc-Nek2A-TA and myc-Nek2A-TE constructs for 24 hours. Cells were fixed with methanol and stained with a myc antibody to detect Nek2 (red), a C-Nap1 antibody to detect the centrosome (green) and Hoechst 33258 to detect the DNA (blue). Scale bar, 10 μm. White arrowheads point to centrosomes. Inserts are enlargements of the centrosome region. **E.** Approximately 100 transfected cells were counted in three independent experiments and the centrosomes scored as either split or non-split. Counts for U2OS cells are shown. Similar results were obtained for HeLa cells. Untransfected cells were scored as a control (–).

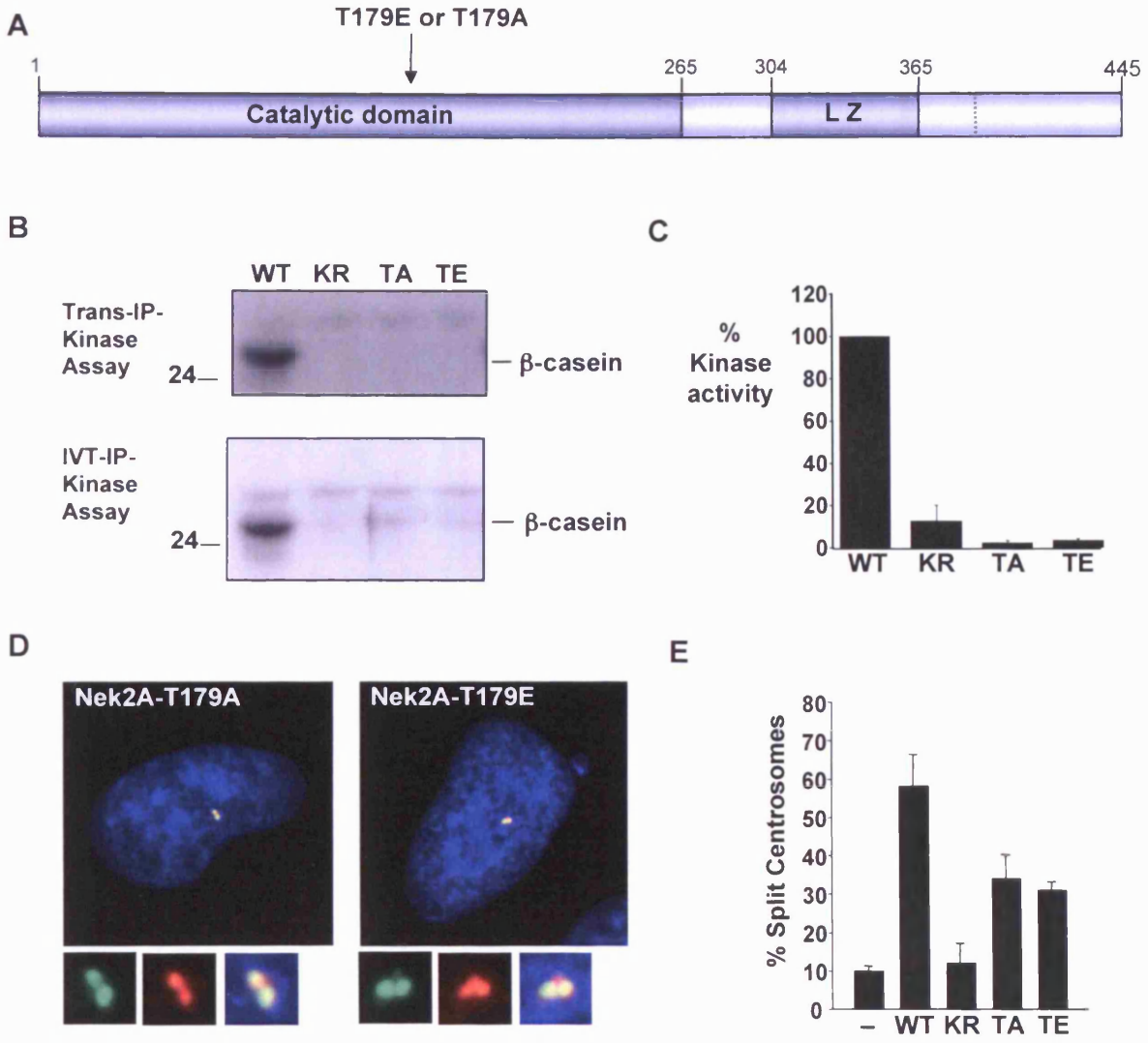

Figure 3.7 Threonine 179 is required for Nek2A kinase activity

A. A schematic diagram of Nek2A indicating the position of the T179 mutation within the catalytic domain. **B**. IP-kinase assays were performed as in Figure 3.5. The upper autoradiograph represents a kinase assay of Nek2A-WT, Nek2A-KR, Nek2A-T179A and Nek2A-T179E which have been transfected and immunoprecipitated from U2OS cells. The lower autoradiograph represents a kinase assay of Nek2A-WT, Nek2A-KR, Nek2A-T179A and Nek2A-T179E constructs immunoprecipitated from constructs translated *in vitro*. **C**. Histogram represents the kinase activity of each mutant as measured by scintillation counting in four separate IVT-IP kinase assay experiments. **D**. U2OS cells were transfected with the myc-Nek2A-T179A and myc-Nek2A-T179E constructs. At 24 hours cells were fixed with methanol and stained with a myc antibody to detect Nek2 (red), a C-Nap1 antibody to detect the centrosome (green) and Hoechst 33258 to detect the DNA (blue). Scale bar, 10 μm. Inserts are enlargements of the centrosome region. **E.** Approximately 100 transfected cells were counted in three independent experiments and the centrosomes scored as either split or non-split. Counts for U2OS cells are shown. Similar results were obtained for HeLa cells. Untransfected cells were scored as a control (–).

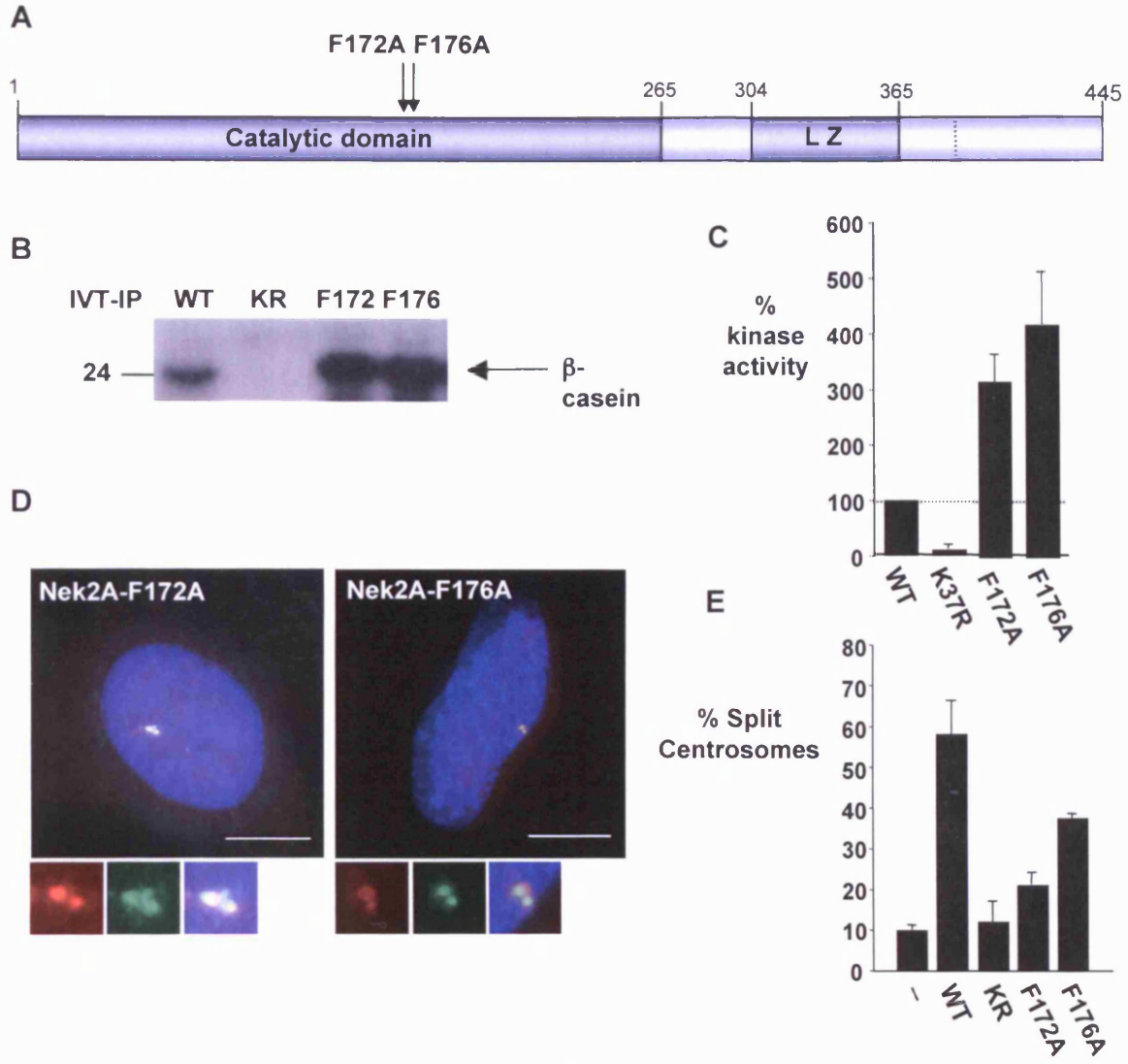

Figure 3.8 Mutation of F172 and F176 increases Nek2A activity *in vitro* but reduces Nek2A activity *in vivo*

A. A schematic diagram highlighting the location of the mutated phenylalanines within the catalytic domain of Nek2A. **B.** The myc-tagged Nek2A-WT, Nek2A-KR, Nek2A-F172A and Nek2A-F176A proteins were translated *in vitro,* immunoprecipitated using the Myc antibody and the beads mixed with β-casein and kinase buffer containing ^{32}P-[γ-ATP] for 30 mins at 30°C. The products were separated by SDS-PAGE and the gel subjected to autoradiography. **C.** Histogram to demonstrate % of kinase activity of the three mutants over three separate experiments. **D.** The myc-Nek2-F172A and myc-Nek2A-F176A mutants were transfected into U2OS cells and after 24 hours the cells were methanol-fixed and stained using the γ-tubulin antibody (green) to detect centrosomes and the Myc antibody (red) to detect myc-Nek2A protein and the DNA stained with Hoechst 33258 (blue). Both proteins can still localise to the centrosome. Scale bar, 5 μm. Inserts are the enlargement of the centrosome region. **E.** Approximately 100 transfected cells were counted in three independent experiments and the centrosomes scored as either split or non-split.

Following transfection into U2OS cells, the myc-tagged Nek2A-F172A and Nek2A-F176A mutants still localised to the centrosome (Figure 3.8D). However, the frequency of centrosome splitting was reduced in cells transfected with the Nek2A-F172A or Nek2A-F176A constructs as compared to cells transfected with the wild-type protein. This suggests that these mutant proteins have reduced activity *in vivo*. These results support the importance of these phenylalanine residues. However, it is not clear why the result of the *in vitro* and *in vivo* assays should be so contradictory. It is possible that the answer lies in the particular substrate used. *In vitro* the mutant kinases are extremely active upon β-casein. However, *in vivo* it is possible that the kinase is no longer able to phosphorylate centrosomal proteins involved in centrosome splitting.

3.2.8 T170 and S171 have no effect on Nek2 activity *in vivo*

Mass spectrometry analysis revealed another putative autophosphorylation site at either T170 or S171. It was possible that both these residues were phosphorylated, but it was equally possible that only one was phosphorylated. Autophosphorylation site data obtained from Invitrogen identified S171 but not T170 to be autophosphorylated. To determine the role of these sites individual T170A, T170E, S171A and S171D mutations were made in myc-tagged Nek2A constructs and transfected into U2OS cells (Figure 3.8). All the proteins localised correctly to the centrosome and stimulated a similar degree of centrosome splitting as compared to the wild-type kinase. As mutations to alanine did not decrease the levels of centrosome splitting these results suggest that these sites do not play a role in regulating Nek2 activity (Figure 3.8). However, kinase assays will need to be performed to verify these conclusions.

3.2.9 S241 phosphorylation is required for Nek2A activity *in vitro* and *in vivo*

The only putative Nek2 autophosphorylation site identified in the catalytic domain outside of the activation loop was serine 241. Ser 241 is located toward the C-terminal end of the kinase domain (Figure 3.3). It seems unlikely that a site so distant from the activation loop could have an effect on Nek2 activity. However, kinase assays using *in vitro* translated proteins showed that mutation to either alanine or aspartate renders the kinase inactive (Figure 3.10 B/C).

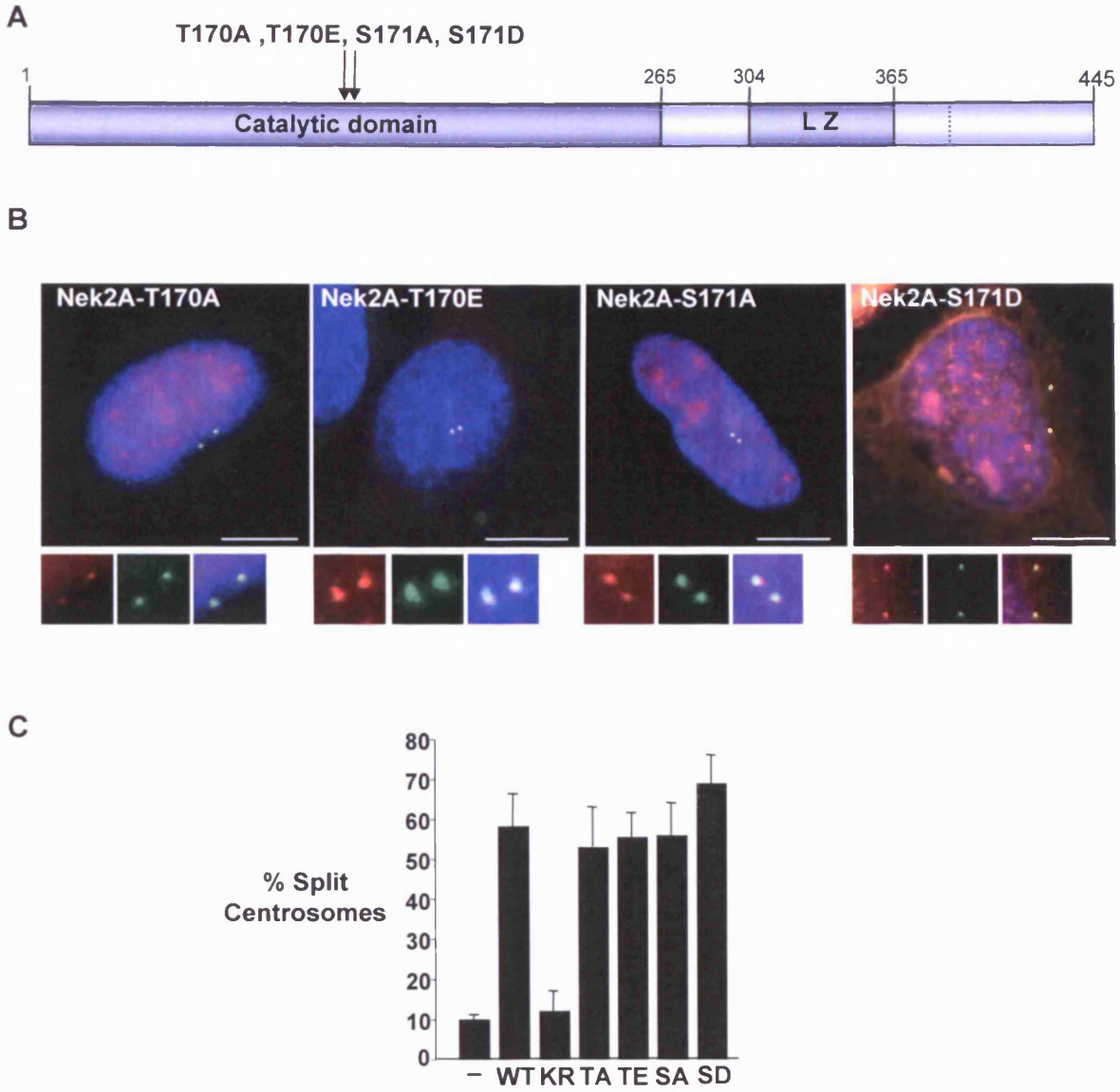

Figure 3.9 Mutation of T170 or S171 does not alter Nek2A activity in cells

A. A schematic diagram of Nek2A indicating the position of the T170 and S171 residues within the catalytic domain of Nek2A. **B.** U2OS cells were transfected with the myc-Nek2A-T170A, myc-Nek2A-T170E, myc-Nek2A-S171A or myc-Nek2A-S171D constructs for 24 hours. Cells were fixed with methanol and stained with a myc antibody to detect Nek2 (red), a C-Nap1 antibody to detect the centrosome (green) and Hoechst 33258 to detect the DNA (blue). Scale bar, 10 μm. Inserts are the enlargement of the centrosome region. **C.** Approximately 100 transfected cells were counted in two independent experiments and the centrosomes scored as either split or non-split. Similar results were obtained for HeLa cells. Untransfected cells were scored as a control (–).

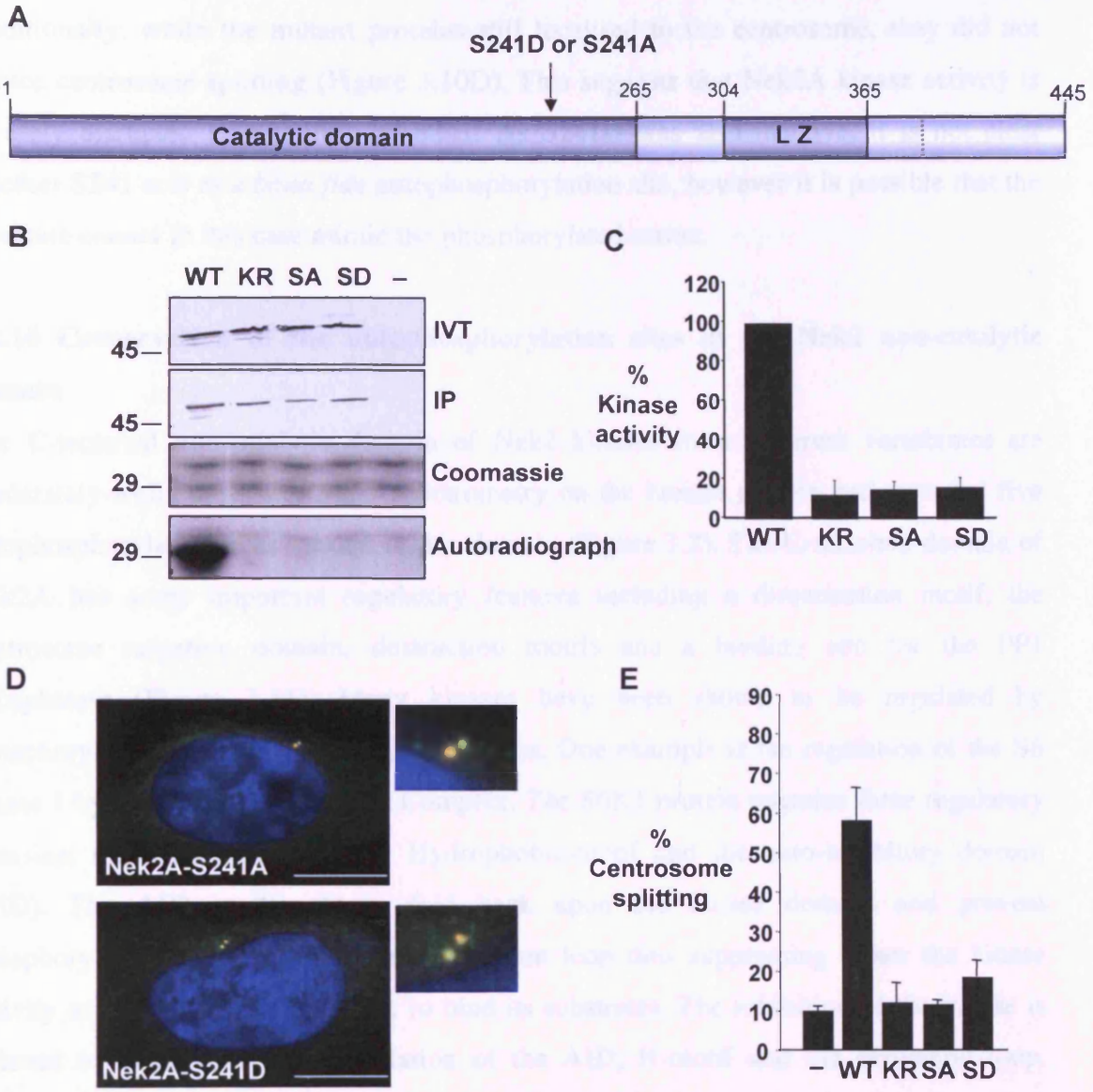

Figure 3.10 Mutation of Serine 241 inhibits Nek2 kinase activity

A. A schematic diagram representing the position of the S241 mutation within the catalytic domain of Nek2A. **B.** The myc-Nek2A-WT, Nek2A-KR, Nek2A-S241A (SA) and Nek2A-S241D (SD) constructs were translated *in vitro* (IVT) and immunoprecipitated using an anti myc antibody (IP). Radioactivity is incorporated into the substrate β-casein specifically by the Nek2A-WT kinase but not with the mutants (autoradiograph). **C.** Histogram representing the kinase activity in each mutant as measured by scintillation counts in three separate experiments. **D.** U2OS cells were transfected with the myc tagged Nek2A-S241A and Nek2A-S241D constructs for 24 hours. Cells were fixed with methanol and stained with a myc antibody to detect Nek2 (red), a C-Nap1 antibody to target the centrosome (green) and Hoechst 33258 to highlight the DNA (blue). Scale bar, 10 μm. Inserts are enlargements of the centrosome region. **E.** The Nek2A mutant kinases do not induce centrosome splitting. Approximately 100 transfected cells were counted in three independent experiments and the centrosomes scored as either split or non-split. This work was carried out under my supervision by an undergraduate project student, Anastasia Shen.

Additionally, while the mutant proteins still localised to the centrosome, they did not induce centrosome splitting (Figure 3.10D). This suggests that Nek2A kinase activity is severely disrupted by mutation of S241. As S241D was also inactive, it is not clear whether S241 acts as a *bona fide* autophosphorylation site, however it is possible that the aspartate cannot in this case mimic the phosphorylated serine.

3.2.10 Conservation of the autophosphorylation sites in the Nek2 non-catalytic domain

The C-terminal non-catalytic domain of Nek2 kinases from different vertebrates are moderately-well conserved. Mass spectrometry on the human protein had revealed five autophosphorylation sites located in this domain (Figure 3.2). The C-terminal domain of Nek2A has some important regulatory features including a dimerisation motif, the centrosome targeting domain, destruction motifs and a binding site for the PP1 phosphatase (Figure 3.11). Many kinases have been shown to be regulated by phosphorylation in their non-catalytic domains. One example is the regulation of the S6 kinase 1 by the Tuberous Sclerosis Complex. The S6K1 protein contains three regulatory domains: the activation loop, the Hydrophobic-motif and the auto-inhibitory domain (AID). The AID is thought to fold back upon the kinase domain and prevent phosphorylation of the H-motif and activation loop thus suppressing either the kinase activity or the ability of the kinase to bind its substrates. The inhibition of the kinase is relieved by sequential phosphorylation of the AID, H-motif and the activation loop. Indeed the phosphorylation and activation of the activation loop by PDK1 is facilitated when the H-motif is phosphorylated as this event enhances the binding of PDK1 (Shah and Hunter, 2004).

Interestingly, a group of autophosphorylation sites are clustered in the CTD of Nek2 around the PP1 binding site. This raised the possibility that phosphorylation of these sites might contribute to Nek2 activity by regulating PP1 binding and subsequent inhibition. Mutagenesis of these sites followed by *in vitro* binding assays were used to address this question. It is also possible that the CTD of Nek2 acts as an auto-inhibitory domain and that phosphorylation of the CTD is required to relieve this inhibition. Indeed, inhibitory

C-terminal domains have been suggested as a mode of regulation in Plk1 and NIMA (Mundt et al., 1997; O'Connell et al., 2003).

3.2.11 Mutation of the PP1 binding site does not alter Nek2A activity *in vitro*

As Nek2A can bind protein phosphatase 1 (PP1), it has been proposed that PP1 acts as a negative regulator of Nek2A (Helps et al., 2000). PP1 binds to Nek2A in its non-catalytic C-terminal domain (CTD) at the motif ^{383}KVHF^{386}. Mutation of the phenylalanine residue completely abolishes binding of PP1 to Nek2A (Helps et al., 2000). To test the role of PP1 in regulating Nek2A, F386 was mutated to alanine to prevent PP1 binding. Later experiments confirmed that this mutation abolished PP1 binding (see 3.14). Creating this mutant would (i) generate a suitable control for PP1 binding assays, and (ii) possibly create a hyperactive Nek2 protein. Production of a hyperactive Nek2 kinase would be beneficial for use in various *in vitro* and *in vivo* assays.

Following *in vitro* translation and immunoprecipitation, the Nek2A-F386A protein exhibited a similar level of kinase activity to that of the wild-type protein. This could be because there is little if any PP1 present in the rabbit reticulocyte lysate. Indeed, an immunoblot of the rabbit reticulocyte lysate used in the *in vitro* translations revealed no detectable PP1 (data not shown). Moreover, rabbit PP1 may not bind human Nek2A. Following transfection into cells, the Nek2A-F386A protein induced a similar level of centrosome splitting as the wild-type protein. As for the T175E mutant, this may suggest that there is a mechanism that exists to prevent 100% of cells undergoing premature centrosome splitting (Figure 3.12). Although these experiments did not support a critical role for PP1 in regulating Nek2A activity, we believe that this is likely to be a result of the experimental system used.

3.2.12 Generation of a GST-PP1α fusion protein

To study the consequences of autophosphorylation on the ability of PP1 to bind Nek2A, a GST-PP1α construct was made by subcloning amino acids 1-327 of human PP1α into pGEX-4T (Appendix). The construct was expressed in *E. coli* BL21 and purified using

A

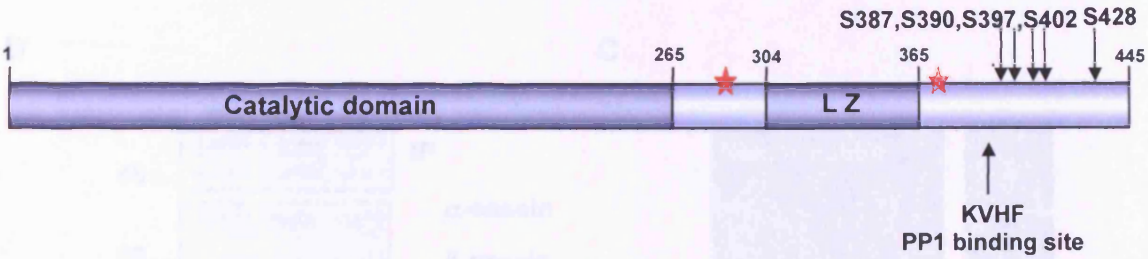

B

C-terminal autophosphorylation sites

Human	KVHFSGESKE NIMRSENSES QLTSKSKCKD
Rat	KVHFHGESKE NTTRSENSES QLAKSKCRDL
Chicken	KVHFGGSEED GMPSVNVENY PLSKGKCSDL
Dog	KVHFSGESKE NVMRSKNSES LLTSKSKCKD
X. tropicalis	HVHFGSNSKE NSSTDRYREQ EKCSDLQKRL
X. laevis	HVHFGSNSKE NRSSDRYLEQ EKCSDLQKRL
Mouse	KVHFHGESKE NTARSENSES YLAKSKCRDL

Figure 3.11 Autophosphorylation sites in the Nek2A non-catalytic domain are highly conserved

A. Schematic diagram of Nek2A with the C-terminal phosphorylation sites highlighted. The stars represent the two additional sites identified by Invitrogen but not studied here. **B.** The phosphorylation sites clustered around the PP1 binding site (blue) are highlighted in red and are shown for different vertebrates.

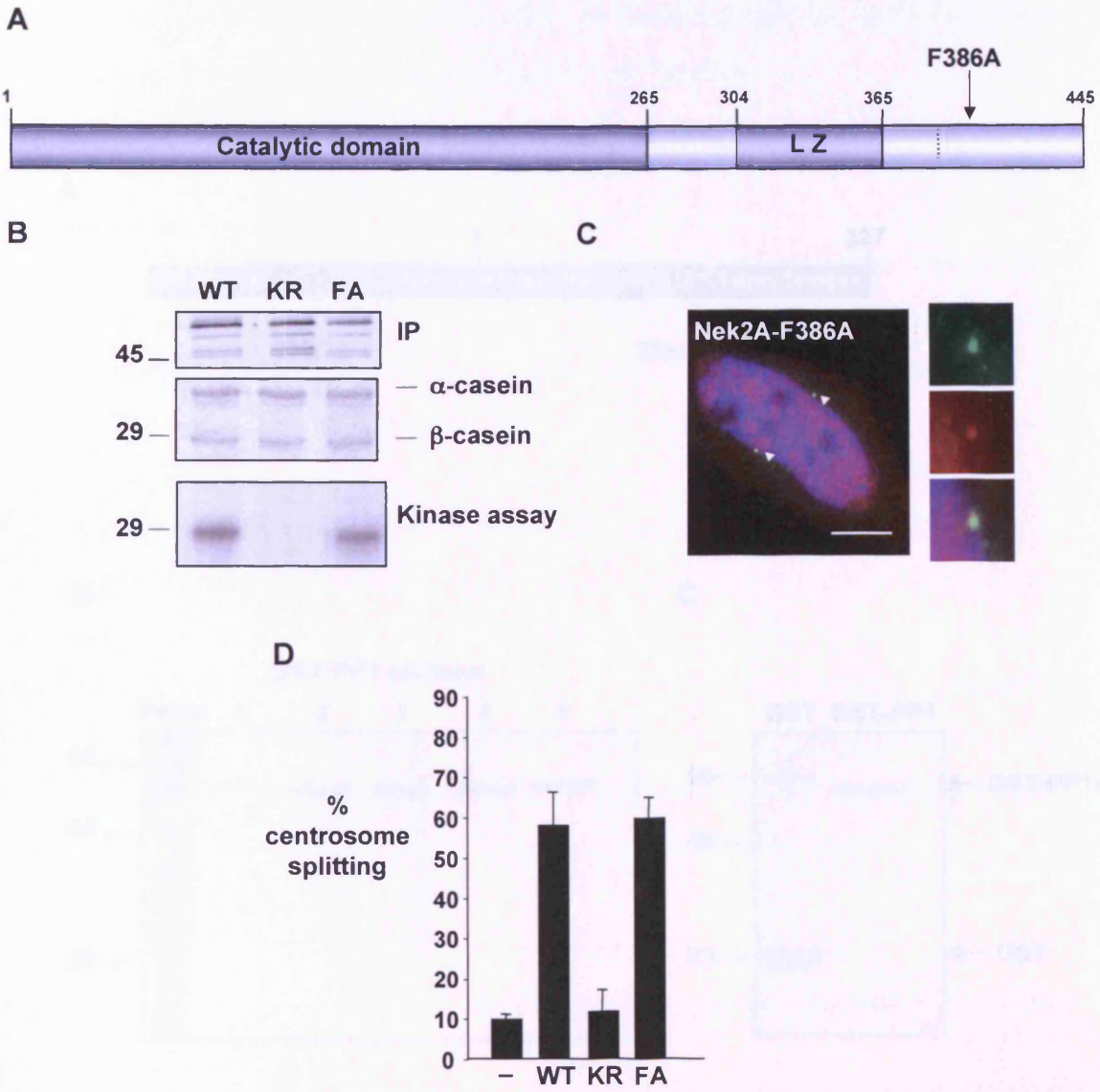

Figure 3.12 Mutation of the PP1 binding site has no effect on Nek2A activity *in vitro*
A. A schematic diagram of Nek2A indicating the position of the F386 mutation. **B.** The myc tagged Nek2A-WT, Nek2A-KR and Nek2A-FA constructs were *in vitro* translated and tested as described in Figure 3.5. **C.** U2OS cells were transfected with the myc-tagged Nek2A-WT and Nek2A-F386A constructs for 24 hours. Cells were fixed with methanol and stained with a myc antibody to highlight Nek2 (red), a C-Nap1 antibody to target the centrosome (green) and Hoechst 33258 to highlight the DNA (blue). Scale bar, 10 μm. White arrowheads point to centrosomes. Inserts are enlargements of the centrosome region. **D.** Approximately 100 transfected cells were counted in three independent experiments and the centrosomes scored as either split or non-split. Similar results were obtained for HeLa cells. Untransfected cells were scored as a control (–).

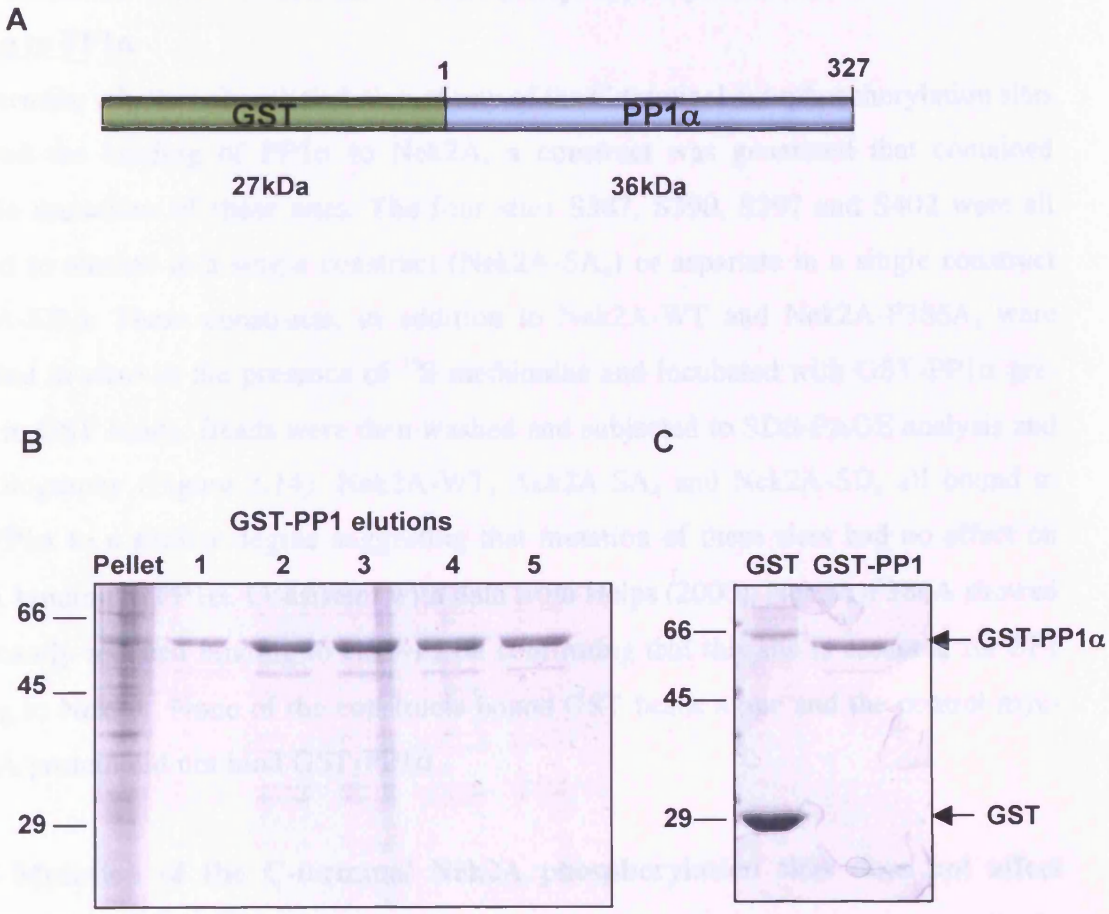

Figure 3.13 Cloning and expression of a GST-PP1α protein

A. Schematic diagram of the GST-PP1α construct. **B.** The protein was expressed in BL21 *E. coli.* The expressed protein was purified using glutathione sepharose and the eluted fractions (1-5) separated by SDS-PAGE and stained with Coomassie Blue. **C.** The GST protein alone was also expressed and both the GST and GST-PP1α dialyzed and analysed on a Coomassie Blue stained gel. Protein concentrations are 7 mg/ml for the GST-PP1α construct and 25 mg/ml for GST. M.wt markers (kDa) are indicated on the left.

glutathione beads. A single band of 63 kDa, the predicted size for GST-PP1α, was obtained giving, after dialysis, a protein preparation of 7 mg/ml.

3.2.13 Mutation of the C-terminal Nek2A autophosphorylation sites does not affect binding to PP1α

To determine whether phosphorylation of any of the C-terminal autophosphorylation sites regulated the binding of PP1α to Nek2A, a construct was generated that contained multiple mutations of these sites. The four sites S387, S390, S397 and S402 were all mutated to alanine in a single construct (Nek2A-SA_4) or aspartate in a single construct (Nek2A-SD_4). These constructs, in addition to Nek2A-WT and Nek2A-F386A, were translated *in vitro* in the presence of ^{35}S-methionine and incubated with GST-PP1α pre-bound to GST beads. Beads were then washed and subjected to SDS-PAGE analysis and autoradiography (Figure 3.14). Nek2A-WT, Nek2A-SA_4 and Nek2A-SD_4 all bound to GST-PP1α to a similar degree suggesting that mutation of these sites had no effect on Nek2A binding to PP1α. Consistent with data from Helps (2000), Nek2A-F386A showed significantly reduced binding to GST-PP1α confirming that this site is essential for PP1 binding to Nek2A. None of the constructs bound GST beads alone and the control myc-lamin A protein did not bind GST-PP1α.

3.2.14 Mutation of the C-terminal Nek2A phosphorylation sites does not affect Nek2A activity *in vitro* or *in vivo*

As mutation of the four autophosphorylation sites clustered around the PP1 binding site appear to have little effect on binding of PP1α to Nek2A, we decided to determine whether these mutations had any effect on Nek2 activity. Upon transfection into U2OS cells, both myc-Nek2A-SA_4 and myc-Nek2A-SD_4 localised to the centrosome and induced similar levels of centrosome splitting as the wild-type kinase (Figure 3.15). However, *in vitro* kinase assays performed on immunoprecipitated proteins generated either by *in vitro* translation or transient transfection into U2OS cells demonstrated that the myc-Nek2A-SA_4 and myc-Nek2A-SD_4 proteins had very similar activities to the wild-type kinase (Figure 3.16).

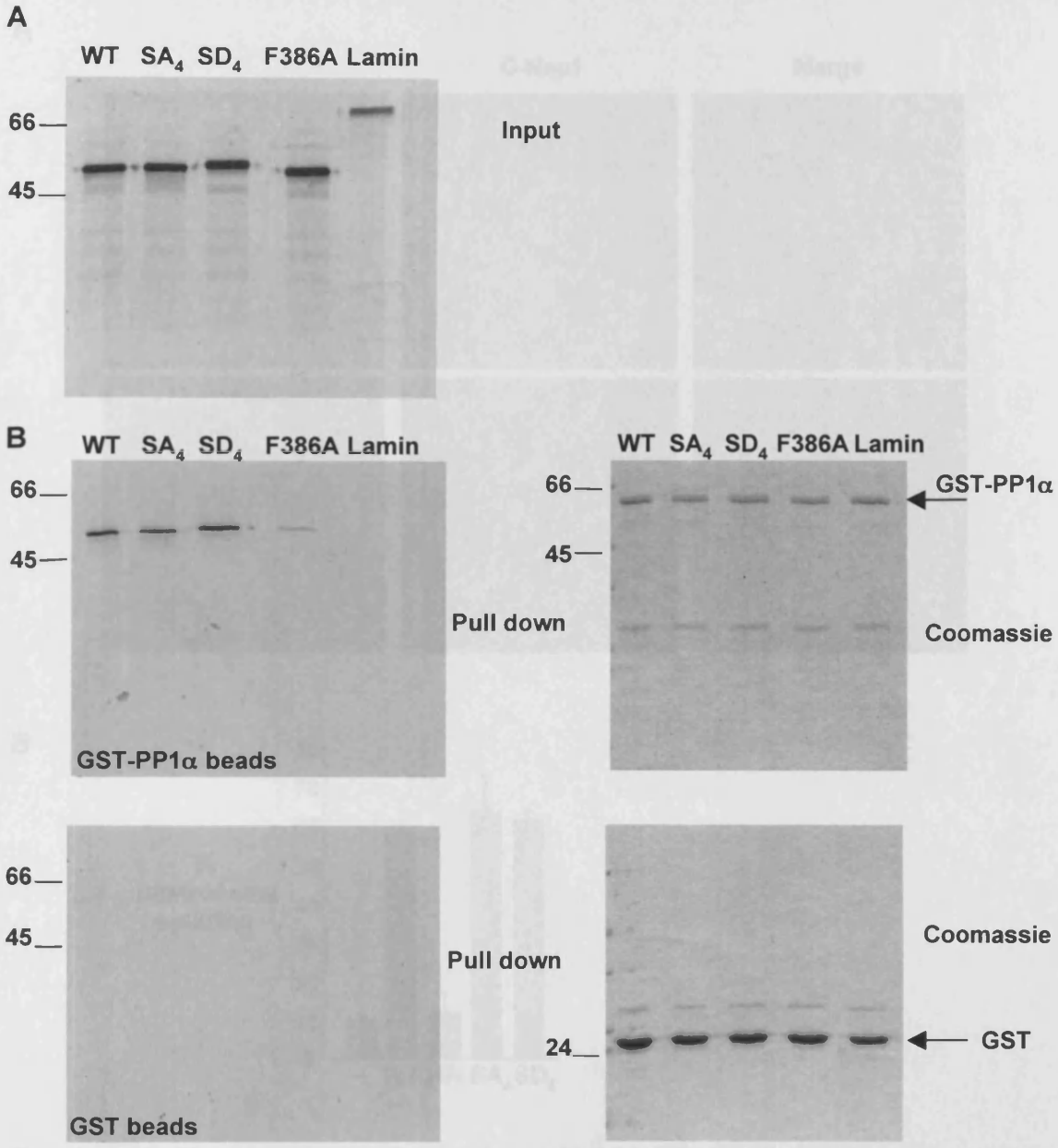

Figure 3.14 Nek2A CTD autophosphorylation sites do not affect PP1 binding
A. Nek2A constructs, myc-Nek2A wild type (WT), myc-Nek2A(SA_4), myc-Nek2A(SD_4), myc-Nek2-F386A and myc-Lamin A were translated *in vitro* in the presence of ^{35}S-methionine and 10% of the reaction analysed by SDS-PAGE gel and exposed to X-ray film. **B.** The remaining IVT mixes were bound for two hours to glutathione beads pre-bound to GST-PP1α (top panels) or GST alone (bottom panels). The beads were then washed in NETN buffer and analysed by SDS-PAGE and autoradiography (left panels). The Coomassie Blue stained gels are also shown (right panels).

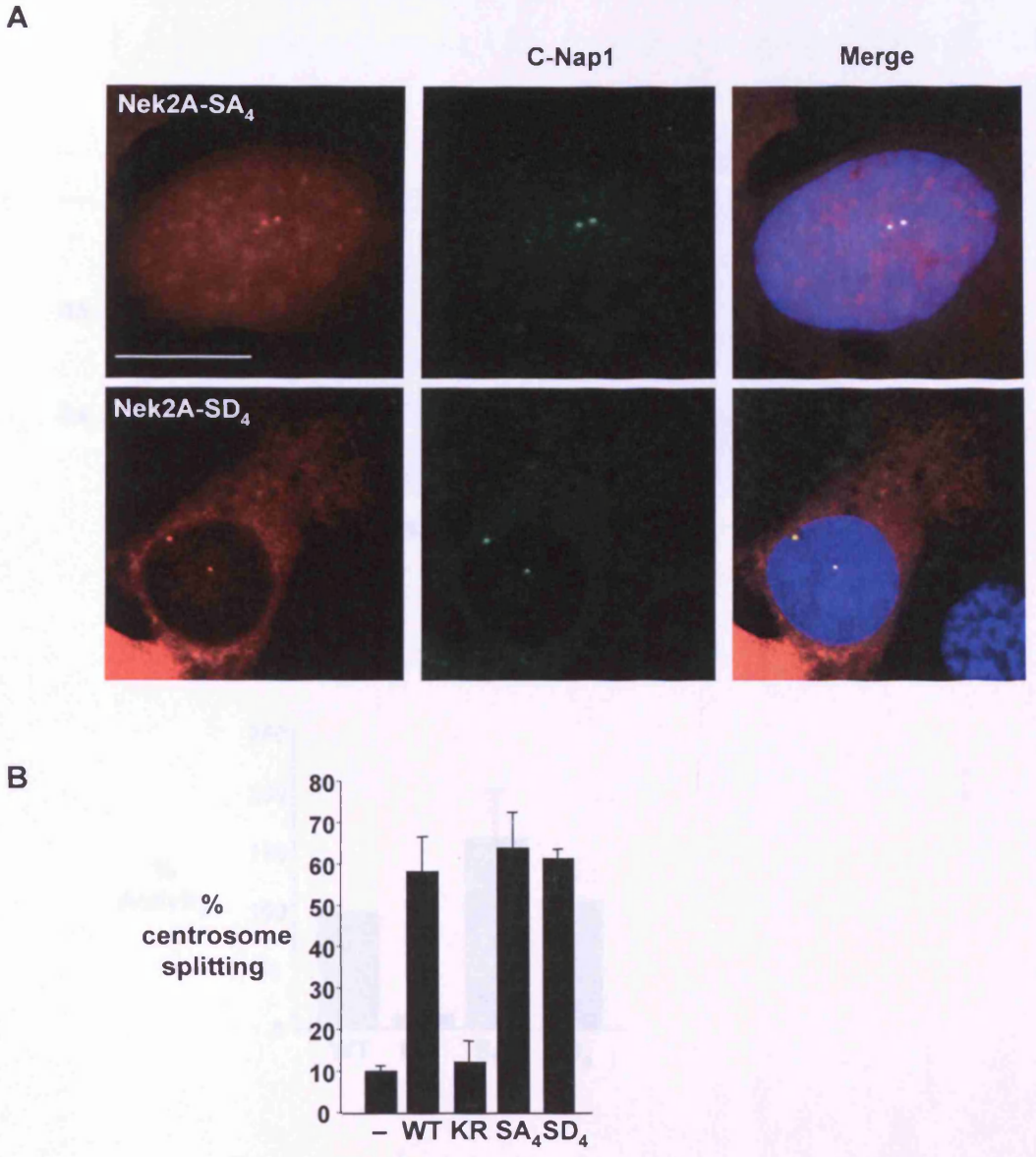

Figure 3.15 The myc-Nek2A-SA_4 and myc-Nek2A-SD_4 localize to the centrosomes and induce centrosome splitting similar to that of the Nek2A-WT kinase

A. U2OS cells were transfected with the myc-Nek2A-SA_4, and myc-Nek2A-SD_4 constructs for 24 hours. Cells were fixed with methanol and stained with a myc antibody to highlight Nek2 (red), a C-Nap1 antibody to reveal the centrosome (green) and Hoechst 33258 to highlight the DNA (blue). Scale bar, 10 μm. **B.** Approximately 100 transfected cells were counted in three independent experiments and the centrosomes scored as either split or non-split. Untransfected cells were scored as a control (–).

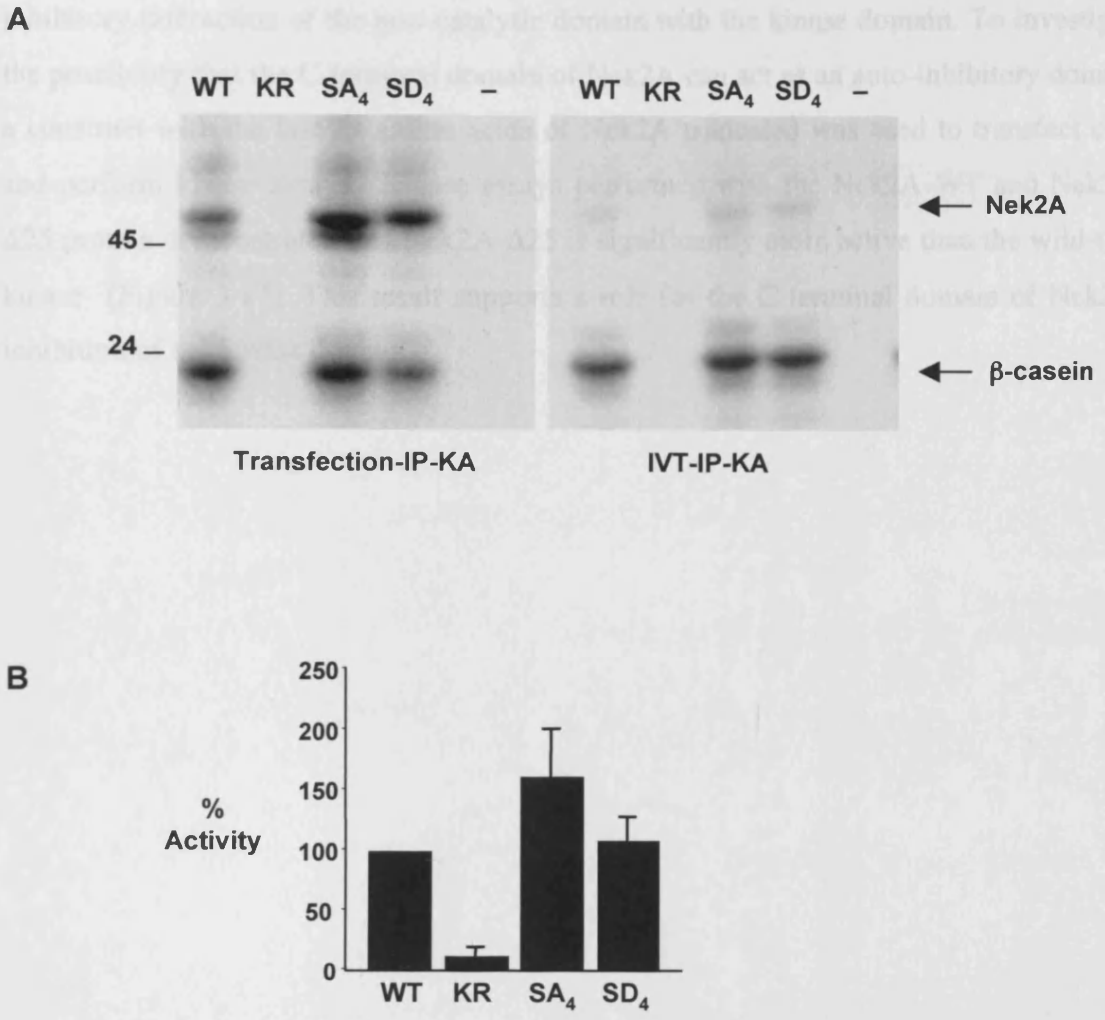

Figure 3.16 The activity of myc-Nek2A-SA_4 is increased but myc-Nek2A-SD_4 is similar to that of the wild-type kinase

A. U2OS cells were transfected (left panel) with myc-Nek2A-WT, myc-Nek2A-KR, myc-Nek2A-SA_4, myc-Nek2A-SD_4 and pRcCMV vector alone. Cells were harvested and lysed in Neb buffer and proteins immunoprecipitated with a Myc antibody. The immune complexes were used in a kinase assay with casein as a substrate. Alternatively, the constructs were translated *in vitro*, immunoprecipitated and subjected to a kinase assay (right panel). **B.** The relative activity of each construct was calculated by scintillation counting the individual Coomassie Blue stained β-casein bands of the IVT-IP kinase assays. The histogram represents the mean of three separate experiments. Wild type activity is taken as 100%.

3.2.15 The C-terminal domain of Nek2A may act as an auto-inhibitory domain

A number of protein kinases, including Plk1, are negatively regulated through an auto-inhibitory interaction of the non-catalytic domain with the kinase domain. To investigate the possibility that the C-terminal domain of Nek2A can act as an auto-inhibitory domain, a construct with the last 25 amino acids of Nek2A truncated was used to transfect cells and perform kinase assays. Kinase assays performed with the Nek2A-WT and Nek2A-Δ25 protein demonstrated that Nek2A-Δ25 is significantly more active than the wild-type kinase (Figure 3.17). This result supports a role for the C-terminal domain of Nek2 in inhibition of the kinase domain.

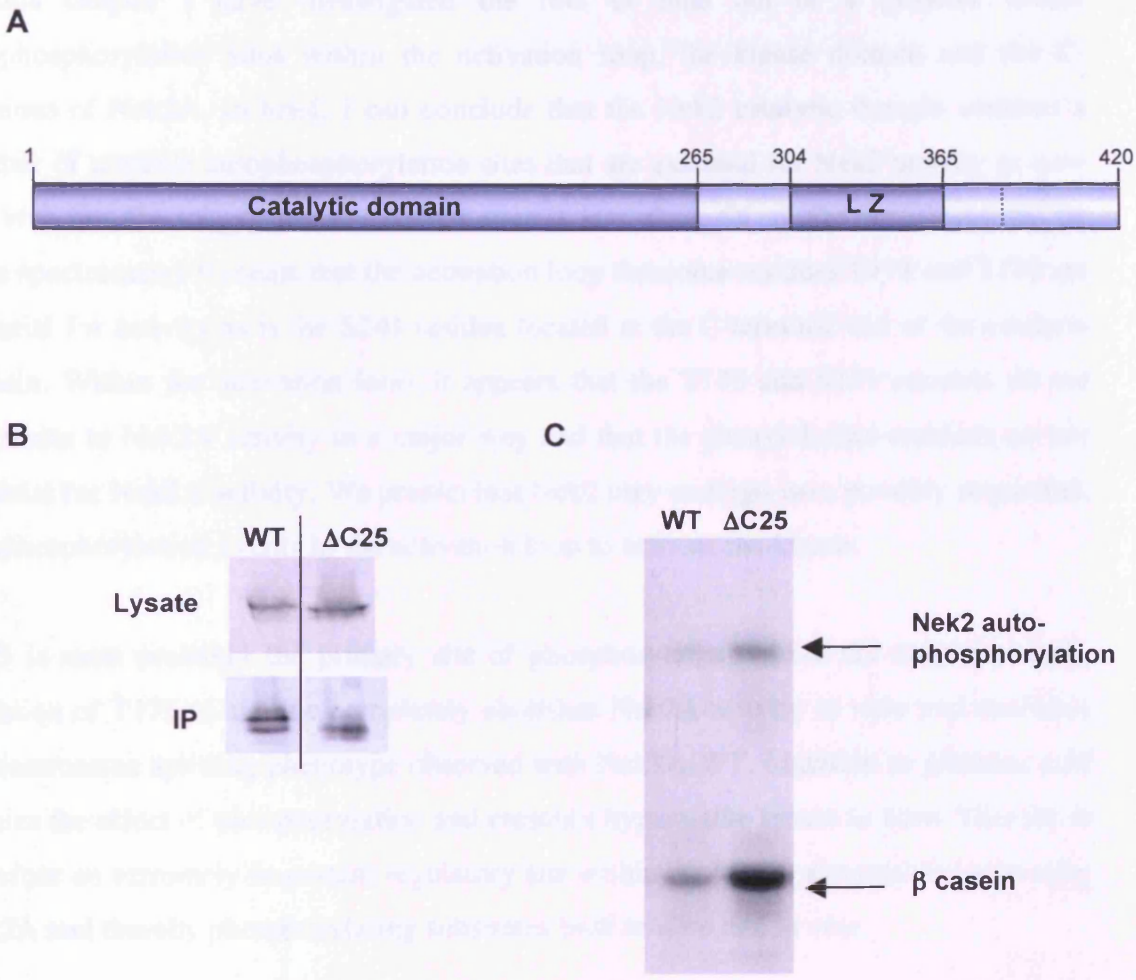

Figure 3.17 Nek2A-ΔC25 has elevated kinase activity compared to Nek2A-WT
A. Schematic diagram representing the Nek2A-Δconstruct. **B.** GFP-Nek2A-WT and GFP-Nek2A-ΔC25 were transiently transfected into HeLa cells for 24 hrs followed by lysis and immunoprecipitation using an anti-GFP antibody. Western blots of lysate (anti-GFP, top panel) and immunoprecipitation (anti-Nek2, bottom panel) show equalized protein levels. **C.** The immunoprecipitations were incubated with kinase buffer containing ^{32}P γ-[ATP] and casein for 30 mins at 30°C. Samples were analysed by SDS-PAGE and autoradiography. The experiments were carried out three times and each demonstrated that Nek2A-ΔC25 was more active than the wild-type. Plasmid construction, transfections and immunoprecipitations were carried out by Dr. Michelle Hayes.

3.3 Discussion

In this chapter I have investigated the role of nine out of a possible twelve autophosphorylation sites within the activation loop, the kinase domain and the C-terminus of Nek2A. In brief, I can conclude that the Nek2 catalytic domain contains a number of possible autophosphorylation sites that are essential for Nek2 activity *in vitro* and *vivo* but the role of the C-terminal sites is less clear. Of all the sites identified by mass spectrometry it seems that the activation loop threonine residues T175 and T179 are essential for activity as is the S241 residue located at the C-terminal end of the catalytic domain. Within the activation loop, it appears that the T170 and S171 residues do not contribute to Nek2A activity in a major way and that the phenylalanine residues are not essential for Nek2A activity. We predict that Nek2 may undergo two, possibly sequential, autophosphorylation events in the activation loop to activate the kinase.

T175 is most probably the primary site of phosphorylation within the activation loop. Mutation of T175 to alanine completely abolishes Nek2A activity *in vitro* and abolishes the centrosome splitting phenotype observed with Nek2A-WT. Mutation to glutamic acid mimics the effect of phosphorylation and creates a hyperactive kinase *in vitro*. This site is therefore an extremely important regulatory site within the kinase essential for activating Nek2A and thereby phosphorylating substrates both *in vitro* and *in vivo*.

Mutation of T179 to alanine or glutamate completely abolished Nek2 kinase activity *in vitro* and reduced it *in vivo*. It is plausible that the mutation of T179 to glutamate did not mimic phosphorylation of this site and therefore the phenotype observed mimicked that of the mutation to alanine. However, it is also plausible that this site plays a structural role within the activation loop. As mentioned previously, this site is equivalent to the anchor residue T165 of Cdk2. Structually, this residue is required to anchor the activation loop within Cdk2. Interestingly, the preceding residue in Nek2 is glycine and mutation of this glycine residue in PKA abolishes kinase activity (Nolen et al., 2004). One conclusion therefore maybe that T179 acts structurally to retain the integrity of the Nek2 activation loop and its mutation abolishes kinase activity via structural damage to the kinase. However, if mutation of this site were to cause any major conformational change then it

may be expected to cause the protein to mis-localise. In contrast, the mutant protein still localises to the centrosome (Figure 3.7). Therefore, it remains plausible that along with T175, T179 represents a second important regulatory phosphorylation site required for Nek2 activity.

In addition to the primary sites of phosphorylation, a number of additional sites may be required for full activation of the kinase. These, however, may elicit only weak effects. T170 and S171 when mutated to alanine or aspartate/glutamate showed no significant difference in activity compared to the wild-type kinase. These sites therefore are either (i) not *in vivo* phosphorylation sites, or (ii) play only a small role in Nek2 activation that cannot be detected in the assays performed. In addition to the activation loop phosphorylation sites, identified by mass spectrometry a fifth site resides toward the C-terminal end of the catalytic domain (S241). This site is conserved within Nek2 kinases but is not a recognised site within wider kinase families. Mutation to alanine or aspartate rendered the kinase inactive *in vitro* and *in vivo*. This suggests that the site is essential for Nek2 activity. Phosphorylation of this site may allosterically position the kinase into a more active conformation. The aspartate group though did not activate the kinase. Again this could be because it cannot mimic the effect of phosphorylation, or that the site may be required to maintain the structure of the kinase domain.

In addition to the *bona fide* autophosphorylation sites identified through mass spectrometry, I have also investigated two sites within the activation loop which may contribute to Nek2A activity, namely F172 and F176. F172 and F176 were mutated to alanine to determine whether they are essential residues within a Nek2A consensus site. If so this motif may be found in other Nek2 substrates. Unfortunately, though, the assays performed have given conflicting results as to the importance of these sites. Kinase assays (*in vitro*) of Nek2A-F172A and Nek2A-F176A reveal the proteins to have increased activity to that of the wild type kinase. However, *in vivo* the level of kinase activity as judged by centrosome splitting assays is decreased to nearly 50% of the wild-type kinase. The discrepancies between the two assays may suggest that the Nek2A mutant proteins are behaving differently in these two environments or that these

phenylalanines are only required for phosphorylation of genuine *in vivo* substrates like C-Nap1 or rootletin.

Many kinases are involved in cell cycle processes each with specificity for discrete substrates. In contrast there are only a few phosphatases, one of which is PP1. PP1 is brought into close proximity to its substrates via regulatory subunits which possess a KVHF binding motif. Some of these regulatory subunits may themselves be substrates of PP1. Nek2A contains a KVHF motif in its C-terminal domain. In Nek2A this motif is immediately followed by a serine residue and, upon inspection of other PP1 regulatory subunits several also have either a serine or threonine at this site (Terrak et al., 2004). Although the KVHF motif is conserved, the area around the motif has little conservation of residues. This suggests that this serine residue may play an important role in PP1 binding. Mutation of this residue and three other serine residues in the C-terminal domain of Nek2A had little effect on kinase activity and did not affect PP1 binding *in vitro*. In conclusion, the results demonstrate that the four sites located around the PP1 binding site do not play a role in regulating Nek2 activity structurally or in PP1 binding. Further investigation into these sites may reveal whether they are involved in substrate targeting or other as yet unidentified processes. Mutation of F386 of the 'KVHF' motif to alanine was predicted to produce a hyperactive protein both *in vitro* and *in vivo*. The site has been demonstrated by Helps (2002) and in this study as essential for PP1 binding. However, the activity of Nek2A-F386A *in vitro* and *in vivo* was similar to that of the wild-type protein. *In vitro* this result can be explained by the lack of PP1 in the rabbit reticulocyte lysate and as such mutation of the PP1 binding site would have little or no effect on Nek2A-F386A activity. Centrosome splitting assays confirm that Nek2A-F386A activity is similar to that of the wild type kinase. However, *in vivo* there appears to be an upper limit to the frequency of centrosome splitting that can be achieved suggesting other mechanisms are in place to prevent 100% centrosome splitting from occurring. Therefore further investigation of the F386 site upon Nek2A activity needs to be performed.

Many kinases although activated by activation loop phosphorylation have different regulatory mechanisms which contribute to their activity (Huse and Kuriyan, 2002). One

such mechanism may be through inhibition by the non-catalytic domain. This is true for Plk1 where truncation of the C-terminal non-catalytic domain leads to increased kinase activity (Mundt et al., 1997). We have performed initial experiments with Nek2A-Δ25 which lacks the C-terminal 25 amino acids. This mutant appears to have increased kinase activity compared to the wild-type kinase. This suggests that, like Plk1, Nek2A may also exhibit control over its activity through use of an auto-inhibitory domain. This however, is not affected by the autophosphorylation of the C-terminal residues identified within Nek2A. It would be interesting to express the C-terminal 25 amino acids of Nek2A and determine if this construct inhibits the activity of the Nek2A kinase.

A summary of the various Nek2A mutants and their relative activities compared to the wild type kinase can be seen in Figure 3.19. In conclusion, Nek2A activity is regulated by phosphorylation at T175, and by structural or possibly secondary autophosphorylation events at position T179 and S241. In addition Nek2A behaviour may be mediated by PP1 inhibition and by inhibition via its own C-terminal domain.

A

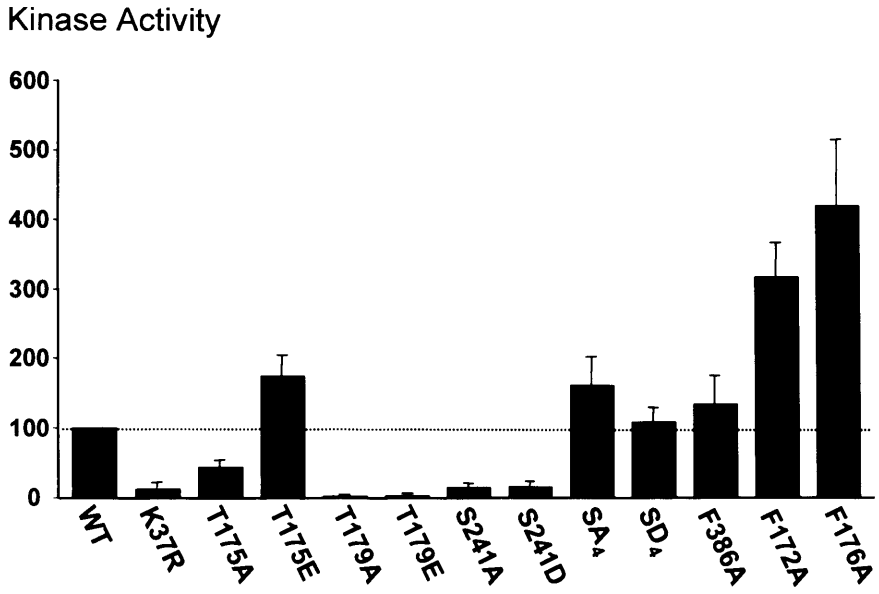

B

	WT	K37R	T175A	T175E	T179A	T179E	S241A	S241D	SA4	SD4	F386A	F172A	F176A
Average	100	4	33	165	37	27	15	16	162	109	135	318	420
Std.Error	0	7	8	29	1	1	5	5	39	20	39	47	93

C

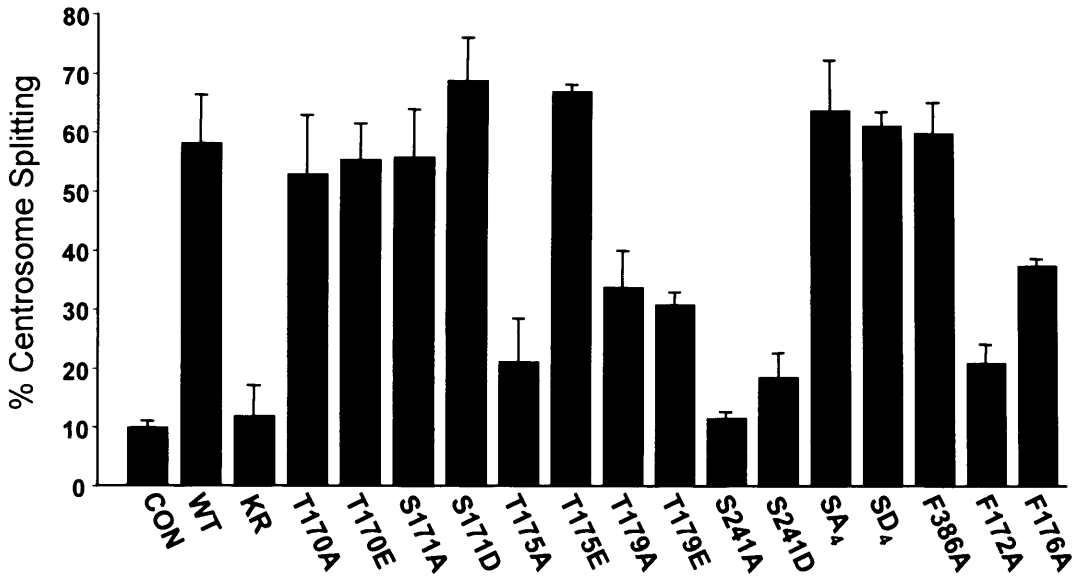

D

	CON	WT	KR	T170A	T170E	S171A	S171D	T175A	T175E
Average	11	58	12	53	56	56	69	21.	67
Std.Error	1	8	5	10	6	8	7	7	1

	T179A	T179E	S241A	S241D	SA_4	SD_4	F386A	F172A	F176A
Average	34	31	12	19	64	61	60	21	37
Std.Error	6	2	1	4	8	2	5	3	1

Figure 3.18 A summary of the Nek2A mutations and their activity

A. Histogram to represent the relative activity of the Nek2A mutations compared to wild-type kinase using *in vitro* kinase assays. **B.** Table showing the average percentage activity of Nek2A mutants compared to those of wild-type kinase. **C.** Histogram to represent the relative levels of centrosome splitting of the Nek2A mutations compared to wild-type kinase following transfection in U2OS cells. **D.** Table showing the average percentage of centrosome splitting of Nek2A mutants compared to those of wild-type kinase.

Chapter 4

Nlp (Ninein like protein): its regulation by Nek2 and Plk1 kinases

4.1 Introduction

Nlp was first identified in a yeast two-hybrid screen using Plx1 as bait and was found to be an important substrate for Plk1 (Casenghi et al., 2003). Nlp is a centrosomal protein during interphase but is absent from mitotic spindle poles. Nlp is phosphorylated by Plk1 at up to eight sites and the phosphorylation of Nlp by Plk1 regulates the interaction of Nlp with both centrosomes and γ-TuRCs (Casenghi et al., 2003). The function of Nlp at the interphase centrosome may be to recruit γ-tubulin and other components of the γ-TuRC such as hGCP4. Nlp may then be involved in microtubule nucleation up to the G2/M transition when its phosphorylation by Plk1 causes its displacement from centrosomes, possibly to allow centrosome maturation and spindle assembly to occur. Overexpression of a mutant that can no longer be phosphorylated by Plk1 causes severe defects in spindle formation (Casenghi et al., 2003).

Plk1 is a cell-cycle regulated kinase with protein levels low in G1, increasing in S through to G2/M and decreasing rapidly after mitosis. It appears at the centrosome during G2 and early mitosis (Golsteyn et al., 1995). The kinase is phosphorylated at G2/M giving it maximal activity and its activity is reduced 5-10 fold when dephosphorylated (Hamanaka et al., 1995). Plk1, in common with all Plk kinases, shares a conserved structure consisting of an amino-terminal kinase domain and a carboxy-terminal regulatory domain containing two conserved polo boxes. Together, these polo boxes constitute the Polo box domain (PBD). The PBD has been implicated in the regulation of Plk1 kinase activity and its localisation. The PBD has recently been shown to be a region by which the kinase can dock onto a pre-phosphorylated substrate at the consensus SpS/T and then proceed to phosphorylate the same protein at a different site (Elia et al., 2003a; Elia et al., 2003b).

This model for recognition of substrates by Plk1 requires a priming kinase to pre-phosphorylate Plk1 targets. So far, Cdk1 and Plk1 itself have been proposed as priming kinases (Nigg, 1998). Nek2 is also cell cycle-regulated with maximal levels at the G2/M transition and therefore may be a perfect candidate to prime Nlp for phosphorylation by Plk1 at the centrosome. In this chapter, I discuss results that suggest that Nek2 may

indeed be a priming kinase for Plk1 upon Nlp. Through *in vitro* kinase assays and cotransfection we have demonstrated that the Nek2 protein kinase can phosphorylate Nlp at sites distinct from those targeted by Plk1 (this work, and Rapley et al., 2005). In addition we demonstrate that wild-type Nek2A can stimulate the phosphorylation of Nlp by Plk1 while the presence of inactive Nek2A can inhibit the phosphorylation of Nlp by Plk1 *in vitro* and *in vivo*.

Large aggregates of Nlp form around centrosomes in cells overexpressing GFP-Nlp suggesting that Nlp can form oligomers. These aggregates can be displaced from the centrosome by coexpression of the Nek2A-WT protein but not the Nek2A-KR protein suggesting that phosphorylation of Nlp by Nek2A can interfere with its oligomerisation state (Rapley et al., 2005). Overexpression of the active Nek2A protein in human cells can also displace endogenous Nlp from the centrosome. Meanwhile, addition of the Nek2A-KR protein prevents displacement of endogenous Nlp from cells expressing active Plk1. This suggests that inactive Nek2A may block the phosphorylation of Nlp by Plk1 (Rapley et al., 2005).

Nlp is primarily concentrated around the mother centriole of interphase centrioles (Rapley et al., 2005). This suggests that it may contribute to microtubule anchoring, possibly as a result of binding microtubules capped at their minus ends with γ-TuRCs. Overexpression of GFP-Nlp alone leads to an increased density of microtubules surrounding the centrosome (Casenghi et al., 2003). However, we show here that these disappear upon co-expression of either active Nek2A or active Plk1. These results provide further information regarding the mechanism by which Nlp is regulated by phosphorylation.

4.2 Results

4.2.1 Expression and purification of GST-Nlp-NTD and GST-Nlp-NTDΔ8

To investigate whether Nek2A can phosphorylate Nlp i*n vitro* it was first necessary to express and purify the Nlp-NTD (N-terminal domain, amino acids 1-702) protein for use in *in vitro* kinase assays. We also wished to test whether Nek2A could phosphorylate an Nlp-NTD protein that lacked the Plk1 phosphorylation sites. These two constructs were provided by Prof. E. Nigg (Martinsreid, Germany) and consisted of either a wild-type or mutant NTD region of Nlp fused to an N-terminal GST tag. The mutant NTD lacked the eight putative Plk1 sites due to mutation of the relevant serines or threonines to alanine. Four of these residues had been confirmed as *in vitro* Plk1 target sites by mass spectrometry and the others were chosen based on their homology to the known Plk1 consensus target site (Figure 4.1). The NTD of Nlp was chosen for this study as we wished to explore the possibility that Nek2A may be a priming kinase, and as the Plk1 phosphorylation sites are located within the NTD, this region was chosen.

The two constructs were introduced into BL21 *E. coli* and induced at 24°C for 12 hours with 1 mM IPTG. The Nlp-NTD is approximately 80 kDa and the GST tag 28 kDa making a total of 108 kDa. Following induction with IPTG, the expressed proteins migrated at the predicted size on a polyacrylamide gel (Figure 4.1). These proteins were then purified on glutathione-sepharose beads according to standard procedures. Following elution and subsequent dialysis into 25 mM Hepes pH 7.4, both proteins were ready for use in kinase assays.

4.2.2 Nek2 phosphorylates Nlp at sites distinct from those targeted by Plk1

It was important to determine whether Nek2 can phosphorylate Nlp at sites distinct from those which Plk1 targets. If the target sites are the same, Nek2 and Plk1 phosphorylation of Nlp may be considered to be redundant. However, if the sites are distinct it suggests that a pathway or particular sequence of phosphorylation may be required and this opens the possibility that Nek2 can act as a priming kinase for Plk1.

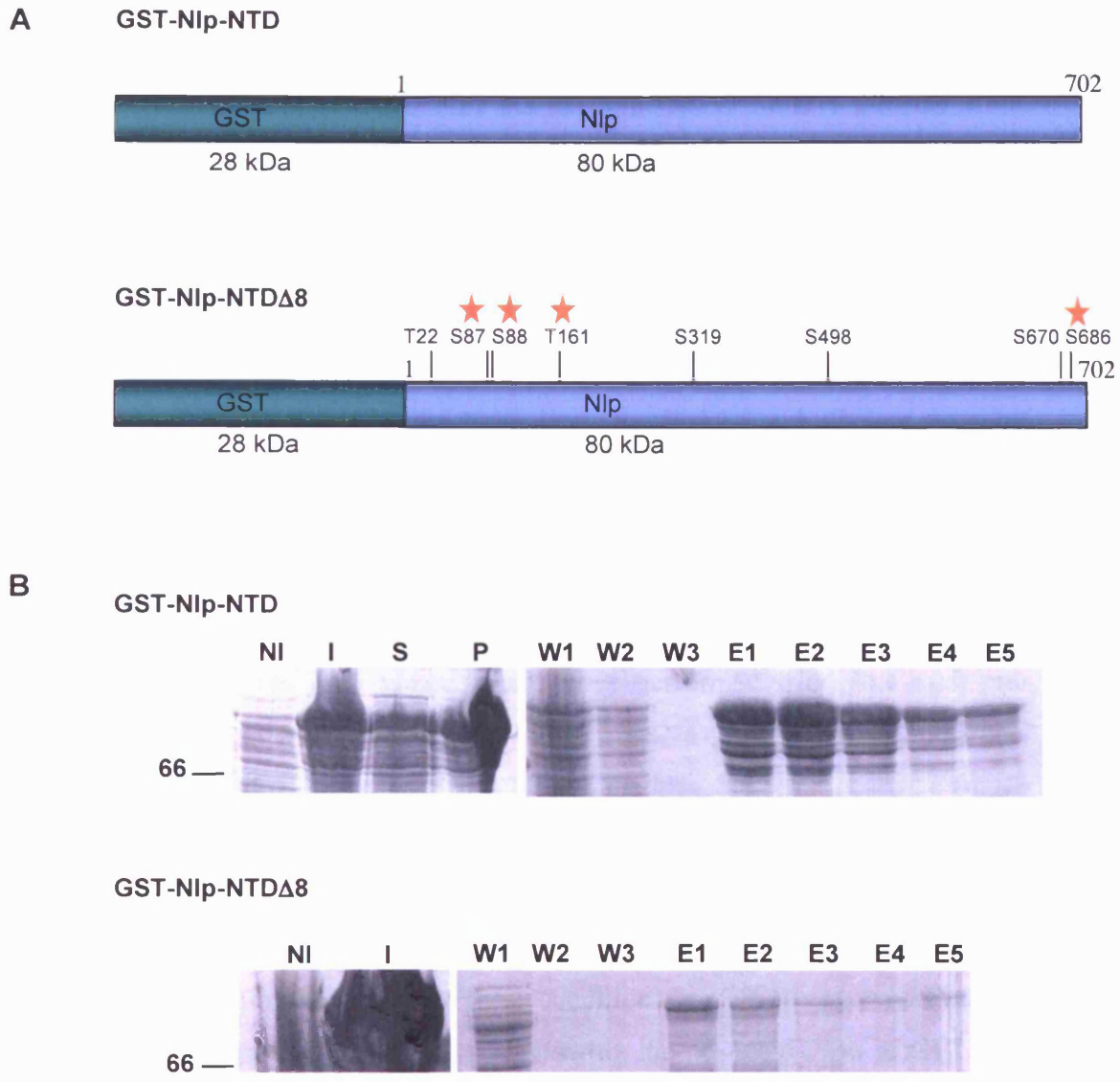

Figure 4.1 Expression and purification of GST-Nlp-NTD and GST-Nlp-NTDΔ8

A. Diagram representing the GST-Nlp-NTD and GST-Nlp-NTDΔ8 constructs. These constructs consist of the first 702 amino acids of Nlp fused to an N-terminal GST tag. The GST-Nlp-NTDΔ8 protein contains mutations of serines and threonines to alanine as indicated. Four of these sites have been identified by mass spectrometry as target phosphorylation sites of Plk1 (star); the remaining four are likely phosphorylation sites of Plk1. **B.** GST-Nlp-NTD and GST-Nlp-NTDΔ8 were expressed from the relevant pGEX vectors in BL21 *E. coli* by induction with 1 mM IPTG. The non-induced (NI), induced (I), supernatant (S) and pellet (P) fractions were separated on a 12% SDS-PAGE protein gel to determine expression and solubility of the protein. The proteins were bound to glutathione beads, washed (W1-3) and eluted in five 1 ml fractions (E1-5). M. wts (kDa) are indicated on the left.

In vitro kinase assays were performed using immunoprecipitated myc-Nek2A-WT and myc-Nek2A-KR kinases (generated as described in 3.1.1) on both the purified GST-Nlp-NTD and GST-Nlp-NTDΔ8 proteins. Plk1-T210D hyperactive kinase, purified from insect cells following expression from a recombinant baculovirus, was also used as a positive control (provided by Prof. E. Nigg, Martinsreid, Germany). The results indicate that Nek2A can phosphorylate both the Nlp-NTD and the Nlp-NTDΔ8 proteins to a similar extent (Figure 4.2A). In contrast, Plk1 can only phosphorylate Nlp-NTDΔ8 to a fraction of that of the Nlp-NTD. The inactive Nek2A-KR protein does not phosphorylate either protein (Figure 4.2B). These results demonstrate that Nek2A and Plk1 are targeting different sites within Nlp *in vitro*.

4.2.3 Nek2A kinase stimulates phosphorylation of Nlp by Plk1

To address the question of whether Nek2A phosphorylation can prime Nlp for phosphorylation by Plk1, *in vitro* kinase assays were performed with Plk1 after pre-incubating GST-Nlp-NTD with myc-Nek2A-WT or myc-Nek2A-KR kinases. The pre-incubation was performed using unlabelled ATP and the kinase assays incubated for 40 minutes to ensure complete saturation of phosphorylation sites by Nek2A. Complete saturation was confirmed by pre-incubation of GST-Nlp-NTD with Nek2A-WT with unlabelled ATP; following this initial incubation, ^{32}P-γ-[ATP] was added and the reaction incubated for a further 40 minutes. Under these conditions, no ^{32}P was incorporated into the GST-Nlp-NTD substrate (Figure 4.3A). Following the pre-incubation of GST-Nlp-NTD with Nek2A protein and unlabelled ATP, Plk1 kinase was added together with ^{32}P-γ-[ATP]. After a further 40 minute incubation, the reaction products were separated by SDS-PAGE and analysed by autoradiography. The results revealed that more ^{32}P was incorporated into the GST-Nlp-NTD substrate by Plk1 as a result of pre-incubation with the wild-type Nek2A kinase than after pre-incubation with no kinase or kinase-inactive Nek2 (Figure 4.3). This result was observed in 5 independent experiments suggesting that pre-phosphorylation of Nlp by Nek2A increases its subsequent phosphorylation by Plk1.

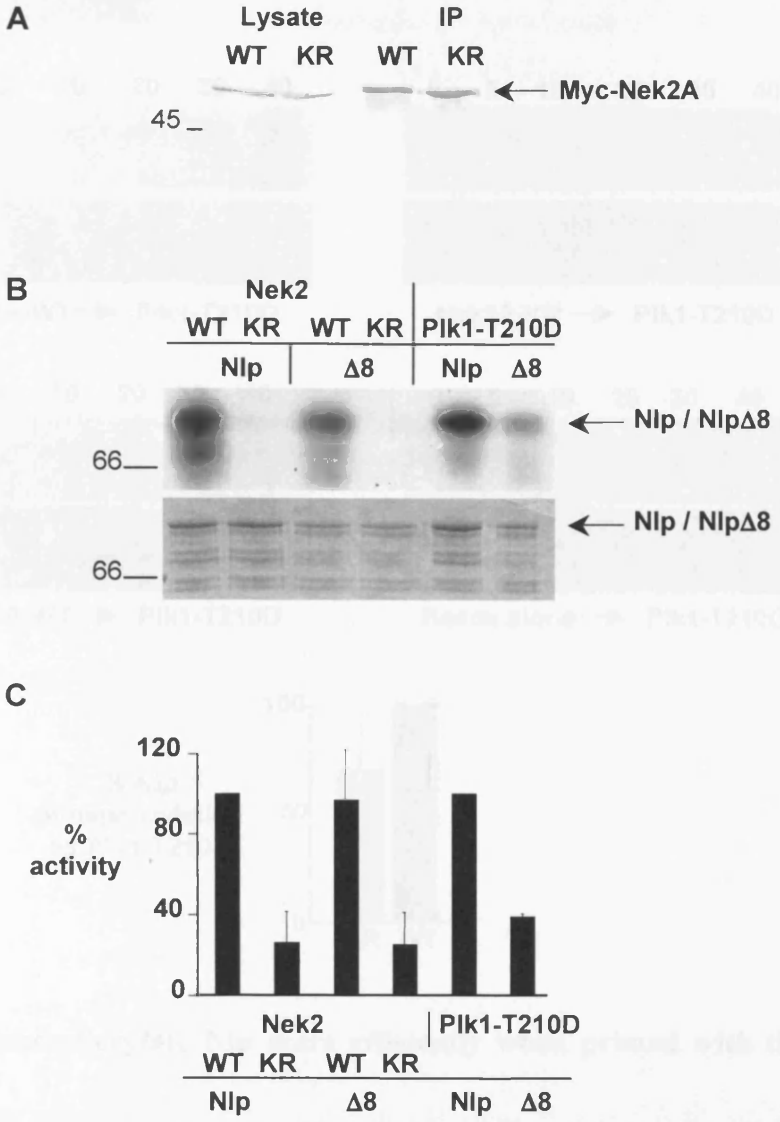

Figure 4.2 Nek2A phosphorylates Nlp at sites distinct from Plk1

A. HeLa cells were transiently transfected with myc-Nek2A-WT and myc-Nek2A-KR for 24 hours. The Nek2A kinases were harvested by cell lysis and immunoprecipitation using an anti-Myc antibody. Lysates and immunoprecipitated proteins were Western blotted using the anti-Myc or Nek2-LZ antibody respectively, to confirm transfection and purification. **B.** GST-Nlp-NTD or the GST-Nlp-NTDΔ8 were mixed with kinase buffer containing ^{32}P-γ-[ATP] for 30 minutes at 30°C with either Nek2A-WT, Nek2A-KR or Plk1-T210D kinases. The reactions were separated by SDS-PAGE and analysed by Coomassie Blue staining (bottom panel) and autoradiography (top panel). M.wts (kDa) are indicated on the left. **C.** The assays were quantified by scintillation counting of the Coomassie Blue stained Nlp or NlpΔ8 proteins and the activity expressed as a percentage of the each active kinase. The reactions were repeated three times and error bars represent the standard deviation. M. wts (kDa) are indicated on the left.

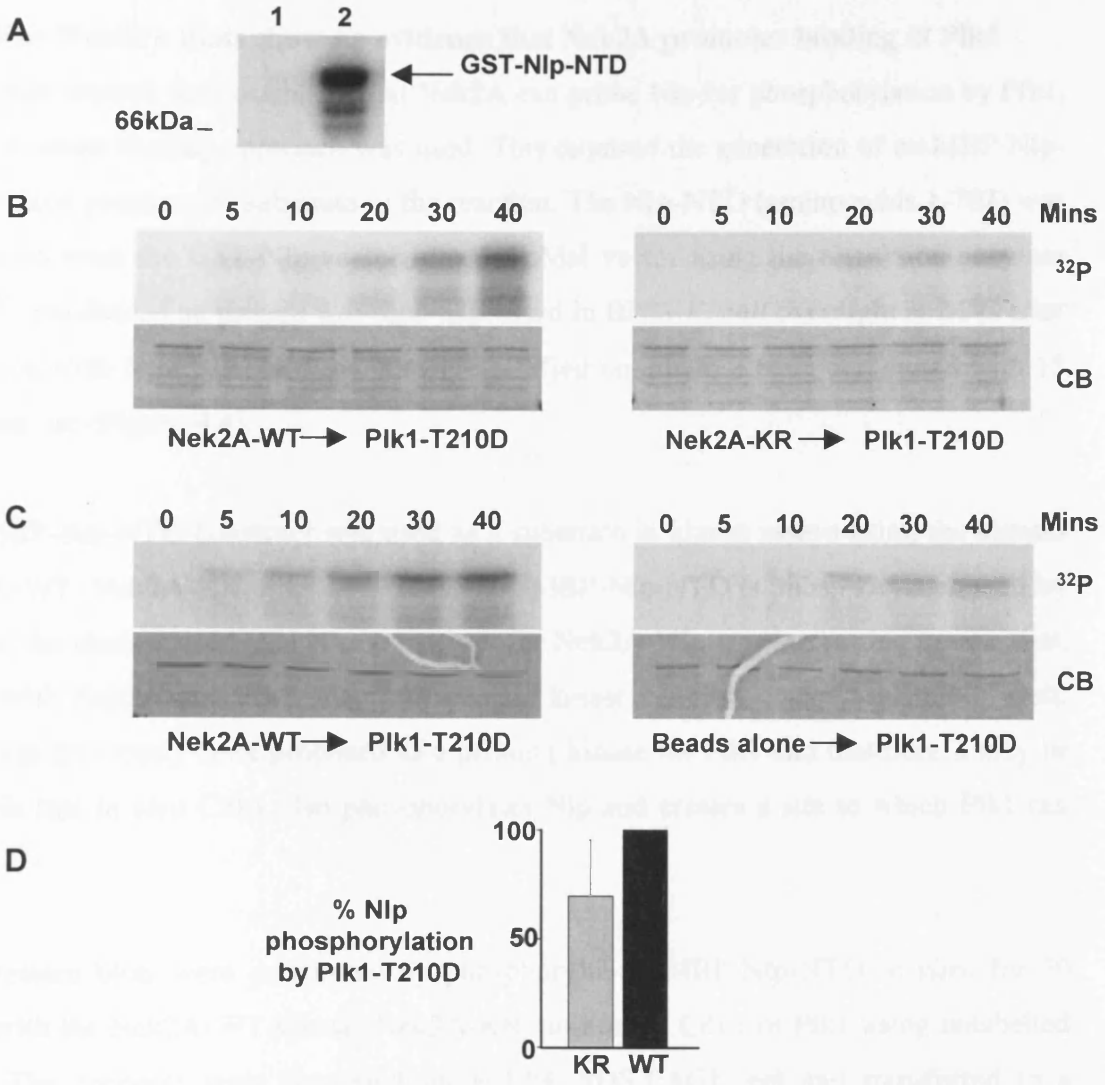

Figure 4.3 Plk1 can phosphorylate Nlp more efficiently when primed with the Nek2 kinase

A. GST-Nlp-NTD was pre-incubated with either Nek2A-WT and unlabelled ATP for 40 minutes followed by the addition of ^{32}P-γ-[ATP] and further incubation for 40 minutes (lane 1) or direct incubation of GST-Nlp-NTD with Nek2A-WT and ^{32}P-γ-[ATP] for 40 minutes (lane 2). **B.** GST-Nlp-NTD was incubated with either immunoprecipitated Nek2A-WT kinase (left panels) or Nek2A-KR (right panels) for 40 minutes in the presence of unlabelled ATP. Purified Plk1 was then added together with ^{32}P-γ-[ATP] and samples taken at the times indicated before separation by SDS-PAGE. Gels were stained with Coomassie Blue (CB) and exposed to autoradiography (^{32}P). In each of five separate experiments, the phosphorylation of Nlp by Plk1 was greater after incubation with Nek2A-WT than Nek2A-KR. **C.** Kinase assays were performed as in panel B, except that phosphorylation of GST-Nlp-NTD by Plk1 was assayed after incubation with either immunoprecipitated Nek2A-WT (left panels) or protein G-sepharose beads alone (right panels). **D.** Histogram represents the relative level of ^{32}P incorporation into GST-Nlp-NTD after 40 minutes incubation with Plk1 following pre-incubation with either Nek2A-WT or Nek2A-KR kinases.

4.2.4 Far-Western blots show no evidence that Nek2A promotes binding of Plk1

To further explore the possibility that Nek2A can prime Nlp for phosphorylation by Plk1, a Far-Western blotting approach was used. This required the generation of an MBP-Nlp-NTD fusion protein as a substrate in the reaction. The Nlp-NTD (amino acids 1-702) was subcloned from the GST-Nlp vector into the pMal vector using the restriction enzymes *BamH1* and *Sal1*. The protein was then expressed in BL21 *E. coli* overnight at 24°C after induction with 1 mM IPTG. Proteins were purified on amylose resin and eluted with 15 mM maltose (Figure 4.4).

The MBP-Nlp-NTD construct was used as a substrate in kinase assays using the kinases Nek2A-WT, Nek2A-KR, Plk1 and Cdk1. The MBP-Nlp-NTD is phosphorylated well by each of the kinases used in this assay except for Nek2A-KR. It is interesting to note that, along with Nek2A and Plk1, the Cdk1 protein kinase can also phosphorylate Nlp well. Cdk1 has previously been proposed as a priming kinase for Plk1 and therefore it may be possible that *in vivo* Cdk1 also phosphorylates Nlp and creates a site to which Plk1 can dock.

Far-Western blots were performed by phosphorylating MBP-Nlp-NTD *in vitro* for 30 mins with the Nek2A-WT kinase, Nek2A-KR, no kinase, Cdk1 or Plk1 using unlabelled ATP. The products were separated on a 12% SDS-PAGE gel and transferred to a membrane via Western Blotting. The membrane was then incubated with 1 μg/ml His-GST-Plk1-PBD (amino acids 300-603) protein (kind gift from Dr. F. Barr, Martinsreid, Germany) for 12 hours at 4°C, washed and then probed using an anti-GST antibody.

If Nek2 phosphorylates Nlp to create a binding site for the Plk1 PBD, then the GST-PBD probe should bind more strongly to Nlp on the membrane after pre-treatment with Nek2A. However, the results demonstrated no significant increase in binding of the GST-PBD to Nlp after phosphorylation by Nek2A-WT. Therefore, this suggests that either there is no binding site created or that the binding site is obscured when Nlp is bound to the membrane (Figure 4.7). However, there was a small increase in GST-PBD binding after phosphorylation of Nlp by Plk1 and a significant increase after phosphorylation by

Cdk1. This could demonstrate that these kinases are capable of creating a PBD binding site upon Nlp. Alternatively, the higher degree of phosphorylation of Nlp generated by these kinases could lead to an increase in non-specific binding of the GST-PBD.

4.2.5 Nek2 depletion does not alter the abundance of Nlp at the centrosome

Overexpression of active Nek2A kinase causes fragmentation of GFP-Nlp aggregates *in vivo* and also displaces endogenous Nlp from the interphase centrosome (Rapley et al., 2005). If Nek2A phosphorylation of Nlp is essential to create a docking site for Plk1, then the removal of Nek2 from the cell should prevent Plk1 from phosphorylating and displacing Nlp. Therefore, Nek2 RNAi was performed by transfection for 48 hours of double-stranded RNA oligonucleotides directed at against Nek2 or lamin (Dharmacon) to deplete endogenous Nek2 from U2OS cells. The intensity of Nlp at the centrosome in prophase and in interphase was measured. The Nek2 depletion was effective in 80% of cells as determined by immunofluorescence microscopy (Figure 4.6).

Depletion of Nek2 did not alter the abundance of Nlp on interphase centrosomes. This demonstrates that the presence of Nlp at interphase centrosomes is not dependent upon Nek2. During prophase Nlp is normally displaced from the centrosome. Depletion of Nek2 did not appear to affect the displacement of Nlp from the centrosome during prophase. Hence, it is possible that the Nek2 kinase is not required for triggering the removal of Nlp from the centrosome at the G2/M transition. However, the depletion may not have been complete.

4.2.6 Kinase-inactive Nek2A inhibits Plk1 phosphorylation of Nlp

To determine the extent of phosphorylation of Nlp by Nek2A and Plk1 *in vivo,* U2OS cells were transiently transfected with the GFP-Nlp construct, alongside myc-tagged Nek2A-WT, Nek2A-KR and Plk1-T210D in various combinations. The aim was to determine whether Nek2A and Plk1 had an additive effect on Nlp phosphorylation and more importantly to determine whether Nek2A-KR prevented Plk1 phosphorylation of Nlp. Upon co-transfection of Nlp with Nek2A and Plk1, a major smear appears above the protein band for GFP-Nlp on a Western blot. This smear is indicative of phosphorylation

A

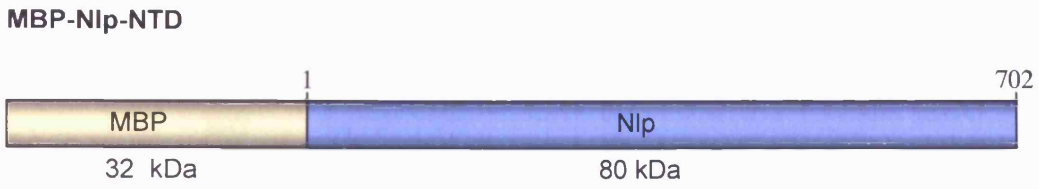

B

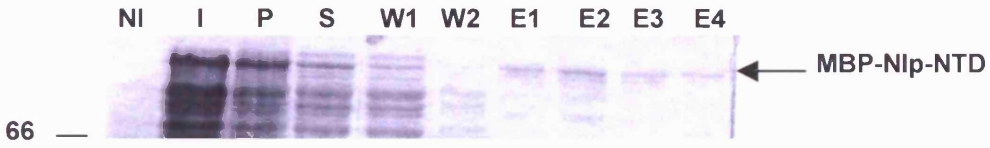

Figure 4.4 MBP-Nlp-NTD expression and purification

A. The Nlp-NTD (amino acids 1-702) was subcloned from the GST-Nlp vector into the pMAL vector using the restriction enzymes *BamH1* and *Sal1*. **B.** MBP-Nlp-NTD was expressed in BL21 *E. coli* by induction with 1 mM IPTG. The non-induced (NI), induced (I), supernatant (S) and pellet (P) fractions were separated on a 12% SDS-PAGE protein gel to determine expression and solubility of the protein. The proteins were bound to amylose beads, washed (W1-2) and eluted in four 1 ml fractions (E1-4). M. wts (kDa) are indicated on the left.

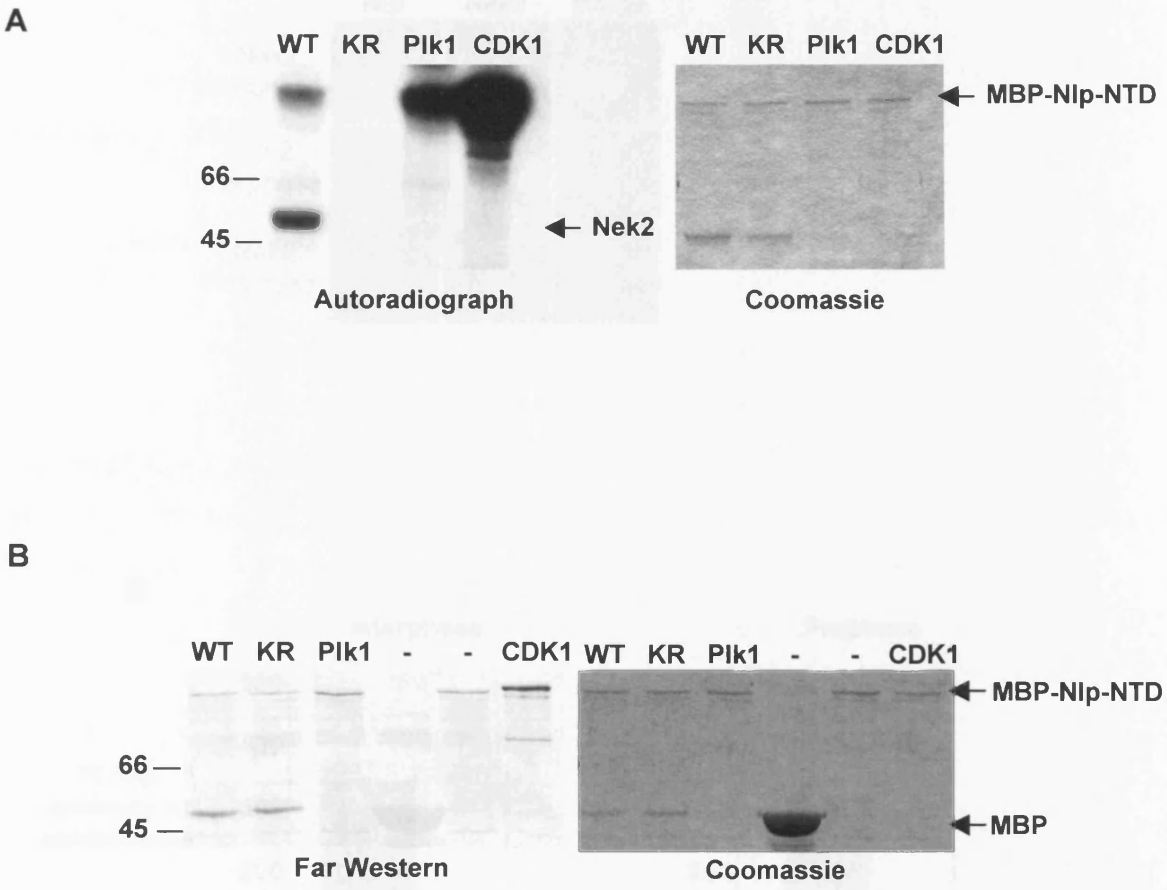

Figure 4.5 Phosphorylation of Nlp by Nek2 does not increase binding of Plk1
A. The purified MBP-Nlp-NTD protein was phosphorylated *in vitro* with Nek2A-WT, Nek2A-KR, Plk1-T210D or Cdk1 as indicated. Nek2A kinases were generated by transfection and immunoprecipitation, whereas Plk1 and Cdk1/cyclin B were obtained as purified proteins. Following the kinase assay, proteins were separated by SDS-PAGE, stained with Coomassie Blue (right panel) and exposed to autoradiography (left panel). **B.** Kinase assays were performed using unlabelled ATP and either Nek2A-WT, Nek2A-KR, Plk1-T210D, Cdk1/cyclin B or no kinase (-) with either MBP-Nlp-NTD or MBP alone. The products were then separated by SDS-PAGE and transferred to a membrane by Western Blotting. The membrane was probed with a purified GST-PBD (1 μg/ml) for 12 hours. After washing, the membrane was probed with an anti-GST antibody (left panel). The Far-Western blot was repeated three times with similar results. A Coomassie Blue stained SDS-PAGE gel is shown (right panel) to demonstrate the relative abundance of each protein. M. wts (kDa) are indicated on the left.

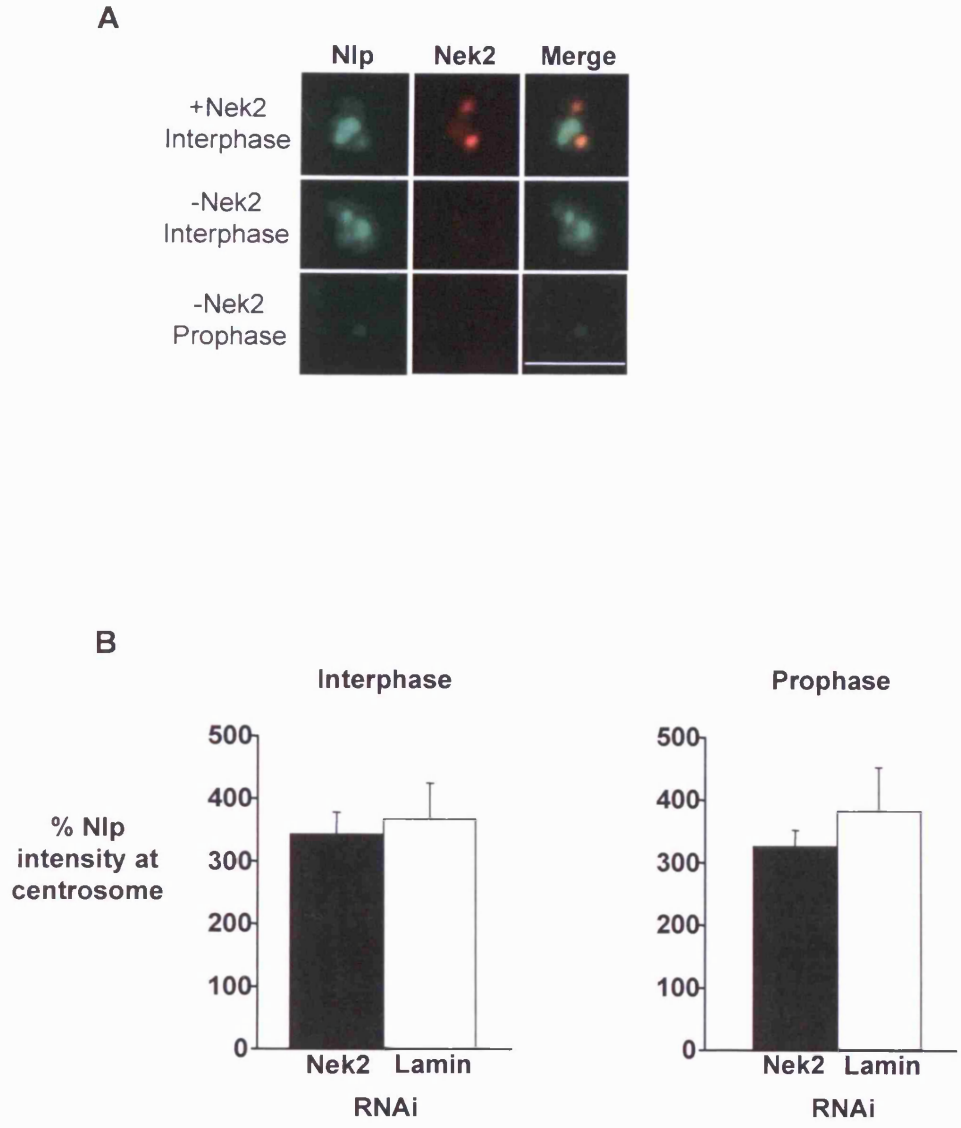

Figure 4.6 Depletion of Nek2 does not significantly alter the abundance of Nlp at the centrosome during interphase or prophase

A. Nek2 was depleted from U2OS cells using dsRNA oligonucleotides directed against the Nek2 mRNA. Cells were processed for immunofluorescence microscopy using anti-Nek2 (red) and anti-Nlp (green) antibodies. High resolution images of the centrosomes alone are shown. Scale bar, 2 μm. **B.** The intensity of Nlp at interphase and prophase centrosomes was measured in Nek2-depleted and lamin-depleted cells. Approximately 30 interphase cells and 10 prophase cells were measured over two separate experiments.

of the Nlp protein and is not present when GFP-Nlp was transfected alone. A weak smear can be observed when GFP-Nlp is transfected with Plk1-T210D but this is not present when GFP-Nlp, Plk1-T210D and Nek2A-KR are co-transfected (Figure 4.7). This suggests that the Nek2A-KR protein interferes with the phosphorylation of Nlp by Plk1 *in vivo*. This could be a result of the NekA-KR protein binding to GFP-Nlp therefore sterically inhibiting Plk1 from docking and phosphorylating Nlp.

4.2.7 Kinase-inactive Nek2A inhibits the fragmentation of GFP-Nlp aggregates by Plk1

To confirm that the Nek2A-KR protein could interfere with phosphorylation of Nlp by Plk1 *in vivo*, cells were co-transfected with GFP-Nlp, myc-Plk1-T210D and myc-Nek2A-KR and analysed by immunofluorescence microscopy. The triple transfections were validated by Dr. J. Rapley to ensure transfection of all three constructs occurred at a similar extent (Rapley, 2004). Examination of transfected cells revealed that in cells co-transfected with GFP-Nlp and Plk1-T210D, 65% of cells had fragmented GFP-Nlp aggregates (Figure 4.8). However, only 41% of cells co-transfected with GFP-Nlp, Plk1-T210D and the Nek2A-KR protein had fragmented GFP-Nlp aggregates.

This confirmed that the Nek2A-KR protein could interfere with the ability of Plk1 to phosphorylate Nlp *in vivo*. Nek2A-KR also prevents Plk1-T210D induced removal of endogenous Nlp from the interphase centrosome (Figure 4.9). Transfection of myc-Plk1-T210D into U2OS cells induces the displacement of endogenous Nlp from the interphase centrosome in approximately 90% of cells. However transfection of both myc-Plk1-T210D and Nek2-KR reduces the ability of Plk1 to displace Nlp to approximately 40%. Therefore, the regulation of both endogenous Nlp and overexpressed GFP-Nlp aggregates by Plk1 is blocked by the inactive Nek2A protein.

4.2.8 Microtubule aster formation is blocked in cells with fragmented GFP-Nlp aggregates

When overexpressed, GFP-Nlp forms large aggregates which surround and encapsulate the centrosome. However, the aggregates are dispersed when either the Nek2A-WT or

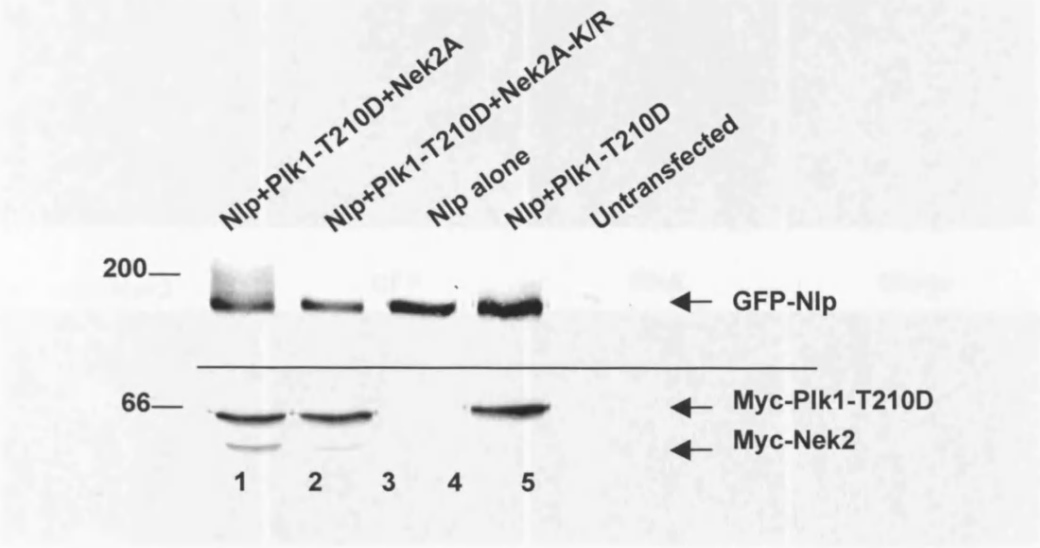

Figure 4.7 Nek2A-KR prevents Plk1-T210D phosphorylation of Nlp in transiently transfected cells

HeLa cells were transiently transfected with GFP-Nlp, myc-Plk1-T210D, myc-Nek2A-WT and myc-Nek2A-KR as indicated. Lysates were prepared, equalised for protein content and separated by SDS-PAGE. The gels were subsequently Western blotted and probed with GFP (top panel) and Myc-tag (lower panel) antibodies. M. wts (kDa) are indicated on the left.

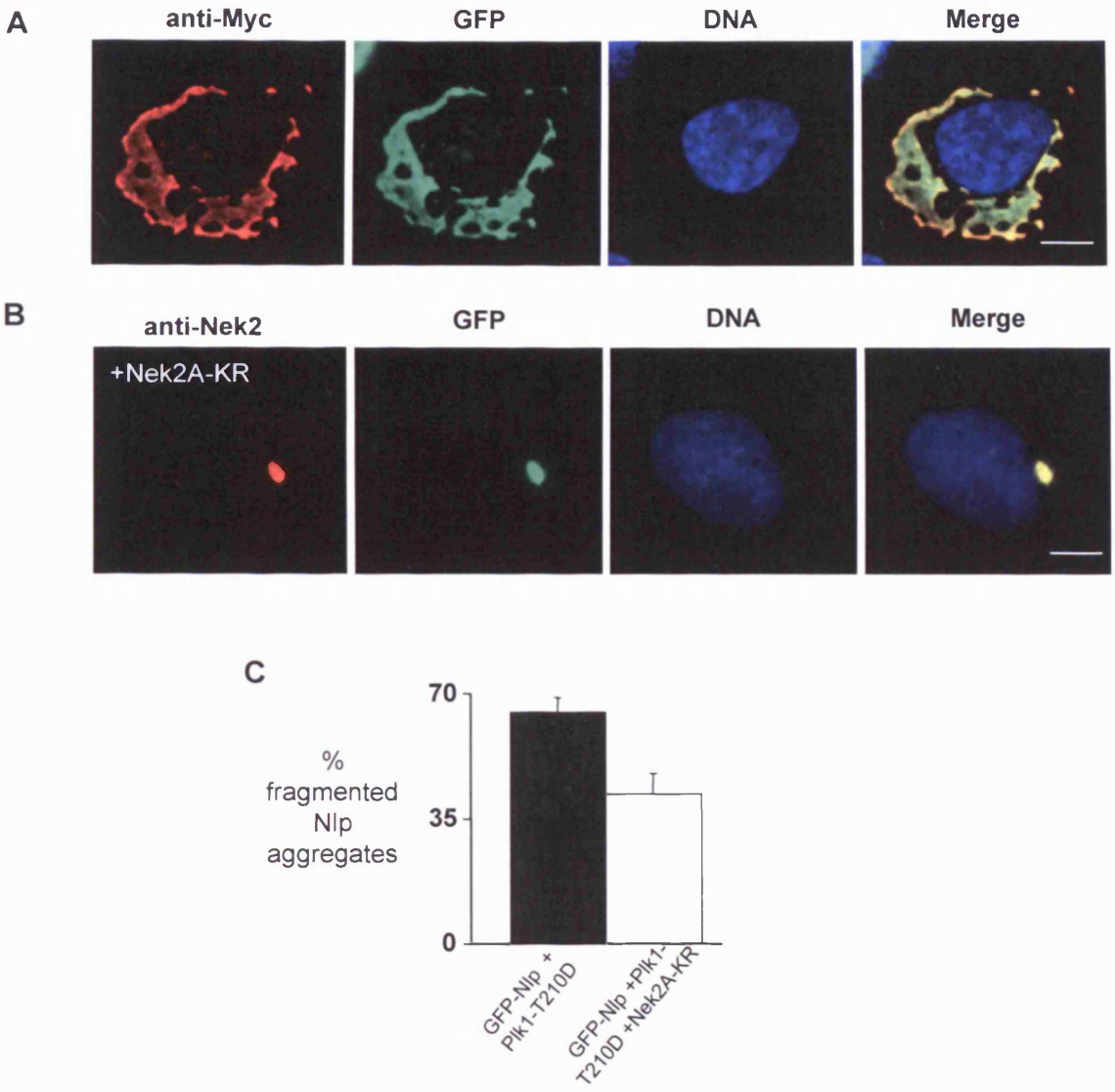

Figure 4.8 The Nek2A-KR protein inhibits Plk1-induced fragmentation of GFP-Nlp aggregates

A. GFP-Nlp and myc-Plk1-T210D were co-transfected into U2OS cells for 24 hours. Cells were stained with the myc antibody (red) and Hoescht 33258 for DNA (blue). **B.** GFP-Nlp, myc-Plk1-T210D and myc-Nek2A-KR kinase were triple transfected and cells fixed with methanol at 24 hours. The cells were stained with the Nek2 antibody (red) and Hoescht 33258 for DNA. **C.** The number of fragmented GFP-Nlp aggregates were counted over four coverslips and two separate experiments and the percentage of cells containing fragmented GFP-Nlp aggregates calculated.

Plk1-T210D proteins are co-transfected, but it is not clear what effect this has on the ability of the centrosome to mediate microtubule nucleation. To address this question microtubule aster formation was observed in cells co-transfected with GFP-Nlp and Nek2A-WT. Transfected cells were put on ice for 30 minutes to depolymerise the microtubule network followed by a shift to warm media for two minutes thereby allowing the initial formation of a new microtubule aster. Cells were then fixed and analysed by immunofluorescence microscopy using an antibody against the α-tubulin protein to observe microtubule asters. A single, robust microtubule aster was observed in 83% of untransfected cells, but only 7.5% of cells co-transfected with GFP-Nlp and Nek2A-WT (Figure 4.10). This suggests that removal of Nlp from the centrosome into the small aggregates may disrupt either the core centrosome structure or remove a component of the centrosome which is essential for the nucleation of microtubules. The co-transfection of GFP-Nlp with Plk1 also inhibits aster formation within cells suggesting that the phosphorylation of Nlp by either kinase disrupts the centrosome's ability to make asters possibly as a result of mislocalization of the γ-TuRC complex (Figure 4.10).

4.2.9 γ-Tubulin colocalises with dispersed GFP-Nlp fragments

To test the hypothesis that the lack of microtubule nucleation in cells co-transfected with GFP-Nlp and Nek2A-WT or Plk1-T210D was due to mislocalisation of the γ-TuRCs, cells were stained with γ-tubulin antibodies. In cells co-transfected with GFP-Nlp and either Nek2A-WT or Plk1-T210D, the aggregates of Nlp were dispersed widely throughout the cytoplasm. The γ-tubulin protein primarily co-localized with the Nlp aggregates although some remained at the centrosome suggesting that the centrosome structure is not completely abolished when Nlp is removed (Figure 4.11). To rule out any possibility that the antibodies were sticking to the GFP-Nlp aggregates, a secondary antibody alone was added and showed no co-localization with the GFP-Nlp aggregates. Additional controls were performed with antibodies to other centrosomal proteins. An antibody against a novel centrosomal protein, Pix (Dr. R. Hames and Dr. A. Fry, unpublished data), showed consistent staining of centrosomes and no co-localization with the GFP-Nlp aggregate, while an antibody raised against the centrosomal RPGR protein (α-C2) (Shu et al., 2005) showed no co-localization with GFP-Nlp aggregate but did

exhibit a loss of centrosome staining in 15% of cells (data not shown). These results suggest a partial breakdown of the centrosome structure at the time that Nlp is displaced with specific loss of the γ-TuRC. The phosphorylation of Nlp by Nek2 or Plk1 may serve to initiate the displacement of Nlp together with other proteins such as C-Nap1 from the centrosome at the G2/M transition.

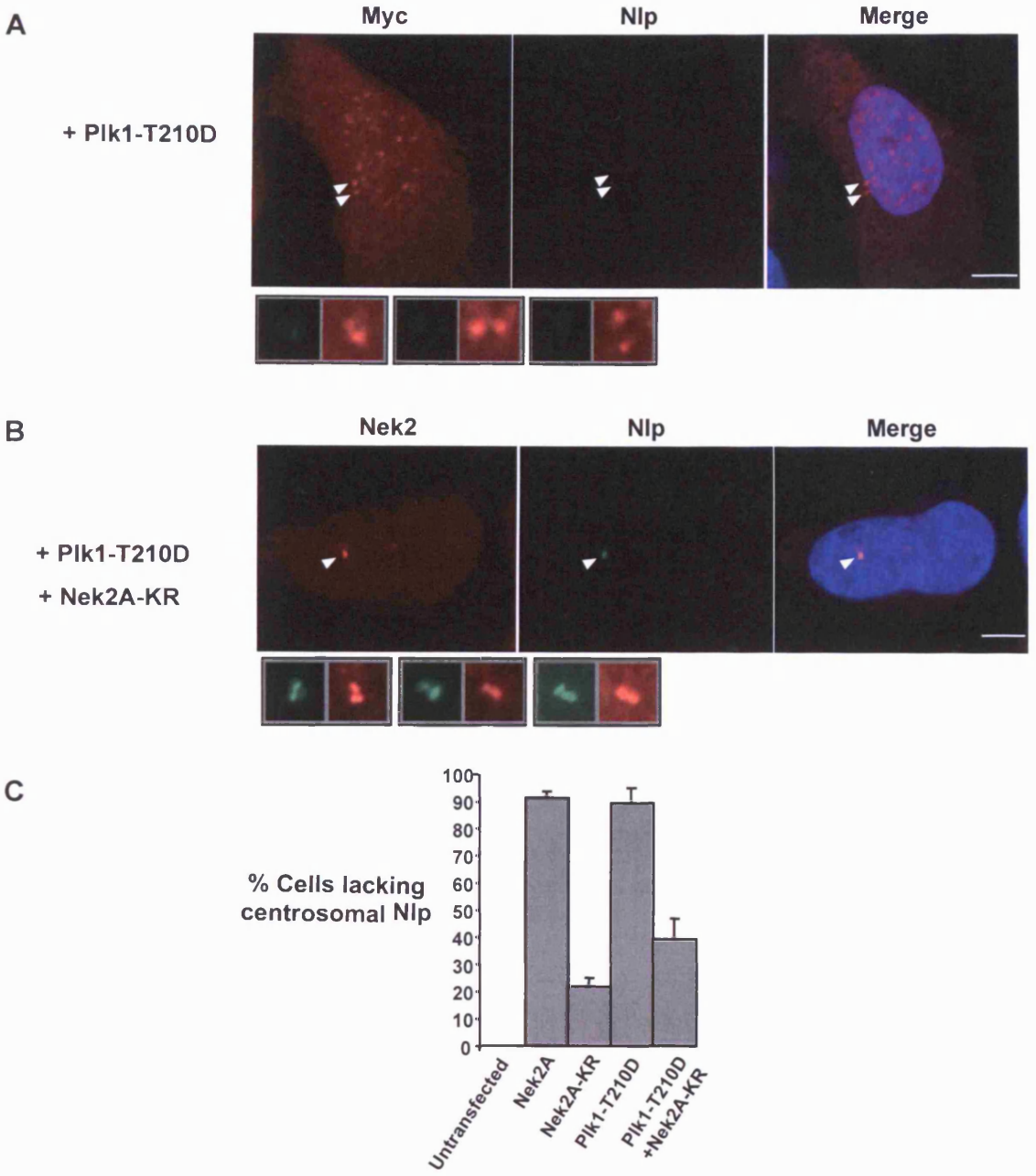

Figure 4.9 Nek2A-KR inhibits the Plk1-induced displacement of endogenous Nlp from the centrosome

A. U2OS cells were transfected with myc-Plk1-T210D for 24 hrs and analysed by immunofluorescence microscopy. The cells were stained with the myc antibody (red), anti-Nlp antibody (green) and Hoescht 33258 to stain the DNA (blue). Additional pictures represent other representative centrosomes. **B.** Plk1-T210D and Nek2A-KR were co-transfected into U2OS cells for 24 hrs and analysed by immunofluorescence microscopy. Cells were stained with the Nek2 antibody (red), anti-Nlp antibody (green) and Hoescht 33258 for DNA (blue). Additional pictures below represent other representative centrosomes. Scale bars in A and B, 5 μm. Arrowheads point to centrosomes. **C.** The percentage of cells lacking Nlp was calculated after transfection with either Nek2A-WT, Nek2A-KR, Plk1-T210D or Plk1-T210D and Nek2A-KR.

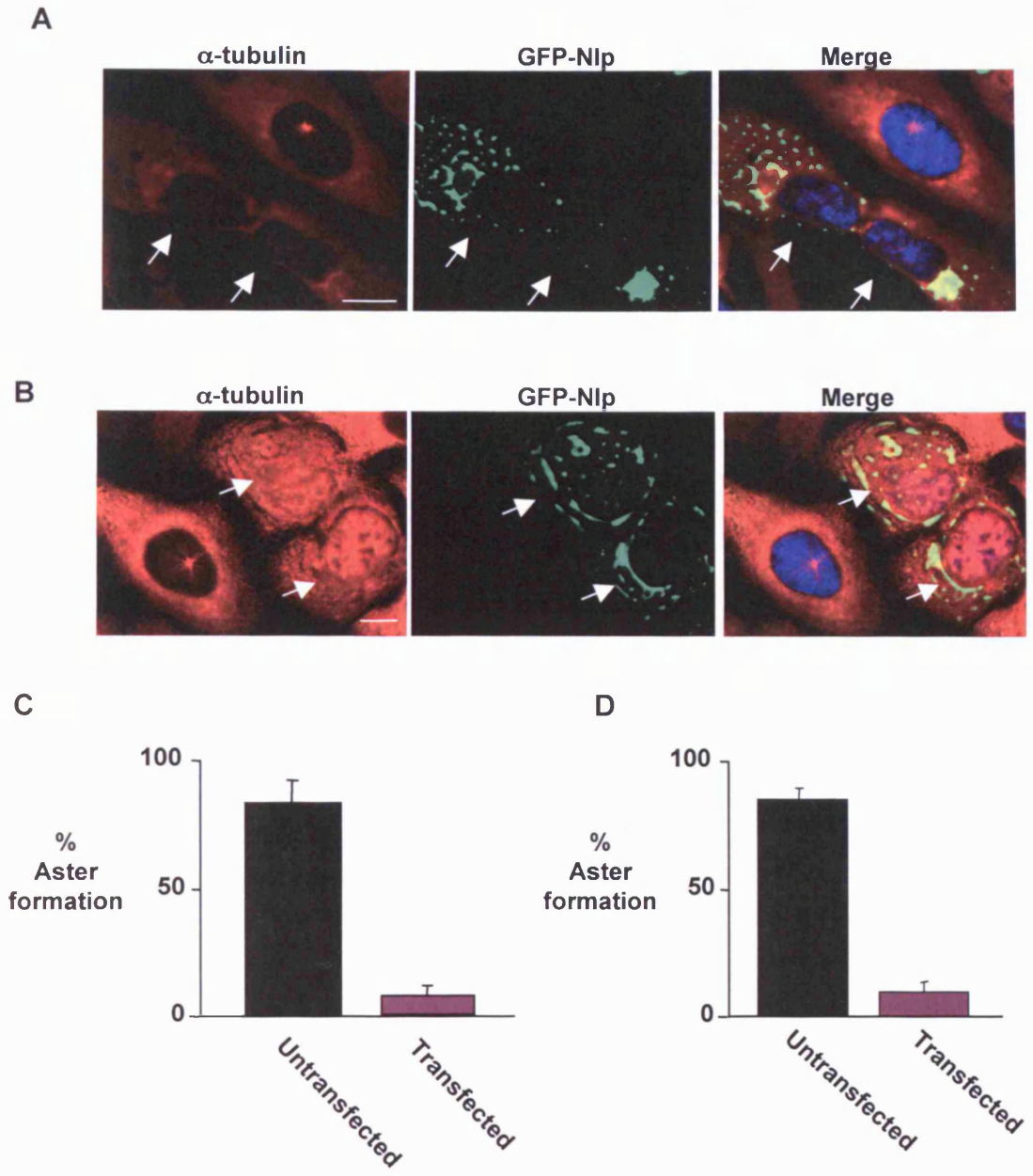

Figure 4.10 Microtubule aster formation is inhibited in cells co-transfected with GFP-Nlp and either Nek2A or Plk1

U2OS cells were co-transfected with GFP-Nlp and either myc-Nek2A-WT (A) or myc-Plk1-T210D (B). At 24 hours microtubules were depolymerised by cold treatment. Microtubule re-growth was achieved by the addition of warm media for 2 minutes followed by analysis by immunofluorescence microscopy. An α-tubulin antibody (red) was used to stain for microtubules and Hoechst 33258 for DNA (blue), GFP-Nlp is observed in green. Arrows point to transfected cells. Scale bar 5 μm. The presence of microtubule asters were counted in a total of 400 cells for cotransfection with myc-Nek2A-WT (C) or myc-Plk1-T210D (D). Aster formation occurred in an average of 83% of non-transfected cells whereas only in 7.5% of Nek2A or 9% of Plk1 co-transfected cells. Graphs are representative of three separate experiments. Error bars show standard deviation.

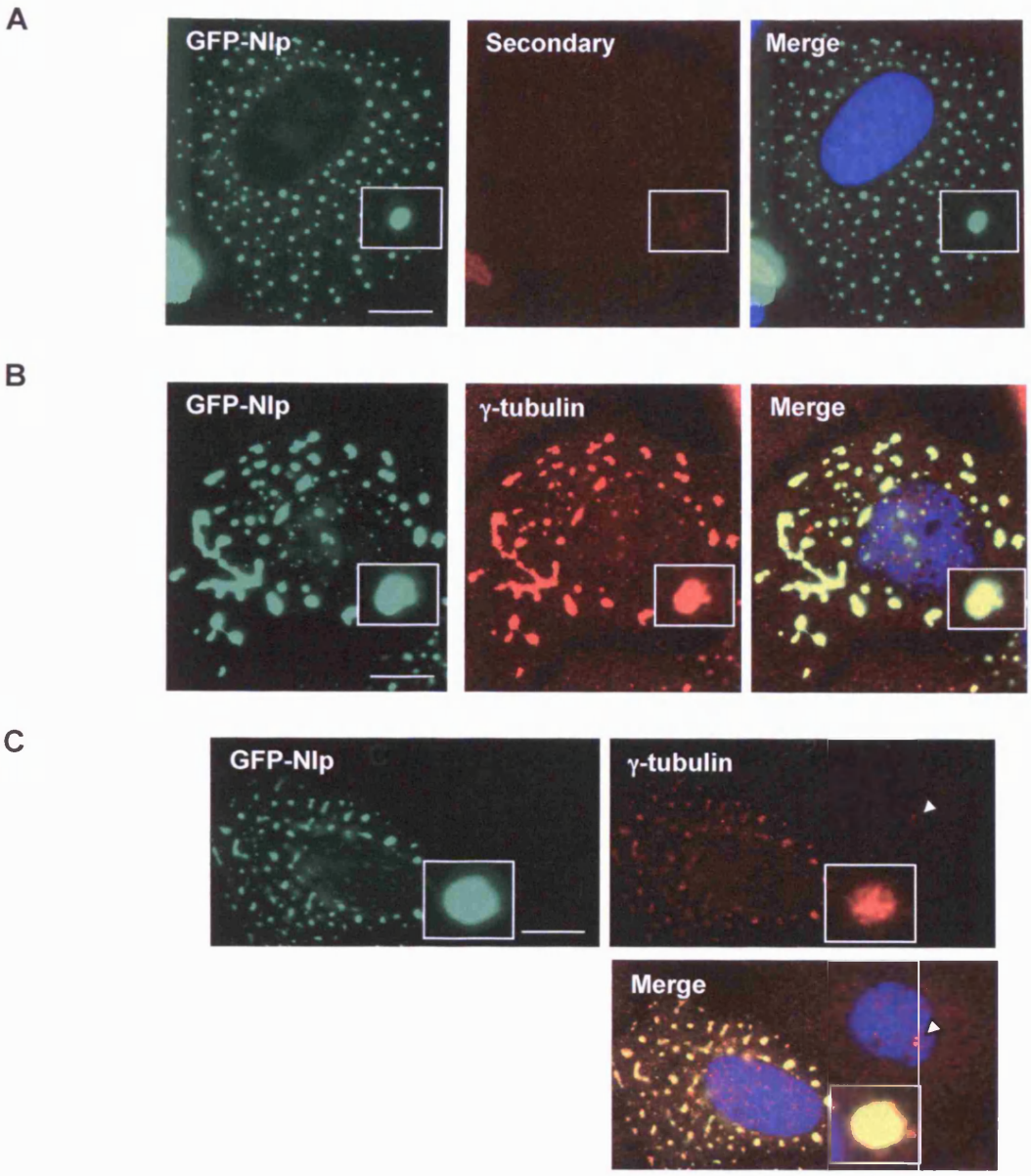

Figure 4.11 γ-tubulin co-localises with dispersed GFP-Nlp aggregates in cells co-transfected with Nek2A-WT or Plk1-T210D

A. U2OS cells were transfected with GFP-Nlp and myc-tagged Nek2A-WT. Cells were analysed by immunofluorescence microscopy at 24 hours post-transfection and stained with secondary antibody (Red) alone, GFP-Nlp (green) and Hoechst (Blue). **B.** Cells were transfected as in A but stained with a γ-tubulin antibody (red) and Hoechst (Blue) GFP-Nlp can be seen in green. As with A the exposure time remained at 1.1 secs. **C.** U2OS cells were transfected with GFP-Nlp and myc-tagged Plk1-T210D for 24 hours. Cells were methanol fixed and stained with γ-tubulin antibody (Red) and Hoechst (Blue), GFP-Nlp can be seen in green . Panels within main picture represent a single GFP-Nlp fragment and demonstrate co-localization of the GFP-Nlp and γ-tubulin. The second cell in this panel demonstrates an untransfected cell where the γ-tubulin still localizes to the centrosome (arrow), (also seen for the GFP-Nlp and Nek2A-WT transfections). Scale bar 10μm.

4.3 Discussion

The centrosome is the major site of microtubule nucleation within the animal cell. This is due to the localization of γ-TuRC within the pericentriolar material. There is evidence that pericentrin/kendrin, CG-Nap, CP309 and Asp all contribute to γ-TuRC recruitment (Bornens, 2002; Delgehyr et al., 2005; Doxsey et al., 1994). However, the anchoring of the γ-TuRC to the centrosome in mammalian cells is not well understood. Nlp has recently been identified as another protein potentially involved in anchoring the γ-TuRC at the centrosome (Casenghi et al., 2003). Nlp co-precipitated with both γ-tubulin and another component of the γ-TuRC and microinjection of antibodies directed against Nlp led to unfocused microtubules and a reduction in microtubule nucleation (Casenghi et al., 2003). Evidence to date supports a role for Nlp in microtubule nucleation at the mammalian centrosome. However, studies in both human and *Xenopus* cells indicate that Nlp is preferentially associated with the mother centriole. This would suggest it is more involved in microtubule anchoring, like its relative ninein, than microtubule nucleation.

In this chapter, I have demonstrated that displacement of Nlp from the centrosome can be triggered independently by overexpression of both the Plk1 and Nek2 kinases. Because of the mechanism by which Plk1 is recruited to its substrates, it is possible that the Nek2 protein kinase may act to prime Nlp for activation by Plk1. In addition, Nlp is shown to have a tight association with γ-tubulin even when not present at the centrosome which may explain its microtubule anchoring properties at the mother centriole.

Kinase assays performed *in vitro* indicated that Nlp is phosphorylated in its N-terminal domain by the Nek2 protein kinase at sites distinct to those phosphorylated by the Plk1 protein kinase. This raised the possibility that Nek2 could act as a priming kinase for Plk1 by phosphorylating Nlp and creating a binding site for the Plk1 PBD. This hypothesis is supported by the fact that when Nlp is pre-incubated with the Nek2A kinase, the level of Plk1 phosphorylation is increased compared to that following pre-incubation with Nek2A-KR. However, the Nek2A-KR protein may also act to inhibit Plk1 phosphorylation of Nlp. The Nek2A-KR protein can inhibit phosphorylation of overexpressed GFP-Nlp and endogenous Nlp by Plk1 in cells. This is demonstrated by (i)

loss of a smear on a Western Blot of transfected cell lysates (Figure 4.7); (ii) prevention of fragmented GST-Nlp aggregates forming in transfected cells (Figure 4.8); and (iii) loss of displacement of endogenous Nlp when Nek2A-KR is present (Figure 4.9). This might place Nek2 phosphorylation of Nlp upstream to that by Plk1 and supports the hypothesis of priming by the Nek2 kinase. However, Far-western blots provided no substantial evidence that Nek2A phosphorylation of Nlp stimulated the binding of the Plk1 PBD. This may be because the level of phosphorylation was not high enough or the phosphorylated sites were masked by membrane binding. At the present time, it really remains to be proven whether or not Nek2 can act as a priming kinase for Plk1.

By Far-western Blotting and *in vitro* kinase assays, we have demonstrated that Cdk1 can phosphorylate Nlp and could possibly prime Nlp for phosphorylation by Plk1 as there was increased binding of the Plk1-PBD following phosphorylation by Cdk1. However, although there are three Cdk1 target sites within the N-terminal domain of Nlp (amino acids 186,191 and 196) none of these form a PBD binding motif. It would be interesting to discover whether Cdk1 does affect the interaction of Nlp with γ-tubulin. This could be achieved by co-transfection of a constitutively active Cdk1 mutant with GFP-Nlp and immunofluorescence microscopy. The interaction of γ-tubulin with GFP-Nlp could also be observed by co-precipitation experiments with and without Cdk1 overexpression.

Nlp is present at the mother centriole during interphase and is displaced upon entry into mitosis (Rapley et al., 2005). The displacement of Nlp is thought to be triggered by the phosphorylation of Nlp by Plk1 and/or Nek2. RNAi mediated interference studies however indicate that depletion of Nek2 had no effect upon the levels of Nlp at the centrosome (Figure 4.6). During interphase, the levels of Nlp at the centrosome in cells depleted of Nek2 remain similar to nontreated cells. This result suggests that Nlp is not dependent upon Nek2 for its interaction with the centrosome during interphase. During prophase, depletion of Nek2 from the centrosome also appeared to have little or no effect upon Nlp localisation (Figure 4.6). This is in contrast to previous evidence that suggested that Nek2 is responsible for the displacement of Nlp at the onset of mitosis. Nek2 depletion would therefore be expected to cause an increase of Nlp at the mitotic spindle

poles. It is possible though that Nek2 was not completely depleted and the residual Nek2 present was still contributing to the displacement of Nlp. Alternatively, it is possible that in U2OS cells, Plk1 is sufficient to displace Nlp. This may not be true though for other cell types.

Co-transfection studies of either Plk1 or Nek2A with GFP-Nlp also revealed a tight association of dispersed GFP-Nlp aggregates with γ-tubulin. The association of γ-tubulin with Nlp aggregates is not affected by the overexpression of either Plk1 or Nek2A and therefore although these kinases are involved in disturbing the interaction of Nlp with itself and Nlp with the centrosome, it is unlikely that they are involved in regulating the binding of Nlp to γ-tubulin. In line with this, aster formation is compromised in cells overexpressing either Plk1 or Nek2A and GFP-Nlp, via the sequestering of γ-tubulin away from the centrosome to the dispersed aggregates. However, as γ-tubulin clearly increases on mitotic spindle poles in normal cells, we assume that the interaction between Nlp and the γ-TuRC must be broken at the onset of mitosis. A third kinase, possibly Cdk1, may then be responsible for the severing of Nlp from γ-tubulin to allow microtubule nucleation and the build up of γ-tubulin to occur at the centrosome ready for microtubule spindle formation.

Further studies need to be performed to address some of the issues raised within this chapter. For instance, it would be interesting to observe the effects of depleting both the Nek2 and Plk1 kinases and determining the effect upon Nlp localisation in mitotic cells. In addition, the role of Cdk1 phosphorylation of Nlp should be explored further. Finally, further work is required to confirm or disprove the hypothesis that Nek2 is a priming kinase for Plk1.

Chapter Five

Identification of sites in the Nlp protein phosphorylated by Nek2

5.1 Introduction

It has been established that Nlp can be phosphorylated by Plk1 and Nek2 kinases at distinct sites (see chapter 4 and Rapley et al., 2005). To date little is known of the consensus site that Nek2 targets except that Nek2 may have a requirement for basic residues close to the phosphorylation site (Fry et al., 1995). Determination of a Nek2 consensus phosphorylation site would be particularly useful in the identification of novel Nek2 substrates. Work within this chapter was performed in collaboration with Mr. F. Ivins and Prof. S. Smerdon at the National Institute of Medical Research (London). To identify Nek2 phosphorylation sites, matrix-assisted laser desorption ionization time of flight (MALDI-TOF) mass spectrometry was performed upon GST-Nlp-NTD fragments phosphosphorylated by Nek2A.

To identify phosphorylation sites by mass spectrometry involves a number of distinct stages. Firstly, it is necessary to phosphorylate your target protein with the desired kinase to as close to saturation of all possible phosphorylation sites as possible. Secondly, the protein is fragmented into a series of peptides by trypsin and the peptides containing phosphate groups isolated from the mixture by metal-affinity or anion-exchange chromatography. Here, the negatively-charged phosphate groups present on the phosphorylated peptides should bind to the resin allowing purification. However, this preparation will also contain any negatively-charged peptides and may lead to the loss of positively-charged phosphorylated peptides. High performance liquid chromatography is then used to further purify and separate the peptides before applying to the mass spectrometer sample matrix. MALDI-TOF involves the use of a matrix whose function is to absorb photons when a laser is fired upon it. This allows the matrix to enter the gas phase carrying the peptide fragments with it. A proton is transferred to the peptide which is subsequently repelled by a large negatively-charged plate. The peptide "flies" through the machine according to its mass-to-charge ratio and is detected. The detector can calculate the exact mass of the peptides according to their time of flight, which are recorded and visualised as a number of peaks.

A predicted map of peptides created by the trypsin digestion of the substrate protein can be generated prior to mass spectrometry using the Mascot peptide mass fingerprint programme (www.matrixscience.com). By comparing the molecular mass of the predicted peptides to that of the peaks found by mass spectrometry and subtracting the molecular weight of a phosphate group one can identify the peptides phosphorylated and then determine where they lie within the protein. However, there are many considerations that can complicate the interpretation. Some of the problems associated with mass spectrometry include a peptide losing its phosphate group during preparation, a peptide not flying because of the negatively-charged phosphate, and sites being identified which are not physiologically relevant. Here, I have phosphorylated the N-terminal domain of Nlp with a bacterially expressed Nek2 construct and have identified six possible phosphorylation sites that Nek2 targets.

5.2 Results

5.2.1 *In vitro* phosphorylation of the Nlp N-terminal domain by Nek2

As discussed in chapter 4, the N-terminal domain (NTD) of the Nlp protein is an excellent substrate for the Nek2 protein kinase. We therefore wished to identify the sites of Nek2 phosphorylation using the GST-Nlp-NTD purified protein as a substrate. For the kinase, we decided to use a Nek2 N-terminal kinase domain fragment (amino acids 2-271) expressed in bacteria by the Smerdon lab. This fragment of Nek2, Nek2-NTD-KR-His, as well as carrying an N-terminal His-tag, also has the K37R point mutation. However, the protein retains sufficient activity when present in high concentrations to phosphorylate both itself and the Nek2 substrate β-casein. This fragment can also phosphorylate the GST-Nlp-NTD and GST-Nlp-NTDΔ8 proteins to near equal levels again proving that the majority of sites phosphorylated by Nek2 are distinct to those targeted by the Plk1 kinase and that this fragment of Nek2 is behaving in a similar manner to the full length kinase (Figure 5.1). There is a small degree of loss of phosphorylation upon GST-Nlp-NTDΔ8 which demonstrates that Nek2 and Plk1 may possibly share one or two target sites.

5.2.2 Mass spectrometry reveals six putative Nek2 phosphorylation sites in the Nlp-NTD.

Nek2-NTD-KR-His was used to phosphorylate approximately 5 μg of GST-Nlp-NTD for 1 hour leading to complete saturation. The sample was analysed in collaboration with Prof. Smerdon (NIMR, London) by mass spectrometry analysis. Two peptides were identified which each contained two phosphorylated amino acids as confirmed by post source decay analysis (Figure 5.2). These peptides spanned amino acids 113-126 and 445-458 and each contained only two possible sites of phosphorylation. Hence, it is certain that the phosphorylated residues are S113, T122, S448 and S452. A third peptide (amino acids 634-640) contained only one phosphate group, however there were two possible sites to which the phosphate may have been attached, T634 and T638 (Figure 5.3). For this reason both sites have been included as possible phosphorylation sites until further analysis can be performed. These sites all differ from those phosphorylated by

Plk1 (T22, S87, S88, T161, S319, S498, S670 and S686) and do not conform to the PBD consensus.

5.2.3 Mutation of the six Nek2 phosphorylation sites within the GST-Nlp-NTD protein eliminates phosphorylation by the Nek2 kinase

To determine whether the Nek2 protein kinase targets the phosphorylation sites identified by mass spectrometry site-directed mutagenesis was used to mutate the 6 putative Nek2 phosphorylation sites within the GST-Nlp-NTD fragment. The S113, T122, S448, S452, T634 and T638 sites were all mutated to alanine in a single construct to prevent phosphorylation. This GST-Nlp-NTDΔ6 construct was then tested in an *in vitro* kinase assay to determine whether Nek2 could still phosphorylate the protein. Unfortunately, following bacterial expression, the majority of the protein remained insoluble with a small amount present in the soluble fraction. After purification the levels of Nlp-NTDΔ6 protein present were too low to perform kinase assays. Therefore the soluble fraction before purification was used in the kinase assays. The GST-Nlp-NTD wild type protein was used as a control in the kinase assay. The assay revealed that although the wild type GST-Nlp-NTD is phosphorylated very well by the Nek2 protein, the Nlp-NTDΔ6 protein is no longer phosphorylated by Nek2. This result demonstrates that the phosphorylation sites identified by the mass spectrometry represent the bulk of sites that Nek2 targets in the Nlp N-terminal domain *in vitro*.

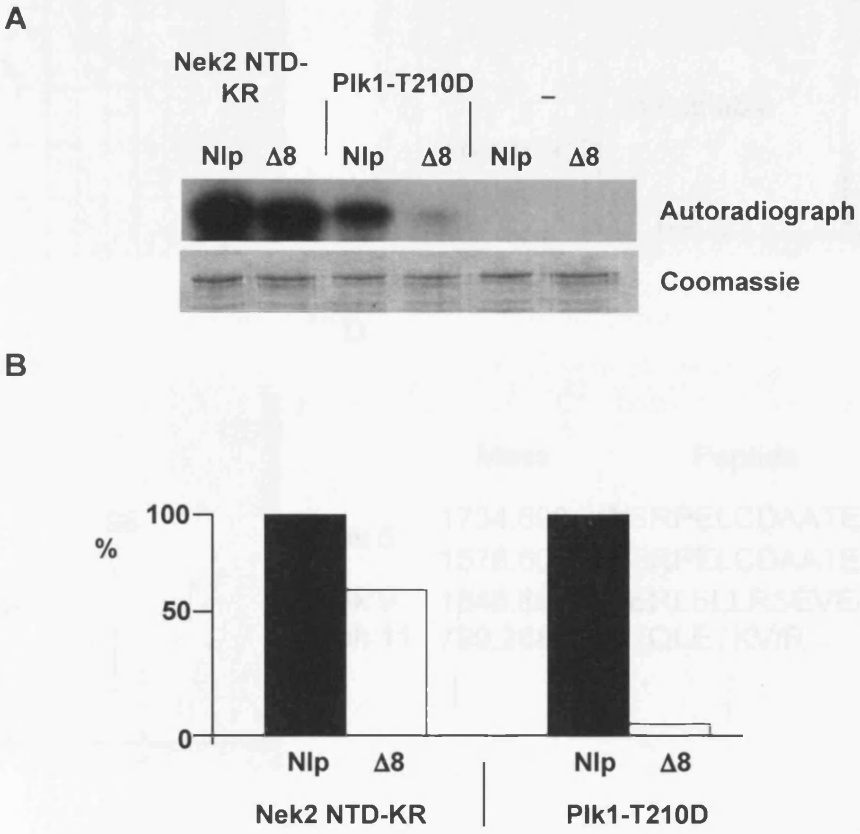

Figure 5.1 The Nlp N-terminal domain is phosphorylated by the Nek2 kinase domain fragment at sites distinct from those phosphorylated by Plk1

A. *In vitro* kinase assays were performed using Nek2-NTD-KR-His, Plk1-T210D or no kinase (-) and the Nlp-NTD or Nlp-NTDΔ8 as substrates in the presence of ^{32}P-γ-[ATP]. Products were separated by SDS-PAGE, stained with Coomassie Blue (lower panel) and analysed by autoradiography (top panel). **B.** The Nlp protein bands were excised from the gel and subjected to scintillation counting. The percentage of ^{32}P incorporated into the substrate is shown with respect to the wild type Nlp fragment. Data is representative of two experiments.

A

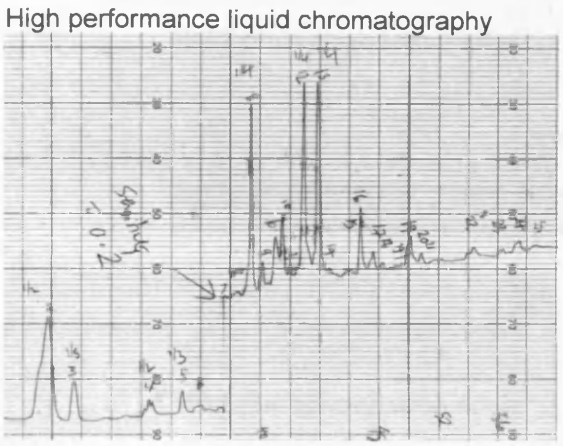

B

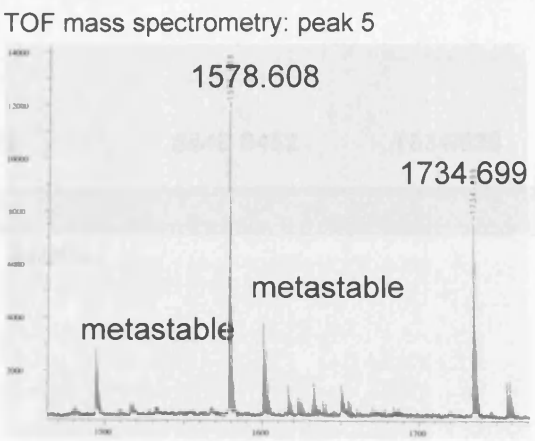

C

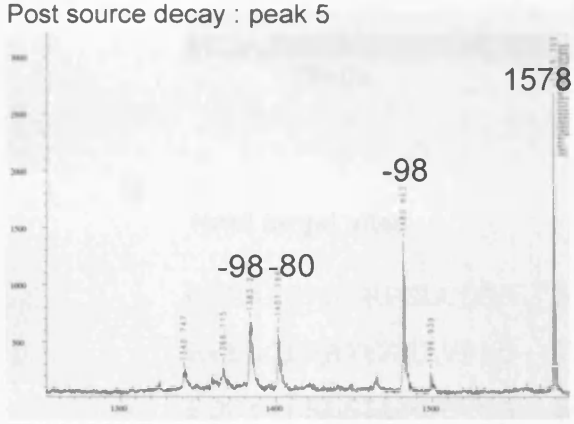

D

	Mass	Peptide
Peak 5	1734.699	R/SRPELCDAATEARR/
	1578.608	R/SRPELCDAATEAR/R
Peak 9	1846.853	R/ERLSLLRSEVEAER/E
Peak 11	799.268	R/TQLETKV/R

Figure 5.2 HPLC and MALDI-TOF mass spectrometry analysis of the Nlp-NTD following Nek2 phosphorylation

A. Kinase assays were performed using the Nek2-NTD-KR protein fragment and GST-Nlp-NTD as a substrate in kinase buffer containing 100 mM ATP for 40 minutes at 30°C. The assays were then subjected to trypsin digestion for 12 hours followed by high performance liquid chromatography. Peaks indicate the peptides as they eluted from the HPLC. **B.** Each HPLC peak was subjected to MALDI-TOF mass spectrometry. The spectra generated from peak five is represented here. **C.** Of the 24 peaks collected from the HPLC column three (peaks 5, 9 and 11) corresponded to an Nlp phosphorylated peptide. Peptides from peaks 5 and 9 showed masses indicating two phosphate groups. Post source decay was then performed on these peaks to prove these peptides contained two phosphate groups as seen by a double loss of a mass of 98 after breakdown of the fragment. Data is shown from peak five. **D.** The peptides identified can be seen in the table. Phosphorylated residues are shaded green and possible sites in red.

A

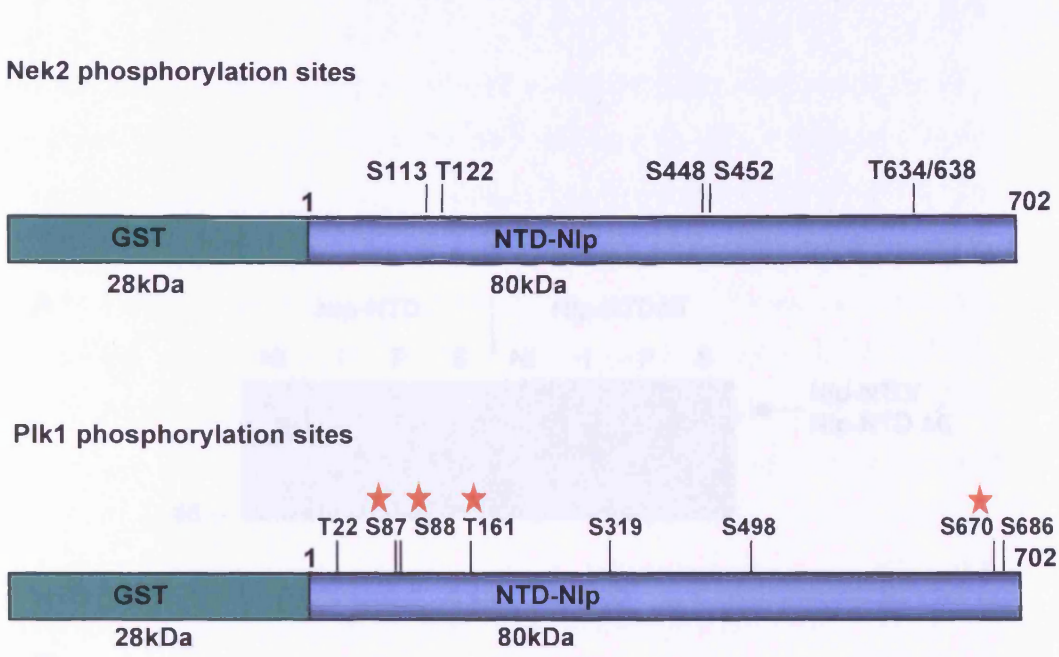

B

Nek2 target sites		Plk1 target sites	
GSKWYGRR**S**RPELCDAA	S113	EVYSSCDT**T**GTGFLDRQEL	T22
RPELCDAA**T**EARRVPEQ	T122	GVRPSDED**SS**SLESAASSA	S87/88
EQGYRERL**S**LLRSEVEA	S448	KSDEEAES**T**KEAQNELFEA	T161
RERLSLLR**S**EVEAEREL	S452	LFSSIDDG**S**GFAFPDQVLA	S319
KEHYQDLR**T**QLE**T**KVNY	T634/T638	LTLALKEN**S**RLQKEIVEVV	S498
		MEQARREV**S**VLEGQKADLE	S670
		DLEELHEK**S**QEVIWGLQEQ	S686

Figure 5.3 Comparison of Nek2 and Plk1 phosphorylation sites in the Nlp N-terminal domain

A. A schematic diagram of the GST-Nlp protein, indicating the phosphorylation sites targeted by Nek2 (upper diagram) and Plk1 (lower diagram). The Plk1 sites indicated with a star are those identified by mass spectrometry. **B.** The phosphorylation sites within GST-Nlp-NTD are shown in red along with the surrounding amino acids for the Nek2 and Plk1 target sites.

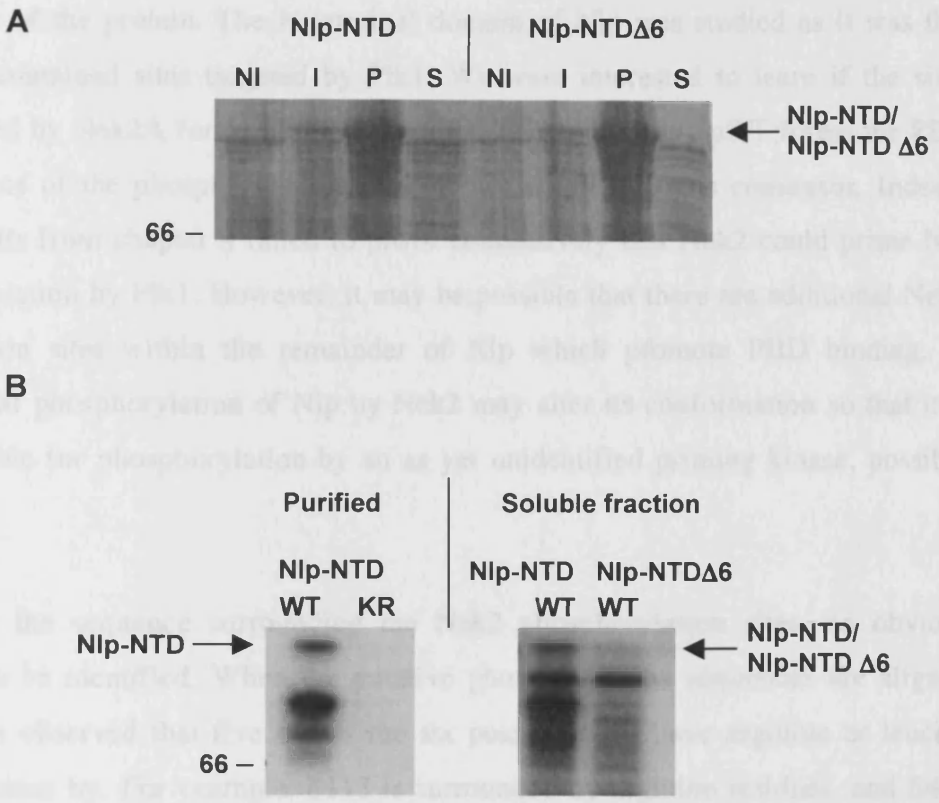

Figure 5.4 Nek2 cannot phosphorylate the Nlp-NTDΔ6 mutant
A. GST-Nlp-NTD and GST-Nlp-NTDΔ6 were expressed in BL21 *E. coli* by indution with 1 mM IPTG. The non-induced (NI), induced (I), pellet (P) and soluble (S) fractions were separated on a 12% SDS-PAGE gel and stained with Coomassie Blue. **B** *In vitro* kinase assays were performed using immunoprecipitated Nek2A-WT and Nek2A-KR protein on purified Nlp-NTD (left panel) and a soluble lysate prepared from *E. coli* expressing Nlp-NTD and Nlp-NTDΔ6 (right panel). These were analysed on an SDS-PAGE gel and subjected to autoradiography. M. wts (kDa) are indicated on the left.

5.3 Discussion

In this chapter, we have identified 5 putative Nek2 phosphorylation sites within the Nlp N-terminal domain: S113, T122, S448, S452 and T634 or T638. Preliminary studies suggest that mutation of these sites significantly reduces phosphorylation of Nlp by Nek2. This suggests that we have identified most of the major Nek2 phosphorylation sites in this region of the protein. The N-terminal domain of Nlp was studied as it was this domain that contained sites targeted by Plk1. We were interested to learn if the sites phosphorylated by Nek2A formed a PBD for Plk1. The consensus SpS/T forms the PBD motif, but none of the phosphorylation sites identified fall into this consensus. Indeed, previous results from chapter 4 failed to prove conclusively that Nek2 could prime Nlp for phosphorylation by Plk1. However, it may be possible that there are additional Nek2 phosphorylation sites within the remainder of Nlp which promote PBD binding. In addition, initial phosphorylation of Nlp by Nek2 may alter its conformation so that it is more acceptable for phosphorylation by an as yet unidentified priming kinase, possibly Cdk1.

By analysing the sequence surrounding the Nek2 phosphorylation sites, no obvious consensus can be identified. When the putative phosphorylation sequences are aligned then it can be observed that five out of the six possible sites have arginine or leucine amino acids close by. For example, S113 is surrounded by arginine residues, and S448 S452 and T634 have the motif RL or LR immediately preceding them. This is interesting to note as Nek2 has previously been described as having a preference for positive residues surrounding its target site. It is also interesting to note that these three sites are also present within *Xenopus* Nlp and the consensus surrounding the sites are the same (Figure 5.5). It is therefore possible that of the five sites identified these three may represent the *bona fide* Nek2 target sites upon Nlp. The remaining three sites are not conserved with the *Xenopus* sequence and do not share a similar consensus.

Although these five sites are phosphorylated *in vitro*, it has not been shown which are critical *in vivo*. It is important to determine the functional role of the phosphorylation of Nlp by Nek2. By mutating the phosphorylation sites in a GFP-Nlp construct and

performing transfection studies in conjunction with Nek2A kinase we can determine if these sites are important for regulating the localisation of Nlp. In addition, we may be able to determine whether the mutated Nlp disturbs microtubule organisation or mitotic progression. It would also be interesting to examine whether Plk1 can still phosphorylate and displace the Nlp mutant. In theory, if phosphorylation by Nek2 is a prerequisite for Plk1 phosphorylation then Plk1 may no longer be able to phosphorylate an Nlp mutant that is lacking Nek2 phosphorylation sites.

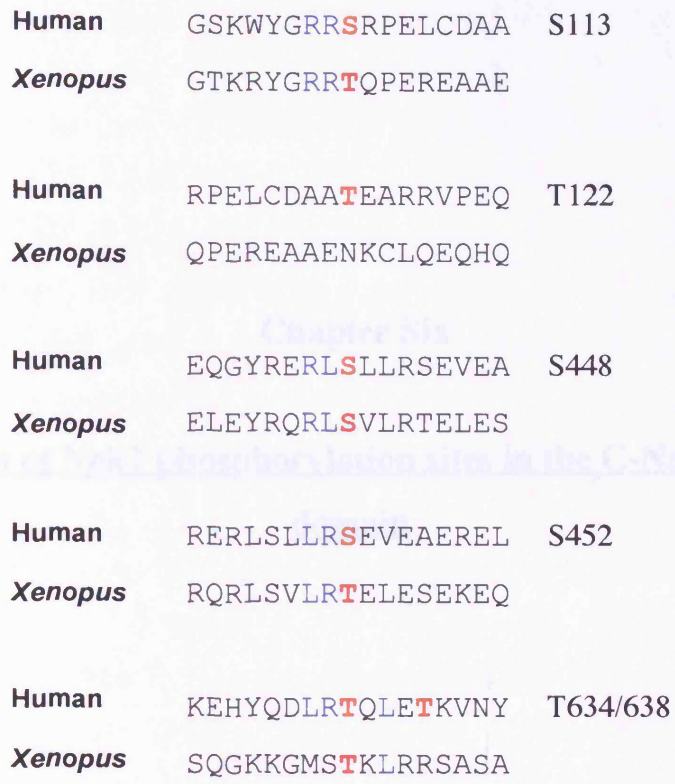

Figure 5.5 Comparison of conserved putative Nek2 phosphorylation sites in the human and *Xenopus* Nlp N-terminal domain

Sequence alignment of the human and *Xenopus* phosphorylation sites identified by mass spectrometry analysis of the human Nlp-NTD. Red letters represent the phosphorylation site, blue letters demonstrate the conserved arginine and leucine residues.

Chapter Six

Identification of Nek2 phosphorylation sites in the C-Nap1 C-terminal domain

6.1 Introduction

The C-Nap1 protein was isolated in a yeast two-hybrid screen using Nek2A as the bait. Nek2 can phosphorylate the C- and N-terminal domains of C-Nap1 *in vitro* (Fry et al., 1998b; Hames and Fry, 2002). Additional evidence that C-Nap1 is a substrate of Nek2 comes from the fact that C-Nap1 protein is specifically phosphorylated in mitosis when Nek2 is active (Mayor et al., 2002). The C-terminus of C-Nap1, encompassing amino acids 1961-2442, has been shown to be an excellent substrate for Nek2. Phosphorylation assays show that there maybe up to 13 sites within this domain that Nek2 can phosphorylate as approximately 13 moles of phosphate can be incorporated per mole of the C-Nap1 C-terminal domain by Nek2 (Helps et al., 2000).

C-Nap1 is predicted by its primary structure to contain two large coiled-coil domains separated by a proline rich hinge region. The C-Nap1 protein when overexpressed forms aggregates throughout the cell. These aggregates are reduced in size when Nek2-WT is co-expressed (Mayor et al., 2002). This suggests that phosphorylation of C-Nap1 by Nek2 may affect the structure of C-Nap1. Indeed in addition to Nek2, C-Nap1 also localises to the centrosome and immunochemical and biochemical studies demonstrate it is part of the core centrosome (Fry et al., 1998a). Antibody interference experiments of C-Nap1 highlighted its role in centrosome cohesion as microinjection of cells with C-Nap1 antibodies resulted in centrosome splitting (Mayor et al., 2000). The ability of C-Nap1 to form aggregates suggested it may form a linker structure between the centrosomes. However, antibodies raised against different parts of C-Nap1 consistently revealed two distinct dots colocalising with centrioles rather than staining the region between them (Mayor et al., 2000). C-Nap1 may therefore form part of the linker structure and which upon phosphorylation by Nek2 is dismantled and centrosome splitting induced. It is possible that the recently identified Rootletin protein is also an integral part of this linkage (Bahe et al., 2005)

In this chapter, I have explored the relationship between C-Nap1 and Nek2 by examining the consequences of Nek2 depletion and in mapping some putative sites of Nek2

phosphorylation within C-Nap1. Firstly, I depleted Nek2 by RNAi and studied the consequences upon C-Nap1 localisation to the centrosome. Secondly, the C-terminal domain of C-Nap1 was expressed in bacteria. This protein was used as a substrate for Nek2 before subjecting it to mass spectrometry. It is important to have an understanding of the sites that Nek2 targets in order to determine a possible consensus motif for Nek2 phosphorylation. Once sites are mapped within C-Nap1, it would be possible to generate phosphospecific antibodies and mutate these sites to examine the consequences of inhibiting phosphorylation.

6.2 Results

6.2.1 C-Nap1 is reduced at interphase centrosomes upon depletion of Nek2

U2OS cells were transiently transfected with RNAi oligonucleotide duplexes directed towards the Nek2 protein kinase. The level of Nek2 knockdown was calculated by immunofluorescence microscopy. After 48 hours, Nek2 could no longer be detected in more than 80% of cells (Figure 6.1). Following Nek2 knockdown, the abundance of C-Nap1 and γ-tubulin at the centrosome was measured by quantitative immunofluorescence microscopy. Measurements made on 50 cells revealed that the abundance of C-Nap1 was reduced in Nek2-depleted cells compared to mock-treated cells (Figure 6.2). This surprising result would seem to contradict the notion that the Nek2 kinase phosphorylates the C-Nap1 protein and initiates its dissolution from the centrosome. However, C-Nap1 is displaced from the centrosome only at the onset of mitosis at the time that Nek2 is thought to become activated. These results therefore suggest that, before it is activated, Nek2 may play a role in anchoring C-Nap1 at the centrosome. It may also have a more general role in maintaining centrosome integrity however γ-tubulin levels remain fairly stable after Nek2 depletion. A loss of centrosome integrity has previously been shown after Nek2 depletion in *Drosophila* cells (Prigent et al., 2005).

6.2.2 The C-Nap1 C-terminal domain is an excellent substrate for the Nek2 protein kinase

The C-Nap1 C-terminal domain was originally identified through its interaction with Nek2 and has been shown to be a substrate of Nek2 *in vitro* (Fry et al., 1998). To identify sites on C-Nap1 which Nek2 targets, the C-Nap1 C-terminal domain (amino acids 1961-2442) was cloned into the pMAL vector and expressed as an MBP fusion protein for use as a substrate in kinase assays (Figure 6.3). The MBP-C-Nap1-CTD domain was expressed at high levels predominately in the soluble fraction and could be easily purified on amylose beads. However, a MBP-C-Nap1-NTD protein expressed to high levels remained insoluble and therefore could not be used as a substrate (data not shown). The MBP fusion protein alone was also purified for use as a control (Figure 6.3).

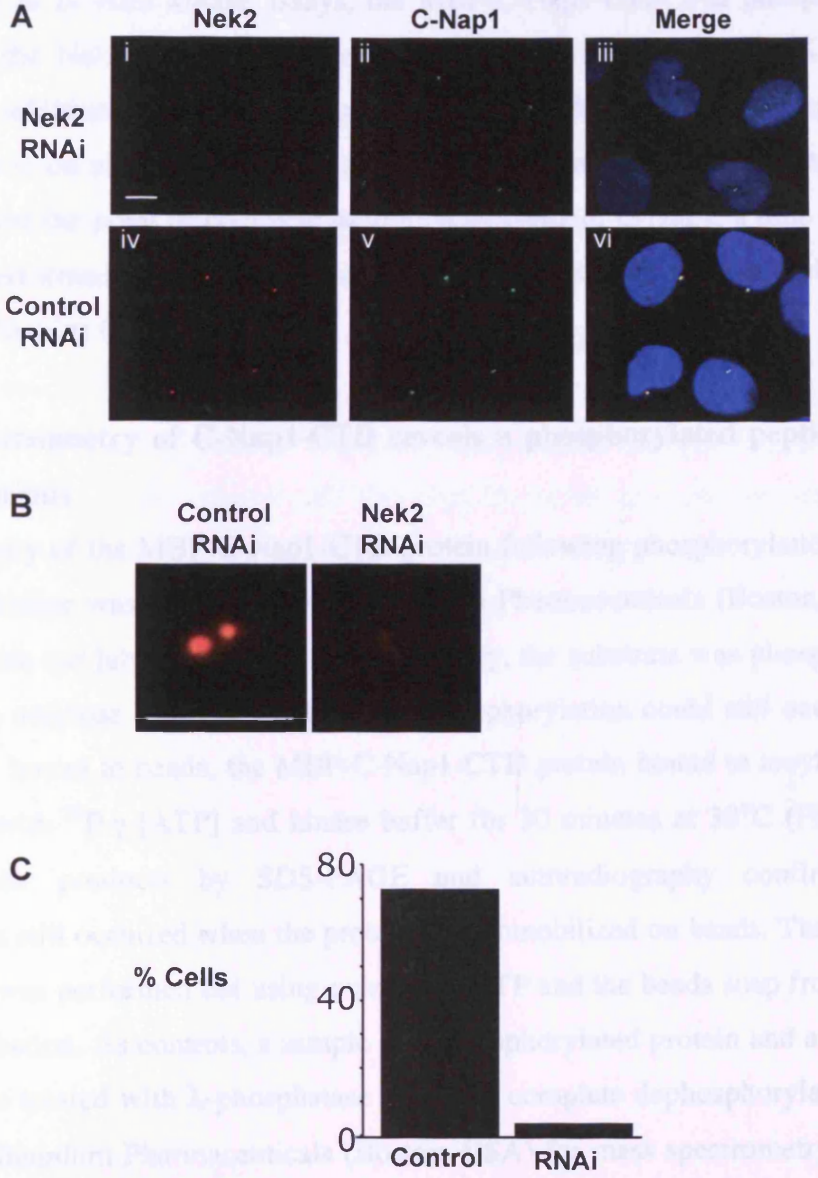

Figure 6.1 RNAi depletion of Nek2 in U2OS cells

A. Asynchronous U2OS cells were transfected with Nek2 RNAi duplexes (i-iii) or control duplexes (iv-vi) using oligofectamine (Invitrogen). Cells were fixed at 48 hours post transfection and co-stained using a monoclonal Nek2 antibody (red), C-Nap1-antibody (green) and Hoechst 33258 (blue). Scale bar 5 μm. **B**. Centrosomes of Nek2 RNAi and control RNAi treated cells as stained with the Nek2 antibody. Scale bar 2 μ m. **C**. Nek2 depletion was assessed by the presence of visible centrosome staining using a Nek2 antibody in 300 treated cells and 100 mock treated cells. The percentage of cells with detectable Nek2 at the centrosome under these conditions is shown, counted on two cover slips during one treatment.

When subjected to *in vitro* kinase assays, the MBP-C-Nap1-CTD was phosphorylated specifically by the Nek2A protein kinase and not by the inactive Nek2A-KR kinase (Figure 6.4). In addition, the MBP tag alone was not phosphorylated indicating that the phosphorylation is on site(s) in the C-Nap1-CTD protein and not the MBP tag (Figure 6.4). To determine the point of complete saturation by Nek2 of C-Nap1, a time course of activity was performed and it was estimated that full saturation was achieved at approximately 30 mins (Figure 6.4).

6.2.3 Mass spectrometry of C-Nap1-CTD reveals a phosphorylated peptide at the extreme C-terminus

Mass spectrometry of the MBP-C-Nap1-CTD protein following phosphorylation *in vitro* by the Nek2A kinase was performed by Millennium Pharmaceuticals (Boston, USA) in collaboration with our lab. Prior to mass spectrometry, the substrate was phosphorylated whilst bound to amylose beads. To ensure that phosphorylation could still occur on the substrate whilst bound to beads, the MBP-C-Nap1-CTD protein bound to amylose beads was incubated with ^{32}P-γ-[ATP] and kinase buffer for 30 minutes at 30°C (Figure 6.5). Analysis of the products by SDS-PAGE and autoradiography confirmed that phosphorylation still occurred when the protein was immobilized on beads. Therefore, an identical assay was performed but using unlabelled ATP and the beads snap frozen at the end of the incubation. As controls, a sample of unphosphorylated protein and a sample of protein that was treated with λ-phosphatase to ensure complete dephosphorylation, were also sent to Millennium Pharmaceuticals (Boston, USA) for mass spectrometry analysis. The results of the mass spectrometry revealed a phosphorylated peptide spanning the extreme C-terminal residues 2413-2442 of C-Nap1.

6.2.4 Mutational analysis of putative C-Nap1 phosphorylation sites

Within the phosphorylated peptide identified by Millennium Pharmaceuticals lie 10 serine and threonine residues (Figure 6.6.). It is not possible at this time to determine exactly which residues are phosphorylated within this fragment but sequence analysis reveal three serines at positions 2417, 2421 and 2433 which lie in a common motif

LxxpS. An MBP-tagged C-Nap1-CTD-S2417A/S2421A construct was produced by site-directed mutagenesis to investigate the possibility that this motif is phosphorylated. In addition, a second mutant construct C-Nap1-CTD-T2419A/T2423A/S2424A was made by an M.Sc. project student, Miss Sunitha Karkarla, under my supervision. These were expressed in *Rosetta E. coli* and induced using 1 mM IPTG for 5 hours at 30°C. The proteins were purified using amylose resin and eluted using 15 mM maltose (Figure 6.6). Nek2 kinase assays were then performed using these purified proteins as substrates. The results showed that the C-Nap1-CTD mutant constructs were still phosphorylated to a similar extent to that of the wild-type protein (Figure 6.6). The C-Nap1-CTD-T2419A/T2423A/S2424A expressed at significantly lower levels; however, clear phosphorylation of this construct was still observed. However, this may not rule out that these residues are target sites for Nek2 as the loss of phosphorylation at these sites may be masked by a high degree of phosphorylation throughout the remainder of the C-Nap1-CTD. It will be necessary to perform quantitative measurements of the phosphate incorporation into these proteins to determine if any loss of phosphorylation has occurred.

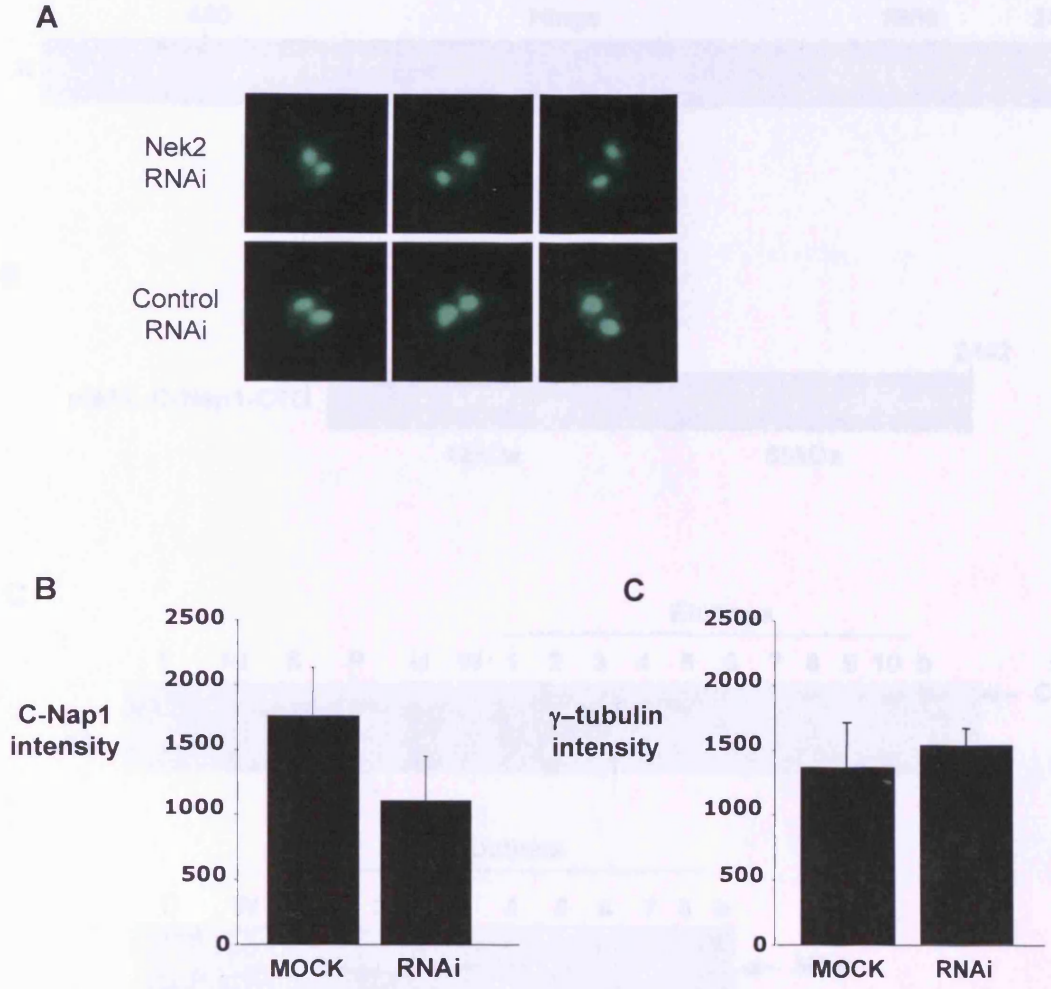

Figure 6.2 C-Nap1 is reduced after Nek2 RNAi treatment

A. Asynchronous U2OS cells were transfected with Nek2 RNAi duplexes (top panels) or control duplexes (bottom panels) using Oliogfectamine (Invitrogen). Cells were fixed at 48 hours post transfection and co-stained using a C-Nap1 (green) antibody. Three representative centrosomes are shown. **B**. The intensity of C-Nap1 at centrosomes in cells treated with Nek2 or control duplexes were quantified using Openlab software. Approximately 50 cells was measured for each condition. **C.** As for B, except the intensity of γ-tubulin was quantified. Error bars represent the standard deviation of intensity between the 50 cells during one treatment.

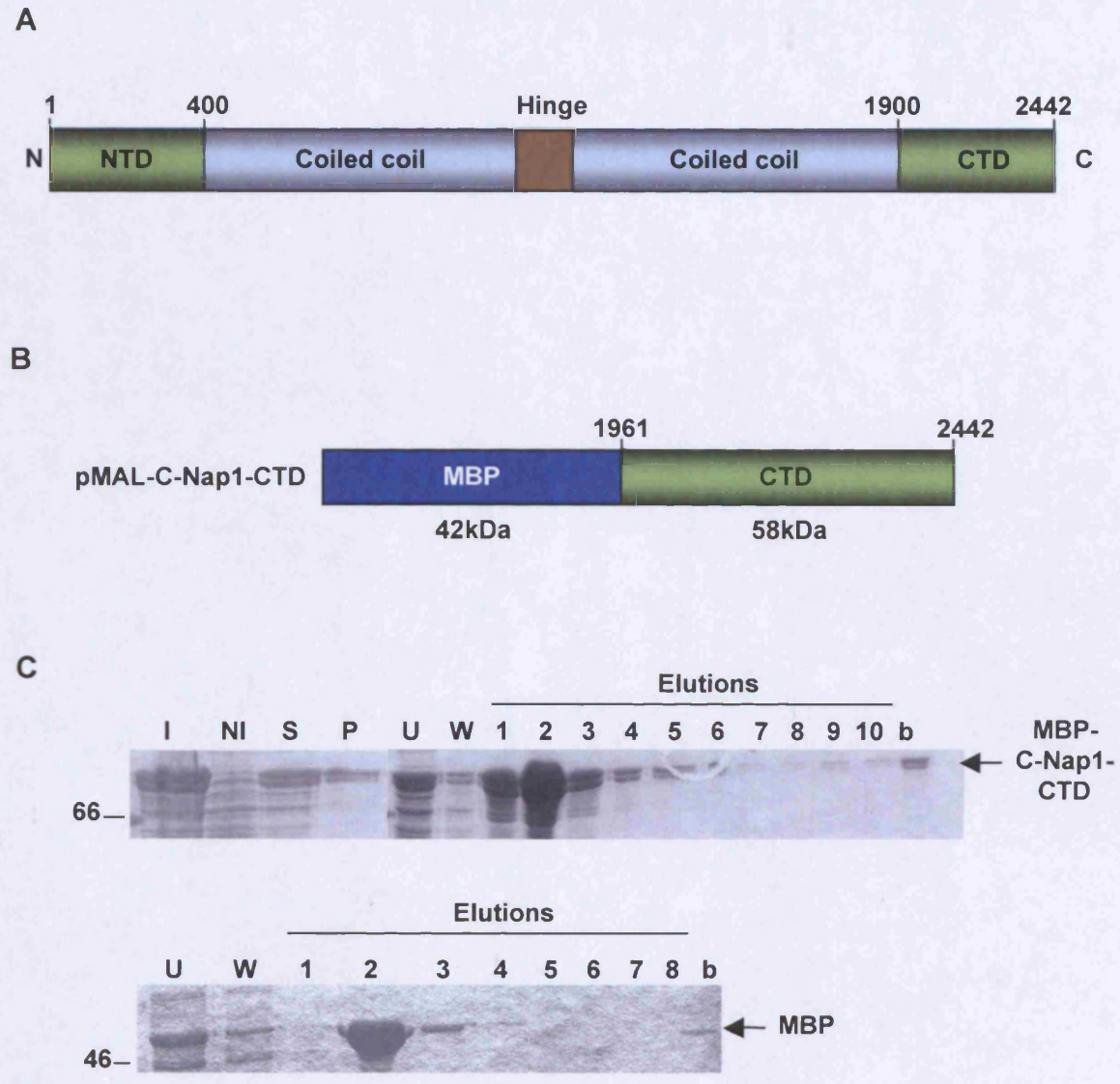

Figure 6.3 Expression of the C-Nap1 C-terminal domain as an MBP fusion protein in bacteria

A. Schematic diagram of the C-Nap1 protein. The C-Nap1 protein contains a globular N-terminal (NTD) and C-terminal (CTD) These regions are separated by two coiled-coils and a hinge motif. **B.** The CTD of C-Nap1 was cloned into the expression vector pMAL which contains an MBP purification tag. **C.** The pMAL-C-Nap1-CTD construct (upper panel) and a pMAL vector alone (lower panel) were transformed into *Rosetta E. coli* and induced with IPTG (NI=non-induced, I=induced). The bacteria were pelleted (S=soluble, P=pellet fraction) and the supernatant run over a column containing amylose beads (W=wash). Protein was eluted (E=elutions) from the column by the addition of 15 mM maltose and 5 μl samples taken at each stage of the procedure and analysed by SDS-PAGE gel and Coomassie Blue staining. Beads (b) were also run on the gel. M. wts (kDa) are indicated on the left of each panel.

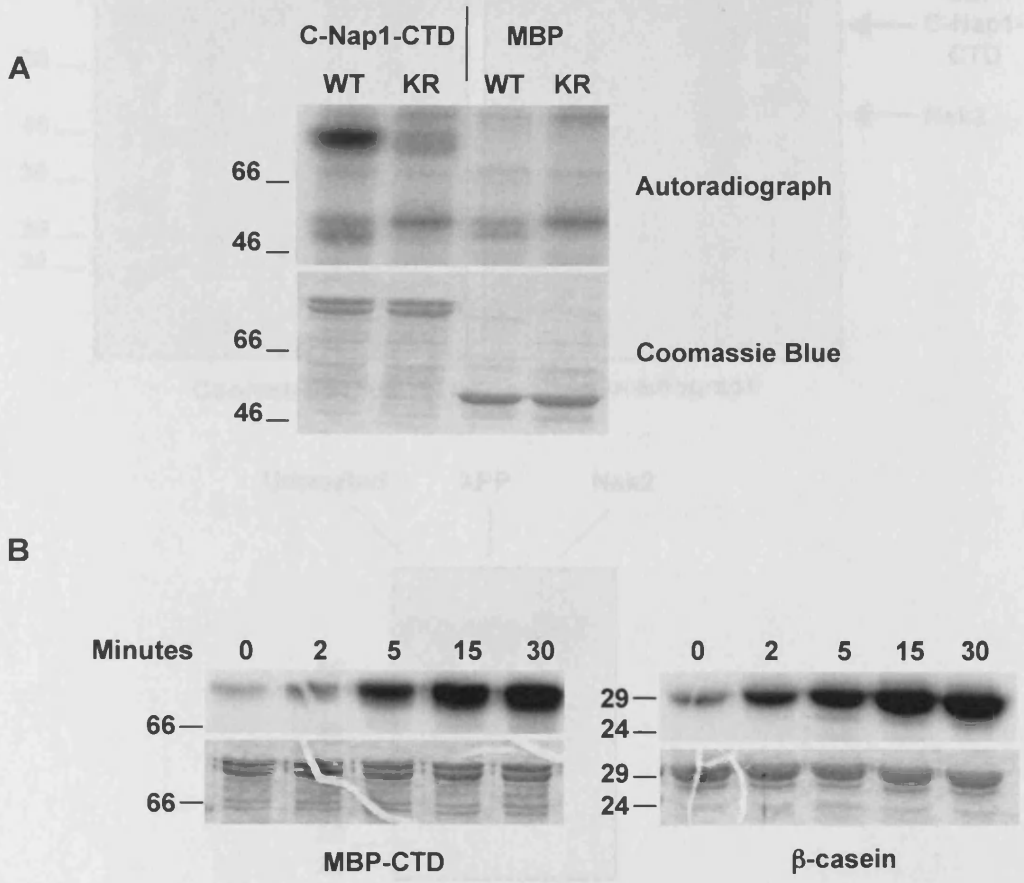

Figure 6.4 The CTD of C-Nap1 is phosphorylated by the Nek2 protein kinase

A. 5 μg of MBP-CTD-C-Nap1 or MBP alone was added to kinase buffer containing ^{32}P-γ-[ATP] and incubated for 30 mins at 30°C. The kinase reaction was stopped by the addition of 50 μl of sample buffer and 20 μl of the reaction was analysed by SDS-PAGE and Coomassie Blue staining (bottom panel) and autoradiography (top panel). The CTD of C-Nap1 is specifically phosphorylated by the Nek2A-WT kinase (lane 1); the MBP tag is not phosphorylated by the Nek2A-WT kinase (lane 3). The Nek2A-KR kinase also does not phosphorylate the proteins (lane 2, 4). **B.** Approximately 5 μg of either the MBP-C-Nap1-CTD or casein was incubated at 30° C in Nek2 kinase buffer containing ^{32}P-γ–[ATP]. 8 μl samples were taken at 0, 2, 5, 15 and 30 minute intervals and combined with the equivalent of sample buffer. Samples were analysed by SDS-PAGE and Coomassie Blue staining (bottom panels) and autoradiography (top panels). M.wts (kDa) are indicated on the left.

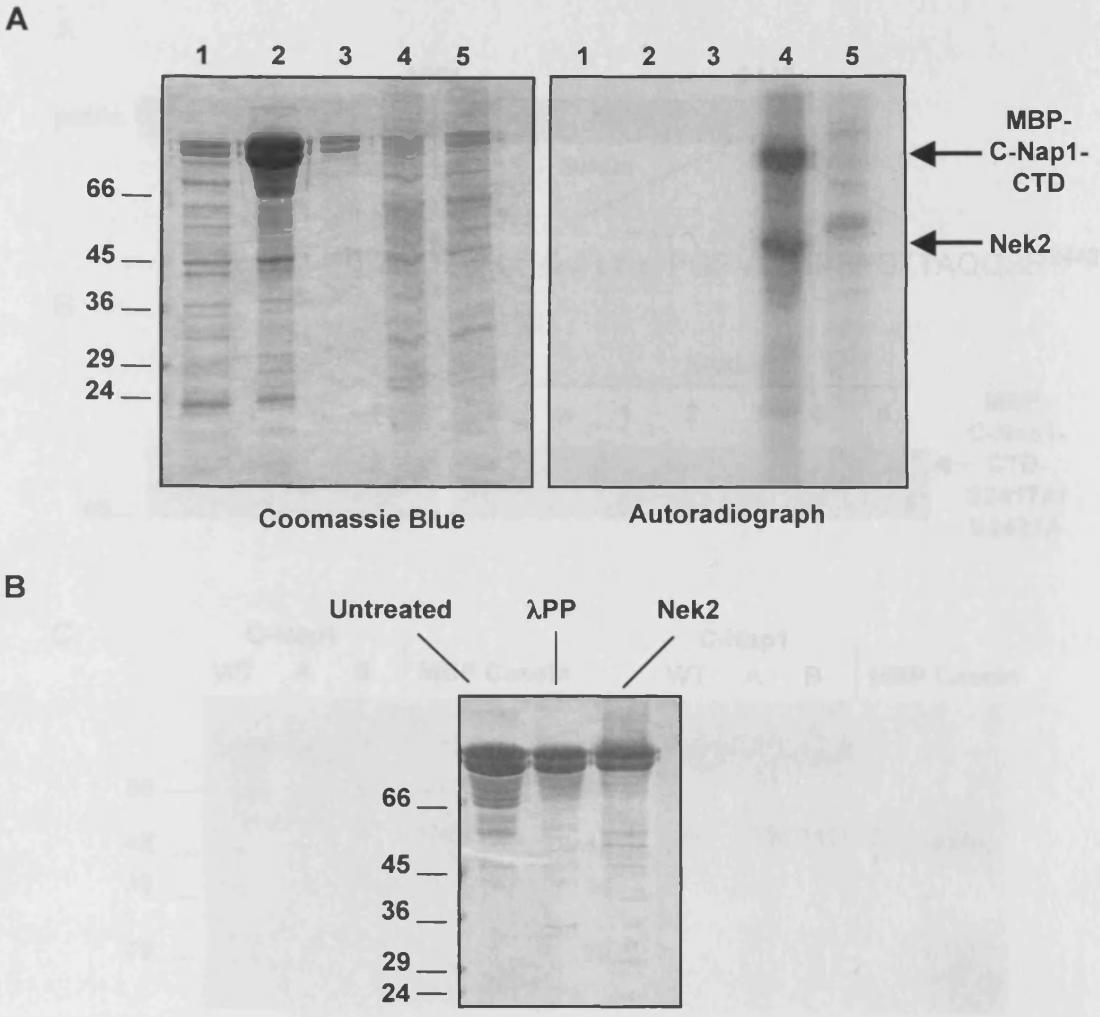

Figure 6.5 Preparation of phosphorylated C-Nap1 C-terminal domain for mass spectrometry

A. 200 μg of soluble MBP-C-Nap1-CTD protein was bound to 250 μl of amylose beads for 2 hrs. A fraction of unbound material was taken as a control (lane 1). Approximately one third of the beads were washed three times in PBS and snap frozen (lane 2, untreated beads). The remaining two thirds were washed in λ-phosphatase buffer three times followed by λ-phosphatase treatment at 30°C for 5 hrs. The beads were washed three times in PBS and half taken and frozen (lane 3, stripped sample). The remaining beads were washed three times in kinase buffer and incubated in kinase buffer containing ^{32}P-γ-[ATP] and either WT (lane 4) or kinase inactive Nek2 (lane 5) for 40 minutes at 30°C. Sample buffer was added and products were separated on a 12% SDS-PAGE gel for analysis. **B.** MBP-C-Nap1-CTD was subjected to the same protocol as (A) with the following changes: 400 μg of soluble fraction was bound to 500 μl of amylose beads and beads incubated with Nek2-WT and unlabelled ATP for 1 hr and washed three times with PBS after the reaction was complete. Lane 1 represents a fraction of the untreated sample, lane two the λPP stripped sample and lane three Nek2 treated sample. Proteins attached to beads were subsequently sent for mass spectrometry analysis to Millennium Pharmaceuticals (Boston, USA). M. wts (kDa) are indicated on the left.

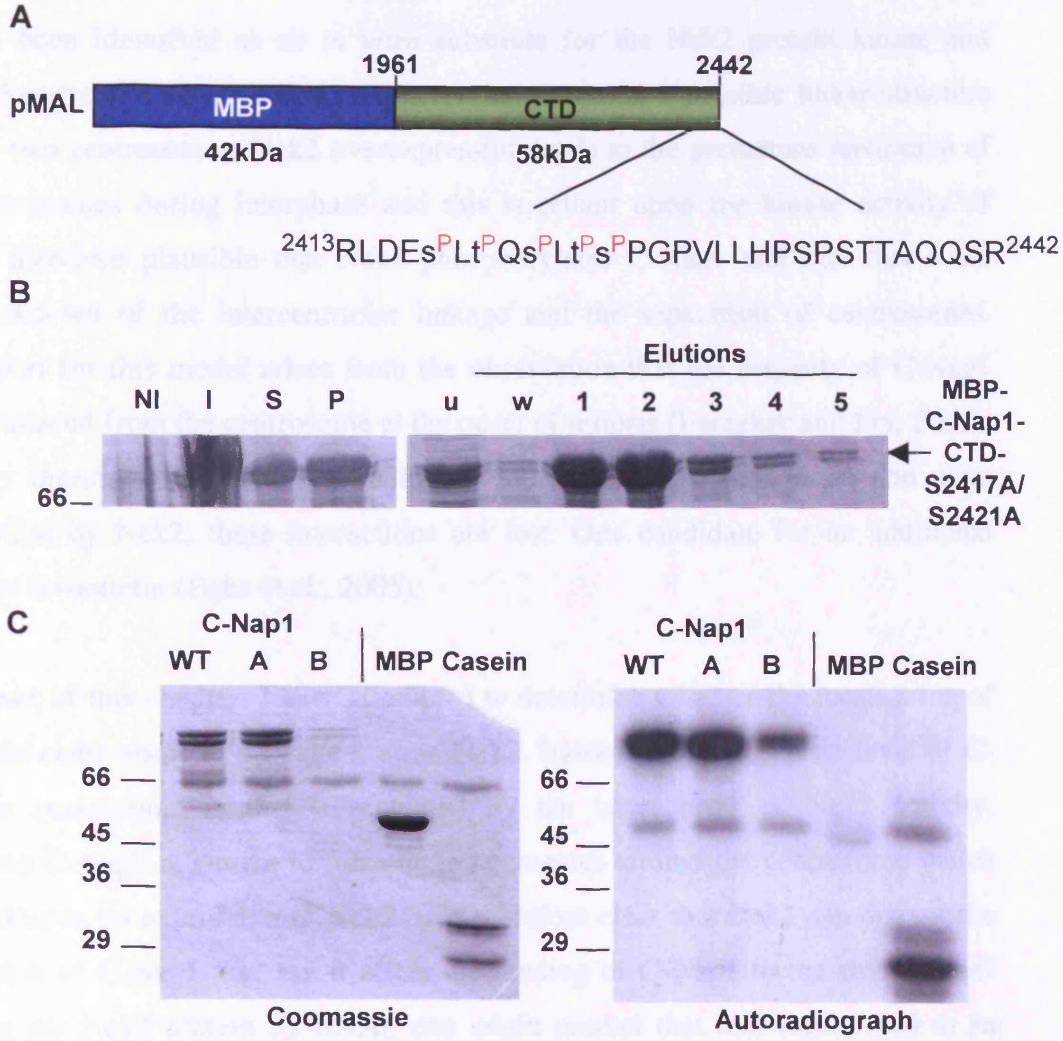

Figure 6.6 Mutation of putative phosphorylation sites does not abolish Nek2 phosphorylation of the C-Nap1 C-terminal domain

A. A schematic diagram of the MBP-C-Nap1-CTD construct. The position of possible phosphate incorporation was narrowed down to the N-terminal region of this tryptic fragment. Possible sites are shown by a ^{P} and these have been mutated to alanine. **B.** The MBP-C-Nap1-CTD mutants S2417A/S2421A (A) and T2419A/T2423A/S2424A (B) were expressed in *Rosetta E. coli* and induced with IPTG (NI=non-induced, I=induced). The bacteria were pelleted (S=soluble, P=pellet fraction) and the supernatant run over a column containing amylose beads (u=unbound, w=wash). Protein was eluted from the column by the addition of 15 mM maltose and 5 µl samples taken at each stage of the procedure and analysed by SDS-PAGE gel and Coomassie Blue staining. MBP-C-Nap1-CTD-T2419A/T2423A/S2424A purification was performed under my supervision by Miss Sunitha Karkarla. Data is just shown for MBP-C-Nap1-CTD-S2417A/S2421A. **C.** The purified constructs were then subjected to an *in vitro* kinase assay using Nek2 kinase (Upstate). Products were separated by SDS-PAGE and analysed by Coomassie Blue staining (left panel) and autoradiography (right panel). M. wts (kDa) are indicated on the left of each panel.

6.3 Discussion

C-Nap1 has been identified as an *in vitro* substrate for the Nek2 protein kinase and functional characterisation of C-Nap1 suggests that it acts as a possible linker structure between the two centrosomes. Nek2 overexpression leads to the premature separation of the two centrosomes during interphase and this is reliant upon the kinase activity of Nek2. It is therefore plausible that Nek2 phosphorylates C-Nap1 and that this event triggers breakdown of the intercentriolar linkage and the separation of centrosomes. Further support for this model arises from the observation that the majority of C-Nap1 protein is displaced from the centrosome at the onset of mitosis (Faragher and Fry, 2003). C-Nap1 may therefore be anchoring additional proteins at the centrosome, and upon phosphorylation by Nek2, these interactions are lost. One candidate for an additional linker protein is rootletin (Bahe et al., 2005).

In the first part of this chapter, I have attempted to determine whether the localisation of C-Nap1 at the centrosome is dependent upon Nek2. Indeed, the steady state level of C-Nap1 at the centrosome might be regulated by the basal level of Nek2 activity. Overexpressed C-Nap1 is known to form large aggregates around the centrosome which are dispersed upon co-expression of Nek2. It is therefore clear that Nek2 can disrupt the oligomerisation of C-Nap1, but can it affect the binding of C-Nap1 to the centrosome? By depleting the Nek2 protein by RNAi, one might predict that this would lead to an increase in the abundance of C-Nap1 at the centrosome. However, the relative abundance of C-Nap1 at the centrosome upon Nek2 depletion was reduced. This suggests either an overall breakdown of centrosome structure which was also observed after prolonged Nek2 overexpression (Fry et al., 1998b), or that Nek2 is required for C-Nap1 localisation at the centrosome during interphase. However, as the levels of γ-tubulin were not disrupted after Nek2 depletion it is possible that Nek2 may be required for C-Nap1 localisation at the centrosome. I have also shown in chapter 4 that Nek2 depletion does not alter Nlp abundance at interphase centrosomes. It will be important to investigate the effect of Nek2 depletion on other core centrosomal proteins such as centrin.

To investigate the consequences of C-Nap1 phosphorylation by Nek2, we have started to map some of the Nek2 phosphorylation sites. The first sites identified in collaboration with Millennium Pharmaceuticals (Boston, USA) are within a long peptide (amino acids 2413-2442) at the extreme C-terminus of C-Nap1. This peptide contains 10 possible sites that include, S2417, T2419, S2421, T2423, S2424, S2433, S2435, T2436, T2437 and S2441. However, additional mass spectrometry analysis suggested the phosphates are within the first five of these sites (S2417, T2419, S2421, T2423, S2424). *In vitro* assays have demonstrated that mutation of these five sites alone, albeit in two different constructs, does not significantly abolish Nek2 phosphorylation of the C-Nap1-CTD by Nek2. However, there are up to 13 Nek2 phosphorylation sites within the C-Nap1 C-terminal domain and so one or more of these sites may be correct. Further studies are required to identify additional sites phosphorylated by Nek2 in the C-Nap1-CTD. Mutation of all these sites together may be required to produce a significant phenotype. It is plausible to assume that mutation of these sites would have profound effects upon the cell. For example, monopolar spindles may occur as a result of the lack of centrosome splitting.

The putative phosphorylation sites identified here are within the C-terminal domain of C-Nap1 (amino acids 2413-2442). Interestingly residues 2362-2442 have been previously identified as a possible Nek2 interacting domain (Hames and Fry, 2002). Indeed, Nek2 has also previously been shown to interact with and phosphorylate the C-Nap1-NTD. Within both the C-Nap1 C- and N-terminal regions lies the common motif LXXS which is present three times within the peptide identified by Millennium Pharmaceuticals and is also present within the N-terminal domain of C-Nap1. A RLXXSL motif has previously been suggested as a possible binding motif for Nek2 in C-Nap1 (Hames and Fry, 2002). It is possible therefore that this motif may represent either or both a phosphorylation and binding motif. It is also possible that phosphorylation of this motif by Nek2 could facilitate binding of Nek2 to C-Nap1. To investigate this further *in vitro* binding studies with mutated C-Nap1 proteins could be used to determine if Nek2 interaction with C-Nap1 is affected.

Multiple sites are phosphorylated within C-Nap1 by Nek2 and it is interesting that these sites lie in the regions also identified as regions of Nek2 binding. C-Nap1 is a large multidomain protein containing coiled-coils, non-coiled C- and N-termini and a hinge region. C-Nap1 can form oligomers and most probably binds other proteins at the centrosome. Nek2 has been shown to disrupt the interaction of C-Nap1 with itself and is a kinase which induces centrosome splitting. It is possible therefore that the phosphorylation by Nek2 at these specific sites causes a change in C-Nap1 structure. The protein may unfold and release bound proteins (for example rootletin) to initiate centrosome splitting. Interestingly, the C- and N-terminal regions of C-Nap1, but not the central region, localise to the centrosome (Mayor et al., 2000). These regions are therefore important for both centrosomal localisation of the protein and Nek2 interaction and phosphorylation. To further our understanding of the importance of the Nek2 phosphorylation sites that lie within the N- and C-terminal domains, mutations can be made. The effect of these mutations on C-Nap1 interactions with the centrosome, rootletin and Nek2 could then be observed. It would also be interesting to determine the effects of overexpressing mutated forms of C-Nap1 *in vivo*, especially in light of the fact that overexpression of the N-terminal region and middle region of C-Nap1 induce centrosome splitting to a similar extent to Nek2 (Mayor et al., 2000). Nek2 may regulate the interaction of the C-terminal domain with the centrosome and the N-terminal domain with other factors which contribute to the integrity of the intercentriolar linkage.

Additionally, these preliminary data could be used to monitor the timing of Nek2 activation within cells by the generation of phosphospecific antibodies against Nek2 phosphorylation sites within C-Nap1. Western blotting and immunofluorescence microscopy using the specific antibodies would reveal the exact timing of C-Nap1 phosphorylation and more importantly shed insight on the events which occur immediately following Nek2 phosphorylation.

Chapter Seven

Final Discussion

7.1 Nek2 regulation by autophosphorylation

Previous studies of the Nek2 protein kinase demonstrated that the active kinase is capable of inducing centrosome splitting in interphase cells (Fry et al., 1998b). This highlighted the possibility that Nek2 plays a major role in centrosome cohesion. There is also evidence that Nek2 contributes to chromatin condensation and the reorganisation of the microtubule network at the G2/M transition. This raises the important question of how Nek2 achieves its timely and precise activation to initiate these processes. Understanding how Nek2 is activated and regulated has been a major goal of this thesis as loss of control of Nek2 activity may have severe consequences for cell division (Hayward et al., 2004). Indeed, the Nek2 protein has been shown to be elevated 2- to 5-fold in cell lines derived from a number of human tumours (Hayward et al., 2004). In addition, ectopic expression of Nek2 in immortalised HBL100 breast epithelial cells leads to the accumulation of multinucleated cells with supernumary centrosomes (Hayward et al., 2004). The prognosis for this type of cell is likely to be poor and therefore the aim of this thesis was to gain insight into how Nek2 is regulated by autophosphorylation, as well as how it regulates other centrosomal partners. Identification of a specific target motif of Nek2 was also a major aim of this thesis as this could be used to generate phosphospecific antibodies and to identify new substrates of Nek2.

Previous work on Nek2 had identified its unique structural features. It contains an N-terminal catalytic domain and a C-terminal regulatory domain which includes a leucine zipper required for homodimerisation (Fry et al., 1999). The leucine zipper is thought to promote homodimerisation which in turn leads to trans-autophosphorylation (Fry et al., 1999). Trans-autophosphorylation is thought to occur predominantly on serine and threonine residues. We have begun to shed further light on the control of Nek2 as we have identified autophosphorylation sites that are important for Nek2 activity.

7.1.1 Is there a common mode of activation for the Nek kinases?

Autophosphorylation of Nek2 may change Nek2 in structure allowing a fully active conformation to be achieved. Nek2 may then proceed to target its substrates for example

C-Nap1, rootletin and Nlp and trigger centrosome splitting and other essential mitotic events. We present data here that, in collaboration with Prof. S. Smerdon, residues T170/S171, T175, T179, S241, S387, S390, S397, S402 and S428 are Nek2 autophosphorylation sites. These sites are phosphorylated in bacteria during expression of the protein. Independently, during the characterization of Nek2 kinase purified from baculovirus expression in insect cells, Invitrogen have identified S171, S296, S368, S387 and S428 as Nek2 autophosphorylation sites. S171, T175 and T179 lie within the activation loop of Nek2 whereas the remaining sites lie in the non-catalytic C-terminal region. S387, S390, S397, S402 are found immediately following the PP1 binding motif, and S428 near to the destruction motifs at the extreme C-terminus of Nek2. I have examined many of these sites through mutagenesis and found a number of them to be absolutely required for Nek2 activity. When autophosphorylation is prevented from occurring on residues T175, T179 and S241 by mutation to alanine we observe that Nek2 activity is abolished. Nek2 therefore absolutely requires the presence of these residues for activity. Mutation of T175 to glutamic acid activated Nek2; in contrast mutation of T179 and S241 to glutamic and aspartic acid, respectively, led to an inactive kinase. This suggests that a glutamate residue can effectively mimic a phosphorylated threonine residue at position T175 and that this site is indeed a *bona fide* autophosphorylation site which is absolutely required for Nek2 activity. However. we cannot conclude the same for position T179 and S241, these are obviously extremely important residues which are required for Nek2 activity. However, they may be playing a structural role and these data cannot conclusively identify them as Nek2 autophosphorylation sites *in vitro*.

Like Nek2, Nek6 and Nek7 are activated by phosphorylation of their T-loop domains. Nek6 activation requires phosphorylation at Ser 206 and Thr 202. The phosphorylation of Ser 206 is the major contributor to Nek6 activation but Thr 202 is also required for full activation to occur. Ser 206 is actually targeted by the Nek9 protein kinase in what has been termed a Nek2 kinase cascade of activation (Belham et al., 2003). By comparing the sequence of Nek6 and Nek2 it is clear that Thr 202 of Nek6 and Thr 191 of Nek7 are equivalent in position to Ser 171 of Nek2 (Figure 7.1). Also the residue preceding this site is always a threonine in all three kinases. In addition, positions equivalent to 206 and

210 of Nek6 are also Thr in both Nek2 and Nek7. It is possible that these kinases all share a common mode of activation. Data on Nek6 suggests that Ser 206 is the major site of phosphorylation and that Thr 202 is required for Nek6 activation but to a lesser degree. This is similar to the results obtained for Nek2. Thr 175 of Nek2 is absolutely required for Nek2 activity with Ser 171 possibly also important. However, Ser 171 needs to be investigated more fully to understand its role in Nek2 regulation. Is it possible therefore that all Nek kinases require phosphorylation of similar residues to achieve their full activation status? This is something that needs to be explored further by investigating the effects of single and double mutations in the Nek2 activation loop.

7.1.2 Is the C-terminus of Nek2A an autoinhibitory domain?

The C-terminal domain of Nek2 contains many regulatory features including the KEN and D-boxes required for Nek2 degradation (Hames et al., 2001), a microtubule and centrosomal targeting motif (Hames et al., 2005) and the PP1 binding site (Helps et al., 2000). Binding of PP1 leads to inhibition of Nek2 presumably through dephosphorylation of the autophosphorylation sites. We have identified an important region within the non-catalytic domain that affects kinase activity. Removal of the C-terminal 25 amino acids of Nek2 creates a hyperactive kinase. It is therefore possible that these 25 amino acids act as an autoinhibitory domain. However, Nek2B which also lacks the C-terminus present in Nek2A does not have increased kinase activity compared to Nek2A as it is less efficient at stimulating centrosome splitting than Nek2A upon overexpression (Hames and Fry, 2002). It is possible therefore that Nek2B is under different control mechanisms than Nek2A.

How the possible C-terminal inhibition is released is a question which remains to be answered. It is possible that autophosphorylation of the C-terminus of Nek2 relieves the inhibition. However, mutation of the autophosphorylation sites identified at positions S387, S390, S397 and S402 to alanine or aspartic acid did not alter Nek2 activity upon its substrate β-casein *in vitro* and had little effect upon centrosome splitting *in vivo*. Interestingly though, when these sites were mutated to alanine or aspartate there was a slight increase in autophosphorylation. These sites lie in close proximity to the PP1

binding site 'KVHF' at position 383-386 but GST-pull down experiments demonstrated that mutation of these sites to alanine or aspartate had no effect on PP1 binding. S428 which has also been identified as a Nek2 autophosphorylation site also needs to be investigated in this regard.

7.1.3 Generation of Nek2 phosphospecific antibodies

Experiments performed during this thesis have provided the first steps into understanding how Nek2 is controlled through autophosphorylation. Indeed, from the information gathered about position T175 within the activation loop, the production of phosphospecific antibodies began. Phosphospecific antibodies and non-phosphospecific antibodies were raised in rabbits in collaboration with Millennium Pharmaceuticals (Boston, USA). The subsequent sera raised against the phospho-peptide ($T175^{P}$) were released to us for testing and purification (Figure A1). Unfortunately, the purification of the T175 phosphospecific antibody was unsuccessful as the purified antibody (i) failed to detect endogenous Nek2 on a Western Blot (Figure A5), (ii) failed to localise to the usual sites of Nek2 localisation in U2OS cells (Figure A6), and (iii) still stained cells after Nek2 depletion by RNAi (Data not shown). It is possible that the antiserum raised was targeting another centrosomal protein. Many kinases have a conserved activation loop and therefore this antibody could quite possibly have been recognising other kinases which share a similar sequence. In addition, following the production of the phosphospecific antibody directed at the phosphorylated T175 residue other residues within this region were identified as being phosphorylation sites. Namely, T170, S171 and T179. It is possible that the antibodies raised would not recognise a fully activated Nek2 kinase because of the structural changes caused by these additional phosphate groups. The knowledge acquired from this thesis will allow further attempts at phosphospecific antibody production. These can be used to determine the exact timing of Nek2 activation within the cell cycle.

7.2 Does a Nek2 target consensus site exist?

Most protein kinases recognise specific sequences surrounding the phosphorylated residue. Specificity is required to ensure that each kinase can target the appropriate

substrates. A number of consensus sites have been identified by numerous methods including mutagenesis, mass spectrometry and more recently by using peptide library screens. The NIMA consensus, defined as FRXS/T (Lu et al., 1994), was identified by phosphorylating degenerate peptide libraries. Nek6 and Nek7 target the sequence FP/LXFS/TF/Y (Belham et al., 2001; Lizcano et al., 2002). So does Nek2 have a consensus sequence? During the work undertaken in this thesis we have identified a total of eleven putative autophosphorylation sites within Nek2, six within Nlp and five within C-Nap1 (Figure 7.2). The alignment of these sites reveals that there is a preference for a hydrophobic group at both position –2 (10 out of 23) and position +2 (14 out of 23) from the target site. However, apart from this it is not clear that a specific consensus sequence exists. Further work to determine the bona fide *in vivo* phosphorylation sites may reveal a clearer picture of the Nek2 consensus. Using degenerate peptide libraries may be another method to identify a Nek2 consensus site however how accurate these are in terms of the behaviour of the protein *in vivo* will still need to be established. It is possible that no clear consensus exists because Nek2 relies on other factors for its target specificity. For example, it may bind at a particular consensus and then phosphorylate its targets at a site distinct from this.

7.3 Nlp interaction with the γTuRC

Mitotic entry requires a major reorganisation of the microtubule cytoskeleton in addition to a structural reorganisation of the centrosome called maturation. During centrosome maturation there is substantial recruitment of γ-tubulin to the centrosome and an increase in microtubule nucleation ready for spindle pole formation. Centrosome maturation is controlled in part by the Aurora A and Plk1 kinases. Recently, the centrosomal protein Nlp has been identified as a target for Plk1 and we have shown it to be targeted by Nek2 (Casenghi et al., 2003; Rapley et al., 2005).

Nlp is a γ-tubulin binding protein that is present on interphase centrosomes but absent from spindle poles. Displacement of Nlp is therefore thought to be an important step in centrosome maturation. Premature phosphorylation of Nlp by overexpression of either Plk1 or Nek2 displaces the protein from the centrosome during interphase whereas

endogenous Nlp is normally displaced only at the onset of mitosis (Figure 7.2). Nlp localisation at the centrosome is also controlled by its association with the dynein-dynactin complex (Casenghi et al., 2005). The transport of Nlp to the centrosome is negatively regulated by Plk1 phosphorylation of Nlp. Therefore, at the onset of mitosis, Nlp protein is displaced by Plk1 and Nek2 and in a second mechanism its transport to the centrosome is blocked. This thesis has demonstrated that overexpressed Nlp aggregates are saturated with γ-tubulin and that Nek2 does not affect the interaction of Nlp with γ-tubulin, but it does effect the interaction of Nlp with itself and the centrosome. A kinase-inactive form of Nek2 also blocks the phosphorylation and displacement of Nlp by Plk1. It is therefore clear that there is a complex level of regulation by phosphorylation of the Nlp protein. This regulation is in place to ensure that changes in microtubule organisation at mitotic onset are properly executed.

Nlp is a mother centriole specific protein. This localisation raises the possibility that it is involved in microtubule anchoring at the centrosome via the distal and subdistal appendages of the mother centriole. Other mother centriole associated proteins implicated in microtubule anchoring include ninein, dynactin and the small GTPase Ran. Microtubule anchoring may be facilitated by the interaction of γ-tubulin with Nlp at the mother centriole. At the onset of mitosis when a major reorganisation of the microtubule network begins this anchoring is replaced by increased nucleating activity at the centrosome. As such Nlp is released form the centrosome and its interaction with γ-tubulin is severed. Nlp displacement form the centrosome occurs through the phosphorylation of Nlp by Plk1 and Nek2. However, its release from γ-tubulin is triggered solely by Plk1. One possibility is that, at the onset of mitosis, Nek2 phosphorylates Nlp which in turn leads to increased phosphorylation of Nlp by Plk1. This prevents both Nlp recruitment by dynactin and severes the interaction of Nlp with the centrosome. It also leads to the release of Nlp from γ-tubulin. Nlp may also be phosphorylated by a second kinase (e.g Cdk1) which may also increase the interaction of Plk1 with Nlp. Plk1 and Nek2 are equally capable of displacing Nlp from the centrosome explaining why Nek2 depletion does not alter centrosomal Nlp. However, primary phosphorylation by Nek2 enhances Plk1 phosphorylation. When inactive Nek2A is

present, the displacement of Nlp is blocked, possibly because inactive Nek2A binds and is not released from Nlp and as such access by Plk1 is hindered. Alternatively, if Nek2 and Plk1 form a complex before their interaction with Nlp, the inactive Nek2A protein may bind Plk1 and sequester it away from the centrosome. However, there is no evidence that Plk1 and Nek2 interact directly. This model of Nlp regulation is complex and therefore further investigation needs to be performed. One possibility is to perform depletion of both Plk1 and Nek2 and measure the effects on Nlp localization at the centrosome. A second major experiment to be carried out would be using the Nlp protein with the Nek2 phosphorylation sites mutated in *in vitro* kinase assays and *in vivo* to determine if Plk1 can, still phosphorylate Nlp and still displace overexpressed Nlp aggregates from the centrosome. This, however, will require confirmation of the key Nek2 phosphorylation sites within Nlp.

7.3.1 Nek2, a priming kinase for Plk1?

Nlp is present at the interphase centrosome but can be displaced by the overexpression of both Plk1 and Nek2 kinases (Casenghi et al., 2005; Rapley et al., 2005). The mechanism by which Plk1 targets its substrates requires a pre-phosphorylation event to occur at the sequence S-pS/pT. Plk1 then binds to the phosphorylated sequence via a motif termed the PBD in its C-terminal non-catalytic domain (Elia et al., 2003a; Elia et al., 2003b; Neef et al., 2003). We have demonstrated that following phosphorylation by Nek2, Plk1 can phosphorylate Nlp to a greater extent than after pre-incubation with inactive Nek2 or no kinase. However further evidence to support priming by Nek2 is slim. The identification of Nek2 phosphorylation sites within Nlp revealed that none lie in a PBD consensus sequence. Likewise, Far-Western blots did not support increased PBD binding after phosphorylation by Nek2. However, although not creating a binding site for Plk1, it is still evident that Nek2 is placed upstream of Plk1 phosphorylation for a number of reasons. One being that Nek2 does increase phosphorylation of Nlp by Plk1. Secondly, the presence of the inactive Nek2 protein prevents the displacement and phosphorylation of Nlp by Plk1. It is therefore possible that inactive Nek2 is somehow blocking the access of Plk1 to Nlp and as such preventing phosphorylation. It is possible that when the

inactive Nek2 protein is present in excessive amounts it binds to Nlp but remains bound and therefore blocks access by Plk1.

Depletion of Nek2 from the centrosome addresses the question of whether one or both of the kinases are required in the physiological setting to displace Nlp from the centrosome. It is clear from these results that Nek2 is not solely responsible for this process and either a third kinase is involved (possibly Cdk1) or Plk1 and Nek2 play slightly redundant roles in this process.

7.3.2 Cdk1, a priming kinase for Plk1?

The Cdk protein kinases are major regulators of cell cycle transitions. Cdk1 activity directly or indirectly triggers the early events of mitosis such as chromosome condensation, nuclear envelope breakdown and spindle formation (McCollum and Gould, 2001). The commitment to mitosis is mediated by the rapid activation of Cdk1-cyclin B, the core component of the M-phase promoting factor MPF (Pines and Rieder, 2001). Within this thesis, we have shown that Cdk1 is another protein kinase that can phosphorylate Nlp. Importantly, this phosphorylation, unlike that of Nek2A, does promote binding of the Plk1 PBD to Nlp. Is it possible therefore that Cdk1 acts as a priming kinase for Plk1 on Nlp. However, closer examination of the Nlp sequence reveals there are three possible Cdk1 consensus sites (amino acids S185, S191 and T196). But phosphorylation of these motifs would not create the preferred docking site for Plk1, Ser-^{P}Ser-Pro. It is possible though that Cdk1 is promoting binding of Plk1 by another as yet unidentified means.

Cdk1 has recently been shown to act as a priming kinase for Plk1 upon the substrate vimentin, an intermediate filament protein which makes up the cytoskeletal network (Yamaguchi et al., 2005). Cdk1 phosphorylation of vimentin induces Plk1 mediated vimentin phosphorylation during mitosis. Cdk1 initially phosphorylates vimentin at Ser 55 creating a docking site for the Plk1-PBD. Plk1 then phosphorylates vimentin at Ser 82 which initiates reorganisation of vimentin filaments. With this in mind it is possible that Cdk1 initiates phosphorylation and activation of proteins by Plk1 in a number of protein

kinase cascades including Nlp. This would ensure that the timing of Nlp phosphorylation is directly co-ordinated to other mitotic events.

Further investigation of Nlp regulation by Cdk1 was beyond the scope of this thesis, but it would be interesting to observe the effects of mutating the putative Cdk1 phosphorylation site within Nlp. Although, from the data gathered, this is unlikely to affect phosphorylation of Nlp by Nek2 it may however prevent phosphorylation by Plk1.

7.4 Nek2, C-Nap1 and the intercentriolar linkage

The most studied role of Nek2 within the cell has been its regulation of centrosome splitting at the G2/M transition. Overexpression of active but not inactive Nek2 causes the premature splitting of interphase centrosomes (Fry et al., 1998b). It has long been established that an intercentriolar linkage exists between the mother and daughter centriole. This linkage has been observed in isolated centrosomes by electron microscopy and is supported by the consistent recovery of isolated centrosomes in pairs (Paintrand et al., 1992). The nature of this intercentriolar linkage is still poorly understood. However, it has been proposed that C-Nap1 and rootletin may form part of this structure (Bahe et al., 2005; Mayor et al., 2000). Part of this thesis has been concerned with the regulation of C-Nap1 by Nek2 in terms of its localisation and phosphorylation. We have identified a number of putative phosphorylation sites upon C-Nap1, however further investigation into these sites need to be explored. In addition to the phospho-site mapping, we have performed Nek2 depletion assays using RNAi and measured the effects of depletion upon the level of C-Nap1 and γ-tubulin at the interphase centrosome. It appears that Nek2 depletion actually induces a small loss of C-Nap1 from the centrosome. It is possible therefore that Nek2 depletion disrupts the localisation or recruitment of C-Nap1 to the centrosome. However Nek2 may also be disrupting other centrosomal proteins. This theory is supported by evidence that prolonged Nek2 overexpression causes the fragmentation of centrosomes. To investigate this further it will be necessary to observe the effects of Nek2 depletion on other core centrosomal proteins such as centrin.

It is possible that Nek2 is responsible for a global change in C-Nap1 conformation which in turn leads to the degradation of the 'molecular glue' which holds the centrosomes together. This global change in C-Nap1 structure may be caused by the combined phosphorylation of C-Nap1 at its N- and C-termini by Nek2 at the G2/M transition. The association of C-Nap1 with the centrosome may then be reduced when Nek2 is degraded, further enhancing centrosome splitting. This is supported by evidence that C-Nap1 levels at the centrosome are reduced at spindle poles upon mitotic entry but are not reduced on split centrosomes induced by Nek2 overexpression. Further studies should therefore involve mutating the putative Nek2 phosphorylation sites in C-Nap1 and investigating how these mutants behave with respect to centrosome localisation and induction of centrosome splitting.

7.5 Concluding remarks

The work presented within this thesis has brought further insight into Nek2 regulation by autophosphorylation and the regulation of Nlp and C-Nap1 by Nek2, and has identified a number of Nek2 phosphorylation sites within these substrates. It has also highlighted a number of issues regarding the control of these proteins within the centrosome duplication cycle. It is clear from the work with Nek2, Plk1 and Nlp that there are no straightforward control mechanisms involved in Nlp localization at the centrosome. There may possibly be a number of kinases involved in just this aspect of microtubule anchoring and release from the centrosome. The release of Nlp from the centrosome is tightly controlled and coupled to more global cellular events. Work within this thesis has also shed further insight into the role that Nek2 plays within the cell cycle. Not only is Nek2 involved in severing the centrosomal linkage but it may also function in bipolar spindle formation through the displacement of Nlp from the mother centriole. Nek2 may also be a critical factor in controlling regulation of Nlp by Plk1 through a possible priming mechanism.

Identification of a number of Nek2 autophosphorylation and substrate phosphorylation sites has allowed us to understand more regarding how this kinase recognises its targets. Identification of these putative Nek2 phosphorylation sites will aid further investigation

into Nek2 regulation of itself and its substrates. The detection of elevated Nek2 mRNA and protein in various tumours (Hayward and Fry, 2005; Vos et al., 2003) means that understanding more about Nek2 targets and regulation is essential. Phosphospecific antibodies may prove invaluable tools for detecting elevated levels of Nek2 activity in cancer cells.

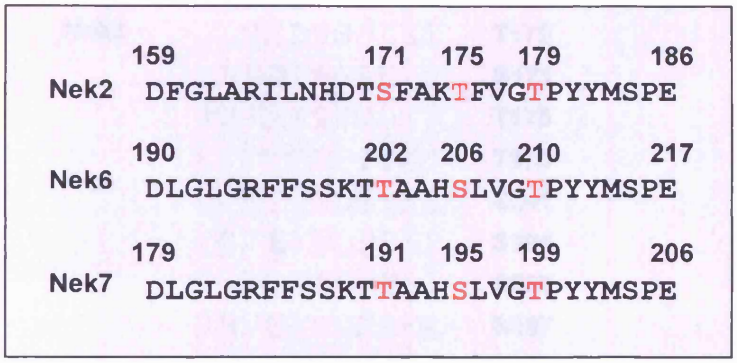

Figure 7.1 Alignment of Nek2, Nek6, and Nek7 activation loop domains
The amino acid sequences of the human Nek2, Nek6 and Nek7 activation domain segments. Conserved putative autophosphorylation sites are highlighted in red. Numbers indicate amino acid residue.

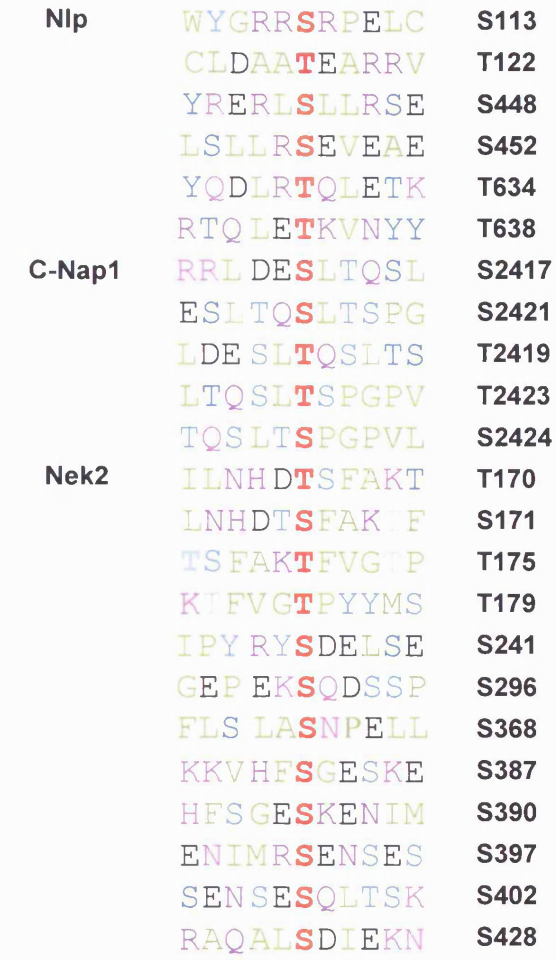

Figure 7.2 Comparison of sites phosphorylated by Nek2 identified in this study
Phosphorylation sites identified by mass spectrometry are aligned and the residues colour coded according to the type of amino acid present. The alignment suggests the possibility that there may be a requirement for a hydrophobic amino acid at position -2 and +2 from the phosphorylation site.

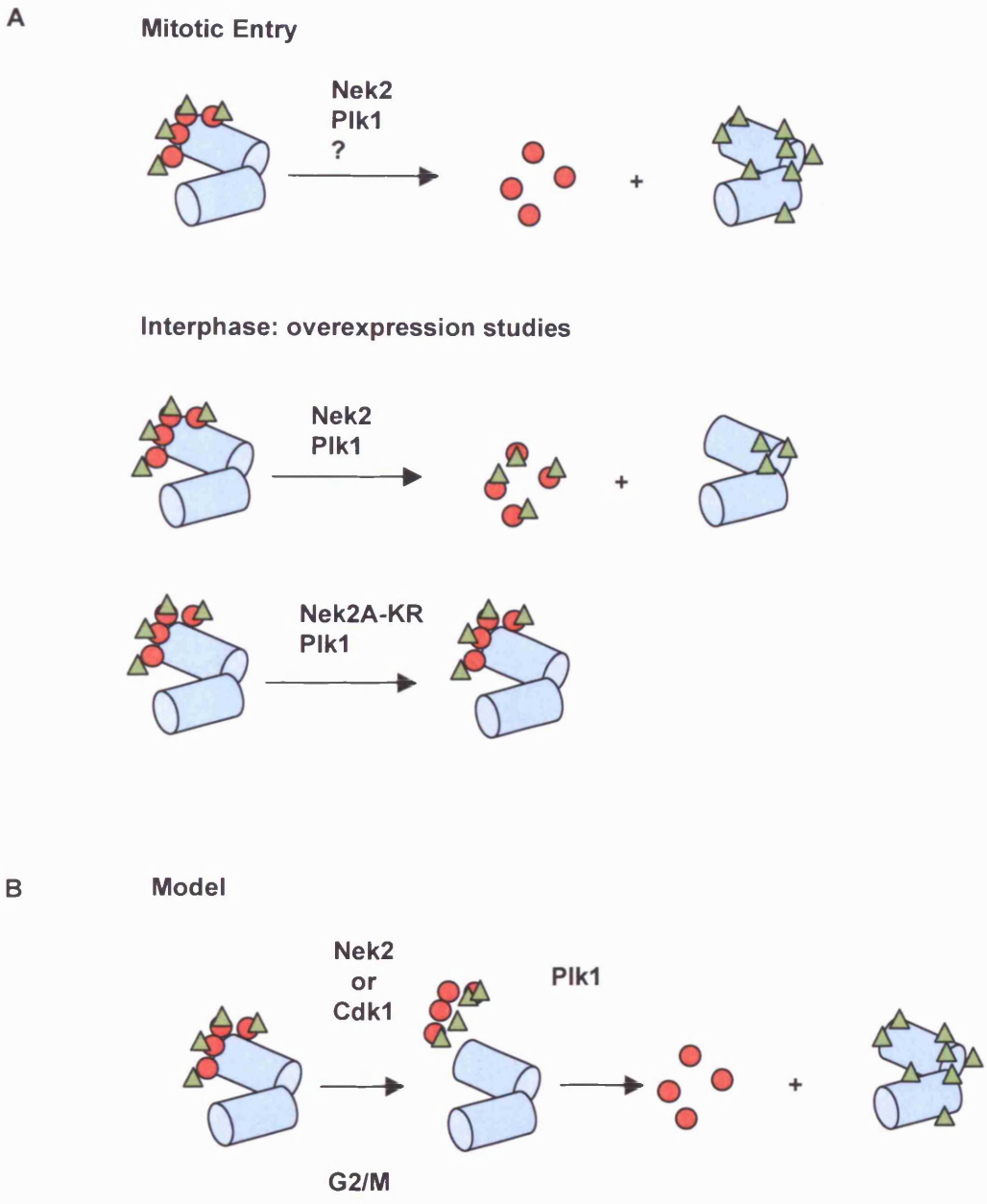

Figure 7.3 Model of Nek2, Plk1 and Nlp interaction at the centrosome
A. In interphase, Nlp (red circle) and γ–tubulin (green triangle) are concentrated around the distal appendages of the mother centriole. As cells enter mitosis Nlp is displaced from the centrosome, while there is an increase of γ–tubulin to the centrosome. During interphase, if either Nek2 or Plk1 is overexpressed then Nlp is displaced from the centrosome and its interactions with itself are also disrupted. However, inactive Nek2 (KR) can prevent Plk1-induced displacement of Nlp from the centrosome. **B.** Nlp may be displaced from the centrosome by a complex set of events involving a number of kinases. Step one would involve the phosphorylation of Nlp by Nek2 or Cdk1 which disrupts its binding to the centrosome. Secondly phosphorylation by Plk1 leads to complete displacement of Nlp from γ–tubulin.

Chapter 8

Bibliography

Alberts, B., Bray, D., Lewis, J., Raff, M., Roberts, K. and Watson, J.D. (1994) **Molecular biology of the cell.** *Garland science publishing.*

Alexandru, G., Uhlmann, F., Mechter, K., Poupart, M.A. and Nasmyth, K. (2001) **Phosphorylation of the cohesin subunit Scc1 by Polo/Cdc5 kinase regulates sister chromatid separation in yeast.** *Cell*, 105, 459-472.

Anderson, S.S.L. (1999) **Molecular characteristics of the centrosome.** *International Review of Cytology*, 187, 51-109.

Avides, M.D.C. and Glover, D.M. (1999) **Abnormal spindle protein, Asp, and the integrity of mitotic centrosomal microtubule orgaizing centers.** *Science*, 283, 1733-1735.

Avides, M.D.C., Tavares, A. and Glover, D.M. (2001) **Polo kinase and Asp are needed to promote the mitotic organizing activity of centrosomes.** *Nature Cell Biology*, 3, 421-424.

Bahassi, E.M., Conn, C.W., Myer, D.L., Hennigan, R.F., McGowan, C.H., Sanchez, Y. and Stambrook, P.J. (2002) **Mammalian polo-like kinase 3 (Plk3) is a multifunctional protein invoved in stress response pathways.** *Oncogene*, 21, 6633-6640.

Bahe, S., Steihof, Y., Wilkinson, C.J., Leiss, F. and Nigg, E.A. (2005) **Rootletin forms centriole-associated filaments and functions in centrosome cohesion.** *The Journal of Cell Biology*, 171, 27-33.

Banerjee, M., Worth, D., Prowse, D.M. and Nikolic, M. (2002) **Pak1 phosphorylation on T212 affects microtubules in cells undergoing mitosis.** *Current Biology*, 12, 1233-1239.

Barr, F.A., Sillje, H.H.W. and Nigg, E.A. (2004) **Polo-like kinases and the orchestration of cell division.** *Nature*, 5, 429-440.

Barros, T.P., Kinoshita, K., Hyman, A.A. and Raff, J.W. (2005) **Aurora A activates D-TACC-Msps complexes exclusively at centrosomes to stabilize centrosomal microtubules.** *The Journal of Cell Biology*, 170, 1039-1046.

Barton, A.B., Davies, C.J., Hutchinson III, C.A. and Kaback, D.B. (1992) **Cloning of chromosome 1 DNA from *Saccharomyces cerevisiae*: analysis of *FUN52* gene, whose product has homology to protein kinases.** *Gene*, 117, 137-140.

Belham, C., Comb, M.J. and Avruch, J. (2001) **Identification of the NIMA family kinases Nek6/7 as regulators of the p70 ribosomal S6 kinase.** *Current Biology*, 11, 1151-1167.

Belham, C., Roig, J., Caldwell, J.A., Aoyama, Y., Kemp, B.E., Comb, M.J. and Avruch, J. (2003) **A mitotic cascade of NIMA protein kinases.** ***The Journal of Biological Chemistry,*** 278, 34897-34909.

Blangy, A., Lane, H.A., d'Herin, P., Harper, M., Kress, M. and Nigg, E.A. (1995) **Phosphorylation by p34cdc2 regulates spindle association of human Eg5, a kinesin-related motor essential for bipolar spindle formation in vivo.** *Cell*, 83, 1159-1169.

Bobinnec, Y., Khodjakov, A., Mir, L.M., Rieder, C.L., Edde, B. and Bornens, M. (1998) **Centriole disassembly in vivo and its effect on centrosome structure and function in vertebrate cells.** *The Journal of Cell Biology*, 143, 1575-1589.

Bornens, M. (2002) **Centrosome composition and microtubule anchoring mechanisms.** *Current Opinion in Cell Biology*, 14, 25-34.

Bouckson-Castaing, V., Moudjou, M., Ferguson, D.J.P., Mucklow, S., Belkaid, Y., Milon, G. and Crocker, P.R. (1996) **Molecular characterisation of ninein, a new coiled-coil protein of the centrosome.** *Journal of Cell Science*, 109, 179-190.

Bowers, A.J. and Boylan, J.F. (2004) **Nek8, a NIMA family kinase member, is overexpressed in primary human breast tumors.** *Gene*, 328, 135-142.

Brinkley, B.R. (2001) **Managing the centrosome numbers game: from chaos to stability in cancer cell division.** *Trends in Cell Biology*, 11, 18-21.

Brinkley, B.R. and Goepfert, T.R. (1998) **Supernumary centrosomes and cancer: Boveri's hypothesis revisited.** *Cell Motility and the Cytoskeleton*, 41, 281-288.

Burns, T.M., Fei, P., Scata, K.A., Dicker, D.T. and El-Deiry, W.S. (2003) **Silencing of the novel p53 target gene *Snk/Plk2* leads to mitotic catastrophe in Paclitaxel (taxol)-exposed cells.** *Molecular and Cellular Biology*, 23, Aug 2003.

Canaday, J., Stoppin-Mellet, V., Mutterer, J., Lambert, A. and Schmidt, A. (2000) **Higher plant cells: Gamma-tubulin and microtubule nucleation in the absence of centrosomes.** *Microscopy Research and Techniques*, 49, 487-495.

Casenghi, M., Barr, F.A. and Nigg, E.A. (2005) **Phosphorylation of Nlp by Plk1 negatively regulates its dynein-dynactin-dependent targeting to the centrosome.** *Journal of Cell Science*, 118, 5101-5108.

Casenghi, M., Meraldi, P., Weinhart, U., Duncan, P.I., Korner, R. and Nigg, E.A. (2003) **Polo-like kinase 1 regulates Nlp, a centrosome protein involved in microtubule nucleation.** *Developmental Cell*, 5, 113-125.

Chen, A., Arama, Y.E. and Motro, K.B. (1999) **NIMA-related kinases: isolation and characterization of murine *nek3* and *nek4* cDNAs, and chromosomal localization of *nek1*, *nek2* and *nek3***. *Gene*, 234, 127-137.

Chen, Y., Riley, D.J., Zheng, J., Chen, P. and Lee, W. (2002) **Phosphorylation of the mitotic regulator protein Hec-1 by Nek2 kinase is essential for faithful chromosome segregation**. *Journal of Biological Chemistry*, 277, 49408-49416.

Cheng, K.Y., Lowe, E.D., Sinclair, J., Nigg, E.A. and Johnson, L.N. (2003) **The crystal structure of the human polo-like kinase-1 polo box domain and its phospho-peptide complex.** *EMBO Journal*, 22, 5757-5768.

Cogswell, J.P., Brown, C.E., Bisi, J.E. and Neill, S.D. (2000) **Dominant-negative polo like kinase 1 induces mitotic catastophe independent of Cdc25C function.** *Cell Growth and Differentiation*, 11, 615-623.

Conn, C.W., Hennigan, R.F., Dai, W., Sanchez, Y. and Stambrook, P. (2000) **Incomplete cytokinesis and induction of apoptosis by overexpression of the mammalian Polo-like kinase, Plk3.** *Cancer Research*, 60, 6826-6831.

Dammermann, A., Desai, A. and Oegema, K. (2003) **The minus end in sight.** *Current Biology*, 13, R614-R624.

Delgehyr, N., Sillibourne, J. and Bornens, M. (2005) **Microtubule nucleation and anchoring at the centrosome are independent processes linked by ninein function.** *Journal of Cell Science*, 118, 1564-1575.

Deng, C. (2002) **Roles of BRCA1 in centrosome duplication**. *Oncogene*, 21, 6222-6227.

Di Agostino, S., Fedele, M., Chieffi, P., Fusco, A., Rossi, P., Geremia, R. and Sette, C. (2004) **Phosphorylation of High Mobility Group protein A2 by Nek2 kinase during the first meiotic division in mouse spermatocytes.** *Molecular Biology of the Cell*, 15, 1224-1232.

Di Agostino, S., Rossi, P., Geremia, R. and Sette, C. (2002) **The MAPK pathway triggers activation of Nek2 during chromosome condensation in mouse spermatocytes**. *Development*, 129, 1715-1727.

Di Fiore, B., Ciciarello, M., Mangiacasale, R., Palena, A., Tassin, A.M., Cundari, E. and Patrizia, L. (2003) **Mammalian RanBP1 regulates centrosome cohesion during mitosis.** *Journal of Cell Science*, 116, 3399-3411.

Dictenberg, J.B., Zimmerman, W., Sparks, C.A., Young, A., Vidair, C., Zheng, J., Carrington, W., Fay, F.S. and Doxsey, S.J. (1998) **Pericentrin and γ-tubulin**

form a protein complex and are organized into a novel lattice at the centrosome. *The Journal of Cell Biology*, 141, 163-174.

Donohue, P.J., Alberts, G.F., Guo, Y. and Winkles, J.A. (1995) **Identification by targeted differential display of an immediate early gene encoding a putative serine/threonine kinase.** *Journal of Biological Chemistry*, 270, 10351-10357.

Dorin, D., Roch, K.L., Sallicandro, P., Alano, P., Poullet, P., Meijer, L. and Doerig, C. (2001) **Pfnek-1, a NIMA-related kinase from the human malaria parasite *Plasmodium falciparum*.** *European Journal of Biochemistry*, 268, 2600-2608.

Doxsey, S. (2001) **Re-evaluating centrosome function.** *Nature Reviews Molecular Cell Biology*, 2, 688-698.

Doxsey, S. (2002) **Duplicating dangerously: linking centrosome duplication and aneuploidy.** *Molecular Cell*, 10, 439-440.

Doxsey, S., Zimmerman, W. and Mikule, K. (2005) **Centrosome control of the cell cycle.** *Trends in Cell Biology*, 15, 303-311.

Doxsey, S.J., Stein, P., Evans, L., Calarco, P.D. and Kirschner, M.W. (1994) **Pericentrin, a highly conserved centrosome protein involved in microtubule organization.** *Cell*, 76, 639-650.

Egloff, M., Johnson, D.F., Moorhead, G., Cohen, P.T.W., Cohen, P. and Barford, D. (1997) **Structural basis for the recognition of regulatory subunits by the catalytic subunit of protein phosphatase 1.** *EMBO Journal*, 16, 1876-1887.

Eckerdt, F., Yuan, J., Saxena, K., Martin, B., Kappel, S., Lindenau, C., Kramer, A., Naumann, S., Daum, S., Fischer, G., Dikic, I., Kaufmann, M. and Strebhardt, K. (2005) **Polo-like kinase 1 (Plk1) mediated phosphorylation of Pin1 stabilizes Pin1 by inhibiting its ubuitination in human cells.** *Journal of Biolocical Chemistry*, 280 (44), 36575-83.

Elia, A.E.H., Cantley, L.C. and Yaffe, M.B. (2003a) **Proteomic screen finds pSer/pThr-binding domain localizing Plk1 to mitotic substrates.** *Science*, 299, 1228-1231.

Elia, A.E.H., Rellos, P., Haire, L.F., Chao, J.W., Ivins, F.J., Hoepker, K., Mohammad, D., Cantley, L.C., Smerdon, S.J. and Yaffe, M.B. (2003b) **The molecular basis for phosphodependent substrate targeting and regulation of Plks by the polo-box domain.** *Cell*, 115, 83-95.

Eto, M., Elliot, E., Prickett, T.D. and Brautigan, D.L. (2002) **Inhibitor-2 regulates protein phosphatase-1 complexed with NimA-related kinase to induce centrosome separation.** *Journal of Biological Chemistry*, 277, 44013-44020.

Faragher, A.J. and Fry, A.M. (2003) **Nek2A kinase stimulates centrosome disjunction and is required for formation of bipolar mitotic spindles.** *Molecular Biology of the Cell*, 14, 2876-2889.

Fardilha, M., Wu, W., Sa, R., Fidalgo, S., Sousa, C., Mota, C., Da Cruz E Silva, O. and Da Cruz E Silva, E. (2004) **Alternatively spliced protein variants as potential therapeutic targets for male infertility and contraception.** *Annual New York Academy of Sciences*, 1030, 468-478.

Ferris, D.K., Maloid, S. and Li, C.H. (1998) **Ubiquitination and proteasome mediated degradation of Polo-like kinase.** *Biochemical and Biophysical Research Communications*, 252, 340-344.

Fisk, H.A. and Winey, M. (2001) **The Mouse Mps1p-Like Kinase Regulates Centrosome Duplication.** *Cell*, 106, 95-104.

Fletcher, L., Cerniglia, G.J., Nigg, E.A., Yend, T.J. and Muschel, R.J. (2004) **Inhibition of centrosome separation after DNA damage: a role for Nek2.** *Radiation Research*, 162, 128-135.

Fletcher, L., Cerniglia, G.J., Yen, T.J. and Muschel, R.J. (2005) **Live cell imaging reveals distinct roles in cell cycle regulation for Nek2A and Nek2B.** *Biochemical and Biophysical Research Communications*, 1744, 89-92.

Fode, C., Motro, B., Yousefi, S., Heffernan, M. and Dennis, J.W. (1994) **Sak, a murine protein-serine/threonine kinase that is related to the *Drosophila* polo kinase and involved in cell proliferation.** *Proceedings of the National Academy of Sciences of the United States of America*, 91, 6388-9392.

Freed, E., Lacey, K.R., Huie, P., Lyapina, S.A., Deshaies, R.J., Stearns, T. and Jackson, P.K. (1999) **Components of an SCF ubiquitin ligase localize to the centrosome and regulate the centrosome duplication cycle.** *Genes and Development*, 13, 2242-2257.

Fry, A.M., Arnaud, L. and Nigg, E.A. (1999) **Activity of the human centrosomal kinase, Nek2, depends on an unusual leucine zipper dimerization motif.** *Journal of Biological Chemistry*, 274, 16304-16310.

Fry, A.M., Descombes, P., Twomey, C., Bacchieri, R. and Nigg, E.A. (2000a) **The NIMA-related kinase X-Nek2B is required for efficient assembly of the zygotic centrosome in *Xenopus laevis*.** *Jounal of Cell Science*, 113, 1973-1984.

Fry, A.M. and Faragher, A.J. (2001) **Identification of centrosome kinases.** *Methods in Cell Biology*, 67, 305-323.

Fry, A.M., Mayor T, Meraldi P, Stierhof Y, Tanaka K and Nigg, E.A. (1998a) **C-Nap1, a novel centrosomal coiled-coil protein and candidate substrate of the cell cycle regulated protein kinase Nek2.** *Journal of Cell Biology*, 141, 1563-1574.

Fry, A.M., Mayor, T. and Nigg, E.A. (2000b) **Regulating centrosomes by protein phosphorylation.** *Current Topics in Developmental Biology*, 49, 291-312.

Fry, A.M., Meraldi, P. and Nigg, E.A. (1998b) **A centrosomal fuction for the human Nek2 protein kinase, a member of the NIMA family of cell cycle regulators.** *EMBO Journal*, 17, 470-481.

Fry, A.M. and Nigg, E.A. (1997) **Characterization of mammalian NIMA-related kinases.** *Methods in Enzymology*, 283, 270-282.

Fry, A.M., Schultz, S.J., Bartek, J. and Nigg, E.A. (1995) **Substrate specificty and cell cycle regulation of Nek2 protein kinase, a potential human homolog of the mitotic regulator NIMA of Aspergillus nidulans.** *The Journal of Biological Chemistry*, 270, 12899-12905.

Fujioka, T., Takebayashi, Y., Ito, M. and Uchida, T. (2000) **Nek2 expression and localization in Porcine oocyte maturation.** *Biochemical and Biophysical Research Communications*, 279, 799-802.

Golsteyn, R.M., Mundt, K.E., Fry, A.M. and Nigg, E.A. (1995) **Cell cycle regulation of the activity and subcellular localization of Plk1, a human protein kinase implicated in mitotic spindle function.** *The Journal of Cell Biology*, 129, 1617-1628.

Golsteyn, R.M., Schultz, S.J., Bartek, J., Ziemiecki, A., Ried, T. and Nigg, E.A. (1994) **Cell cycle analysis and chromosomal localization of human Plk1, a putative homologue of the mitotic kinases *Drosophila* polo and *Saccharomyces cerevisiae* Cdc5.** *Journal of Cell Science*, 107, 1509-1517.

Graf, R. (2002) **DdNek2, the first non-vertebrate homologue of human Nek2, is involved in the formation of microtubule-organizing centers.** *Journal of Cell Science*, 115, 1919-1929.

Grallert, A. and Hagan, I. (2002) ***Schizosaccharomyces pombe* NIMA-related kinase, Fin1, regulates spindle formation and an affinity of Polo for the SPB.** *EMBO Journal*, 21, 3096-3107.

Grallert, A., Krapp, A., Bagley, S., Simanis, V. and Hagan, I.M. (2004) **Recruitment of NIMA kinase shows that maturation of the *S. pombe* spindle-pole body occurs over consecutive cell cycles and reveals a role for NIMA in modulating SIN activity.** *Genes and Development*, 18, 1007-1021.

Gruss, O.J., Carazo-Salas, R.E., Schatz, C.A., Guarguaglini, G., Kast, J., Wilm, M., Le Bot, N., Vernos, I., Karsenti, E. and Mattaj, I.W. (2001) **Ran induces spindle assembly by reversing the inhibitory effect of importin α on TPX2 activity.** *Cell*, 104, 83-93.

Habedanck, R., Steirhof, Y.-D., Wilkinson, C.J. and Nigg, E.A. (2005) **The Polo kinase Plk4 functions in centriole duplication.** *Nature Cell Biology*, 7, 1140-1146.

Hamanaka, R., Maloid, S., Smith, M.R., O'Connell, C.D., Longo, D.L. and Ferris, D.K. (1994) **Cloning and characterization of human and murine homologues of the *Drosophila* polo serine-threonine kinase.** *Cell Growth and Differentiation*, 5, 249-257.

Hamanaka, R., Smith, M.R., O'Connell, P.M., Maloid, S., Mihalic, K., Spivak, J.L., Longo, D.L. and Ferris, D.K. (1995) **Polo-like kinase is a cell cycle-regulated kinase activated during mitosis.** *The Journal of Biological Chemistry*, 270, 21086-21091.

Hames, R.S., Crookes, R.E., Straatman, K.R., Merdes, A., Hayes, J.M., Faragher, A.J. and Fry, A.M. (2005) **Dynamic recruitmant of Nek2 kinase to the centrosome involves microtubules, PCM-1, and localized proteasomal degradation.** *Molecular Biology of the Cell*, 16, 1700-1724.

Hames, R.S. and Fry, A.M. (2002) **Alternative splice variants of the human centrosome kinase Nek2 exhibit distinct patterns of expression in mitosis.** *Biochemical Journal*, 361, 77-85.

Hames, R.S., Wattam, S.L., Yamano, H., Bacchieri, R. and Fry, A.M. (2001) **APC/C-mediated destruction of the centrosomal kinase Nek2A occurs in early mitosis and depends upon a cyclin A-type D-box.** *EMBO Journal*, 20, 7117-7127.

Hanks, S.K. and Hunter, T. (1995) **The eukaryotic protein kinase superfamily: kinase (catalytic) domain structure and classification.** *FASEB Journal*, 9, 576-596.

Hannak, E., Kirkham, M., Hyman, A.A. and Oegema, K. (2001) **Aurora-A kinase is required for centrosome maturation in *Caenorhabditis elegans*.** *Journal of Cell Biology*, 155, 1109-1115.

Hayashi, K., Igarashi, I., Ogawa, M. and Sakaguchi, N. (1999) **Activity and substrate specificity of the murine STK2 serine/threonine kinase that is structually related to the mitotic regulator protein NIMA of Aspergillus nidulans.** *Biochemical and Biophysical Research Communications*, 264, 449-456.

Hayward, D.G., Clarke, R.B., Faragher, A.J., Pillai, M.R., Hagan, I.M. and Fry, A.M. (2004) **The centrosomal kinase Nek2 displays elevated levels of protein expression in human breast cancer**. *Cancer Research*, 64, 7370-7376.

Hayward, D.G. and Fry, A.M. (2005) **Nek2 kinase in chromosomal instability and cancer.** *Cancer Letters*, August 2nd.

Heald, R., Regis, T., Habermann, A., Karsenti, E. and Hyman, A. (1997) **Spindle assembly in *Xenopus* egg extracts: respective roles of centrosome and microtubule self organisation.** *Journal of Cell Biology*, 138, 615-628.

Helps, N.R., Luo, X., Barker, H.M. and Cohen, P.T.W. (2000) **NIMA-related kinase 2, a cell cycle regulated protein kinase localized to centrosomes is complexed to protein phosphatase 1.** *Jounal of Biochemistry*, 349, 509-518.

Hinchcliffe, E.H., Miller, F.J., Charm, M., Khodjakov, A. and Sluder, G. (2001) **Requirement of centrosomal activity for cell cycle progression through G1 into S phase.** *Science*, 291, 1547-1550.

Hinchcliffe, E.H. and Sluder, G. (2001) **"It Takes Two to Tango" : Understanding how centrosome duplication is regulated throughout the cell cycle.** *Genes and Development*, 15, 1167-1181.

Hirota, T., Kunitoku, N., Sasayama, T., Marumoto, T., Zhang, D., Nitta, M., Hatakeyama, K. and Saya, H. (2003) **Aurora-A and an interacting activator, the LIM protein Ajuba, are required for mitotic commitment in human cells.** *Cell*, 114, 585-598.

Holland, P.M., Milne, A., Garka, K., Johnson, R.S., Willis, C., Sims, J.E., Rauch, C.T., Bird, T.A. and Virca, G.D. (2002) **Purification, cloning, and characterizarion of Nek8, a novel NIMA-related kinase, and it's candidate substrate Bic2.** *The Journal of Biological Chemistry*, 277, 16229-16240.

Holtrich, U., Wolf, G., Brauninger, A., Karn, T., Bohme, B., Rubsamen-Waigmann, H. and Strebhardt, K. (1994) **Induction and down-regulation of PLK, a human serine/threonine kinase expressed in proliferating cells and tumors.** *Proceedings of the National Academy of Sciences of the United States of America*, 91, 1736-1740.

Hong, Y., Chen, C., Chang, J.R., Wang, S., Sy, W., Chou, C. and Howng, S. (2000) **Cloning and characterization of a novel human ninein protein that interacts with the glycogen synthase kinase 3β**. *Biochemical and Biophysical Research Communications*, 1492, 513-516.

Hori, T., Haraguchi, T., Hiraoka, Y., Kimura, H. and Fukagawa, T. (2003) **Dynamic behaviour of Nuf2-Hec1 complex that localizes to the centrosome and**

centromere and is essential for mitotic progression in vertebrate cells. *Journal of Cell Science*, 116, 3347-3362.

Huse, M. and Kuriyan, J. (2002) **The conformational plasticity of protein kinases.** *Cell*, 109, 275-282.

Jang, Y.J., Ji, J.H., Ahn, J.H., Hoe, K.L., Won, M., Im, D.S., Chae, S.K., Song, S. and Yoo, H.S. (2004) **Polo-box motif targets a centrosome regulator, RanGTPase.** *Biochemical and Biophysical Research Communications*, 325, 257-264.

Jang, Y.J., Ma, S., Terada, J. and Erikson, R.L. (2002) **Phosphorylation of threonine 210 and the role of ser 137 in the regulation of polo-like kinase.** *Journal of Biolocical Chemistry*, 277, 44115-44120.

Job, D., Valiron, O. and Oakley, B. (2003) **Microtubule nucleation.** *Current Opinion in Cell Biology*, 15, 111-117.

Johnson, L.N., Noble, M.E.M. and Owen, D.J. (1996) **Active and inactive protein kinases: structural basis for regulation.** *Cell*, 85, 149-158.

Jones, D.G.L. and Rosamond, J. (1990) **Isolation of a novel protein kinase-encoding gene from yeast by oligodeoxyribonucleotide probing.** *Gene*, 90, 87-92.

Kandli, M., Feige, E., Chen, A., Kilfin, G. and Motro, B. (2000) **Isolation and characterization of two evolutionaily conserved murine kinases (Nek6 and Nek7) related to the fungal mitotic regulator, NIMA.** *Genomics*, 68, 187-196.

Kauselmann, G., Weiler, M., Wulff, P., Jessburger, S., Konietzko, U., Scafidi, J., Staubli, U., Bereiter-Hahn, J., Strebhardt, K. and Kuhl, D. (1999) **The polo-like protein kinases Fnk and Snk associate with Ca^{2+} - and integrin-binding protein and are regulated dynamically with synaptic plasticity.** *EMBO Journal*, 18, 5528-5539.

Khodjakov, A. and Rieder, C.L. (1999) **The sudden recruitment of γ-tubulin to the centrosome at the onset of mitosis and its dynamic exchange throughout the cell cycle, do not require microtubules.** *The Journal of Cell Biology*, 146, 585-596.

Khodjakov, A. and Rieder, C.L. (2001) **Centrosomes enhance the fidelity of cytokinesis in vertebrates and are required for cell cycle progression.** *Journal of Cell Biology*, 153, 237-242.

Khodjakov, A., Rieder, C.L., Sluder, G., Cassels, G., Sibon, O. and Wang, C. (2002) ***De novo* formation of centrosomes in vertebrate cells arrested during S phase.** *The Journal of Cell Biology*, 158, September 30, 2005.

Kim, Y.H., Choi, J.Y., Jeong, Y., Wolgemuth, D.J. and Rhee, K. (2002) **Nek2 localizes to multiple sites in mitotic cells, suggesting its involvement in multiple cellular functions during the cell cycle.** *Biochemical and Biophysical Research Communications*, 290, 130-136.

Kinoshita, K., Noetzel, T.L., Pelletier, L., Mechtler, K., Drechsel, D.N., Schwager, A., Lee, M., Raff, J.W. and Hyman, A.A. (2005) **Aurora A phosphorylation of TACC3/maskin is required for centrosome-dependent microtubule assembly in mitosis.** *The Journal of Cell Biology*, 17, 1047-1055.

Kitada, K., Johnson, A.L., Johnston, L.H. and Sugino, A. (1993) **A multicopy suppressor gene of the *Saccharomyces cerevisiae* G1 cell cycle mutant gene dbf4 encodes a protein kinase identified as CDC5.** *Molecular Cell Biology*, 13, 4445-4457.

Kochanski, R.S. and Borisy, G.G. (1990) **Mode of centriole duplication and distribution.** *The Journal of Cell Biology*, 100, 1599-1605.

Kotani, S., Tanaka, H., Yasuda, H. and Todokoro, K. (1999) **Regulation of APC activity by phosphorylation and regulatory factors.** *Journal of Cell Biology*, 146, 791-800.

Krien, M.J.E., Bugg, S.J., Palasides, M., Asouline, G., Morimyo, M. and O'Connell, M.J. (1998) **A NIMA homologue promotes chromatin condensation in fission yeast.** *Journal of Cell Science*, 111, 967-976.

Krien, M.J.E., West, R.R., John, U.L., Koniaras, K., Mcintosh, J.R. and O'Connell, M.J. (2002) **The fission yeast NIMA kinase Fin1p is required for spindle function and nuclear envelope integrity.** *EMBO Journal*, 21, 1713-1722.

Krupa, A., Preethi, G. and Srinivasan, N. (2004) **Structural modes of stabilization of permissive phosphorylation sites in protein kinases: Distinct strategies in Ser/Thr and Tyr kinases.** *Journal of Molecular Biology*, 339, 1025-1039.

La Terra, S., English, C.N., Hergert, P., McEwen, B.F., Sluder, G. and Khodjakov, A. (2005) **The *de novo* centriole assembly pathway in HeLa cells: cell cycle progression and centriole assembly/maturation.** *The Journal of Cell Biology*, 168, 713-722.

Lacey, K.R., Jackson, P.K. and Stearns, T. (1999) **Cyclin-dependent kinase control of centrosome duplication.** *The Journal of Cell Biology*, 96, 2817-2822.

Lane, H.A. and Nigg, E.A. (1996) **Antibody microinjection reveals an essential role for Human Polo-like** kinase 1 (Plk1) in the functional maturation of mitotic centrosomes. *The Journal of Cell Biology*, 165, 1701-1713.

Lee, K.S. and Erikson, R.L. (1997) **Plk is a functional homolog of *Saccharomyces cerevisiae* Cdc5, and elevated Plk activity induces multiple septation structures.** *Molecular and Cellular Biology*, 17, 3408-3417.

Lee, K.S., Grenfell, T.Z., Yarm, F.R. and Erikson, R.L. (1998) **Mutation of the polo-box disrupts localization and mitotic functions of the mammalian polo kinase Plk.** *Proceedings of the National Academy of Sciences of the United States of America*, 95, 9301-9306.

Letwin, K., Mizzen, L., Motro, B., Ben-David, Y., Bernstein, A. and Pawson, T. (1992) **A mammalian dual specificity protein kinase, Nek1, is related to the NIMA cell cycle regulator and highly expressed in meiotic germ cells.** *EMBO Journal*, 11, 3521-3531.

Li, B., Ouyang, B., Pan, H., Reissmann, P.T., Slamon, D.J., Arceci, R., Lu, L. and Dai, W. (1996) ***prk*, a cytokine-inducible human protein serine/threonine kinase whose expression appears to be down-regulated in lung carinomas.** *The Journal of Biological Chemistry*, 271, 19402-19408.

Li, J., Tan, M., Li, L., Pamarthy, D., Lawerence, T.S. and Sun, Y. (2005) **SAK, a new polo-like kinase, is transcriptionally repressed by p53 and induces apoptosis upon RNAi silencing.** *Neoplasia*, 7, 312-323.

Lindon, C. and Pines, J. (2004) **Ordered proteolysis in anaphase inactivates Plk1 to contribute to proper mitotic exit in human cells.** *The Journal of Cell Biology*, 164, 233-241.

Liu, S., Lu, W., Obara, T., Kuida, S., Lehoczky, J., Dewer, K., Drummond, I.A. and Beier, D.R. (2002) **A defect in a novel Nek-family kinase causes cystic kidney disease in the mouse and zebrafish.** *Development*, 129, 5839-5846.

Liu, X. and Erikson, R.L. (2003) **Polo-like kinase (Plk)1 depletion induces apoptosis in cancer cells.** *PNAS*, 100, 5789-5794.

Lizcano, J.M., Deak, M., Morrice, N., Kieloch, A., Hastie, C.J., Dong, L., Schutkowski, M., Reimer, U. and Alessi, D.R. (2002) **Molecular basis for the substrate specificity of NIMA-related kinase-6 (NEK6).** *The Journal of Biological Chemistry*, 277, 27839-27849.

Llamazares, S.M., Moreira, A., Tavares, A., Girdham, C., Spruce, B.A., Gonzalez, C., Karess, R.E., Glover, D.M. and Sunkel, C.E. (1991) **Polo encodes a protein kinase homolog required for mitosis in Drosophila.** *Genes and Development*, 5, 2153-2165.

Losada, A., Hirano, M. and Hirano, T. (2002) **Cohesin release is required for sister chromatid resolution, but not for condensin-mediated compaction, at the onset of mitosis.** *Genes and Development*, 16, 3004-3016.

Lou, Y., Xie, W., Zhang, D., Yao, J., Lou, Z., Wang, Y., Shi, Y. and Yao, X. (2004a) **Nek2A specifies the centrosomal localization of Erk2.** *Biochemical and Biophysical Research Communications*, 321, 495-501.

Lou, Y., Yao, J., Zereshki, A., Dou, Z., Ahmed, K., Wang, H., Hu, J., Wang, Y. and Yao, X. (2004b) **Nek2A interacts with MAD1 and possibly functions as a novel integrator of the spindle checkpoint signalling.** *The Journal of Biological Chemistry*, 279, 20049-20057.

Lu, K.P., Kemp, B.E. and Means, R. (1994) **Identification of substrate specificity determinants for the cell cycle-regulated NIMA protein kinase.** *Journal of Cell Biology*, 269, 6603-6607.

Ma, S., Charron, J. and Erikson, R.L. (2003a) **Role of Plk2 (Snk) in mouse development and cell proliferation.** *Molecular and Cellular Biology*, 23, 6936-6943.

Ma, S., Liu, M.-A., Yuan, Y.O. and Erikson, R.L. (2003b) **The serum inducible protein kinase snk is a G1 phase polo-like kinase that is inhibited by the calcium- and integrin-binding protein CIB.** *Molecular Cancer Research*, 1, 376-384.

Mack, G.J., Ou, Y. and Rattner, B.R. (2000) **Integrating centrosome structure with protein composition and function in animal cells.** *Microscopy Research and Techniques*, 49, 409-419.

Mahjoub, M.R., Montpetit, B., Zhao, L., Finst, R.J., Goh, B., Kim, A.C. and Quarmby, L.M. (2002) **The FA2 gene of *Chlamydomonas* encodes a NIMA family kinase with roles in cell cycle progression and microtubule severing during deflagellation.** *Journal of Cell Science*, 115, 1759-1768.

Marshall, W.F. (2001) **Centrioles Take Center Stage.** *Current Biology*, 11, 487-496.

Marshall, W.F., Vucica, Y. and Rosenbaum, J.L. (2001) **Kinetics and regulation of *de novo* centriole assembly: Implications for the mechanism of centriole duplication.** *Current Biology*, 11, 308-317.

Matyakhina, L., Lenhurr, S.M. and Stratkis, C.S. (2002) **Protein kinase A and chromosomal stability.** *Annals of the New York Academy of Sciences,* 968,148-57.

Mayor, T., Hacker, U., Stierhof, Y. and Nigg, E.A. (2002) **The mechanism regulating the dissociation of centrosomal protein C-Nap1 from mitotic spindle poles.** *Journal of Cell Science*, 115, 3275-3284.

Mayor, T., Meraldi, P., Stierhof, Y., Nigg, E.A. and Fry, A.M. (1999) **Protein kinases in control of the centrosome cycle.** *FEBS letters*, 452, 92-95.

Mayor, T., Stierhof, Y., Tanaka, K., Fry, A.M. and Nigg, E.A. (2000) **The centrosomal protein C-Nap1 is required for cell cycle regulated centrosome cohesion.** *Journal of Cell Biology*, 151, 837-846.

McCollum, D. and Gould, K.L. (2001) **Timing is everything: regulation of mitotic exit and cytokinesis by the MEN and SIN.** *Trends in Cell Biology*, 11, 89-95.

Meraldi, P., Honda, R. and Nigg, E.A. (2002) **Aurora-A overexpression reveals tetraploidization as a major route to centrosome amplication in $p53^{-/-}$ cells.** *EMBO Journal*, 21, 483-492.

Meraldi, P. and Nigg, E.A. (2001) **Centrosome cohesion is regulated by a balance of kinase and phosphatase activities.** *Journal of Cell Science*, 114, 3749-3757.

Mogensen, M.M., Mackie, J.B., Doxsey, S., Stearns, T. and Tucker, J.B. (1997) **Centrosomal deployment of γ-tubulin and pericentrin: Evidence for a microtubule-nucleating domain and a minus-end docking domain in certain mouse epithelial cells.** *Cell Motility and the Cytoskeleton*, 36, 276-290.

Mogensen, M.M., Malik, A., Piel, M., Bouckson-Castaing, V. and Bornens, M. (2000) **Microtubule minus-end anchorage at centrosomal and non-centrosomal sites: the role of ninein.** *Journal of Cell Science*, 113, 3013-3023.

Moritz, M. and Agard, D.A. (2001) **γ-Tubulin complexes and microtubule nucleation.** *Current Opinion in Structural Biology*, 11, 174-181.

Moritz, M., Braunfeld, M.B., Sedat, J.W., Alberts, B. and Agard, D.A. (1995) **Microtubule nucleation by γ-tubulin-containing rings in the centrosome.** *Nature*, 378, 638-640.

Mundt, K.E., Golsteyn, R.M., Lane, H.A. and Nigg, E.A. (1997) **On the regulation and function of human Polo-like kinase 1 (PLK1): Effects of overexpression on cell cycle progression.** *Biochemical and Biophysical Research Communications*, 239, 377-385.

Mussman, J.G., Horn, H.F., Carroll, P.E., Okuda, M., Tarapore, P., Donehower, L.A. and Fukasawa, K. (2000) **Synergistic induction of centrosome hyperamplication by loss of p53 and cyclin E overexpression.** *Oncogene*, 19, 1635-1646.

Neef, R., Preisinger, C., Sutcliffe, J., Kopajtich, R., Nigg, E.A., Mayer, T.U. and Barr, F.A. (2003) **Phosphorylation of mitotic kinesin-like protein 2 by polo-like kinase 1 is required for cytokinesis.** *The Journal of Cell Biology*, 162, 863-875.

Nigg, E.A. (1998) **Polo-like kinases: positive regulators of cell division from start to finish.** *Current Opinion in Cell Biology*, 10, 776-783.

Nigg, E.A. (2001) **Mitotic kinases as regulators of cell division and its checkpoints.** *Nature Reviews*, 2, 21-32.

Nigg, E.A. (2002) **Centrosome aberrations: cause or consequence of cancer progression.** *Nature Reviews*, 2, 815-825.

Nigg, E.A. (2004) **Centrosomes in development and disease.** *Wiley-VCH.*

Noguchi, K., Fukazawa, H., Murakami, Y. and Uehara, Y. (2002) **Nek11, a new member of the NIMA family of kinases, involved in DNA replication and genotoxic stress responses.** *Journal of Biolocical Chemistry*, 2002, 39655-39665.

Noguchi, K., Fukazawa, H., Murakami, Y. and Uehara, Y. (2004) **Nucleolar Nek11 is a novel target of Nek2A in G_1/S-arrested cells.** *The Journal of Biological Chemistry*, 279, 32716-32727.

Nolen, B., Taylor, S. and Ghosh, G. (2004) **Regulation of protein kinases: controlling activity through activation segment conformation.** *Molecular Cell*, 15, 661-675.

O'Connell, K.F. (2002) **The ZYG-1 kinase, a mitotic and meiotic regulator of centriole replication.** *Oncogene*, 21, 6201-6208.

O'Connell, K.F., Krien, M.J.E. and Hunter, T. (2003) **Never say never: The NIMA-related kinases in mitotic control.** *Trends in Cell Biology*, 13, 221-228.

Ohkura, H., Hagan, I.M. and Glover, D.M. (1995) **The conserved *Schizosaccharomyces pombe* kinase plo1, required to form a bipolar spindle, the actin ring, and septum, can drive formation in G1 and G2 cells.** *Genes and Development*, 9, 1059-1073.

Okuda, M., Horn, H.F., Tarapore, P., Tokuyama, Y., Smulian, A.G., Chan, P.-K., Knudsen, E.S., Hofmann, I.A., Snyder, J.D., Bove, K.E. and Fukasawa, K. (2000) **Nucleophosmin/B23 is a target of Cdk2/cyclin E in centrosome duplication.** *Cell*, 103, 127-140.

Ou, Y.Y., Mack, G.J., Zhang, M. and Rattner, J.B. (2002) **CEP110 and Ninein are located in a specific domain of the centrosome associated with centrosome maturation.** *Journal of Cell Science*, 115, 1825-1835.

Ouyang, B., Pan, H., Lu, L., Li, J., Stambrook, P., Li, B. and Dai, W. (1997) **Human Prk is a conserved protein serine/threonine kinase involved in regulating M phase functions.** *The Journal of Biological Chemistry*, 272, 28646-28651.

Paintrand, M., Moudjou, M., Delacroix, H. and Bornens, M. (1992) **Centrosome organization and centriole architecture: their sensitivity to divalent cations.** *Journal of Structural Biology*, 108, 107-128.

Peset, I., Seiler, J., Sardon, T., Bejarano, L.A., Rybina, S. and Vernos, I. (2005) **Function and regulation of maskin, a TACC family protein, in microtubule growth during mitosis.** *The Journal of Cell Biology*, 170, 1057-1066.

Piel, M., Meyer, P., Khodjakov, A., Rieder, C.L. and Bornens, M. (2000) **The respective contributions of the mother and daughter centrioles to centrosome activity and behaviour in vertebrate Cells.** *Journal of Cell Biology*, 149, 317-329.

Pines, J. and Rieder, C.L. (2001) **Re-staging mitosis: a contemporary view of mitotic progression.** *Nature Cell Biology*, 3, E3-E6.

Prigent, C., Glover, D.M. and Giet, R. (2005) ***Drosophila* Nek2 protein kinase knockdown leads to centrosome maturation defects while overexpression causes centrosome fragmentation and cytokinesis failure.** *Experimental Cell Research*, 303, 1-13.

Prime, G. and Markie, D. (2005) **The telomere repeat binding protein Trf1 interacts with the spindle checkpoint protein Mad1 and Nek2 mitotic kinase.** *Cell Cycle*, 4, 45-48.

Pu, R.T., Xu, G., Wu, L., Vierula, J., O'Donnell, K., Ye, X.S. and Osmani, S.A. (1995) **Isolation of a functional homolog of the cell cycle-specific NIMA protein kinase of *Aspergillus nidulans* and functional analysis of conserved residues.** *The Journal of Biological Chemistry*, 270, 18110-18116.

Quintyne, N.J., Gill, S.R., Eckley, D.M., Crego, C.L., Comptom, D.A. and Schroer, T.A. (1999) **Dynactin is required for microtubule anchoring at centrosomes.** *The Journal of Cell Biology*, 147, 321-334.

Rapley, J. (2004) **Characterization of Nlp, a novel centrosomal substrate of the Nek2 kinase.** *Biochemistry*. University of Leicester, Leicester.

Rapley, J., Baxter, J.E., Blot, J., Wattam, S.L., Casenghi, M., Meraldi, P., Nigg, E.A. and Fry, A.M. (2005) **Coordinate regulation of the mother centriole component Nlp by Nek2 and Plk1 protein kinases.** *Molecular and Cellular Biology*, 25, 1309-1324.

Ren, B., Cam, **H., Takahashi, Y., Volkert, T., Terragni, J., Young, R.A. and Dynlacht, D. (2002) E2F integrates cell cycle progression with DNA repair, replication, and G2/M checkpoints**. *Genes and Development*, 16, 245-256.

Roig, J., Mikhailov, A., Belham, C. and Avruch, J. (2002) **Nercc1, a mammalian NIMA-family kinase, binds the Ran GTPase and regulates mitotic progression**. *Genes and Development*, 16, 1640-1658.

Saavedra, H.I., Maiti, B., Timmers, C., Altura, R., Tokuyama, Y., Fukasawa, K. and Leone, G. (2003) **Inactivation of E2F3 results in centrosome amplification**. *Cancer Cell*, 3, 333-346.

Salisbury, J.L., Suino, K.M., Busby, R. and Springett, M. (2002) **Centrin-2 is required for centriole duplication in mammalian cells.** *Current Biology*, 12, 1287-1292.

Saunders, R.D.C., Avides, M.D.C., Howard, T., Gonzalez, C. and Glover, D.M. (1997) **The *Drosophila* gene *abnormal spindle* encodes a novel microtubule-associated protein that associates with the polar regions of the mitotic spindle**. *The Journal of Cell Biology*, 137, 881-890.

Saunders, W. (2005) **Centrosomal amplification and spindle multipolarity in cancer cells**. *Seminars in Cancer Biology*, 15, 25-32.

Sawin, K.E. and Mitchison, T.J. (1995) **Mutations in the kinesin-like protein Eg5 disrupt localization to the mitotic spindle**. *Proceedings of the National Academy of Sciences of the United States of America*, 92, 4289-4293.

Schmidt, A., Duncan, P.I., Rauh, N.R., Sauer, G., Fry, A.M., Nigg, E.A. and Mayer, T.U. (2005) ***Xenopus* polo-like kinase Plx1 regulates XErp1, a novel inhibitor of APC/C activity**. *Genes and Development*, 19, 502-513.

Schultz, S.J., Fry, A.M., Sutterlin, C., Reid, T. and Nigg, E.A. (1994) **Cell cycle dependent expression of Nek2, a novel human protein kinase related to the NIMA mitotic regulator of *Aspergillus nidulans*.** *Cell Growth and Differentiation*, 5, 625-635.

Schweitzer, B. and Philippsen, P. (1992) ***NPK1*, a nonessential protein kinase gene in *Saccharomyces cerevisiae* with similarity to *Aspergillus nidulans nimA***. *Molecular and General Genetics*, 234, 164-167.

Seong, Y.S., Kamijo, K., Lee, J.S., Fernandez, E., Kuriyama, R., Miki, T. and Lee, K.S. (2002) **A spindle checkpoint arrest and a cytokinesis failure by the dominant-negative Polo-box domain of Plk1 in U-2OS cells**. *The Journal of Biological Chemistry*, 277, 32282-32293.

Shah, O.J. and Hunter, T. (2004) **Critical role of T-loop and H-motif phosphorylation in the regulation of S6 kinase 1 by the Tuberous Sclerosis Complex**. *The Journal of Biological Chemistry*, 279, 20816-20823.

Simmons, D.L., Neel, B.G., Stevens, R., Evett, G. and Erikson, R.L. (1992) **Identification of an early-growth-response gene encoding a novel putative protein kinase.** *Molecular Cell Biology*, 12, 4164-4169.

Sonn, S., Khang, I., Kim, K. and Rhee, K. (2004) **Suppression of Nek2A in mouse early embryos confirms its requirement for chromosome sgregation.** *Journal of Cell Science*, 117, 5557-5566.

Stearns, T. and Winey, M. (1997) **The cell centre at 100**. *Cell*, 91, 303-309.

Stucke, V.M., Sillje, H.H.W., Arnaud, L. and Nigg, E.A. (2002) **Human Mps1 kinase is required for the spindle assembly checkpoint but not for centrosome duplication.** *EMBO Journal*, 21, 1723-1732.

Sumara, I., Vorlaufer, E., Stukenbereg, P.T., Kelm, O., Redemann, N., Nigg, E.A. and Peters, J.M. (2002) **The dissociation of Cohesin from chromosomes in prophase is regulated by Polo-like kinase**. *Molecular Cell*, 9, 515-525.

Swenson, K.I., Winkler, K.E. and Means, A.R. (2003) **A new Identity for MLK3 as an NIMA-related, cell cycle-regulated kinase that is localized near centrosomes and Influences microtubule organization.** *Molecular Biology of the Cell*, 14, 156-172.

Tan, B.C.M. and Lee, S.C. (2004) **Nek9, a novel FACT-associated protein, modulates interphase progression**. *The Journal of Biological Chemistry*, 279, 9321-9330.

Tanaka, K. and Nigg, E.A. (1999) **Cloning and characterization of the murine Nek3 protein kinase, a novel member of the NIMA family of putative cell cycle regulators.** *Journal of Biological Chemistry*, 274, 13491-13497.

Terrak, M., Kerff, F., Langsetmo, K., Tao, T. and Dominguez, R. (2004) **Structural basis of protein phosphatase 1 regulation**. *Nature*, 429, 780-784.

Tokuyama, Y., Horn, H.F., Kawamura, K., Tarapore, P. and Fukasawa, K. (2001) **Specific phosphorylation of nucleophosmin on Thr^{199} by cyclin-dependent kinase 2-cyclin E and its role in centrosome duplication.** *Journal of Biological Chemistry*, 276, 21529-21537.

Toyoshima-Morimoto, F., Taniguchi, E., Shinya, N., Iwamatsu, A. and Nishida, E. (2001) **Polo-like kinase 1 phosphorylated cyclin B1 targets it to the nucleus during prophase.** *Nature*, 410, 215-220.

Tsai, M.Y., Wiese, C., Cao, K., Martin, O., Donovan, P., Ruderman, J., Prigent, C. and Zheng, J. (2003) **A Ran signalling pathway mediated by the mitotic kinase Aurora A in spindle assembly.** *Nature Cell Biology*, 5, 242-248.

Tsvetkov, L.M., Tsekova, R.T., Xu, X. and Stern, D.F. (2005) **The Plk1 Polo box domain mediates a cell cycle and DNA damage regulated interaction with Chk2.** *Cell Cycle*, 4, 609-617.

Twomey, C., Wattam, S.L., Pillai, M.R., Rapley, J., Baxter, J.E. and Fry, A.M. (2004) **Nek2B stimulates zygotic centrosome assembly in *Xenopus laevis* in a kinase-independent manner.** *Developmental Biology*, 265, 384-398.

Upadhya, P., Birkenmeier, E.H., Birkenmeier, C.S. and Barker, J.E. (2000) **Mutations in a NIMA-related kinase gene, Nek1, cause pleiotropic effects including a progressive polycystic kidney disease in mice.** *PNAS*, 97, 217-221.

Urbani, L. and Stearns, T. (1999) **The Centrosome.** *Current Biology*, 9.

Uto, K., Nakajo, N. and Sagata, N. (1999) **Two structural variants of Nek2 kinase, termed Nek2A and Nek2B, are differentially expressed in *Xenopus* tissues and development.** *Developmental Biology*, 208, 456-464.

Uto, K. and Sagata, N. (2000) **Nek2B, a novel maternal form of Nek2 kinase, is essential for the assembly or maintenance of centrosomes in early *Xenopus* embryos.** *EMBO Journal*, 19, 1816-1826.

van Vugt, MA. and Medema, RH. (2005) **Getting in and out of mitosis with Polo-like kinase-1.** *Oncogene,* 24, 2844-2859.

Vos, S., Hofmann, W.K., Grogan, T.M., Krug, U., Schrage, M., Miller, T.P., Braun, J.G., Wachsman, W., Koeffler, H.P. and Said, J.W. (2003) **Gene Expression Profile of Serial Samples of Transformed B-Cell Lymphomas.** *Laboratory Investigations*, 83, 271.

Wai, D.H., Schaefer, K.L., Scramm, A., Korsching, E., Valen, F.V., Ozaki, T., Boecker, W., Schweigerer, L., Dochhorn-Dworniczak, B. and Poremba, C. (2002) **Expression analysis of pediatric solid tumor cell lines using oligonucleotide microarrays.** *International Journal of Oncology*, 20, 441-451.

Walter, A.O., Seghezzi, W., Korver, W., Sheung, J. and Lees, E. (2000) **The mitotic seine/threonine kinase Aurora2/AIK is regulated by phosphorylation and degradation.** *Oncogene*, 19, 4906-4916.

Wang, Q., Xie, S., Chen, J., Fukasawa, K., Naik, U., Traganos, F., Darzynkiewicz, Z., Jhanwar-Uniyal, M. and Dai, W. (2002) **Cell cycle arrest and apoptosis induced**

by polo-like kinase 3 is mediated through perturbation of microtubule integrity. *Molecular and Cellular Biology*, 22, 3450-3459.

Wang, S., Nakashima, S., Sakai, H., Numata, O., Fujiu, K. and Nozawa, Y. (1998) **Molecular cloning and cell-cycle-dependent expression of a novel NIMA (never in mitosis in *Aspergillus nidulans*)-related protein kinase (*TpNrk*) in *Tetrahymena* cells.** *Journal of Biochemistry*, 334, 197-203.

Warnke, S., Kemmler, S., Hames, R.S., Tsai, H.L., Hoffmann-Roher, U., Fry, A.M. and Hoffmann, I. (2004) **Polo-like kinase-2 is required for centriole duplication in mammalian cells.** *Current Biology*, 14, 1200-1207.

Westermann, S. and Weber, K. (2002) **Identification of CfNek2, a novel member of the NIMA family of cell cycle regulators, as a polypeptide copurifying with polyglutamylation activity in *Crithidia.*** *Journal of Cell Science*, 115, 5003-5012.

Wilson, E.B. (1925) **The cell in development and inheritance**. *MacMillan (New York)*, 85.

Wojcik, E.J., Glover, D.M. and Hays, T.S. (2000) **The SCF ubiquitin ligase protein Slimb regulates centrosome duplication in *Drosophila.*** *Current Biology*, 10, 1131-1134.

Wong, C. and Stearns, T. (2003) **Centrosome number is controlled by a centrosome-intrinsic block to reduplication.** *Nature Cell Biology*, 5, 539-544.

Wonsey, D.R. and Follettie, M.T. (2005) **Loss of the Forkhead transcription factor FoxM1 causes centrosome amplification and mitotic catasrophe**. *Cancer Research*, 65, 5181-5189.

Xie, S., Wu, H., Wang, Q., Cogswell, J.P., Husain, I., Conn, C., Stambrook, P., Jhanwar-Uniyal, M. and Dai, W. (2001) **Plk3 functionally links DNA damage to cell cycle arrest and apoptosis at least in part via the p53 pathway**. *The Journal of Biological Chemistry*, 276, 43305-43312.

Xu, Z., Zou, W., Lin, P. and Chang, K. (2005) **A role for PML3 in centrosome duplication and genome stability.** *Molecular Cell*, 17, 721-732.

Yamaguchi, T., Goto, H., Yokoyama, T., Sillje, H., Hanisch, A., Uldschmid, A., Takai, Y., Oguri, T., Nigg, E.A. and Inagaki, M. (2005) **Phosphorylation by Cdk1 induces Plk1-mediated vimentin phosphorylation during mitosis.** *The Journal of Cell Biology*, 171, 431-436.

Yang, J., Liu, X., Yue, G., M., A., Bulgakov, O. and Li, T. (2002) **Rootletin, a novel coiled-coil protein, is a structural component of the cilary rootlet.** *The Journal of Cell Biology*, 159, 431-440.

Yao, J., Fu, C., Ding, X., Guo, Z., Zenreski, A., Chen, Y., Ahmed, K., Liao, J., Dou, Z. and Yao, X. (2004) **Nek2A kinase regulates the localization of numatrin to centrosome in mitosis.** *FEBS letters*, 575, 112-118.

Yin, M.J., Shao, L., Voehringer, D., Smeal, T. and Jallal, B. (2003) **The serine/threonine kinase Nek6 is required for cell cycle progression through mitosis**. *The Journal of Biological Chemistry*, 278, 52454-52460.

Yoo, J.C., Chang, J.R., Kim, S.H., Jang, S.K., Wolgemuth, D.J., Kim, K. and Rhee, K. (2004) **NIP1/XB51/NECAB3 is a potential substrate of Nek2, suggesting specific roles of Nek2 in Golgi.** *Experimental Cell Research*, 292, 393-402.

Young, A., Dictenberg, J.B., Purohit, A., Tuft, R. and Doxsey, S.J. (2000) **Cytoplasmic dynein-mediated assembly of pericentrin and γ-tubulin onto centrosomes**. *Molecular Biology of the Cell*, 11, 2047-2056.

Zheng, Y., Wong, M.L., Alberts, B. and Mitchison, T. (1995) **Nucleation of microtubule assembly by a γ-tubulin-containing ring complex.** *Nature*, 378, 578-583.

Zhou, H., Kuang, J., Zhong, L., Kuo, W., Gray, J.W., Sahin, A., Brinkley, B.R. and Sen, S. (1998) **Tumour amplified kinase *STK15/BTAK* induces centrosome amplication, aneuploidy and transformation.** *Nature Genetics*, 20, 189-193.

APPENDIX

Nek2 phosphospecific antibody production

Rabbit antiserum was provided from Millennium Pharmaceuticals (Boston, USA) raised against the Nek2 T175 phospho tryptic peptide (Figure A1). The antiserum was analysed by immunofluorescence microscopy and Western blotting to determine the reactivity with Nek2. Following this the antiserum was purified and both Nek2-T175 and Nek2-phospho-T175 specific antibodies were produced. Immunofluorescence microscopy and Western blotting showed that the Nek2-T175, antibody but not the Nek2-phopho-T175, was still able to recognise the Nek2 protein.

Firstly, pre-immune and immune sera were tested for their reactivity against the Nek2 protein. This was performed by transfection of U2OS cells with myc-Nek2A-WT, myc-Nek2A-KR and myc-Nek2A-F386A. These constructs were chosen to detect any possible difference between the wild-type and kinase-dead proteins. Lysates were prepared and Western blotted with the pre-immune and immune sera generated from rabbit 582. Nek2 was detected by the immune sera but not the pre-immune sera (Figure A1). The immune sera could detect all of the Nek2 constructs irrespective of their activity. This suggests that the immune sera contains antibodies reactive to the non-phosphorylated Nek2 protein. However, the antiserum did not detect endogenous Nek2, whereas it did detect a protein of approximately 70 kDa. Immunofluorescence microscopy using the pre-immune sera did not detect centrosomes or show any localisation to any particular structures within cells (Figure A2). However, in contrast, the immune sera localised to centrosomes throughout the cell cycle and also to the DNA in metaphase and the midbody throughout telophase and cytokinesis (Figure A3). Nek2 localises to centrosomes throughout interphase and therefore the localisation of the immune sera to centrosomes and the detection of Nek2 by Western blot suggests that we had raised an antibody that detects Nek2.

Purification of antibodies was performed by passing the serum first over a column with phosphorylated peptide, eluting the antibodies that bound and then passing them over a non-phosphorylated peptide column. The antibodies that passed straight through were

kept as the phospho T175 antibodies, whereas those that bound were eluted as the T-loop antibodies (Figure A4) and once again these were analysed by Western blot and immunofluorescence. Neither the Nek2-T-loop or Nek2-phospho-T175 purified antibodies could detect endogenous immunoprecipitated Nek2 by Western blot (Figure A5). However, a previously generated Nek2 antibody (Zymed) also failed to detect endogenous immunoprecipitated Nek2. In contrast, the immune sera, purified Nek2-T-loop and Zymed antibodies were capable of detecting immunoprecipitated-myc-Nek2A from transfected 293 cells (Figure A5B). This suggests that the purification of the Nek2-T-loop non-phosphospecific antibody was successful. It could not be determined whether the Nek2-phospho-T175 purification was successful or not as it is possible that there are very low levels of phosphorylated Nek2 present in the extracts. To examine this further, immunofluorescence microscopy was performed at various cell stages using the purified antibodies. This demonstrated that the Nek2-T-loop antibody could detect Nek2 in interphase but it also detected other cell structures throughout mitosis which are inconsistent with Nek2 localisation as determined by the use of other Nek2 antibodies (Figure A6). It is possible that the highly conserved nature of the Nek2 activation domain within other protein kinases has lead to an antibody which recognises other protein kinases in addition to Nek2. The Nek2-phospho-T175 antibody failed to detect centrosomes in the majority of cells (data not shown). It is possible that the abundance of activated Nek2 within the cell is so low and occurs at a very narrow point within the cell cycle that detection using the Nek2-phospho-T175 would prove to be difficult if not impossible. To further test this it will be necessary to perform cell synchronisation experiments and to try and pinpoint the time of Nek2 activation.

Finally, to test the specificity of the Nek2-T-loop antibody, Western blots were performed using the bacterially expressed proteins, Nek2A-T175A-His and Nek2A-NTD-His. The Nek2-T-loop antibody was capable of detecting the Nek2-NTD but incapable of detecting Nek2-T175A. This result is promising as it confirms that the antibody raised can detect the activation domain of Nek2 (Figure A7).

Further characterisation of the Nek2-T-loop and Nek2-phospho-T175 antibodies needs to be performed. This can be achieved by performing cell synchronisation experiments and attempts to increase the abundance of phosphorylated Nek2.

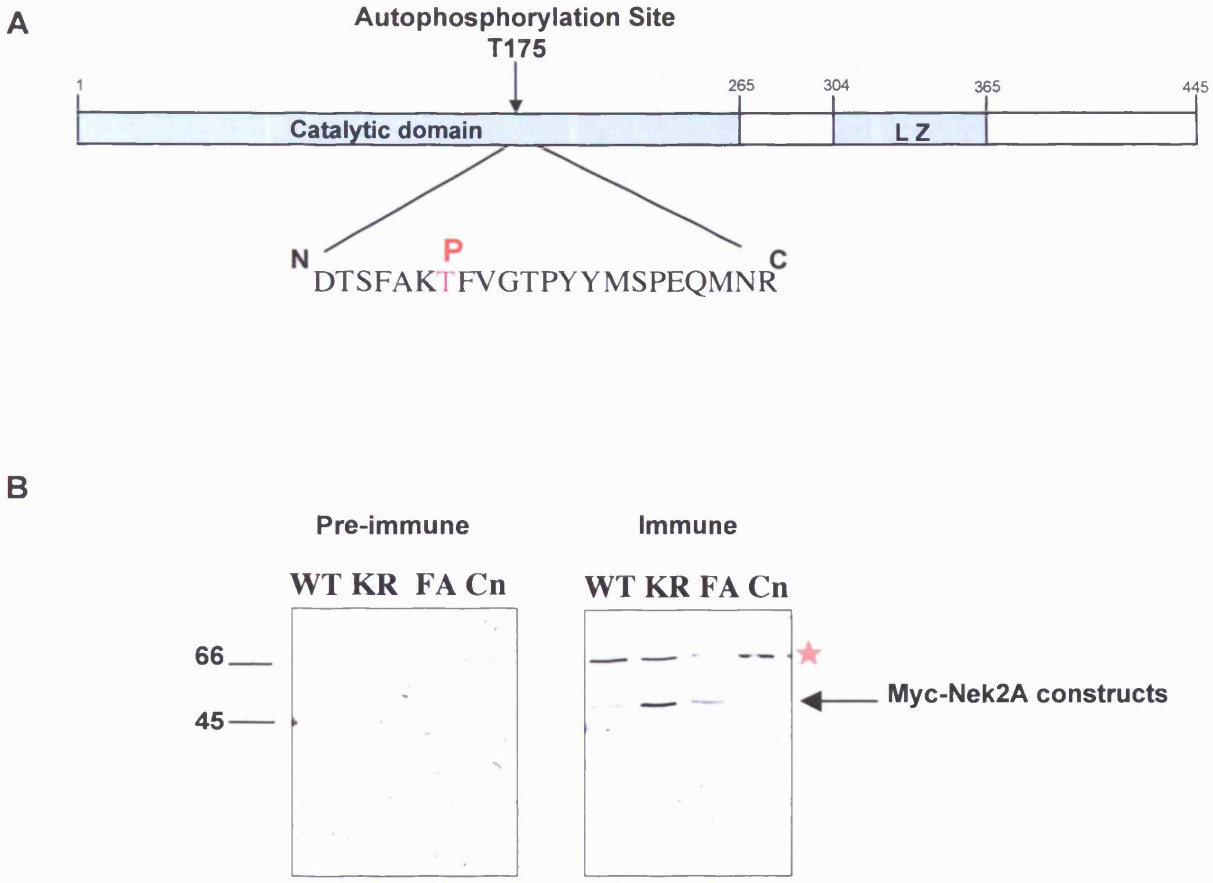

Figure A1 Generation of Nek2 T175 phosphospecific antisera

A. A schematic diagram of the Nek2A protein kinase. The T-loop peptide used for immunization is shown. Millennium Pharmaceuticals used the phosphorylated peptide to raise antisera. **B.** U2OS cells were transfected with myc-tagged Nek2A-WT, Nek2A-KR, Nek2A-FA or left untransfected (control lysate, Cn). Lysates were prepared and Western blotted using the pre-immune and immune serum from rabbit 582. Endogenous Nek2 is not detected by the immune serum. The serum detects a protein of approximately 70 kDa in all extracts (★). M. wts (kDa) are indicated on the left.

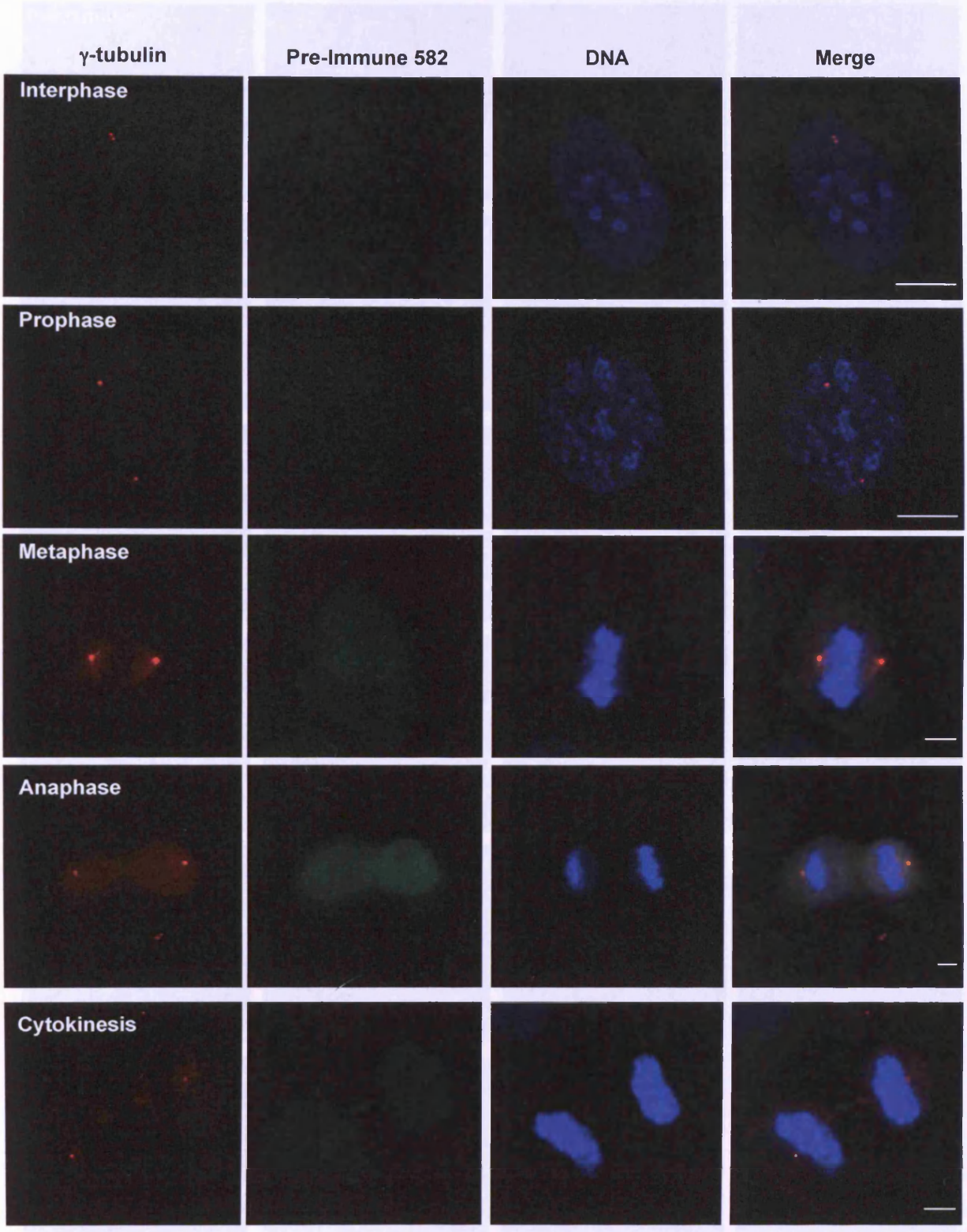

Figure A2 The pre-immune serum 582 does not localise to centrosomes

The pre-immune serum 582 (green) was used to stain HeLa cells fixed in methanol. The γ-tubulin antibody used to stain the centrosomes (red) and Hoescht 33258 to stain the DNA (blue). Merged images are also shown. Images were taken at the cell stages indicated. Scale bar 5 μm.

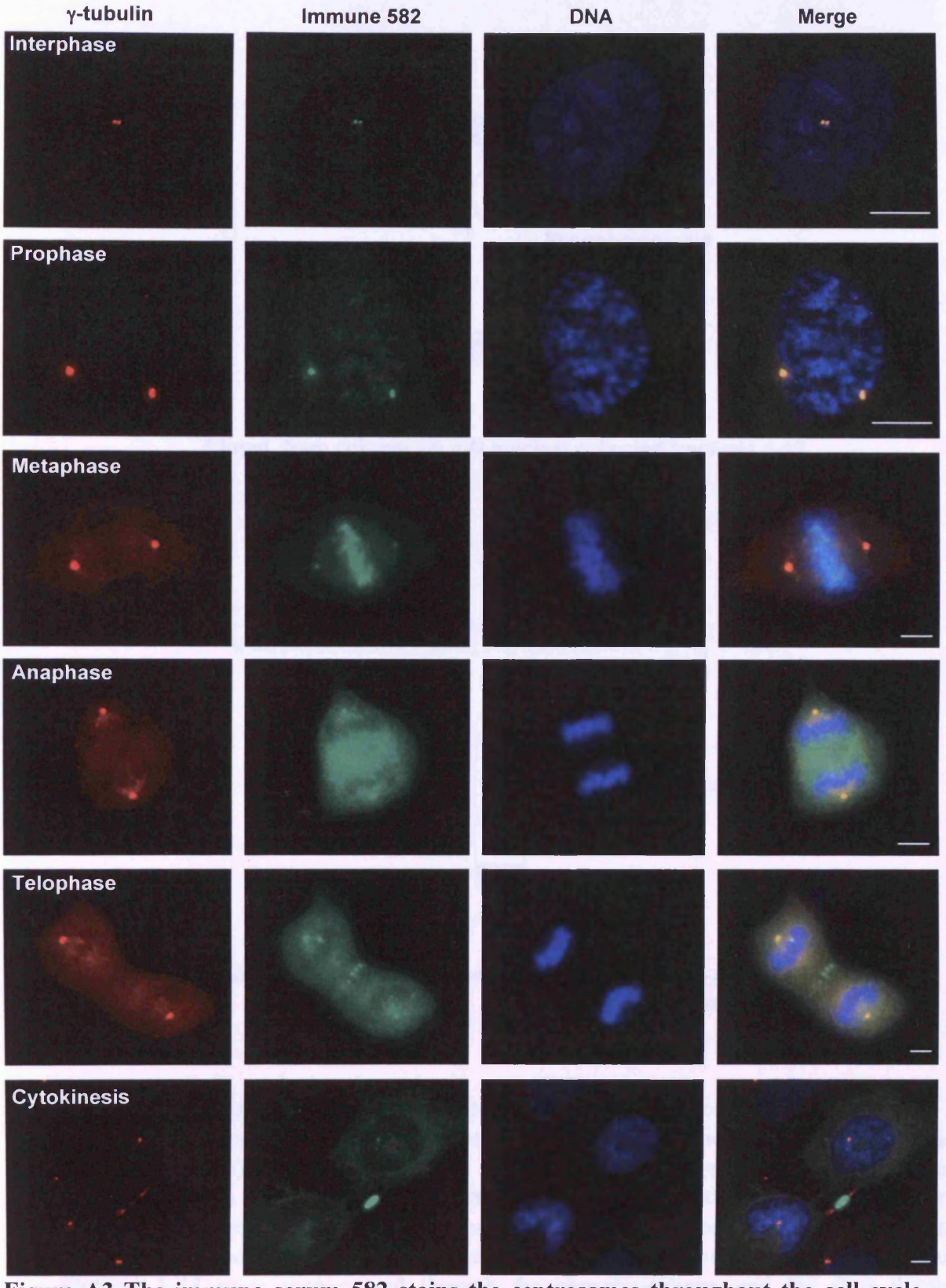

Figure A3 The immune serum 582 stains the centrosomes throughout the cell cycle and also the midbody during cytokinesis

The 582 immune serum (green) was used to stain HeLa cells fixed in methanol. The γ-tubulin antibody used to stain the centrosomes (red) and Hoescht 33258, to stain the DNA (blue). Merged images are also shown. Images were taken at the cell stages indicated. Scale bar, 5 μm.

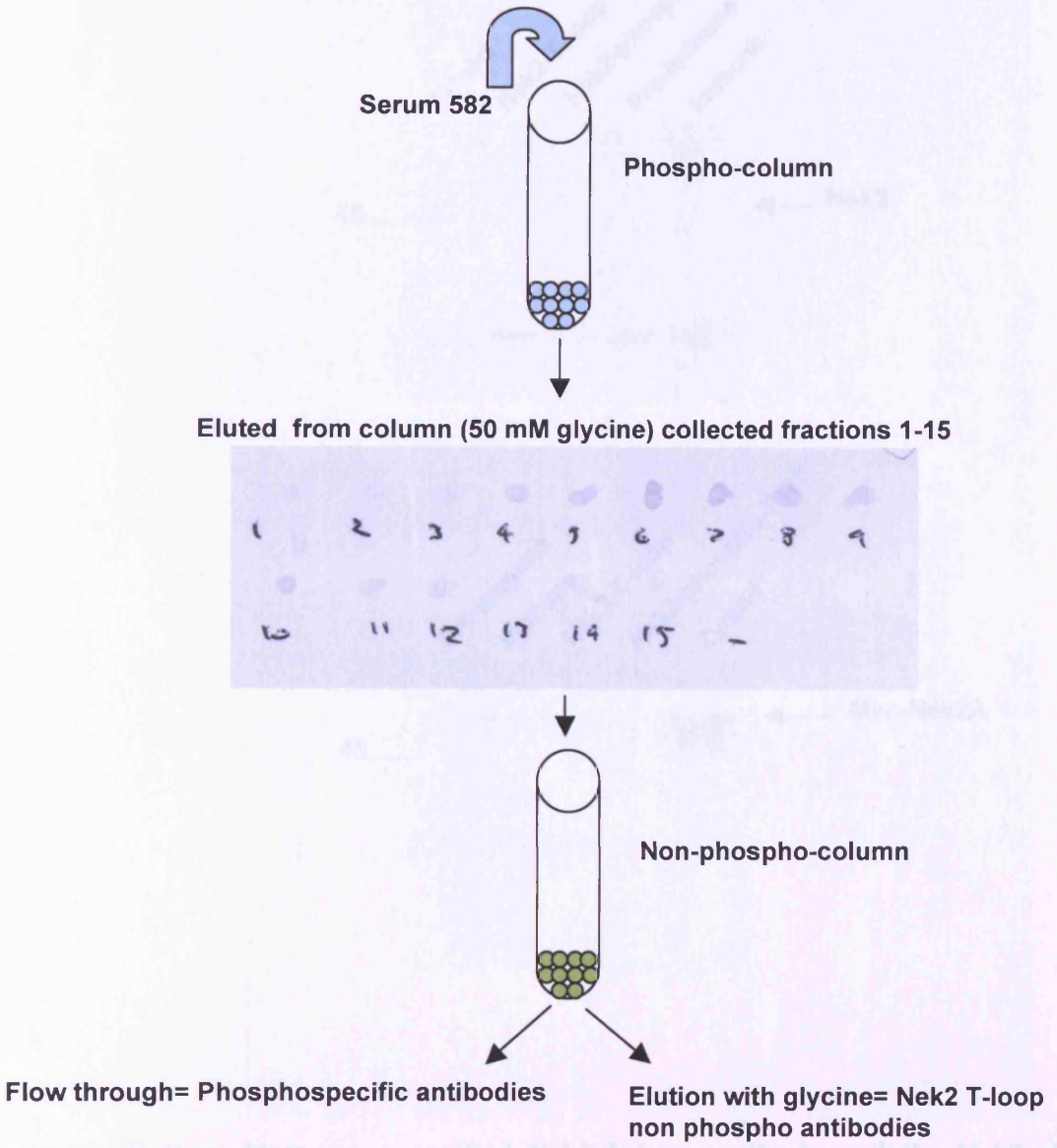

Figure A4 Nek2 phosphospecific antibody purification protocol
Two columns were prepared: CH-sepharose beads bound to the phosphorylated peptide (phospho-column), CH-sepharose beads bound to the non-phosphorylated peptide (Non-phospho-column). The immune serum 582 was incubated with the phospho-column for 4 hours, the column was subsequently washed and bound antibodies eluted using glycine (see Materials and Methods). Elutions were analysed by dot blot using ponceau red stain. Elutions 1-13 were then passed through the phospho-column and the flow through collected. This is the phosphospecific antibody. Glycine elutions were carried out to elute the non-phosphospecific T-loop antibodies.

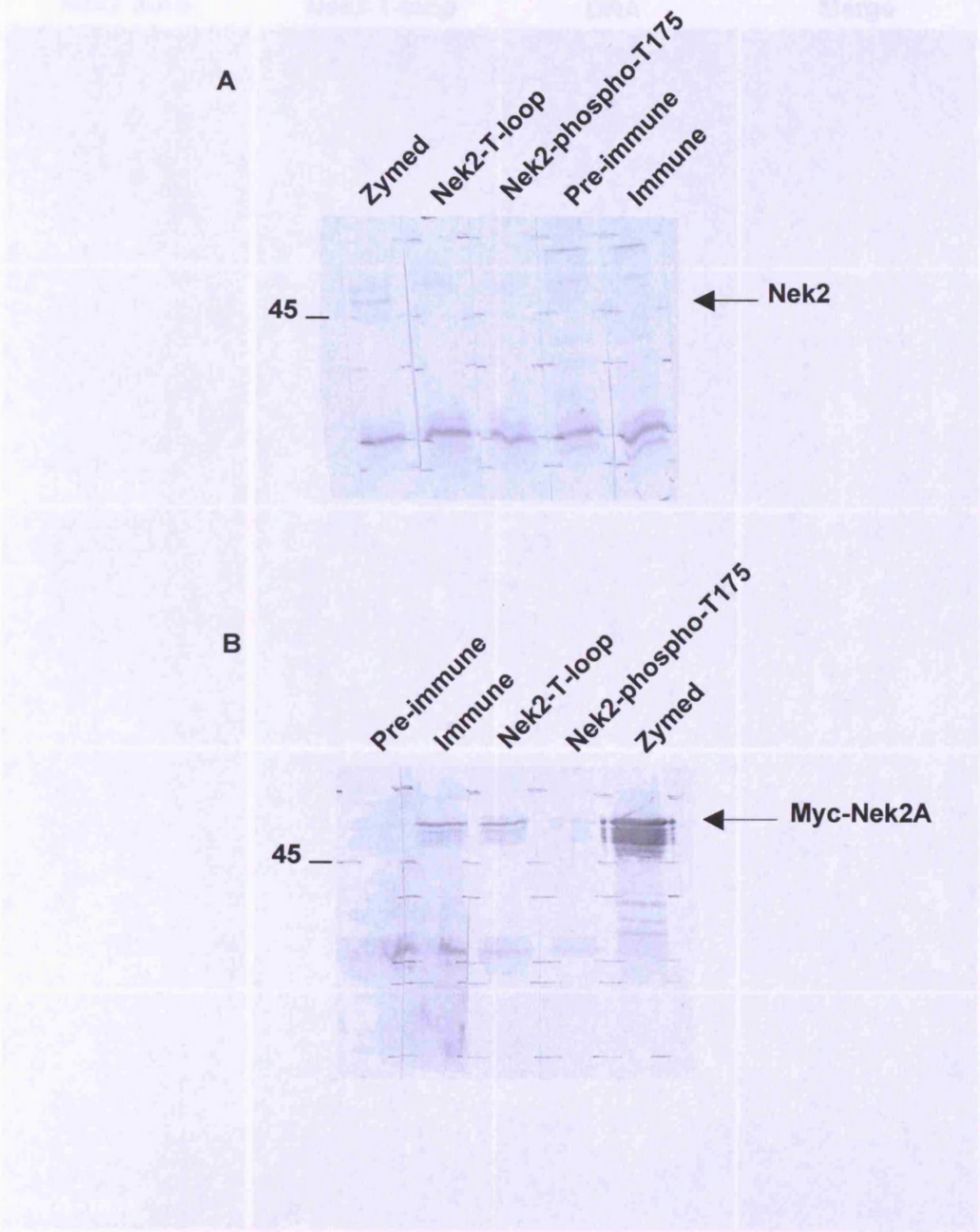

Figure A5 Western blots using purified Nek2-T-loop antibody and the Nek2-phospho-T175 antibody

A. 293 cells were lysed with Neb buffer and Nek2 immunoprecipitated with a commercial Nek2 monoclonal antibody. The beads were washed and subjected to SDS-PAGE followed by Western blotting. The membrane was probed with the Zymed Nek2 antibody (rabbit) to detect Nek2, the pre-immune (PI) and immune (I) 582 serum and the purified Nek2-T-loop and the Nek2-phospho-T175 antibody. **B.** As for A, except the 293 cells were first transfected with a myc-Nek2A-WT construct and immunoprecipitated using a Myc antibody (Cell Signaling). M. wts (kDa) are indicated on the left.

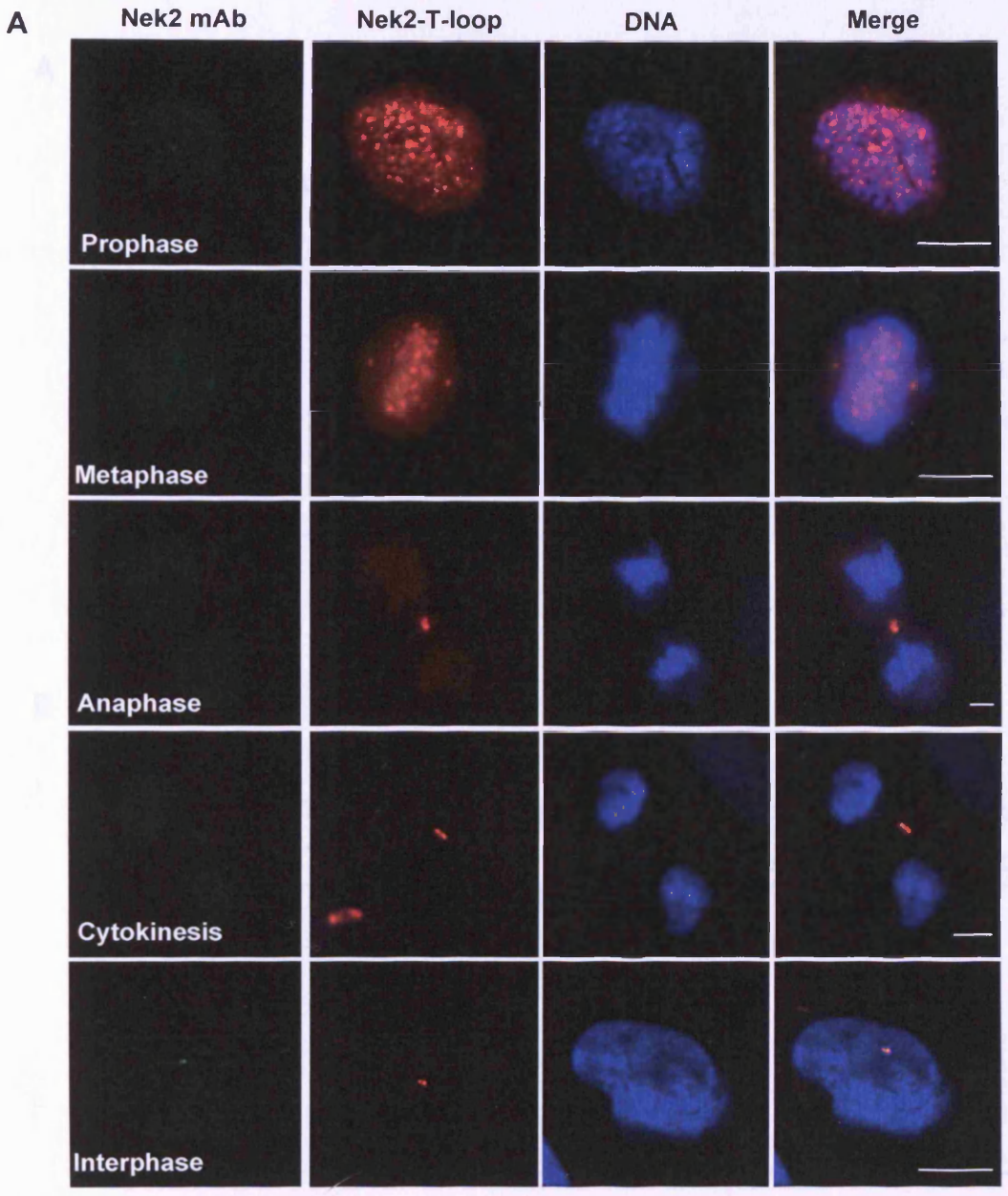

Figure A6 Immunofluorescence microscopy using the Nek2-T-loop purified antibody

A. U2OS cells were methanol-fixed and stained using the monoclonal Nek2 antibody (Cell Signalling, green) or the purified Nek2-T-loop antibody (red). DNA was stained with Hoechst 33258 (blue) and merged images are also shown. Pictures were taken at the various cell cycle stages as indicated. Scale bar, 5 μm

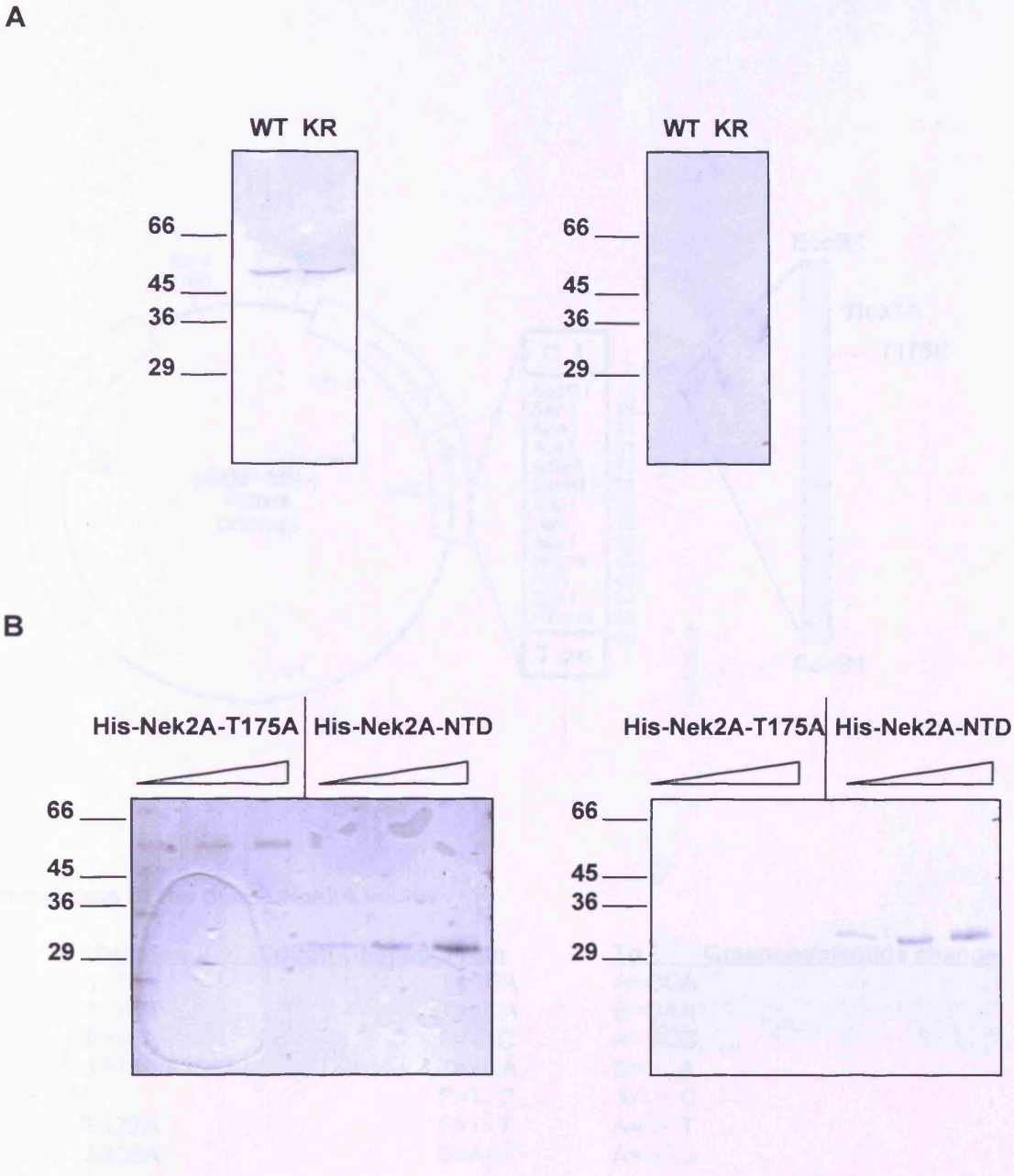

Figure A7 Characterisation of the Nek2-T-loop and Nek2-phospho-T175 antibodies by Western blot

A. Nek2A-WT and Nek2A-KR proteins were transfected into U2OS cells for 24 hours. Lysates were prepared and Western blotted with either Nek2-T-loop antibody (left panel) or the Nek2-phospho-T175 antibody (right panel). **B.** The Nek2A-T175A-His and Nek2A-NTD-His bacterially expressed proteins were analysed on a SDS-PAGE gel at three concentrations by Coomassie Blue (left panel). The same concentrations were analysed by Western blot with the Nek2-T-loop antibody (right panel). M. wts (kDa) are indicated on the left.

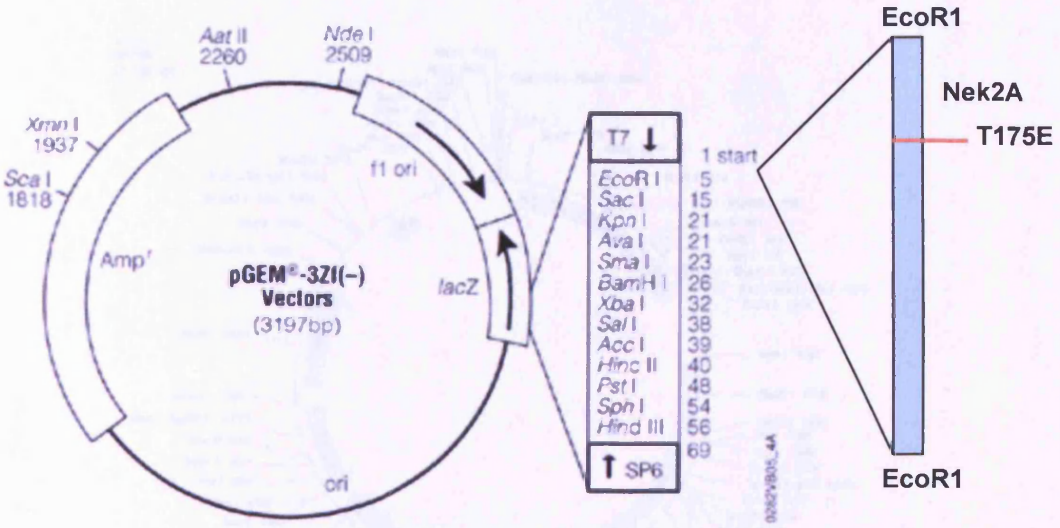

Mutant constructs of the pGEM Nek2A vector

Code	Mutation	Codon Change: From	To	Green=nucleotide change
JEB2	T175A	T=ACA	A=GCA	
JEB4	T175E	T=ACA	E=GAA	
JEB10	F386A	F=TTC	A=GCC	
JEB12	T175E/F386A	T=ACA	E=GAA	
		F=TTC	A=GCC	
JEB13	F172A	F=TTT	A=GCT	
JEB21	S438A	S=AGC	A=GCG	

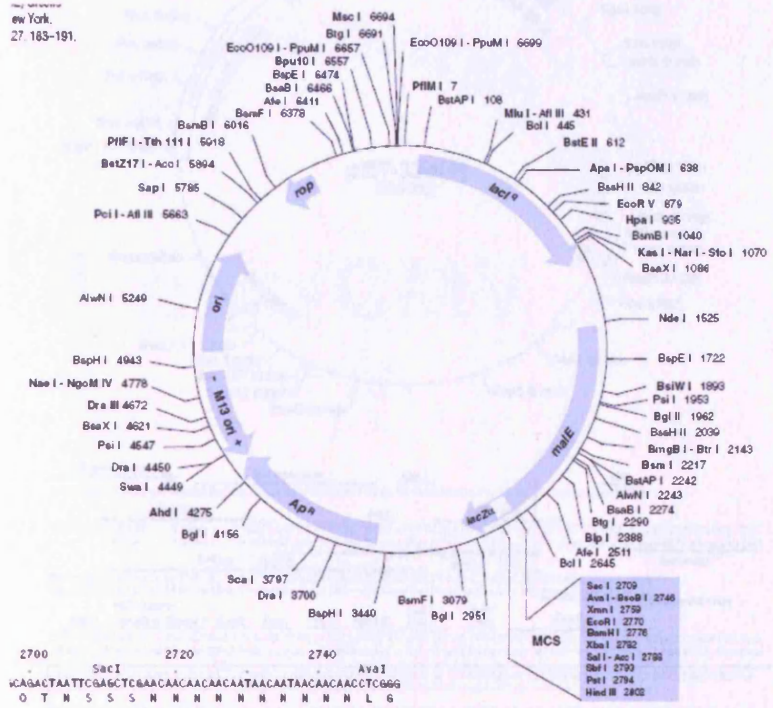

pMAL-p2X MCS

XmnI EcoRI BamHI XbaI SalI PstI HindIII
ATCGAGGGAAGG ATTTCAGAATTCGGATCCTCTAGAGTCGACCTGCAGGCAAGCTTGGCACTGGCCGTCGTT...
I E G R . I S E F G S S R V D L Q A S L A ... *lacZα*

Factor Xa

Constructs made using the pMAL vector (NEB):

pMAL-C-Nap1-CTD (amino acids 1961-2442) Cloned into pMAL-p2X MCS using EcoR1 and HindIII restriction sites

pMAL-Nlp-NTD (amino acids 1-488) Cloned into pMAL-p2X MCS using EcoR1 and HindIII restriction sites

pMAL-C-Nap1-CTD-S2417A/S2421A S=TCC» A=GCC Green=nucleotide change
S=AGT» A=GCT

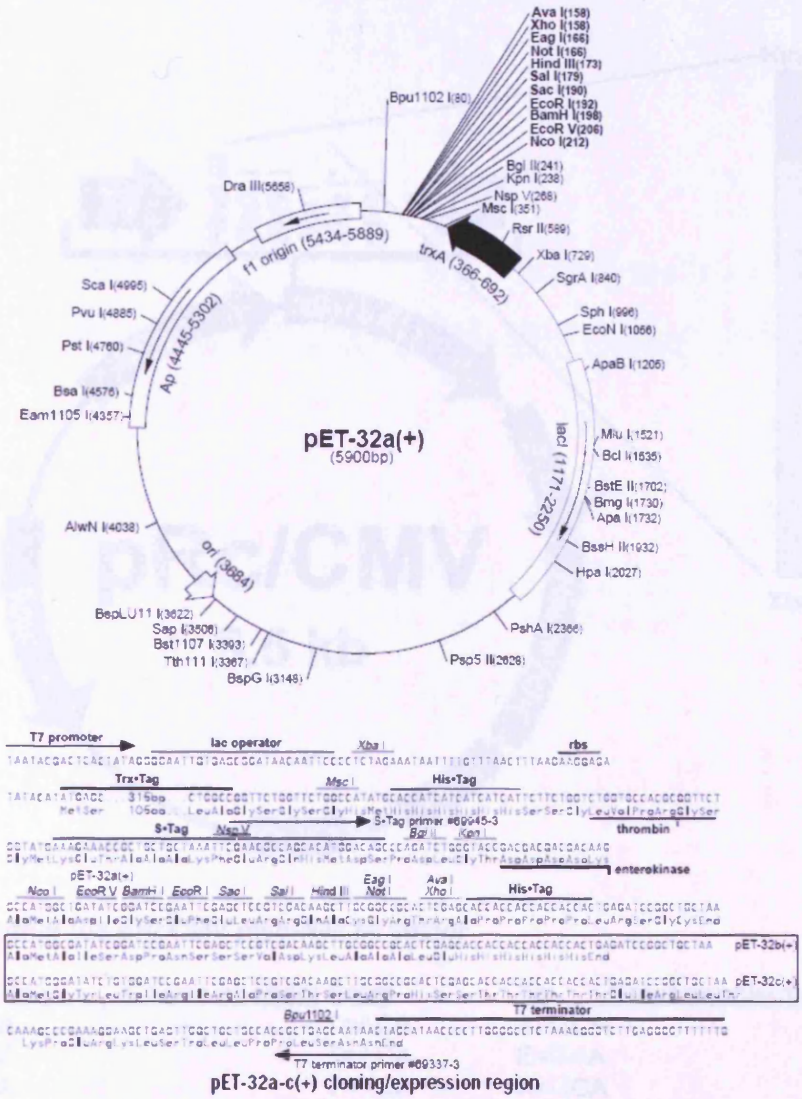

pET-32a-c(+) cloning/expression region

Constructs made with the pET-32a vector (Novagen)

Code	Construct
JEB39	Nek2-CTD (amino acids 304-445) Cloned into pET-32a using BamH1 and HindIII restriction sites
JEB40	Nek2-CTDΔLZ (amino acids 365-445) Cloned into pET-32a using BamH1 and HindIII restriction sites

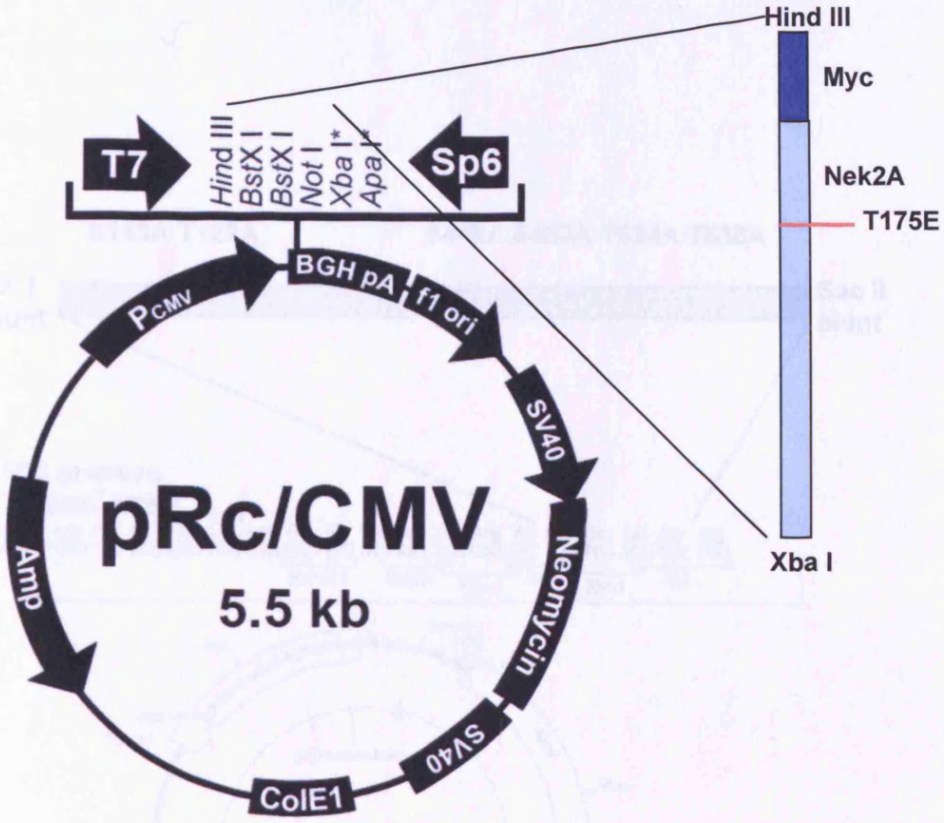

Mutant constructs within the pRcCMV myc-Nek2A vector

Code	Mutation	Codon change: From	To Green=nucleotide change
JEB1	T175A	T=ACA	A=GCA
JEB3	T175E	T=ACA	E=GAA
JEB5	T179A	T=ACA	A=GCA
JEB6	T179E	T=ACA	E=GAA
JEB7	F172A	F=TTT	A=GCT
JEB8	F176A	F=TTT	A=GCA
JEB9	F386A	F=TTC	A=GCC
JEB11	T175E/F386A	T=ACA	E=GAA
		F=TTC	A=GCC
JEB14	S300A	S=AGC	A=GCC
JEB32	S387/390/397/402A	S=AGT	A=GCA
		S=AGT	A=GCA
		S=AGT	A=GCA
		S=AGT	A=GCA
JEB33	S387/390/397/402D	S=AGT	D=GAC
		S=AGT	D=GAC
		S=AGT	D=GAC
		S=AGT	D=GAC
JEB34	T170A	T=ACG	A=GCT
JEB35	T170E	T=ACG	E=GAG
JEB36	S171A	S=AGT	A=GCT
JEB37	S171D	S=AGT	D=GAT

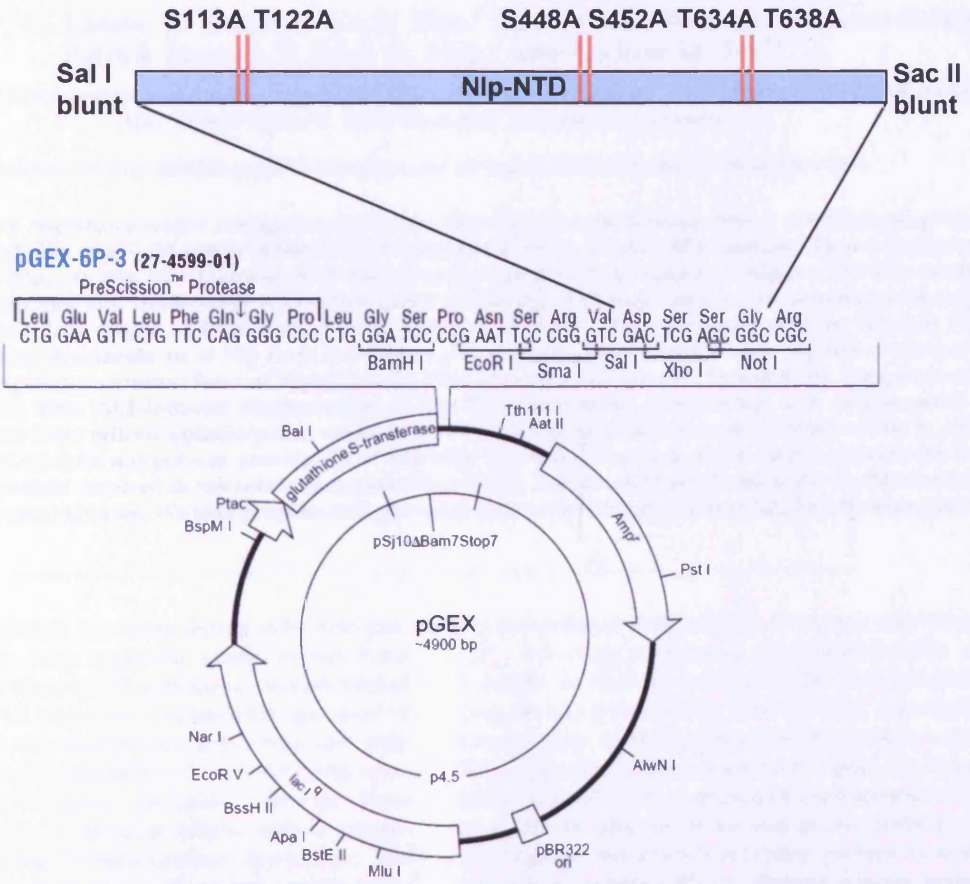

GST-Nlp-NTD was kindly given to us by Prof. E. Nigg. GST-Nlp-Δ6 was made using the site directed mutagenesis.

MOLECULAR AND CELLULAR BIOLOGY, Feb. 2005, p. 1309–1324 Vol. 25, No. 4
0270-7306/05/$08.00+0 doi:10.1128/MCB.25.4.1309–1324.2005

Coordinate Regulation of the Mother Centriole Component Nlp by Nek2 and Plk1 Protein Kinases

Joseph Rapley,[1]†‡ Joanne E. Baxter,[1]† Joelle Blot,[1] Samantha L. Wattam,[1] Martina Casenghi,[2] Patrick Meraldi,[2]§ Erich A. Nigg,[2] and Andrew M. Fry[1]*

Department of Biochemistry, University of Leicester, Leicester, United Kingdom,[1] and Department of Cell Biology, Max Planck Institute of Biochemistry, Martinsried, Germany[2]

Received 16 July 2004/Returned for modification 17 August 2004/Accepted 12 November 2004

Mitotic entry requires a major reorganization of the microtubule cytoskeleton. Nlp, a centrosomal protein that binds γ-tubulin, is a G_2/M target of the Plk1 protein kinase. Here, we show that human Nlp and its *Xenopus* homologue, X-Nlp, are also phosphorylated by the cell cycle-regulated Nek2 kinase. X-Nlp is a 213-kDa mother centriole-specific protein, implicating it in microtubule anchoring. Although constant in abundance throughout the cell cycle, it is displaced from centrosomes upon mitotic entry. Overexpression of active Nek2 or Plk1 causes premature displacement of Nlp from interphase centrosomes. Active Nek2 is also capable of phosphorylating and displacing a mutant form of Nlp that lacks Plk1 phosphorylation sites. Importantly, kinase-inactive Nek2 interferes with Plk1-induced displacement of Nlp from interphase centrosomes and displacement of endogenous Nlp from mitotic spindle poles, while active Nek2 stimulates Plk1 phosphorylation of Nlp in vitro. Unlike Plk1, Nek2 does not prevent association of Nlp with γ-tubulin. Together, these results provide the first example of a protein involved in microtubule organization that is coordinately regulated at the G_2/M transition by two centrosomal kinases. We also propose that phosphorylation by Nek2 may prime Nlp for phosphorylation by Plk1.

Microtubules have diverse functions during cell cycle progression. In interphase, long, relatively stable microtubules contribute to the determination of cell shape, morphological changes required for cell migration, intracellular transport of proteins, mRNAs, and macromolecular assemblies, and positioning of membrane-bound organelles such as the Golgi complex and endoplasmic reticulum. In mitosis, shorter, more dynamic microtubules are involved in mitotic spindle organization, spindle positioning through cortical attachment, and determination of the cleavage plane via central spindle interactions (5, 36). These quite distinct sets of activities require significant changes to take place in the organization of microtubules at the transition between interphase and mitosis. These are regulated largely by posttranslational modifications of microtubule- and centrosome-associated proteins.

The centrosome is the primary site of microtubule nucleation in animal cells, consisting of two cylindrical centrioles surrounded by a meshwork of fibrous and globular proteins that together constitute the pericentriolar material (1, 8). Within the pericentriolar material, γ-tubulin ring complexes are concentrated through interaction with γ-tubulin binding proteins, including pericentrin, pericentrin B/kendrin, CG-NAP, CP309, and Asp (6, 7, 28, 50). γ-Tubulin ring complexes promote the nucleation of microtubules, probably through acting as structural templates for the minus ends of microtubules (27). Following nucleation, some microtubules are released from the centrosome with γ-tubulin ring complexes still capping the minus ends (29). Alternatively, microtubules may be severed close to their minus ends by proteins such as katanin (23). Released microtubules may migrate to distant locations within the cell or be captured by anchoring proteins that bind to either the plus or minus end of microtubules (1, 47). One microtubule minus-end-anchoring protein is ninein, a large coiled-coil protein with no obvious enzyme activity (39, 45). Ninein is localized at the centrosome in most cells but is also found at noncentrosomal apical sites of microtubule anchoring in specialized cell types such as cochlear epithelial cells (2, 39). At the centrosome, ninein is preferentially concentrated on the distal appendages of the older of the two centrioles, the mother, leading to the hypothesis that these appendages act as sites of microtubule anchoring (44). However, the mechanism by which ninein anchors microtubules is not known.

A protein with substantial sequence similarity to ninein was recently identified as a binding partner of the centrosomal protein kinase Plk1 (Polo-like kinase 1). This protein, termed ninein-like protein (Nlp), is concentrated at the centrosome in interphase cells but barely detectable on mitotic spindle poles (3). Nlp interacts with components of the γ-tubulin ring complex, raising the possibility that it contributes to microtubule nucleation during interphase but not mitosis. When overexpressed, Nlp forms large assemblies surrounding the centrosome that can be dispersed by coexpression of active but not inactive Plk1. As Plk1 itself becomes localized to the centrosome in late G_2 and has peak activity at the G_2/M transition (19), a model was proposed in which Plk1 phosphorylation stimulates removal, by either displacement or degradation, of Nlp from the centrosome. In support of this hypothesis, mu-

* Corresponding author. Mailing address: Department of Biochemistry, University of Leicester, University Rd., Leicester LE1 7RH, United Kingdom. Phone: 44 116 252 5024. Fax: 44 116 252 3369. E-mail: amf5@le.ac.uk.

† J.R. and J.E.B. contributed equally to this work.

‡ Present address: Department of Molecular Biology, Massachusetts General Hospital, Boston, Mass.

§ Present address: Department of Biology, Massachusetts Institute of Technology, Cambridge, Mass.

tation of eight putative Plk1 phosphorylation sites in the N-terminal half of Nlp prevented Plk1 from triggering Nlp removal from the centrosome and consequently led to severe defects in mitotic spindle formation (3).

One mechanism of substrate recognition by Plks has recently been described. Plks contain a highly conserved polo box domain in the noncatalytic C-terminal half of the protein. This domain, which is required for centrosome localization (26, 46, 48, 49), forms a cleft that binds a phosphoserine or phosphothreonine in an S-(pS pT) motif (4, 10). Thus, efficient recognition of certain substrates by Plks may require prior phosphorylation by a so-called priming kinase. So far, Cdk1 and Plk1 itself have been proposed as priming kinases for substrate recognition by Plk1 (11, 41). However, other kinases active at the G_2 M transition (43) may also function in priming substrates for recognition by Plk1.

One such kinase that is active in late G_2 and localized to the centrosome is Nek2. Nek2 is a member of the NIMA-related kinase family and contributes to centrosome separation at the G_2 M transition (13). During interphase, mother and daughter centrioles are held in close proximity to each other through a specialized portion of pericentriolar material known as the intercentriolar linkage. Following duplication of centrioles, Nek2 triggers dissolution of this linkage, possibly as a result of phosphorylation of a core centriolar component C-Nap1 (16, 34, 35). Expression of kinase-inactive Nek2 interferes with bipolar spindle formation and chromosome segregation, raising the possibility that Nek2 has multiple centrosomal substrates at the G_2 M transition (12).

We were therefore led to ask whether Nlp might also be a Nek2 substrate. In this article, we report that Nlp is a mother centriole-specific protein that is displaced from the centrosome at the G_2 M transition. We also show that Nlp can indeed be phosphorylated by Nek2 both in vitro and in vivo. Overexpression of Nek2 and of Plk1 has similar consequences in that it can displace Nlp from interphase centrosomes as well as fragment recombinant Nlp assemblies. However, phosphorylation of Nlp by Nek2 occurs on sites that are distinct from those phosphorylated by Plk1, and kinase-inactive Nek2 can interfere with phosphorylation of Nlp by Plk1. These results highlight the complex mechanisms of phosphorylation that are employed to ensure proper regulation of microtubule organization during mitotic onset and raise the possibility that Nek2 is a priming kinase for Plk1.

MATERIALS AND METHODS

Cell culture, synchronization, and transfection. *Xenopus laevis* A6 adult kidney and XTC cells were grown at 23°C in modified (60% medium, 40% water) Leibovitz L15 medium (Invitrogen, Paisley, United Kingdom) supplemented with 10% heat-inactivated fetal calf serum (Invitrogen) and penicillin-streptomycin (100 IU ml and 100 mg ml, respectively). The U2OS osteosarcoma cell line expressing Nek2A K37R-Myc-His from a tetracycline-inducible cytomegalovirus promoter has been described (12). These, together with standard U2OS cells, were grown in Dulbecco's modified Eagle's medium (Invitrogen) supplemented with 10% heat inactivated fetal calf serum, 100 IU of penicillin per ml, and 100 mg of streptomycin per ml at 37°C in a 5% CO_2 atmosphere. To induce and maintain expression from tetracycline-responsive promoters, tetracycline or doxycycline (1 μg ml) was added to the culture medium every 24 h (12).

For synchronization, A6 cells were grown to approximately 50% confluency and then treated accordingly. For G_0, cells were transferred to serum-free medium for 48 h. For G_1/S, hydroxyurea was added to a 1 mM final concentration for 24 h. For S/G_2 and G_1 populations, a G_1/S block was imposed, followed by replacement with drug-free medium for 8 and 16 h, respectively. A mitotic population was generated by addition of nocodazole to a final concentration of 500 ng ml for 24 h. The percentage of cells in each phase of the cell cycle was calculated by standard flow cytometry following propidium iodide staining. For transient transfections, A6 or U2OS cells were grown to approximately 70% confluency and transfected with Lipofectamine 2000 according to the manufacturer's instructions (Invitrogen). Unless otherwise indicated, transfected cells were incubated for 24 h prior to fixation for immunofluorescence microscopy or cell extraction.

Plasmid constructions. Expressed sequence tags (ESTs) containing overlapping *Xenopus laevis* Nlp (X-Nlp) sequences were obtained from the National Institute for Basic Biology, Okazaki, Japan (XL076, XL082, and XL088) and MRC Geneservice, Cambridge, United Kingdom (image clone 6630669). A short X-Nlp cDNA lacking the 439-amino-acid insertion was first generated by introducing a SalI restriction site into XL082 and XL076 with the GeneTailor site-Directed mutagenesis kit (Invitrogen). An EcoRI-SalI fragment was then excised from XL082 and subcloned into the EcoRI and SalI sites of XL076. The SalI site was then mutated back to the original sequence, creating pBS:X-Nlp-ΔN, which lacks the N-terminal 260 amino acids. A 951-bp EcoRI fragment from image clone 6630669 containing the N-terminal sequence was then subcloned into the EcoRI sites of the newly generated pBS:X-Nlp-ΔN construct, giving pBS:X-Nlp-short. To generate the complete full-length X-Nlp cDNA encoding a protein of 1,836 amino acids, overlapping PCRs were performed on image clone 6630669 with primers SW013 (GCGCTCTAGAATGGACAAGGAAGAAGAGAAT) and SW014 (AATGTTCCACCTCCTTCC) and pBS:X-Nlp-short with primers SW015 (ATGGAGCTCTGCCGTCTG) and SW016 (GCGCAAGCTTTCAGACTGCAAGAGAGGC).

The two PCR products were mixed and a further PCR was performed with primers SW013 and SW016. The product was subcloned into pGEM-Teasy (Promega, Southampton, United Kingdom) to generate pGEM:X-Nlp-FL. Fragments encoding amino acid residues 262 to 552 and 1239 to 1836 were subcloned into the pET32-C1 vector (containing an N-terminal Trx-His-S tag; Merck Biosciences, Nottingham, United Kingdom) to generate pET32:X-$Nlp_{262\text{-}552}$ and pET32:X-$Nlp_{1239\text{-}1836}$, respectively. The fragment encoding amino acids 262 to 552 was also subcloned into the pMAL-c2G vector (containing an N-terminal maltose-binding protein [MBP] tag; New England Biolabs UK Ltd., Hitchin, United Kingdom) to generate pMAL:X-$Nlp_{262\text{-}552}$. Yeast two-hybrid constructs were generated by inserting the full-length X-Nek2A-K37R cDNA into the Gal4 DNA binding domain vector pGBDU (25), creating pGBDU:X-Nek2A-K37R. The X-Nlp fragment in the Gal4 activation domain vector pACT2 (BD Biosciences, Oxford, United Kingdom) has been described (3). New constructs were sequenced by Lark Technologies, Inc. (Saffron Walden, United Kingdom). All other Nek2 (15, 17), Nlp (3), Plk1 (37), and Aurora A (37) constructs used here have been described previously.

Bacterial expression and protein purification. The pET32-X-Nlp constructs were expressed in *Escherichia coli* Rosetta DE3 (Merck Biosciences) following induction at 37°C with 1 mM isopropylthiogalactopyranoside (IPTG) and purified with the His tag under denaturing conditions by Ni^{2+}-agarose affinity chromatography according to the manufacturer's instructions (Qiagen Ltd., Crawley, United Kingdom). The pMAL-X-$Nlp_{262\text{-}552}$ construct was expressed in *E. coli* Rosetta DE3 following induction at 37°C with 0.4 mM IPTG and purified by amylose resin chromatography according to the manufacturer's instructions (New England Biolabs UK Ltd.).

Antibody generation. Antibody production was carried out by Cambridge Research Biochemicals (Cleveland, United Kingdom). Rabbits were first screened to eliminate those with centrosome-reactive sera before five (R688) or seven (R1679) injections of selected rabbits with 0.5 mg of Trx-S-His-X-Nlp fusion protein according to standard immunization protocols. Rabbit bleeds were screened by Western blotting of A6 cell lysates and immunofluorescence microscopy of methanol-fixed A6 cells. For affinity purification of R1679 antiserum, an MBP-X-$Nlp_{262\text{-}552}$ Affigel column was made according to the manufacturer's instructions (Bio-Rad, Hemel Hempstead, United Kingdom). After extensive column washes with 10 mM Tris-HCl (pH 7.5) followed by 10 mM Tris-HCl (pH 7.5) 500 mM NaCl, specific antibodies were eluted with 100 mM glycine (pH 2.5) into tubes containing neutralizing quantities of 1 M Tris-HCl (pH 8.0). For competition with antigen, 375 ng of affinity-purified antibody was incubated with 2 μg of MBP-X-$Nlp_{262\text{-}552}$ prior to immunofluorescence staining of A6 cells.

Preparation of extracts, protein electrophoresis, and Western blotting. Extracts of cultured human and *Xenopus* cells were prepared in NP-40 lysis buffer (150 mM NaCl, 1% NP-40, 50 mM Tris-HCl, pH 8). Low-speed cytoplasmic extracts of metaphase II (cytostatic factor [CSF])-arrested eggs or eggs induced to enter interphase by addition of calcium ionophore were prepared as described previously (22). Sodium dodecyl sulfate (SDS)-polyacrylamide gel electrophore-

sis and Western blotting were performed as previously described (16). For Western blotting of X-Nlp, 5% polyacrylamide gels were used; otherwise, all gels were 12% polyacrylamide. Primary antibodies used were anti-X-cyclin B2 (2 μg/ml; gift from H. Yamano, South Mimms, United Kingdom), anti-Eg2 (1:500), anti-green fluorescent protein (anti-GFP) (0.1 μg/ml; Abcam, Cambridge, United Kingdom), anti-Myc (1:1,000; Cell Signaling Technologies, Beverly, Mass.), anti-X-Nlp (2.5 μg/ml for purified R1679; 1:500 for R668), anti-Nek2 (1 μg/ml; Zymed) (14), and anti-α-tubulin (1:2,000; Sigma, Poole, United Kingdom), while secondary antibodies were alkaline phosphatase-conjugated anti-rabbit or anti-mouse immunoglobulin G (1:7,500; Promega).

Immunofluorescence microscopy. Immunofluorescence microscopy was performed as previously described (12). Cells were fixed with either methanol (−20°C) for 6 min or paraformaldehyde solution (3% paraformaldehyde, 2% sucrose, 1× phosphate-buffered saline) for 10 min at room temperature. Paraformaldehyde-fixed cells were permeabilized by 5 min of incubation in 0.5% Triton X-100 (in 1× phosphate-buffered saline). Primary antibodies used were raised against human Nek2 (1 μg/ml Zymed polyclonal [14] or 1 μg/ml Transduction Laboratories monoclonal), *Xenopus* Nek2 (2 μg/ml; R81) (15), human Nlp (1 μg/ml (3), *Xenopus* Nlp (2.5 μg/ml), γ-tubulin (0.15 μg/ml; Sigma), C-Nap1 (1 μg/ml; R63) (16), Myc (1:2,000; Cell Signaling Technologies), or polyglutamylated tubulin (GT335; 0.3 μg/ml; gift from B. Edde, Montpellier, United Kingdom). Secondary antibodies used were Alexa Fluor 488 or 594 goat anti-rabbit and anti-mouse immunoglobulin G (1 μg/ml; Invitrogen), donkey anti-rabbit and sheep anti-mouse biotinylated whole antibodies (1:100; Amersham Biosciences, Little Chalfont, United Kingdom). Streptavidin-Texas Red (1:200; Amersham Biosciences) was used to detect biotinylated antibodies, while DNA was stained with Hoechst 33258 (0.2 μg/ml; Calbiochem, San Diego, Calif.).

Fluorescence images were captured on a TE300 inverted microscope (Nikon United Kingdom, Ltd., Kingston upon Thames, United Kingdom) with an Orca ER charge-coupled device camera (Hamamatsu, Hamamatsu, Japan) with Openlab 3.14 software (Improvision, Coventry, United Kingdom) and processed with Adobe Photoshop (San Jose, Calif.). Quantitative imaging was performed by measuring the mean pixel intensity at nonsaturating exposure conditions with Openlab 3.14 software (Improvision) within a fixed region of interest (1 μm^2). Background readings were taken on neighboring regions of the cell and subtracted from the centrosome intensity measurements.

Miscellaneous techniques. Yeast two-hybrid analysis was performed with the PJ694A strain as previously described (25). *lacZ* reporter gene expression was assayed with the β-galactosidase substrate *O*-nitrophenyl-β-D-galactopyranoside, as described (9). In vitro kinase assays were performed with wild-type or kinase-inactive human Plk1 (31), human Nek2 (18), or *Xenopus* Nek2 (51) kinases purified from insect cells following infection with recombinant baculoviruses or Myc-tagged Nek2 kinases immunoprecipitated with anti-Myc antibodies (Cell Signaling Technologies) from transfected U2OS cells as described (18). X-Nlp was translated in vitro from pGEM:X-Nlp-FL with a T7 polymerase in conjunction with the TnT-coupled transcription-translation kit according to the manufacturer's instructions (Promega). Destruction assays in *Xenopus* egg extracts were performed as previously described (22). Microtubule regrowth assays were performed as described previously (38).

Nucleotide sequence accession number. The GenBank accession number for X-Nlp is AY566230.

RESULTS

***Xenopus laevis* Nlp is a centrosomal protein.** Nlp was first identified in a yeast two-hybrid interaction screen of a *Xenopus* oocyte cDNA library with the kinase-inactive version of *Xenopus* Plx1 (N172A) as the bait. The cDNA fragment isolated matched a full-length human cDNA (KIAA0980), and hence, the human clone was used to characterize the properties and regulation of Nlp (3). To extend these studies, we have now obtained overlapping EST sequences from *Xenopus laevis* that encode an X-Nlp protein of 1,836 amino acids with a predicted molecular mass of 213 kDa. This is somewhat larger than the published human Nlp sequence (156 kDa) but close to the predicted size of a rat Nlp homologue present in the database. We note that one *Xenopus* EST lacked an internal sequence encoding 439 amino acids after residue 792 that would lead to a putative protein of 162 kDa. Thus, it is possible that vertebrates express at least two splice variants of Nlp.

X-Nlp protein shares 60% similarity with human Nlp in the N-terminal half of the protein (amino acids 1 to 691) and 86% similarity over the C-terminal 80 amino acids (Fig. 1A). Between these two regions there is little sequence similarity, but both proteins are predicted to form extended coiled coils (33). Like human Nlp and ninein, X-Nlp also has two putative Ca^{2+}-binding EF-hand motifs within its N terminus. Antibodies were raised in rabbits with bacterially expressed His-tagged fusions of two distinct regions of X-Nlp (R1679 to amino acids 262 to 552 and R688 to amino acids 1239 to 1836). R1679 was affinity purified with a bacterially expressed fusion of amino acids 262 to 552 to MBP. On Western blots of *Xenopus* A6 adult kidney cell extracts, both antibodies (plus four other rabbit immune antisera not described) recognized a common band at 210 kDa, the predicted size of X-Nlp (Fig. 1B).

Translation of X-Nlp in vitro generated a product that was recognized by the affinity-purified R1679 antibody and that comigrated with the band detected in A6 cells (Fig. 1C). By immunofluorescence microscopy, both antibodies stained centrosomes in methanol (Fig. 1D and E) and paraformaldehyde (data not shown) fixed A6 cells as indicated by colocalization with γ-tubulin. Centrosome staining and reactivity of the 210-kDa protein on Western blots with the affinity-purified R1679 was completely blocked by preincubation with the MBP:X-$Nlp_{262-552}$ protein (Fig. 1D and data not shown). Depolymerization of microtubules by incubating A6 cells on ice in the presence of 6 μg of nocodazole per ml had no effect on the centrosome staining pattern (data not shown). X-Nlp is therefore a bona fide core centrosomal protein in adult *Xenopus* cells.

Nlp is displaced from spindle poles but not degraded in mitosis. Immunofluorescence microscopy of *Xenopus* A6 cells at different stages of the cell cycle revealed that X-Nlp is strongly associated with interphase centrosomes, but much less prominent on mitotic spindle poles (Fig. 2A). Quantitative imaging revealed that X-Nlp began to disappear from centrosomes in prophase and by metaphase had decreased to <20% of the abundance during interphase (Fig. 2B). This reduced level of X-Nlp was maintained in anaphase and telophase cells, with X-Nlp only reaccumulating at the centrosome following cytokinesis. Identical results were obtained in two cell lines (A6 and XTC) with both antibodies, making the possibility of epitope masking highly unlikely.

These findings fall in line with studies in human cells, although it is worth noting that, in prophase, Nlp is virtually undetectable in human U2OS cells (3) (see Fig. 6A) but is only beginning to diminish in *Xenopus* A6 cells (Fig. 2B). Previous work did not distinguish whether the reduction in Nlp intensity was due to displacement from the centrosome or degradation. We therefore performed Western blots on extracts of A6 cells synchronized at different stages of the cell cycle (Fig. 2C). Synchrony was confirmed by Western blotting for cyclin B2 and the *Xenopus* Aurora A protein Eg2 (Fig. 2C) and by flow cytometry (data not shown).

The total abundance of X-Nlp was unchanged throughout the cell cycle and clearly was not reduced in mitotic cells. Furthermore, destruction assays confirmed that in vitro-translated X-Nlp was stable in mitotic extracts of *Xenopus* eggs

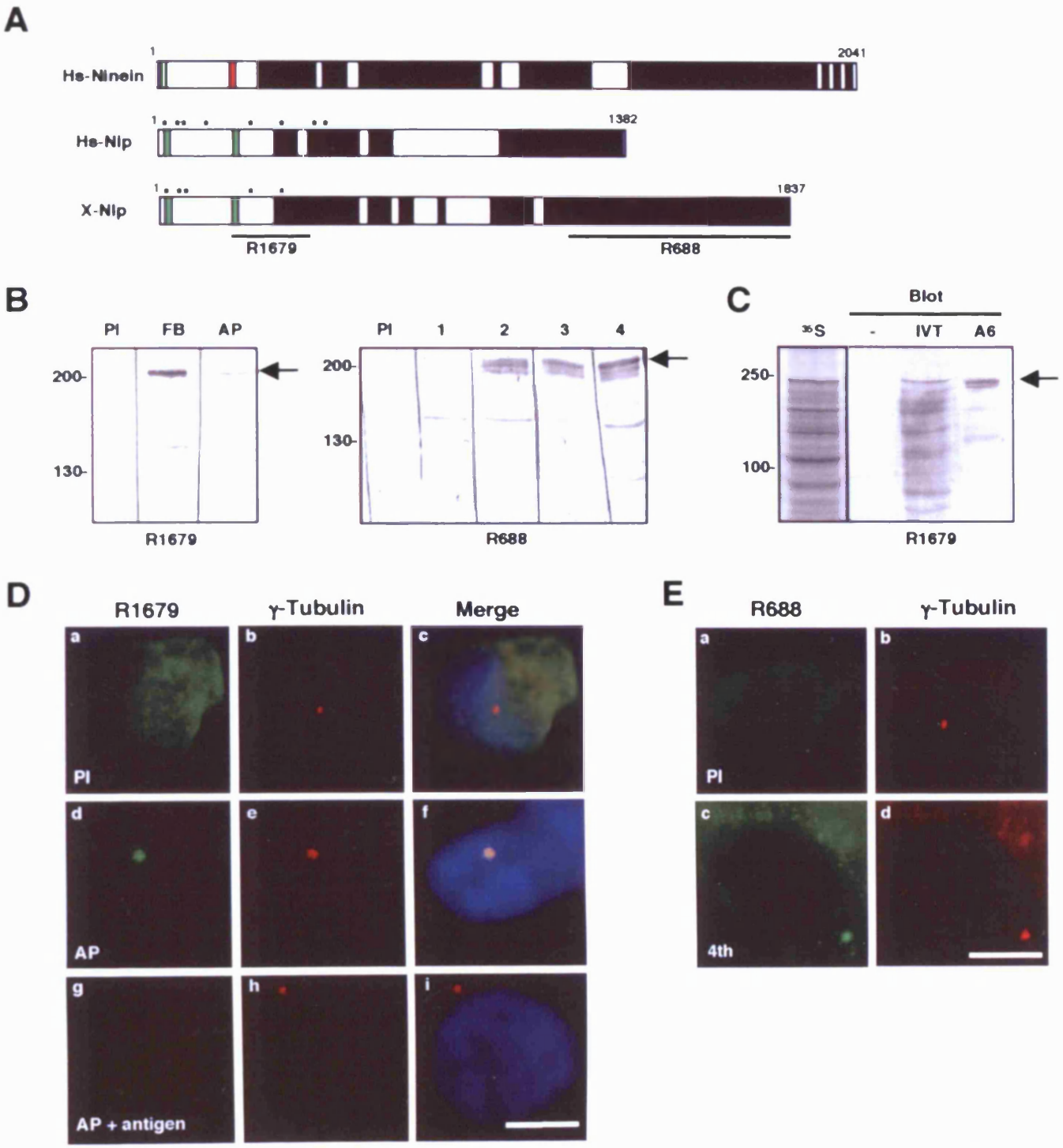

FIG. 1. X-Nlp is a *Xenopus laevis* centrosomal protein. (A) Schematic comparison of human ninein (Hs-Ninein), human Nlp (Hs-Nlp), and *Xenopus laevis* Nlp (X-Nlp) proteins. Numbers represent amino acids; putative Ca^{2+}-binding EF-hands (green boxes), GTP-binding site (red box), and coiled coils (black boxes) are indicated. Asterisks represent eight putative Plk1 phosphorylation sites identified in human Nlp (3), of which five are conserved in X-Nlp. The regions of the X-Nlp protein used to generate antisera R1679 and R688 are also indicated. (B) Western blots of *Xenopus* A6 whole-cell extracts with anti-X-Nlp antibodies R1679 (left panel; PI, preimmune serum; FB, final bleed serum; AP, affinity-purified antibodies) and R688 (right panel; PI, preimmune serum; 1 to 4, crude serum from bleeds 1 to 4). (C) Full-length X-Nlp was translated in vitro in the presence of [^{35}S]methionine and, following SDS-PAGE, was either exposed to autoradiography (^{35}S) or Western blotted with affinity-purified R1679 (IVT). In vitro-translated samples lacking input DNA (−) or A6 whole-cell extracts (A6) were Western blotted in parallel. In panels B and C, the positions of molecular size markers are indicated on the left (in kilodaltons), and the X-Nlp protein is indicated by an arrow on the right. (D) Immunofluorescence microscopy of methanol-fixed *Xenopus* A6 cells costained with preimmune (a) or affinity-purified (d and g) R1679 anti-X-Nlp (green) and anti-γ-tubulin (b, e, and h; red) antibodies. Merged images including DNA stain (blue) are also shown (c, f, and i). In panels g to i, affinity-purified anti-X-Nlp antibodies were incubated with an excess of MBP-X-Nlp$_{262-552}$ protein. (E) Immunofluorescence microscopy of methanol-fixed A6 cells costained with preimmune (a) or immune (c; fourth bleed) R688 anti-X-Nlp and anti-γ-tubulin (b and d) antibodies. Scale bars in panels D and E, 10 μm.

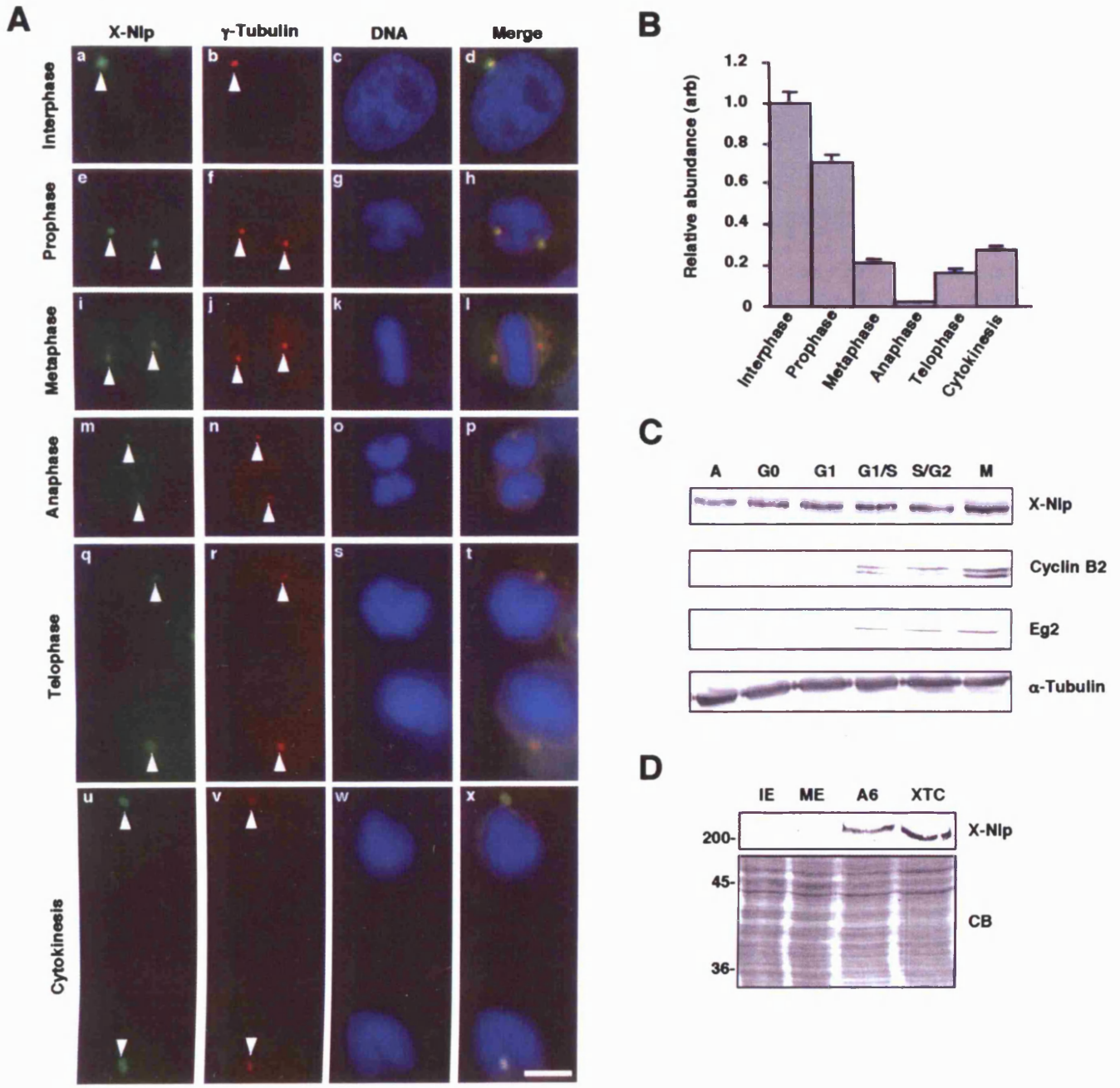

FIG. 2. Localization of X-Nlp at the centrosome is cell cycle dependent. (A) Immunofluorescence microscopy of methanol-fixed *Xenopus* A6 cells at different stages of the cell cycle, as indicated, costained with purified R1679 anti-X-Nlp (green) and anti-γ-tubulin (red) antibodies. DNA was stained with Hoechst 33258 (blue), and merged images are shown. Arrowheads indicate positions of centrosomes/spindle poles. (B) The abundance of X-Nlp at a pair of interphase centrosomes (given an arbitrary value of 1.0) was compared with that at the two spindle poles (added together) in different stages of mitosis by quantitative fluorescence imaging as described in Materials and Methods. The centrosomes/spindle poles in 20 cells were analyzed for each bar of the histogram, and error bars represent standard deviations. (C) *Xenopus* A6 cells were synchronized in different stages of the cell cycle, as indicated (A, asynchronous), with the procedures described in Materials and Methods. Cell extracts were separated by SDS-PAGE and Western blotted for X-Nlp (purified R1679 antibodies), cyclin B2, Eg2, and α-tubulin. (D) Interphase (IE), and metaphase II (ME)-arrested *Xenopus* egg extracts as well as extracts of A6 and XTC cells were Western blotted for X-Nlp protein (purified 1679 antibodies, upper panel). Equal protein loading was confirmed by Coomassie blue (CB) staining of an equivalent SDS-polyacrylamide gel (lower panel). The positions of molecular size markers are indicated on the left (in kilodaltons).

(data not shown). Hence, the disappearance of Nlp from the spindle poles is best explained by a change in localization and not degradation. Surprisingly, X-Nlp was not detected on Western blots of cytoplasmic extracts prepared from CSF-arrested eggs or eggs induced to enter interphase by calcium addition (Fig. 2D). Nor could X-Nlp be detected by immunofluorescence microscopy on the centrosome of demembranated sperm either before or after incubation in egg ex-

tracts (data not shown). These data reveal that X-Nlp protein is not expressed in gametes and does not appear on the zygotic centrosome generated in vitro. This implies that centrosomes in early frog embryos are unlikely to require Nlp for organization of interphase microtubules.

Nlp is a mother centriole-specific protein. The hypothesis that ninein contributes to microtubule anchoring is based in large part on its preferential localization to the mother centriole (44). Hence, we examined the distribution of Nlp at centrosomes in interphase A6 cells with purified X-Nlp antibodies. In this cell type, centrosomes as stained with γ-tubulin often appear as a single large spot that is clearly recognized by Nlp antibodies (see Fig. 1D and E). However, in some cells, two γ-tubulin-staining spots can be distinguished, and in this case X-Nlp is restricted to one of the two spots (Fig. 3A).

To determine whether this spot contained the mother or daughter centriole, A6 cells were serum starved, inducing production of primary cilia that could be detected with antibodies against polyglutamylated tubulin (GT335). Antibody costaining demonstrated that X-Nlp is present specifically on the centriole subtending the cilium, i.e., the mother centriole (Fig. 3B). Overexpression of full-length human GFP-Nlp induces the formation of large assemblies that encompass the centrosome (3). Costaining with the centriolar marker C-Nap1 revealed that the two centrioles were frequently separated by ~2 μm (Fig. 3C) and, while sometimes both centrioles remained within the large GFP-Nlp assembly, often the bulk of GFP-Nlp was clustered around just one centriole (Fig. 3D). The other centriole was completely devoid of GFP-Nlp, consistent with Nlp protein's only being capable of associating with one centriole. A review of the staining pattern produced by human Nlp antibodies confirmed the presence of three small dots surrounding one centriole and one weaker dot colocalizing with the second centriole (data not shown) (3). This staining pattern is identical to that reported for ninein (39) and provides further support to the notion that ninein and Nlp are both preferentially localized to mother centrioles.

Displacement of endogenous Nlp from the centrosome by active Nek2 kinase. To test the hypothesis that Nlp might be regulated by the Nek2 kinase in addition to Plk1, we first asked whether Nek2 and Nlp can interact in the yeast two-hybrid assay. Vertebrate Nek2 is expressed as two splice variants, Nek2A and Nek2B, which differ in their extreme C termini (21, 52). In embryonic systems, only Nek2B is expressed, whereas in adult cells, Nek2A is the predominant isoform. When cotransformed in *Saccharomyces cerevisiae*, X-Nlp and a kinase-inactive mutant of X-Nek2A (K37R) activated reporter genes to a similar extent as the positive control pairing of SNF1 and SNF4, whereas when transformed with control plasmids, little or no activation of reporters was detected (Fig. 4A).

We next tested whether Nek2A kinase was capable of influencing the distribution of X-Nlp in vivo. For this purpose, A6 cells were transfected with wild-type Nek2A or kinase-inactive Nek2A-K37R and stained for endogenous X-Nlp (Fig. 4B). Wild-type Nek2A led to loss of X-Nlp at the centrosome in 85% of interphase cells, whereas kinase-inactive Nek2A triggered loss in only 22% cells (Fig. 4C). In human U2OS cells, wild-type Nek2A induced a comparable displacement of Nlp from the centrosome in ~80% of cells (Fig. 4D), whereas wild-type and kinase-inactive enhanced green fluorescent protein (EGFP)-Aurora A induced Nlp displacement in <10% of cells (Fig. 4E).

The efficient displacement of endogenous Nlp from the interphase centrosome by active Nek2A was highly reminiscent of that seen following transfection of a hyperactive Plk1 (T210D) construct (3). We therefore decided to test whether the kinase-inactive (K/R) mutants could act in a dominant-negative manner to prevent the displacement of Nlp from the centrosome caused by the active enzymes. After 24 h, transfection of either wild-type Nek2A or hyperactive Plk1 alone or the two active kinases together led to loss of Nlp from the centrosome in >80% of U2OS cells, as expected, while the kinase-inactive mutants led to between 25 and 35% loss when transfected alone (Fig. 5A). Intriguingly, when transfected in combination, Plk1-K/R did not prevent wild-type Nek2A from stimulating Nlp displacement, but Nek2A-K/R substantially reduced the ability of hyperactive Plk1 to induce Nlp displacement. The moderate loss of Nlp in the presence of overexpressed inactive kinases may result from either disruption of centrosome structure (17) or steric interference with Nlp association with the centrosome. By analyzing cells after only 16 h of transfection, we found that Nek2A-K/R alone had a less pronounced effect on Nlp localization but that its ability to suppress Nlp displacement by hyperactive Plk1 was undiminished (Fig. 5B and C).

Dominant-negative Nek2A interferes with Nlp displacement from spindle poles. We next tested whether kinase-inactive Nek2A could interfere with displacement of endogenous Nlp from the centrosome during mitosis. For this experiment, we made use of U2OS cells, which express Nek2A-K/R from a tetracycline-inducible promoter (12). In the absence of Nek2A-K/R induction, Nlp abundance was severely diminished at mitotic spindle poles as expected. However, following 24 h of induction, Nlp was much more readily detected on spindle poles during both prophase and metaphase (Fig. 6A and B). Interphase cells expressing kinase-dead Nek2A did not have increased levels of Nlp at the centrosome (data not shown). Hence, kinase-inactive Nek2A acts in a dominant-negative manner to inhibit displacement of Nlp from the mitotic spindle poles.

Nek2A and Plk1 phosphorylation sites are distinct. As shown earlier (Fig. 3D), recombinant GFP-Nlp forms large assemblies, presumably through oligomerization, that surround the mother centriole. Coexpression with wild-type Nek2A but not the kinase-inactive mutant caused the dramatic fragmentation of this large assembly into smaller particles that were distributed throughout the cytoplasm (Fig. 7A). Importantly, the overexpressed Nek2A protein strongly colocalized with Nlp irrespective of whether it was active, supporting the notion that these proteins are capable of interaction in vivo (Fig. 7A). Plk1 is also capable of fragmenting GFP-Nlp assemblies in a kinase-dependent manner (3).

One reason why both Plk1 and Nek2 can disrupt GFP-Nlp oligomerization may be that they target the same critical phosphorylation site(s). A consensus motif for phosphorylation by Plk1 (E/DxS/T) has been proposed (31), whereas the amino acid requirements for phosphorylation by Nek2 are less clear. By scanning the human Nlp sequence, eight putative Plk1 phosphorylation sites have been identified in the N-terminal half of Nlp, and four of these sites (S87 or S88, T161, and S686)

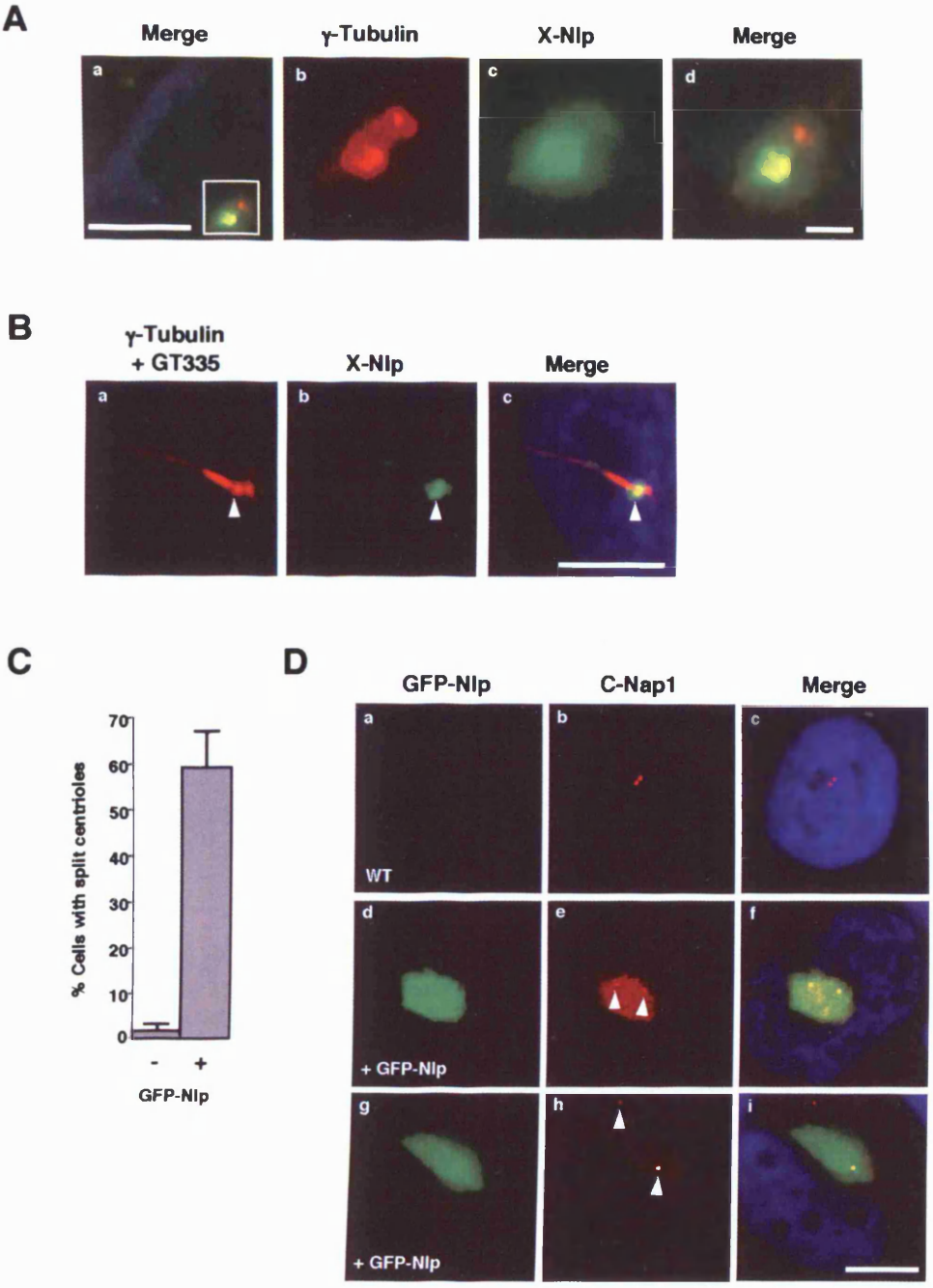

FIG. 3. X-Nlp localizes to the mother centriole in interphase cells. (A) Methanol-fixed *Xenopus* A6 cells were processed for immunofluorescence microscopy with anti-X-Nlp (R1679; green) and anti-γ-tubulin (red) antibodies; DNA was stained with Hoechst 33258 (blue). A merged image of an interphase cell is shown, demonstrating that X-Nlp is only present on one centriole (a). Higher magnification of the boxed area in panel a is shown in panels b (γ-tubulin), c (X-Nlp), and d (merge). Scale bar in panel a, 10 μm; in panel d, 1 μm. (B) *Xenopus* A6 cells were induced to grow primary cilia by serum starvation before processing for immunofluorescence microscopy as in A, except that anti-polyglutamylated tubulin antibodies (GT335) were also added. The red signal (a) is therefore a combination of γ-tubulin (revealing the two centrioles) and polyglutamylated tubulin (revealing the primary cilium). The primary cilium is nucleated from the distal end of the mother centriole (arrowhead), and X-Nlp clearly colocalizes with the mother, and not daughter, centriole. Scale bar, 10 μm. (C) The percentage of cells with centrioles separated by >2 μm was determined in untransfected (−) and GFP-Nlp transfected (+) cells; 100 cells were counted for each sample in three independent experiments. (D) U2OS cells were transfected with GFP-Nlp (green) for 24 h before methanol fixation and processing for immunofluorescence microscopy with antibodies against human C-Nap1 (R63; red). Merged images including DNA stained with Hoechst 33258 (blue) are shown. Centrioles, as indicated by C-Nap1 staining, are often split and, in some cases (d to f), both centrioles are still within the GFP-Nlp assembly, whereas in others (g to i), only one centriole remains within the assembly. Scale bar, 10 μm.

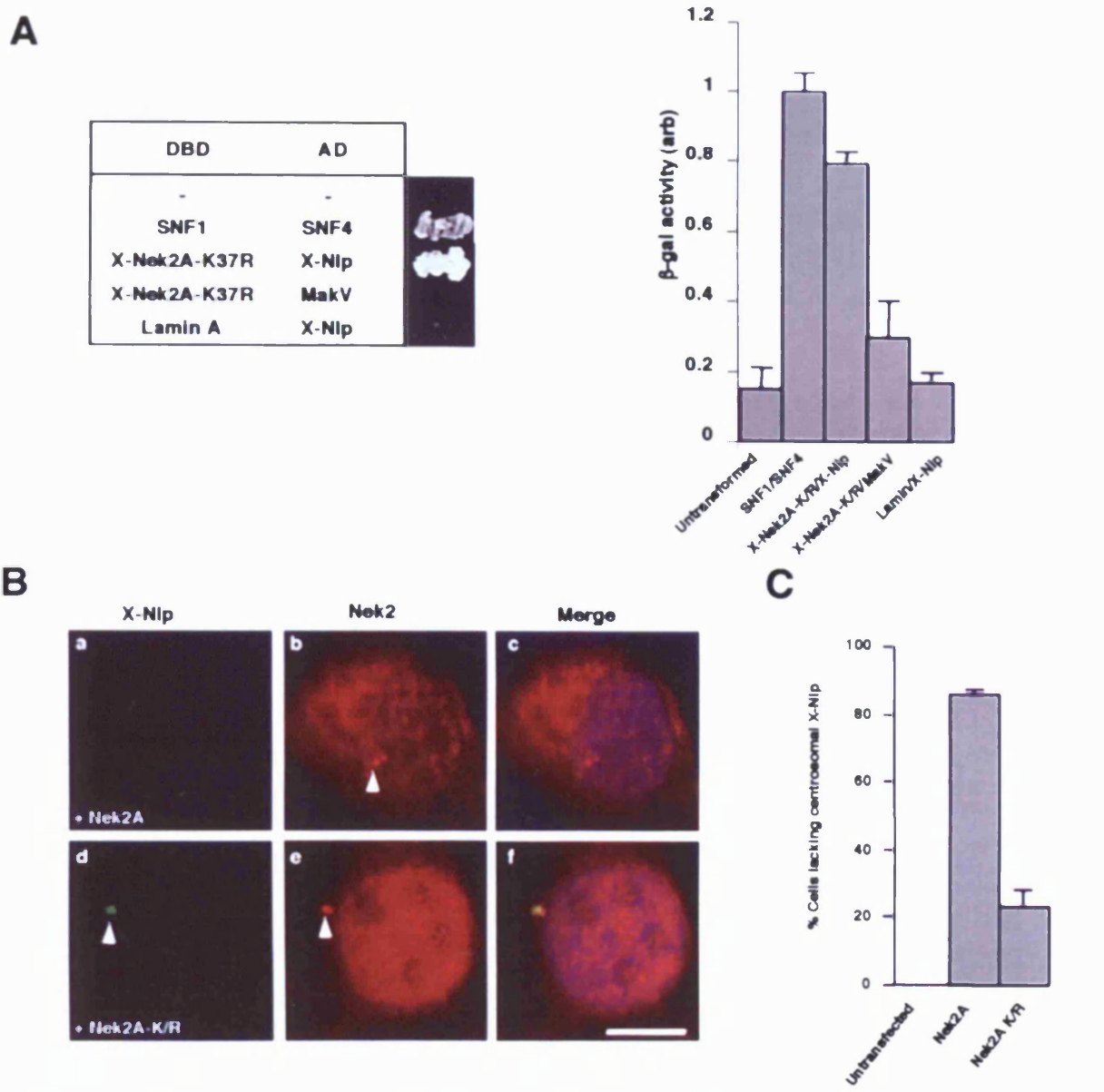
A
DBD
AD
-
-
SNF1
SNF4
X-Nek2A-K37R
X-Nlp
X-Nek2A-K37R
MakV
Lamin A
X-Nlp
β-gal activity (arb)
1.2
1
0.8
0.6
0.4
0.2
0
Untransformed
SNF1/SNF4
X-Nek2A-K/R/X-Nlp
X-Nek2A-K/R/MakV
Lamin/X-Nlp
B
X-Nlp
Nek2
Merge
+ Nek2A
+ Nek2A-K/R
C
% Cells lacking centrosomal X-Nlp
100
80
60
40
20
0
Untransfected
Nek2A
Nek2A K/R
D
Nlp
Nek2
Merge
Untransfected
+ Nek2A
+ Nek2A-K/R
E
Aurora A
Nlp
+ Aurora A
+ Aurora A-K/R

were shown to be phosphorylated by Plk1 in vitro by mass spectrometry (3). Of these, S87, S88, and S686 are conserved between the human and *Xenopus* Nlp proteins (Fig. 1A). Centrosomal assemblies formed by overexpressing a GFP-Nlp mutant lacking all eight phosphorylation sites (NlpΔ8) were no longer fragmented by Plk1 (3). In contrast, active but not inactive Nek2A could still trigger fragmentation of the large NlpΔ8 assemblies around the centrosome (Fig. 7B). Western blotting of these cell extracts revealed a distinct gel mobility shift of both wild-type Nlp and NlpΔ8 in the presence of wild-type but not inactive Nek2A (Fig. 7C). In combination, Nek2A and Plk1 caused an even greater electrophoretic mobility shift, while kinase-inactive Nek2A blocked the electrophoretic shift induced by hyperactive Plk1 (Fig. 7D) and reduced the ability of Plk1 to induce fragmentation of Nlp assemblies (Fig. 7B). These data indicate that Plk1 and Nek2A do not phosphorylate the same sites within the Nlp protein but that kinase-dead Nek2A can interfere with Plk1 phosphorylation and regulation of Nlp.

Nek2 phosphorylation does not prevent interaction of Nlp with γ-tubulin. Immunostaining cells cotransfected with GFP-Nlp and Nek2A with the GT335 antibody revealed that the Nlp fragments were no longer associated with centrioles (Fig. 8A). Indeed, centrioles were often widely separated, consistent with observations that active Nek2A kinase stimulates centriole splitting (12, 17). Thus, Nek2A phosphorylation regulates not only Nlp oligomerization but also its association with the centrosome. Intriguingly, γ-tubulin was present not only in the large assembly in the presence of kinase-inactive Nek2A, but also in the smaller Nlp fragments that had been displaced from the centrosome by active Nek2A (Fig. 8B). This was not true of other unrelated centrosomal proteins (data not shown). Based on this result, we predicted that the ability of the centrosome to organize a radial array of microtubules would be compromised. Microtubule regrowth assays confirmed that cells containing Nek2A-induced GFP-Nlp fragments failed to produce radial microtubule asters, in contrast to surrounding untransfected cells (Fig. 8C and D). Thus, Nek2A stimulates release of Nlp from the centrosomes but not release of γ-tubulin from Nlp. Furthermore, this indicates that association with the centrosome and the γ-tubulin ring complex are independent properties of the Nlp protein.

Phosphorylation of Nlp by Nek2 in vitro regulates Plk1 phosphorylation. To show that Nek2 is capable of phosphorylating Nlp, in vitro kinase assays were first carried out with the MBP-X-Nlp$_{262-552}$ fusion protein. Active but not inactive X-Nek2A expressed in insect cells (51) strongly phosphorylated this protein but not MBP alone (Fig. 9A). This fragment was similarly phosphorylated by the *Xenopus* Nek2B kinase and by *Xenopus* Plx1 (data not shown). The N-terminal half of human Nlp containing the eight putative Plk1 phosphorylation sites (GST-Nlp N-term) (3) was also strongly phosphorylated by active but not inactive human Nek2A immunoprecipitated from transfected cells (Fig. 9B and C). Mutation of the eight Plk1 phosphorylation sites significantly reduced phosphorylation by Plk1 but not Nek2A, confirming that the sites phosphorylated by Plk1 and Nek2 are distinct (Fig. 9C and D).

To determine whether phosphorylation of Nlp by Plk1 is regulated by Nek2, we performed Plk1 in vitro kinase assays with the GST-Nlp fragment that had been incubated with either wild-type or kinase-inactive Nek2A in the presence of unlabeled ATP. Strikingly, Nlp that had been incubated with immunoprecipitated active Nek2A was more efficiently phosphorylated than Nlp incubated with kinase-inactive Nek2A (Fig. 9E) or beads alone (Fig. 9F). Taken together, these data support a model in which Nek2A and Plk1 coordinately regulate the association of Nlp with the mother centriole and γ-tubulin ring complex at the G_2/M transition and in which Nek2A might act as a priming kinase for Plk1.

DISCUSSION

Centrosomes play a dominant role in generating both the long, relatively stable microtubules present in interphase cells and the highly dynamic microtubule asters present during mitosis (24). For this reason, centrosome abnormalities could contribute to the cell polarity defects and chromosome instability that typify many cancer cells (42). Yet the mechanistic basis by which microtubule asters are organized at centrosomes and spindle poles remains poorly understood, and still less is known about how these are regulated at the G_2/M transition. Important progress in this direction came with the identification of a novel centrosomal protein, Nlp, which binds the γ-tubulin ring complex and is a substrate of the mitotic Plk1 kinase. Through characterization of both *Xenopus* and human Nlps, we show here that Nlp is a component of the mother centriole. Furthermore, we demonstrate that Nlp is specifically displaced from centrosomes upon mitotic entry rather than being degraded. Most importantly, we present evidence that Nlp can be phosphorylated not only by Plk1 but also by a second centrosomal kinase, Nek2. We propose that the coordinate regulation of Nlp by Plk1 and Nek2 triggers loss

FIG. 4. Nek2A interacts with Nlp and displaces it from the centrosome. (A) Yeast two-hybrid interaction assay. The table on the left indicates the Gal4 DNA-binding domain (DBD) and activation domain (AD) fusion proteins expressed in *S. cerevisiae* with a photograph of the appropriate colonies after 5 days of growth on plates lacking histidine and adenine. The histogram on the right indicates β-galactosidase activity (arbitrary units) of the yeast strains as measured with an *o*-nitrophenylgalactopyranoside assay. Experiments were repeated three times, and error bars show the standard deviation. The activity of the positive control interaction between SNF1 and SNF4 was set at 1.0. (B) *Xenopus* A6 cells were transiently transfected with either human wild-type Myc-Nek2A (a to c) or the Myc-Nek2A-K/R kinase-inactive mutant (d to f) and, after 24 h, methanol fixed and processed for immunofluorescence microscopy with anti-Nek2 (R81, red) and anti-X-Nlp (R1679, green) antibodies. (C) The percentage of A6 cells in which the intensity of X-Nlp at the centrosome was significantly reduced or undetectable was calculated in untransfected cells and cells transfected with wild-type Nek2A or kinase-inactive Nek2A by counting >100 cells in three independent experiments. (D) Human U2OS cells were either untransfected (a to c) or transfected for 24 h with human Myc-Nek2A (d to f) or Myc-Nek2A-K/R (g to i) and stained with antibodies against human Nek2 (red) and Nlp (green). (E) Similarly, U2OS cells were transfected for 24 h with wild-type EGFP-Aurora A (a and b; green) or kinase-inactive EGFP-Aurora A-K162R (c and d; green) before processing with antibodies against endogenous Nlp (red). Scale bars in panels B, D, and E, 10 μm.

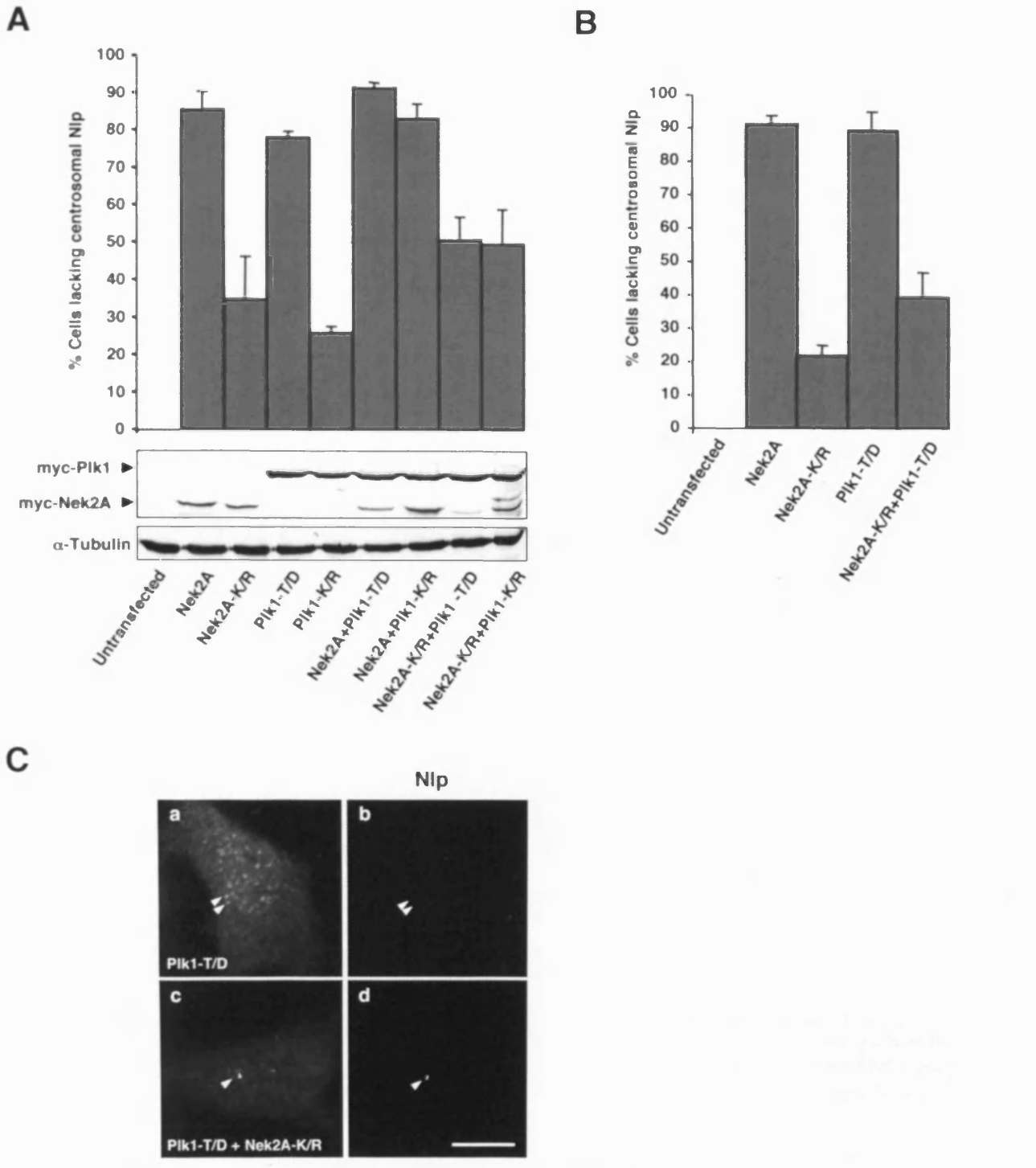

FIG. 5. Displacement of centrosomal Nlp by Plk1 is blocked by kinase-inactive Nek2A. (A) Human U2OS cells were cotransfected for 24 h with Myc-tagged Nek2A, Nek2A-K37R (K/R), Plk1-T210D (T/D), or Plk1-K82R (K/R), as indicated, before methanol fixation and processing by immunofluorescence microscopy with appropriate antibodies to detect transfected proteins (α-Myc) and endogenous Nlp. The percentage of cells with reduced or absent Nlp at interphase centrosomes was calculated in >100 cells for each sample in three independent experiments. Western blots show the level of expression of the transfected proteins (Myc), and equal loading was confirmed with an antitubulin blot. (B) Transient transfections were performed and analyzed as in A except that after only 16 h of transfection. (C) Representative images of endogenous Nlp (b and d) in cells transfected with Plk1-T/D alone (a and b) or in combination with Nek2A-K/R (c and d) are shown. Scale bar, 10 μm.

of interaction of Nlp with both the γ-tubulin ring complex and mother centriole as cells enter mitosis.

Role for Nlp in microtubule anchoring? Microtubules are nucleated from γ-tubulin ring complexes that are evenly distributed within the pericentriolar material (27). Indeed, microtubule regrowth assays demonstrate that the pericentriolar material associated with mother and daughter centrioles has a similar capacity for microtubule nucleation even when well

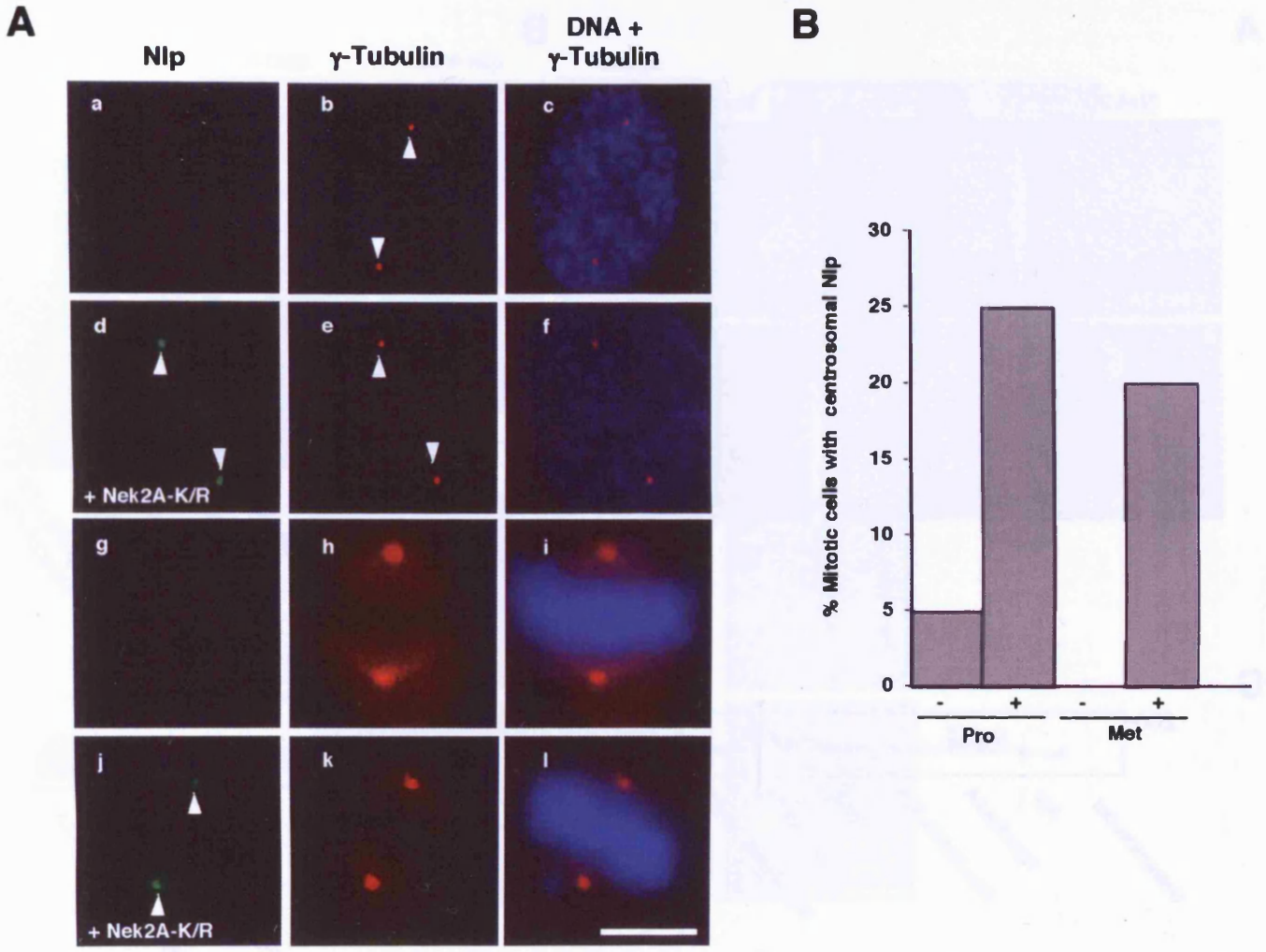

FIG. 6. Kinase-inactive Nek2 interferes with Nlp displacement from mitotic spindle poles. (A) U2OS:Nek2A-K37R-Myc-His cells were either uninduced (a to c and g to i) or induced with tetracycline for 24 h (d to f and j to l) before methanol fixation and processing for immunofluorescence microscopy with antibodies against γ-tubulin (red) or Nlp (green). Merged images of γ-tubulin stain (red) and DNA stained with Hoechst 33258 (blue) are also shown. a to f, prophase cells; g to l, metaphase cells. Scale bar, 5 μm. (B) The percentages of prophase (Pro) and metaphase (Met) cells in which Nlp was readily detected at the spindle poles were calculated in uninduced (−) and induced (+) cells; 40 cells were analyzed for each condition.

separated (38, 44). However, at steady state, most centrosomal microtubules in interphase are associated with the mother centriole, leading to the hypothesis that mother centrioles are associated with microtubule-anchoring activity (1). Our observation that Nlp is a mother centriole-specific protein in *Xenopus* A6 cells supports the hypothesis that it is a microtubule-anchoring protein. Other candidates in vertebrate cells that are mother centriole specific include the related protein ninein as well as dynactin and the small GTPase Ran. Ninein is localized specifically on the subdistal appendages of the mother centriole, and these structures have been proposed as sites of microtubule anchoring (44). Furthermore, ninein is present at noncentrosomal sites of microtubule anchoring in the apical region of cochlear epithelial cells (39). Dynactin is implicated independently of cytoplasmic dynein in interphase microtubule anchoring, as overexpression of dynactin subunits leads to loss of a radially organized centrosomal array of microtubules (45). Ran is also present on mother centriolar appendages, microtubule minus ends, and apical sites of microtubule anchoring, although whether it contributes to microtubule anchoring is unclear (32).

How might Nlp anchor microtubules? During interphase, microtubule minus ends are relatively stable consistent with the idea that they are capped by the γ-tubulin ring complex (30, 40, 53). Hence, microtubule anchoring could occur through direct binding of Nlp to γ-tubulin ring complex components. Indeed, Casenghi and colleagues demonstrated interaction between Nlp and two of the γ-tubulin ring complex components, γ-tubulin and human GCP4 (3). If Nlp anchors microtubules via γ-tubulin ring complex caps, this raises the important question of what regulates the release of γ-tubulin ring complexes from the γ-tubulin binding proteins present throughout the pericentriolar material. One possibility is that microtubule elongation alters the conformation of the γ-tubulin ring complex at its minus end, promoting release from the pericentriolar material-distributed γ-tubulin binding protein.

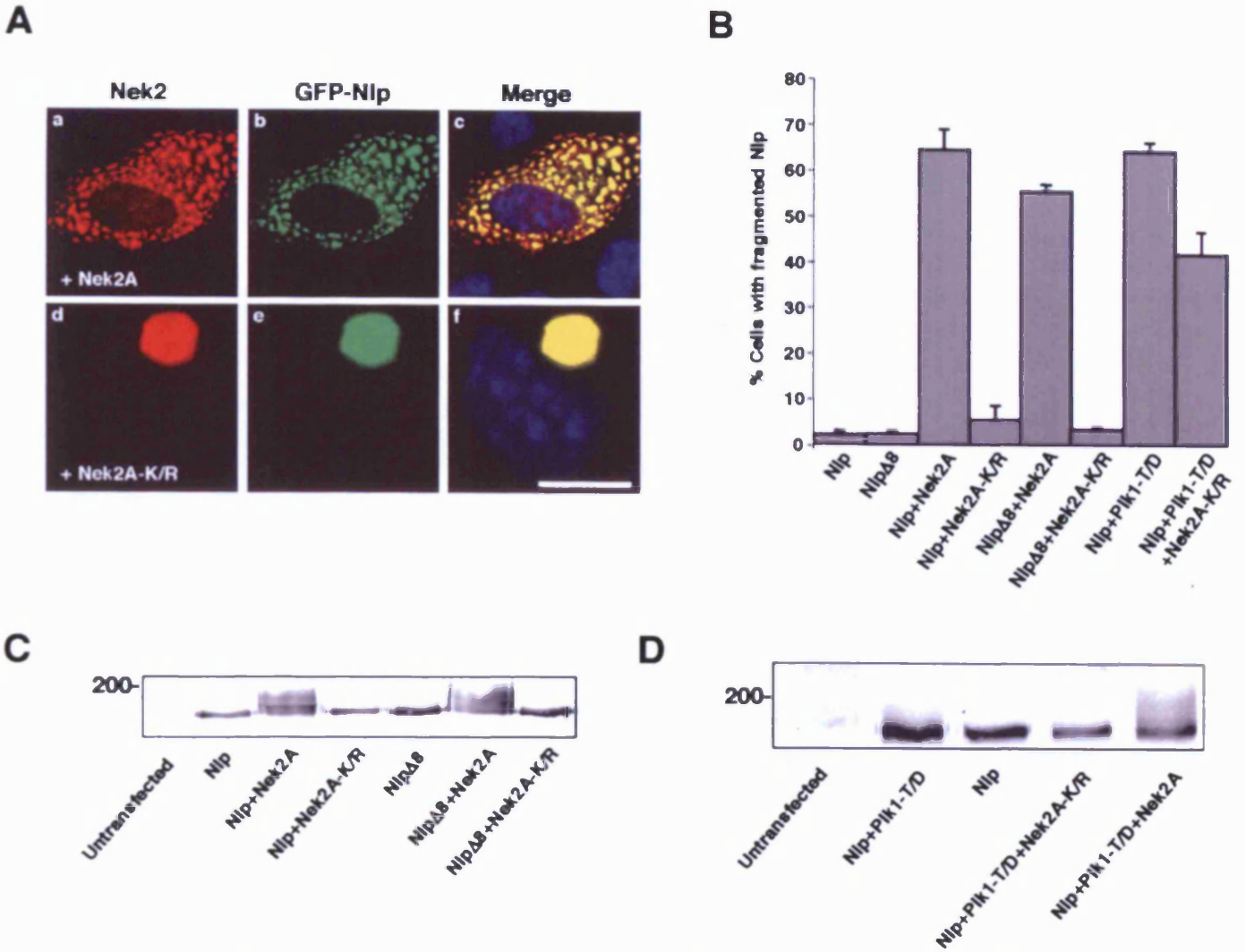

FIG. 7. Nek2 displaces GFP-Nlp assemblies from the centrosome. (A) U2OS cells were cotransfected with GFP-Nlp and either wild-type Myc-Nek2A (a to c) or Myc-Nek2A-K/R (d to f) before methanol fixation after 24 h and processing for immunofluorescence microscopy. Anti-Nek2 antibodies (red), GFP signals (green), and merged images including DNA stained with Hoechst 33258 (blue) are shown. Scale bar, 10 μm. (B) The percentage of cells in which recombinant Nlp is fragmented (as opposed to a single large assembly) is presented for each set of cotransfections as indicated; 100 cells were counted for each set, and independent experiments were performed three times. (C) Extracts were prepared from U2OS cells transfected with the Nek2A and GFP-Nlp constructs as indicated and Western blotted with anti-GFP antibodies. An electrophoretic gel mobility shift indicative of phosphorylation was detected in the GFP-Nlp and GFP-NlpΔ8 proteins only in the presence of wild-type Nek2A. (D) An electrophoretic mobility shift of GFP-Nlp induced by Plk1-T/D is lost upon cotransfection with Nek2A-K/R. HeLa cells were transfected as indicated and processed as in panel C.

Alternatively, Nlp may be capable of interacting directly with the minus ends of microtubules, allowing it to anchor microtubules that have been released from nucleation complexes or severed by proteins such as katanin (23). At acentrosomal sites of microtubule anchoring, such as the apical regions of cochlear epithelial cells, γ-tubulin is not present, indicating that microtubule attachment here cannot be via γ-tubulin ring complexes (39). To confirm a role in microtubule anchoring for Nlp, it will be important to examine its precise centriolar localization by immunoelectron microscopy as well as to determine whether, like ninein, it is also present at acentrosomal sites of microtubule anchoring in differentiated cells.

Regulation of Nlp localization through the cell cycle. Previous data suggested that Nlp is present on interphase centrosomes but absent from mitotic spindle poles (3). However, this study had not been able to distinguish whether this was a result of protein degradation or displacement from the centrosome. The generation of antibodies against *Xenopus* Nlp allowed us to quantitate the change in both centrosomal and total cellular abundance of Nlp through the cell cycle. Our results indicated a 10-fold decrease in Nlp association with metaphase spindle poles compared to interphase centrosomes. However, we found no overall change in abundance of total Nlp between interphase and mitotic cells. While localized degradation of

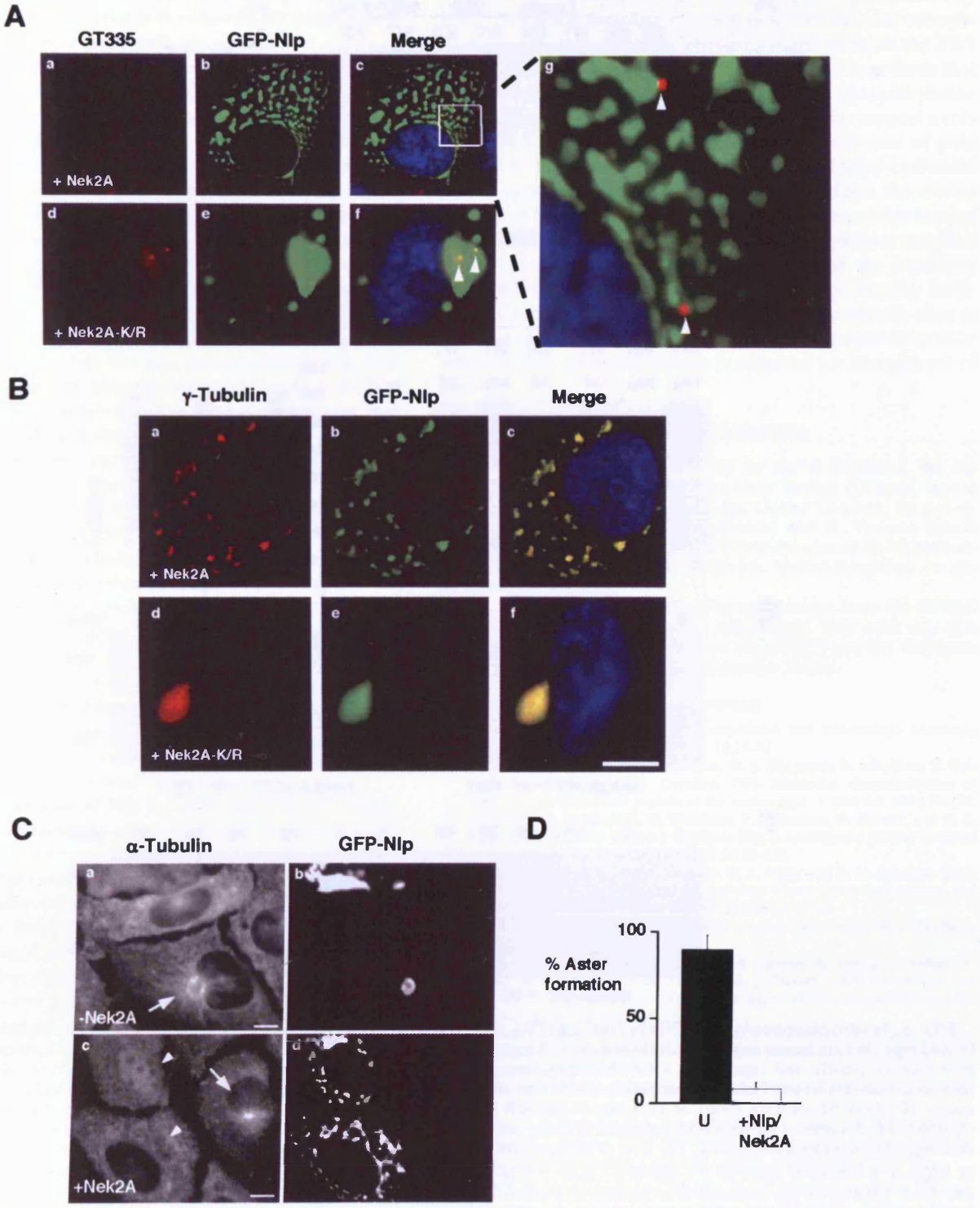

FIG. 8. Nek2 does not prevent association of Nlp with γ-tubulin. (A) U2OS cells were cotransfected with GFP-Nlp and either wild-type Myc-Nek2A (a to c) or Myc-Nek2A-K/R (d to f) before methanol fixation after 24 h and processing for immunofluorescence microscopy. Centrioles stained with GT335 (red), GFP signals (green), and merged images including DNA stained with Hoechst 33258 (blue) are shown. Magnification of the inset box in panel c (g) highlights the fact that GFP-Nlp fragments do not colocalize with centrioles (arrows), whereas centrioles do colocalize with the large GFP-Nlp assembly when coexpressed with kinase-inactive Nek2 (arrows, panel f). (B) Cells processed as for panel A were stained with anti-γ-tubulin antibodies (red). GFP signals (green) and merged images including DNA stained with Hoechst 33258 (blue) are shown. (C) Microtubule regrowth assays were performed on cells transfected with GFP-Nlp alone (a and b) or GFP-Nlp plus Nek2A (c and d). Untransfected cells contain small radial microtubule asters emanating from the centrosome (c, arrow). Cells transfected with GFP-Nlp alone have large microtubule asters surrounding the single GFP-Nlp assembly (a, arrow). However, cells containing fragmented GFP-Nlp lack any such aster (c, arrowheads). (D) Histogram indicating the percentage of untransfected cells (U) with microtubule asters compared to cells cotransfected with GFP-Nlp and Nek2A. Scale bars, 10 μm.

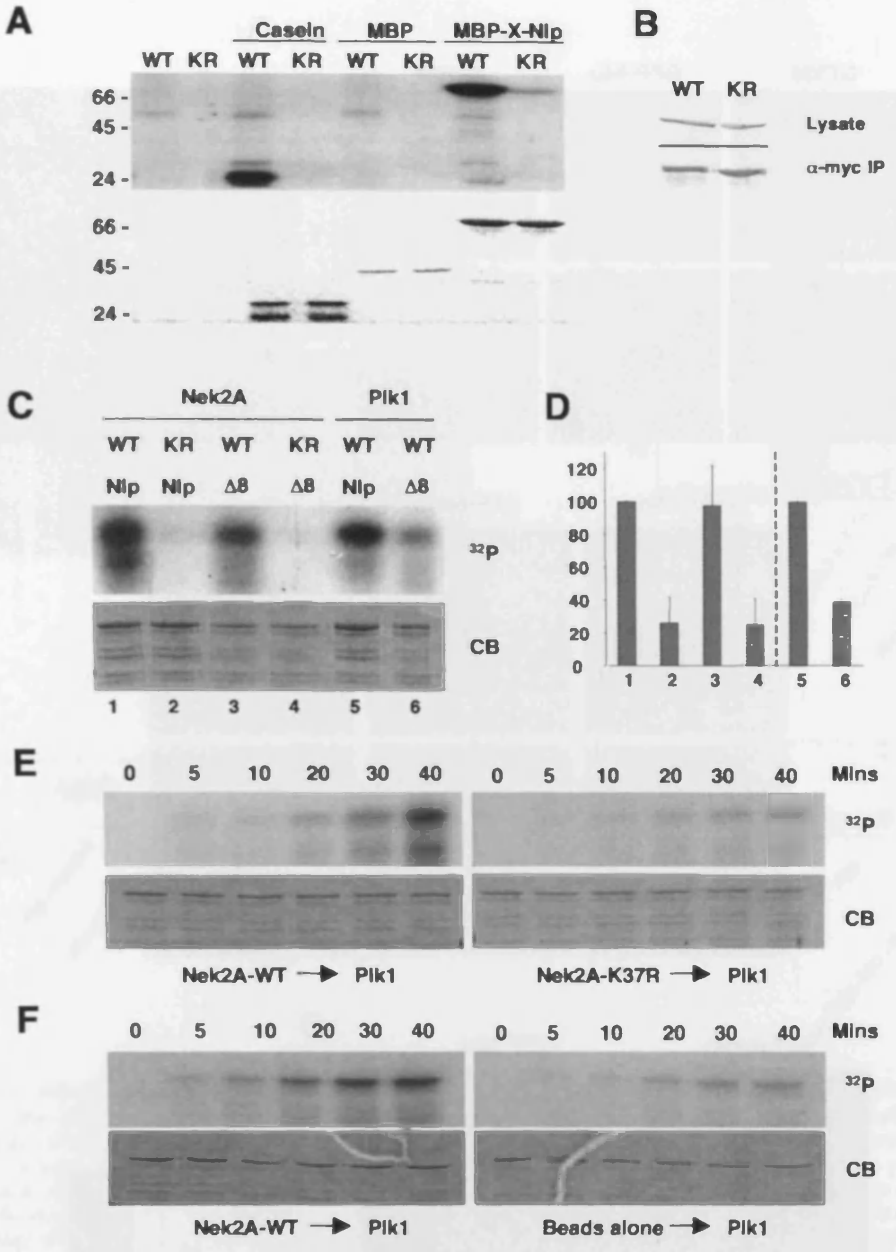

FIG. 9. In vitro phosphorylation of Nlp by Nek2 and Plk1. (A) Purified MBP-X-Nlp$_{262-552}$, MBP alone, and casein were phosphorylated in vitro by wild-type (WT) or kinase-inactive (KR) human Nek2A expressed in insect cells. Samples were separated by SDS-PAGE, stained with Coomassie blue (bottom panel), and exposed to autoradiography (top panel). (B) Western blots indicating equal expression (anti-Myc, top panel) and immunoprecipitation (anti-Nek2, bottom panel) of wild-type and kinase-inactive Myc-Nek2A proteins from transfected HeLa cells for use in kinase assays. (C) GST-Nlp-N-term (Nlp) or GST-Nlp-N-term-Δ8 (Δ8) was phosphorylated in vitro with Nek2A kinases immunoprecipitated from transfected HeLa cells or purified Plk1 expressed in insect cells, as indicated. (D) ^{32}P incorporation into the Nlp proteins as shown in panel C was determined by scintillation counting. The level of phosphorylation of the GST-Nlp-N-term protein by wild-type Nek2 (1–4) and Plk1 (5, 6) was set as 100%. The histogram presents the average of three independent experiments. (E). GST-Nlp-N-term was incubated with either wild-type (left panels) or kinase-inactive (right panels) immunoprecipitated Nek2A for 40 min in the presence of unlabeled ATP. Purified Plk1 was then added together with [γ-^{32}P]ATP and samples were taken at the times indicated before separation by SDS-PAGE. Gels were stained with Coomassie blue (CB) and exposed to autoradiography (^{32}P). In each of five independent experiments, the phosphorylation of Nlp by Plk1 was always greater after incubation with wild-type compared to kinase-inactive Nek2A. (F) Kinase assays were performed as in panel E except that phosphorylation of Nlp by Plk1 was assayed after incubation with either immunoprecipitated Nek2A (left panels) or protein G-Sepharose beads alone (right panels).

Nlp at the centrosome remains a theoretical possibility, our results strongly support a change in localization as being the main cause of loss of Nlp staining at mitotic spindle poles. In this respect, Nlp localization is regulated very similarly to another centriolar protein, C-Nap1, which is also a substrate of Nek2 (16, 34). Interestingly, Nlp was not present in cytoplasmic extracts of either mitotic or interphase eggs, nor was it detected on the basal bodies of sperm either before or after

incubation in egg extract. Thus, it appears that Nlp is not a core component of basal bodies, nor is it required for microtubule organization during early embryonic development.

Nlp is a novel substrate of the Nek2 kinase. The specific displacement of Nlp from the centrosome at the G_2/M transition makes it a likely target for regulation by cell cycle-dependent phosphorylation. Indeed, there is good evidence that Nlp is a target for the Plk1 kinase and that Plk1 activity can regulate its association with the centrosome (3). However, recent studies have revealed that recognition of certain substrates by Plk1 is promoted by prior phosphorylation by other kinases (11), and here we show that Nlp is also a target for the Nek2 centrosomal kinase. Nlp can interact with and be phosphorylated by Nek2 both in vitro and in vivo. Meanwhile, overexpression of active Nek2, like Plk1, displaces both endogenous and recombinant Nlp from the interphase centrosome. The fact that Nek2 can equally phosphorylate and displace the Nlp mutant lacking Plk1 phosphorylation sites demonstrates that Nek2 is targeting different sites to Plk1.

Intriguingly, while Nek2 perturbs the association of Nlp with the centrosome, it does not appear to interfere with the interaction of Nlp with γ-tubulin. As a result, cells with fragmented Nlp assemblies fail to nucleate radial microtubule asters because the bulk of the γ-tubulin ring complexes is associated with noncentrosomal recombinant Nlp. Previously, we reported that overexpressing Nek2 alone also leads to loss of γ-tubulin from the centrosome and failure to organize radial microtubule arrays (17). At the time, we interpreted this as a result of dispersal of centrosome structure, but our current study highlights the possibility that this is the direct result of displacement of endogenous Nlp. Certainly, our results on the effect of Nek2 overexpression on microtubule organization are consistent whether Nlp is coexpressed or not.

Coordinate regulation of Nlp by Nek2 and Plk1. Recognition of mitotic substrates by polo-like kinases is promoted by direct interaction between the substrate and polo box motifs in the C-terminal noncatalytic domain of the kinase (46). Plk1 contains two highly conserved polo boxes that together comprise a polo box domain that is important for subcellular localization and autoinhibition. Structural studies have revealed that each polo box motif forms a single six-stranded β-sheet, which come together in the polo box domain to form a 12-stranded beta sandwich (4, 10). This acts as a novel recognition motif for phosphorylated peptides, which sit in the middle of the sandwich.

Degenerate-peptide library screening revealed that the optimal target site for the polo box domain was S-p(S/T) (11). Thus, tight interaction of Plk1 with its substrates is stimulated by their prior phosphorylation on serine or threonine in this consensus. Both Cdk1 and Plk1 have been proposed as priming kinases for Plk1 (11, 41), with two of the putative Plk1 sites identified in Nlp being within a polo box domain recognition consensus (S88 and T161). Our data, however, raise the possibility that Nek2 is a third priming kinase for Plk1. First, kinase-dead Nek2A interfered with the ability of Plk1 to displace Nlp from the large aggregates around the centrosome but not vice versa, putting Nek2 upstream of Plk1 in the regulation of Nlp. Second, expression of kinase-dead Nek2A led to a significant increase in the amount of endogenous Nlp present on mitotic spindle poles. Third, incubation of Nlp with Nek2 in vitro stimulated the level of Nlp phosphorylation by Plk1. This study therefore not only describes the first example of a centrosomal substrate phosphorylated by both the Plk1 and Nek2 kinases in vitro, but also supports the hypothesis that phosphorylation of Nlp by Nek2 promotes its phosphorylation by Plk1. Importantly, studies in fission yeast also support a role for NIMA-related kinases in promoting recruitment of polo kinases to the spindle pole body (SPB), the fungal equivalent of the centrosome (20). Overexpression of Fin1, the closest relative of Nek2 in *S. pombe*, leads to premature recruitment of the polo kinase Plo1 to the SPB. There is no evidence that Plo1 can be phosphorylated by Fin1, leaving open the possibility that Fin1 is phosphorylating SPB components, thereby facilitating the binding of Plo1. The goal now is to identify sites in Nlp that are phosphorylated by the Nek2 kinase and determine whether their phosphorylation is required for recruitment of Plk1.

ACKNOWLEDGMENTS

We thank all members of the lab for useful discussion. We are grateful to the National Institute for Basic Biology (Okazaki, Japan) and the MRC Geneservice (Cambridge, United Kingdom) for providing ESTs, B. Edde (Montpellier, France) and H. Yamano (South Mimms, United Kingdom) for GT335 and *Xenopus* cyclin B2 antibodies, respectively, and D. Stott (Warwick, United Kingdom) for the pGAD-MakV plasmid.

J.R. and J.E.B. were supported by studentships from the BBSRC and Millennium Pharmaceuticals, respectively. This work was also supported by grants to A.M.F. from the BBSRC and the Wellcome Trust. A.M.F. is a Lister Institute Research Fellow.

REFERENCES

1. **Bornens, M.** 2002. Centrosome composition and microtubule anchoring mechanisms. Curr. Opin. Cell Biol. **14**:25–34.
2. **Bouckson-Castaing, V., M. Moudjou, D. J. Ferguson, S. Mucklow, Y. Belkaid, G. Milon, and P. J. Crocker.** 1996. Molecular characterization of ninein, a new coiled-coil protein of the centrosome. J. Cell Sci. **109**:179–190.
3. **Casenghi, M., P. Meraldi, U. Weinhart, P. I. Duncan, R. Korner, and E. A. Nigg.** 2003. Polo-like kinase 1 regulates Nlp, a centrosome protein involved in microtubule nucleation. Dev. Cell **5**:113–125.
4. **Cheng, K.-Y., E. D. Lowe, J. Sinclair, E. A. Nigg, and L. N. Johnson.** 2003. The crystal structure of the human polo-like kinase-1 polo box domain and its phospho-peptide complex. EMBO J. **22**:5757–5768.
5. **Compton, D. A.** 2000. Spindle assembly in animal cells. Annu. Rev. Biochem. **69**:95–114.
6. **Dictenberg, J. B., W. Zimmerman, C. A. Sparks, A. Young, C. Vidair, Y. Zheng, W. Carrington, F. S. Fay, and S. J. Doxsey.** 1998. Pericentrin and g-tubulin form a protein complex and are organized into a novel lattice at the centrosome. J. Cell Biol. **141**:163–174.
7. **do Carmo Avides, M., and D. M. Glover.** 1999. Abnormal spindle protein, Asp, and the integrity of mitotic centrosomal microtubule organizing centers. Science **283**:1733–1735.
8. **Doxsey, S.** 2001. Re-evaluating centrosome function. Nat. Revs: Mol. Cell. Biol. **2**:688–698.
9. **Durfee, T., K. Becherer, P.-L. Chen, S.-H. Yeh, Y. Yang, A. E. Kilburn, W.-H. Lee, and S. J. Elledge.** 1993. The retinoblastoma protein associates with the protein phosphatase type 1 catalytic subunit. Genes Dev. **7**:555–569.
10. **Elia, A. E., P. Rellos, L. F. Haire, J. W. Chao, F. J. Ivins, K. Hoepker, D. Mohammad, L. C. Cantley, S. J. Smerdon, and M. B. Yaffe.** 2003b. The molecular basis for phosphodependent substrate targeting and regulation of Plks by the Polo-box domain. Cell **115**:83–95.
11. **Elia, A. E. H., L. C. Cantley, and M. B. Yaffe.** 2003a. Proteomic screen finds pSer/pThr-binding domain localizing Plk1 to mitotic substrates. Science **299**: 1228–1231.
12. **Faragher, A. J., and A. M. Fry.** 2003. Nek2 kinase stimulates centrosome disjunction and is required for formation of bipolar mitotic spindles. Mol. Biol. Cell **14**:2876–2889.
13. **Fry, A. M.** 2002. The Nek2 protein kinase: a novel regulator of centrosome structure. Oncogene **21**:6184–6194.
14. **Fry, A. M., L. Arnaud, and E. A. Nigg.** 1999. Activity of the human centrosomal kinase, Nek2, depends upon an unusual leucine zipper dimerization motif. J. Biol. Chem. **274**:16304–16310.
15. **Fry, A. M., P. Descombes, C. Twomey, R. Bacchieri, and E. A. Nigg.** 2000.

The NIMA related kinase X Nek2B is required for efficient assembly of the zygotic centrosome in *Xenopus laevis*. J. Cell Sci. **113**:1973–1984.
16. **Fry, A. M., T. Mayor, P. Meraldi, Y.-D. Stierhof, K. Tanaka, and E. A. Nigg.** 1998b. C-Nap1, a novel centrosomal coiled-coil protein and candidate substrate of the cell cycle-regulated protein kinase Nek2. J. Cell Biol. **141**:1563–1574.
17. **Fry, A. M., P. Meraldi, and E. A. Nigg.** 1998a. A centrosomal function for the human Nek2 protein kinase, a member of the NIMA-family of cell cycle regulators. EMBO J. **17**:470–481.
18. **Fry, A. M., and E. A. Nigg.** 1997. Characterization of mammalian NIMA-related kinases. Methods Enzymol. **283**:270–282.
19. **Golsteyn, R. M., K. E. Mundt, A. M. Fry, and E. A. Nigg.** 1995. Cell cycle regulation of the activity and subcellular localization of Plk1, a human protein kinase implicated in mitotic spindle function. J. Cell Biol. **129**:1617–1628.
20. **Grallert, A., and I. M. Hagan.** 2002. *S. pombe* NIMA-related kinase, Fin1, regulates spindle formation and an affinity of Polo for the SPB. EMBO J. **21**:3096–3107.
21. **Hames, R. S., and A. M. Fry.** 2002. Alternative splice variants of the human centrosomal kinase Nek2 exhibit distinct patterns of expression in mitosis. Biochem. J. **361**:77–85.
22. **Hames, R. S., S. L. Wattam, H. Yamano, R. Bacchieri, and A. M. Fry.** 2001. APC/C-mediated destruction of the centrosomal kinase Nek2A occurs in early mitosis and depends upon a cyclin A type D box. EMBO J. **20**:7137–7147.
23. **Hartman, J. J., J. Mahr, K. McNally, K. Okawa, A. Iwamatsu, S. Thomas, S. Cheesman, J. Heuser, R. D. Vale, and F. J. McNally.** 1998. Katanin, a microtubule-severing protein, is a novel AAA ATPase that targets to the centrosome using a WD40-containing subunit. Cell **93**:277–287.
24. **Heald, R., R. Tournebize, A. Habermann, E. Karsenti, and A. Hyman.** 1997. Spindle assembly in Xenopus egg extracts: respective roles of centrosomes and microtubule self-organization. J. Cell Biol. **138**:615–628.
25. **James, P., J. Halladay, and E. A. Craig.** 1996. Genomic libraries and a host strain designed for highly efficient two-hybrid selection in yeast. Genetics **144**:1425–1436.
26. **Jang, Y., C. Lin, S. Ma, and R. L. Erikson.** 2002. Functional studies on the role of the C-terminal domain of mammalian polo-like kinase. Proc. Natl. Acad. Sci. U.S.A. **99**:1984–1989.
27. **Job, D., O. Valiron, and B. Oakley.** 2003. Microtubule nucleation. Curr. Opin. Cell Biol. **15**:111–117.
28. **Kawaguchi, S., and Y. Zheng.** 2004. Characterization of a Drosophila centrosome protein CP309 that shares homology with kendrin and CG-NAP. Mol. Biol. Cell **15**:37–45.
29. **Keating, T. J., and G. G. Borisy.** 1999. Centrosomal and non-centrosomal microtubules. Biol. Cell **91**:321–329.
30. **Keating, T. J., and G. G. Borisy.** 2000. Immunostructural evidence for the template mechanism of microtubule nucleation. Nat. Cell Biol. **2**:352–357.
31. **Kelm, O., M. Wind, W. D. Lehmann, and E. A. Nigg.** 2002. Cell cycle-regulated phosphorylation of the *Xenopus* polo-like kinase Plx1. J. Biol. Chem. **277**:25247–25256.
32. **Keryer, G., B. Di Fiore, C. Celati, K. F. Lechtreck, M. Mogensen, A. Delouvee, P. Lavia, M. Bornens, and A.-M. Tassin.** 2003. Part of Ran is associated with AKAP450 at the centrosome: involvement in microtubule-organizing activity. Mol. Biol. Cell **14**:4260–4271.
33. **Lupas, A.** 1996. Prediction and analysis of coiled-coil structures. Methods Enzymol. **266**:513–525.
34. **Mayor, T., U. Hacker, Y.-D. Stierhof, and E. A. Nigg.** 2002. The mechanism regulating dissociation of the centrosomal protein C-Nap1 from mitotic spindle poles. J. Cell Sci. **115**:3275–3284.
35. **Mayor, T., K. Tanaka, Y.-D. Stierhof, A. M. Fry, and E. A. Nigg.** 2000. The centrosomal protein C-Nap1 displays properties supporting a role in cell cycle-regulated centrosome cohesion. J. Cell Biol. **151**:837–846.
36. **McIntosh, J. R., E. L. Grishchuk, and R. R. West.** 2002. Chromosome-microtubule interactions during mitosis. Annu. Rev. Cell Dev. Biol. **18**:193–219.
37. **Meraldi, P., R. Honda, and E. A. Nigg.** 2002. Aurora-A overexpression reveals tetraploidization as a major route to centrosome amplification in p53−/− cells. EMBO J. **21**:483–492.
38. **Meraldi, P., and E. A. Nigg.** 2001. Centrosome cohesion is regulated by a balance of kinase and phosphatase activities. J. Cell Sci. **114**:3749–3757.
39. **Mogensen, M. M., A. Malik, M. Piel, V. Bouckson-Castaing, and M. Bornens.** 2000. Microtubule minus-end anchorage at centrosomal and non-centrosomal sites: the role of ninein. J. Cell Sci. **113**:3013–3023.
40. **Moritz, M., M. B. Braunfeld, V. Guenebaut, J. Heuser, and D. A. Agard.** 2000. Structure of the γ-tubulin ring complex: a template for microtubule nucleation. Nat. Cell Biol. **2**:365–370.
41. **Neef, R., C. Preisinger, J. Sutcliffe, R. Kopajtich, E. A. Nigg, T. U. Mayer, and F. A. Barr.** 2003. Phosphorylation of mitotic kinesin-like protein 2 by polo-like kinase 1 is required for cytokinesis. J. Cell Biol. **162**:863–875.
42. **Nigg, E. A.** 2002. Centrosome aberrations: cause or consequence of cancer progression? Nat. Rev. Cancer **2**:815–825.
43. **Nigg, E. A.** 2001. Mitotic kinases as regulators of cell division and its checkpoints. Nat. Rev. Mol. Cell Biol. **2**:21–32.
44. **Piel, M., P. Meyer, A. Khodjakov, C. L. Rieder, and M. Bornens.** 2000. The respective contributions of the mother and daughter centrioles to centrosome activity and behaviour in vertebrate cells. J. Cell Biol. **149**:317–329.
45. **Quintyne, N. J., S. R. Gill, D. M. Eckley, C. L. Crego, D. A. Compton, and T. A. Schroer.** 1999. Dynactin is required for microtubule anchoring at fibroblast centrosomes. J. Cell Biol. **147**:321–334.
46. **Reynolds, N., and H. Ohkura.** 2003. Polo boxes form a single functional domain that mediates interactions with multiple proteins in fission yeast polo kinase. J. Cell Sci. **116**:1377–1387.
47. **Schroer, T. A.** 2001. Microtubules don and doff their caps: dynamic attachments at plus and minus ends. Curr. Opin. Cell Biol. **13**:92–96.
48. **Seong, Y.-S., K. Kamijo, J.-S. Lee, E. Fernandez, R. Kuriyama, T. Miki, and K. S. Lee.** 2002. A spindle checkpoint arrest and a cytokinesis failure by the dominant-negative polo-box domain of Plk1 in U-2 OS cells. J. Biol. Chem. **277**:32282–32293.
49. **Song, S., T. Z. Grenfell, S. Garfield, R. L. Erikson, and K. S. Lee.** 2000. Essential function of the polo box of Cdc5 in subcellular localization and induction of cytokinetic structures. Mol. Cell. Biol. **20**:286–298.
50. **Takahashi, M., A. Yamagiwa, T. Nishimura, H. Mukai, and Y. Ono.** 2002. Centrosomal proteins CG-NAP and kendrin provide microtubule nucleation sites by anchoring gamma-tubulin ring complex. Mol. Biol. Cell **13**:3235–3245.
51. **Twomey, C., S. L. Wattam, M. R. Pillai, J. Rapley, J. E. Baxter, and A. M. Fry.** 2004. Nek2B stimulates zygotic centrosome assembly in *Xenopus laevis* in a kinase-independent manner. Dev. Biol. **265**:384–398.
52. **Uto, K., N. Nakajo, and N. Sagata.** 1999. Two structural variants of Nek2 kinase, termed Nek2A and Nek2B, are differentially expressed in *Xenopus* tissues and development. Dev. Biol. **208**:456–464.
53. **Wiese, C., and Y. Zhang.** 2000. A new function for the gamma-tubulin ring complex as a microtubule minus-end cap. Nat. Cell Biol. **2**:358–364.

Available online at www.sciencedirect.com
SCIENCE DIRECT®
Developmental Biology 265 (2004) 384–398
DEVELOPMENTAL BIOLOGY
www.elsevier.com/locate/ydbio

Nek2B stimulates zygotic centrosome assembly in *Xenopus laevis* in a kinase-independent manner

Ciara Twomey,[1] Samantha L. Wattam, Meenu R. Pillai,[2] Joe Rapley, Joanne E. Baxter, and Andrew M. Fry*

Department of Biochemistry, University of Leicester, University Road, Leicester LE1 7RH, UK

Received for publication 15 August 2003, accepted 1 October 2003

Abstract

Pronuclear migration and formation of the first mitotic spindle depend upon assembly of a functional zygotic centrosome. For most animals, this involves both paternal and maternal contributions as sperm basal bodies are converted into centrosomes competent for microtubule nucleation through recruitment of egg proteins. Nek2B is a vertebrate NIMA-related protein kinase required for centrosome assembly, as its depletion from egg extracts delays microtubule aster formation from sperm basal bodies. Using *Xenopus* as a model system, we now show that protein expression of Nek2B begins during mid-oogenesis and increases further upon oocyte maturation. This is regulated, at least in part, at the level of protein translation. Nek2B protein is weakly phosphorylated in mitotic egg extracts but its recruitment to the sperm basal body, which occurs independently of its kinase activity, stimulates its phosphorylation, possibly through sequestration from a phosphatase present in mitotic egg cytoplasm. Importantly, although Nek2B is not required to organize acentrosomal microtubule asters, we show that addition of either active or kinase-dead recombinant Nek2B can restore centrosome assembly in a dose-dependent manner to a depleted extract. These results support a model in which maternal Nek2B acts to promote assembly of a functional zygotic centrosome in a kinase-independent manner.

Keywords: Nek2; Cell cycle; Centrosome; Centriole; Mitosis; Oogenesis; Kinase; NIMA; *Xenopus*

Introduction

The centrosome plays a critical role in the development of metazoans. It represents the major site of microtubule nucleation in cells and orchestrates many of the microtubule-based processes that occur within the cytoplasm (Doxsey, 2001). The centrosome also plays a dominant role in mitosis directing formation of the bipolar microtubule-based spindle upon which chromosomes are segregated (Heald et al., 1997). Surprisingly, experimental elimination of the centrosome does not prevent bipolar spindle formation indicating that cells have additional pathways that can lead to spindle bipolarity (Khodjakov et al., 2000). These are likely to include Ran-GTP stimulated microtubule nucleation near the chromatin and focusing of microtubule minus ends by motor proteins capable of crosslinking microtubules (reviewed in Dasso, 2001; Wittmann et al., 2001). However, spindle formation in the absence of centrosomes could lead to incorrectly positioned spindles due to lack of centrosome-nucleated astral microtubules which anchor the spindle in the correct axis by attachment to the cell cortex. This may not be critical in cultured cells but is likely to be of the utmost importance during the many asymmetric and oriented cell divisions that are necessary for the development of multicellular organisms.

Although spindle formation can occur without centrosomes, their removal by experimental means interferes with other aspects of cell cycle progression, including cytokinesis and entry into S phase (Hinchcliffe et al., 2001; Khodjakov and Rieder, 2001; Piel et al., 2001). Furthermore, in a classic experiment, it was shown that parthenogenetic development can be induced in the African clawed toad, *X. laevis*, simply by injection of a centrosome into an unfertilized egg (Maller et al., 1976). Activating eggs by pricking, without addition of centrosomes, leads to contractile waves and MPF oscil-

* Corresponding author. Fax: +44-116-252-3369.
E-mail address: amf5@le.ac.uk (A.M. Fry).
[1] Current address: Millennium Pharmaceuticals Limited, Granta Park, Great Abington, Cambridge CB1 6ET, UK.
[2] Current address: Department of Immunology, Institute for Animal Health, Ash Road, Pirbright, Surrey GU24 0NF, UK.

0012-1606/$ - see front matter © 2003 Elsevier Inc. All rights reserved.
doi:10.1016/j.ydbio.2003.10.001

lations, but not cleavage. Hence, the centrosome is essential for cleavage of early embryos.

The centrosome is composed of two centrioles surrounded by pericentriolar material (Doxsey, 2001). Each centriole is a 200 nm (diameter) by 400 nm (height) cylinder made up of nine sets of triplet microtubules that do not undergo the dynamic growth and shrinkage typical of cytoplasmic microtubules (Marshall, 2001). Structurally, centrioles are almost identical to basal bodies, which are found at the base of cilia and flagella (Preble et al., 2000). Indeed, the older of the two centrioles, called the mother, is often found at the surface of cultured cells subtending the primary cilium. These two types of structure are also interchangeable. In the unicellular biflagellate *Chlamydomonas reinhardtii*, the basal bodies responsible for production of the flagella are withdrawn into the cell as it enters mitosis and used to generate the two poles of the spindle (Gaffal, 1988; Johnson and Porter, 1968). Furthermore, in many organisms, it is the sperm basal body, which nucleates the flagellar microtubules, that is converted into a centrosome and acts as the microtubule-organizing centre in the fertilized zygote. This is essential both for pronuclear migration and generation of the first mitotic spindle (Schatten, 1994).

Molecular dissection of the centrosome has now identified many of its structural and regulatory components. Those which appear to be tightly associated with centrioles include Nek2, a cell cycle-regulated serine–threonine kinase, and a proposed substrate of the Nek2 kinase called C-Nap1 (Fry et al., 1998a,b). Both proteins have been localized by immunoelectron microscopy to the proximal ends of the two centrioles. The proximal end of a centriole, like that of a basal body, contains a cartwheel structure with a central hub and spokes. Connecting fibers have been detected running between the proximal ends of centrioles as well as between the pair of basal bodies in *Chlamydomonas* (Paintrand et al., 1992; Preble et al., 2000). Functional studies have implicated the Nek2 and C-Nap1 proteins in regulating this intercentriolar connection during cell cycle progression (Fry, 2002). Furthermore, introduction of kinase-inactive Nek2 constructs into human cells or *Xenopus* embryos causes centrosome dispersal implying an additional function for Nek2 in maintenance of an intact centrosome structure (Fry et al., 1998a; Uto and Sagata, 2000).

In vertebrates, two alternative splice variants of the Nek2 kinase have been detected which can both localize to the centrosome (Hames and Fry, 2002; Uto et al., 1999). Nek2A is a 48-kDa protein with an N-terminal kinase domain, a leucine zipper which promotes homodimerization and trans-autophosphorylation (Fry et al., 1999), and a C-terminal regulatory domain containing motifs for APC/C-mediated destruction and interaction with PP1c, the catalytic subunit of protein phosphatase 1 (Hames et al., 2001; Helps et al., 2000). Nek2B is a 44-kDa protein and differs from Nek2A in its extreme C-terminus. It retains the catalytic domain and leucine zipper, but lacks the destruction and PP1c binding motifs. In adult human cells, both splice variants are detected although Nek2A is consistently more abundant (Hames and Fry, 2002). However, in eggs and early embryos of *Xenopus*, only Nek2B is detected (Fry et al., 2000; Uto et al., 1999).

In a previous set of experiments, we showed that endogenous Nek2B is rapidly recruited to the basal body of sperm upon incubation in a mitotic egg extract (Fry et al., 2000). This recruitment precedes the appearance of an astral array of microtubules around the site of the basal body indicative of functional centrosome assembly. Furthermore, removal of Nek2B from the egg extract delayed recruitment of γ-tubulin and the appearance of a microtubule aster. Hence, Nek2 appeared to play an important role in assembly, as well as maintenance, of the centrosome structure. However, reconstitution of the depleted extracts to prove the requirement for Nek2 had not been done. We have now extended these earlier studies by investigating the precise expression and phosphorylation pattern of Nek2 splice variants in *Xenopus* oocytes, eggs and sperm. We also present reconstitution experiments using recombinant proteins that show that Nek2 can restore efficient assembly of a functional centrosome to a depleted extract independently of its kinase activity.

Materials and methods

Preparation of eggs, sperm and oocytes

CSF and activated (interphase) egg extracts and demembranated sperm were prepared as previously described (Desai et al., 1999; Murray, 1991). Collection and staging of oocytes were done according to Smith et al. (1991). To induce maturation, oocytes were treated with 5 μg/ml progesterone (prepared in high-grade 100% ethanol and filter sterilized) for 12 h. Germinal vesicle breakdown was usually observed after 4–5 h. Oocyte extracts were prepared according to Gerhart et al. (1984) and protein concentrations determined using BCA protein assay reagent (Pierce). For immunodepletion of egg extracts, magnetic protein A beads (Dynal) were pre-coated with R81 α-X-Nek2 purified IgGs (Fry et al., 2000) or rabbit IgGs at 1 μg per microlitre of beads by 30-min incubation on ice. After extensive washing first in sodium hydrogen phosphate buffer, then in CSF-XB buffer (0.1 M KCl, 1 mM $MgCl_2$, 0.1 mM $CaCl_2$, 50 mM sucrose, 10 mM HEPES pH 7.7, 5 mM EGTA), beads were gently resuspended in egg extract (equal volume of bead to extract) and incubated on ice for a further 30 min. Beads were concentrated on a magnetic rack (Dynal) and the extract collected by pipette. To obtain dialysed egg extract, dialysis was performed for 4 h at 4 °C against a large volume of CSF-XB using a 2.5 kDa cut-off Slide-A-Lyzer cassette (Pierce) according to manufacturer's instructions. High-speed supernatants for glycerol gradient analysis were

obtained by centrifugation of CSF extracts at 100 K rpm for 30 min.

Protein electrophoresis and Western blotting

Proteins were resolved on 12% SDS-polyacrylamide gels. For increased resolution, gels were run according to Andersen et al. (1973) with ProSieve 50 gel solution (FMC Bioproducts) where indicated. For immunoblotting, proteins were transferred to nitrocellulose membrane by semidry blotting. Primary antibodies used for immunoblotting were R81 α-X-Nek2-purified IgGs (5.0 μg/ml; Fry et al., 2000) or anti-His antibodies (1:3000 dilution; Sigma). Proteins were detected using alkaline phosphatase-conjugated anti-rabbit or anti-mouse secondary antibodies (1:7500 dilution; Promega).

Protein phosphatase treatment

Protein phosphatase treatment was performed with λ protein phosphatase (New England Biolabs Inc.) as described (Sharp-Baker and Chen, 2001). In brief, sperm were washed twice in λPP buffer (50 mM Tris, pH 7.5, 2 mM $MnCl_2$, 0.1 mM EDTA, 5 mM DTT, 0.01% Brij35) then incubated with 80 U λPP in λPP buffer for 30 min at 30°C. Control reactions were incubated under the same conditions in the presence of 50 mM EDTA to inhibit λPP. Phosphatase treatment of egg extract was carried out by adding λPP

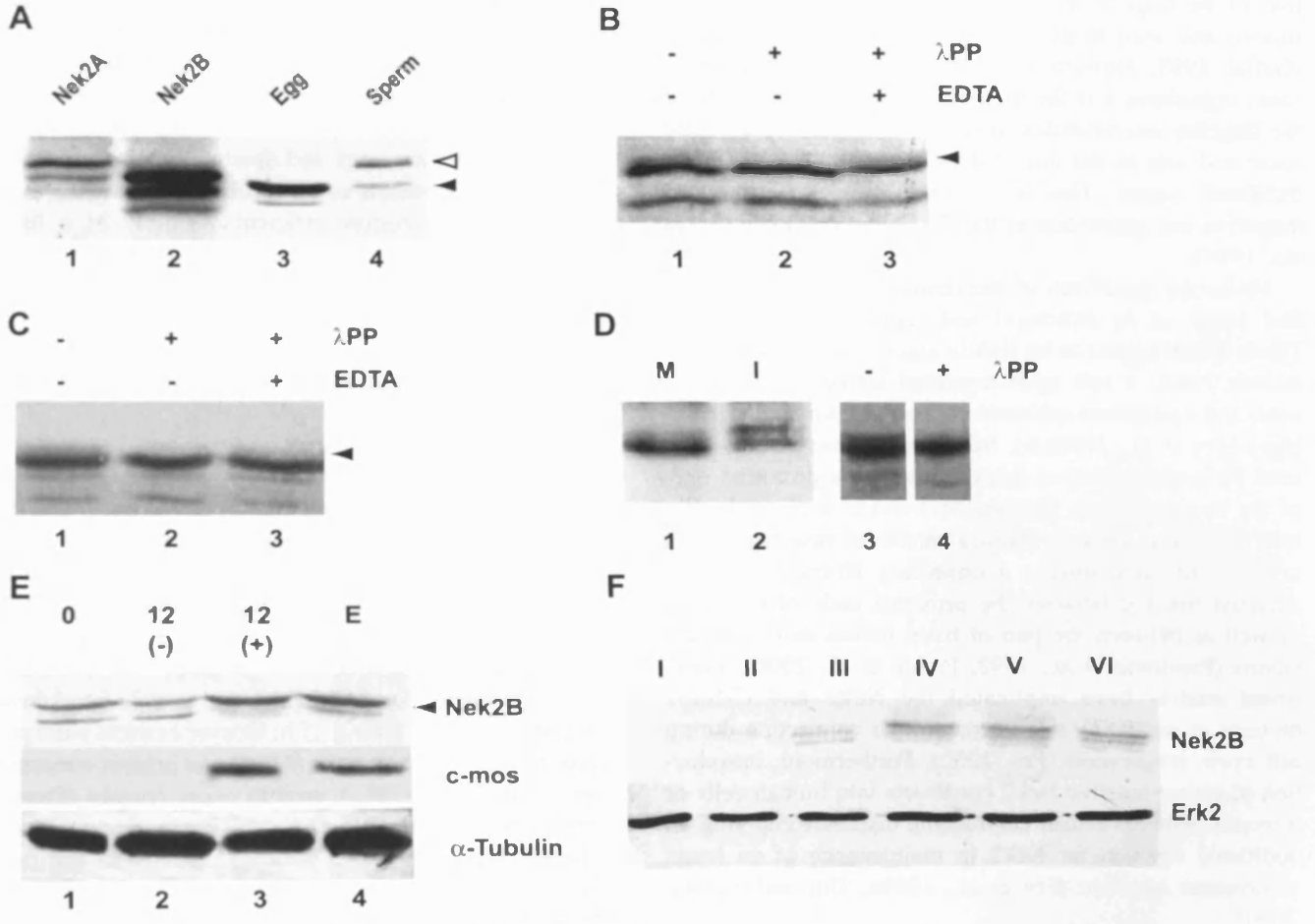

Fig. 1. Expression and phosphorylation of Nek2 splice variants in *Xenopus* sperm, eggs and oocytes. (A) *Xenopus* Nek2A (lane 1) and Nek2B (lane 2) proteins generated by in vitro translation as well as 0.5 μl *Xenopus* CSF egg extract (lane 3) and 3×10^6 *Xenopus* demembranated sperm (lane 4) were separated by 12% SDS-PAGE and immunoblotted with R81 (anti-*Xenopus* Nek2) purified antibodies. Nek2A (open arrowhead) and Nek2B (closed arrowhead) are detected in sperm, whereas only Nek2B is detected in egg. (B) Sperm preparations (9×10^6 per lane), either untreated (lane 1) or treated with λ protein phosphatase (λPP) in the absence (lane 2) or presence (lane 3) of EDTA, were separated on a ProSieve 12% acrylamide gel and immunoblotted with R81 antibodies. A faint smear (arrowhead) indicative of phosphorylation is detected above the Nek2A product that is specifically lost upon phosphatase treatment. (C) CSF egg extracts were subjected to the same examination as shown for sperm in B, indicating that Nek2B is also partially phosphorylated in mitotic egg cytoplasm. (D) CSF (M, lane 1) or interphase (I, lane 2) egg extracts were separated on a ProSieve gel and immunoblotted with R81 antibodies revealing that a more significant fraction of Nek2B is retarded in interphase than mitotic extract. Treatment of interphase extract with (lane 4) or without (lane 3) λPP confirms that this is also a result of phosphorylation. (E) Extracts were prepared from stage VI oocytes (lanes 1–3) or metaphase II-arrested eggs (lane 4), and Western blotted with antibodies against Nek2, c-mos and α-tubulin as indicated. Oocytes were either untreated (lane 1) or treated for 12 h with DMSO (lane 2) or progesterone (lane 3) to induce maturation. Maturation was confirmed not only by the expression of c-mos protein, but also by observation of germinal vesicle breakdown as indicated by white spot formation. (F) Equal amounts of protein were loaded from different stage oocytes (I–VI) and Western blotted for Nek2 and Erk2.

enzyme and buffer, and EDTA where noted, directly to egg and incubating as above. All reactions were stopped by the addition of protein sample buffer.

Generation of recombinant baculoviruses and protein expression

The pBlueBac:His-Nek2B and pBlueBac:His-Nek2B-K37R baculovirus transfer vectors were generated by subcloning the 1327 bp *Bam*HI–*Sal*I fragments from pBS:X-Nek2B and pBS:X-Nek2B-K37R, respectively, into the *Bam*HI–*Sal*I sites of pBlueBacHis2A (Invitrogen Corp.). Similarly, the pBlueBac:His-Nek2A and pBlueBac:His-Nek2A-K37R baculovirus transfer vectors were generated by subcloning the 1400 bp *Bam*HI–*Sal*I fragments from pBS:X-Nek2A and pBS:X-Nek2A-K37R, respectively, into the *Bam*HI–*Sal*I sites of pBlueBacHis2A (Invitrogen Corp.). Cell culture supernatant containing recombinant baculoviruses was generated by co-transfection of Bac-N-Blue DNA (Invitrogen Corp.) and the relevant transfer vectors into Sf9 (*Spodoptera frugiperda* insect larvae ovary) cells using the Insectin Plus™ Kit (Invitrogen Corp.) for 4–5 days and repeated rounds of viral amplification. Sf9 cells were cultured at 27°C in TC100 medium (Invitrogen Life Technologies) with 10% fetal calf serum and antibiotics (100 i.u./ml penicillin, 100 μg/ml strepto-

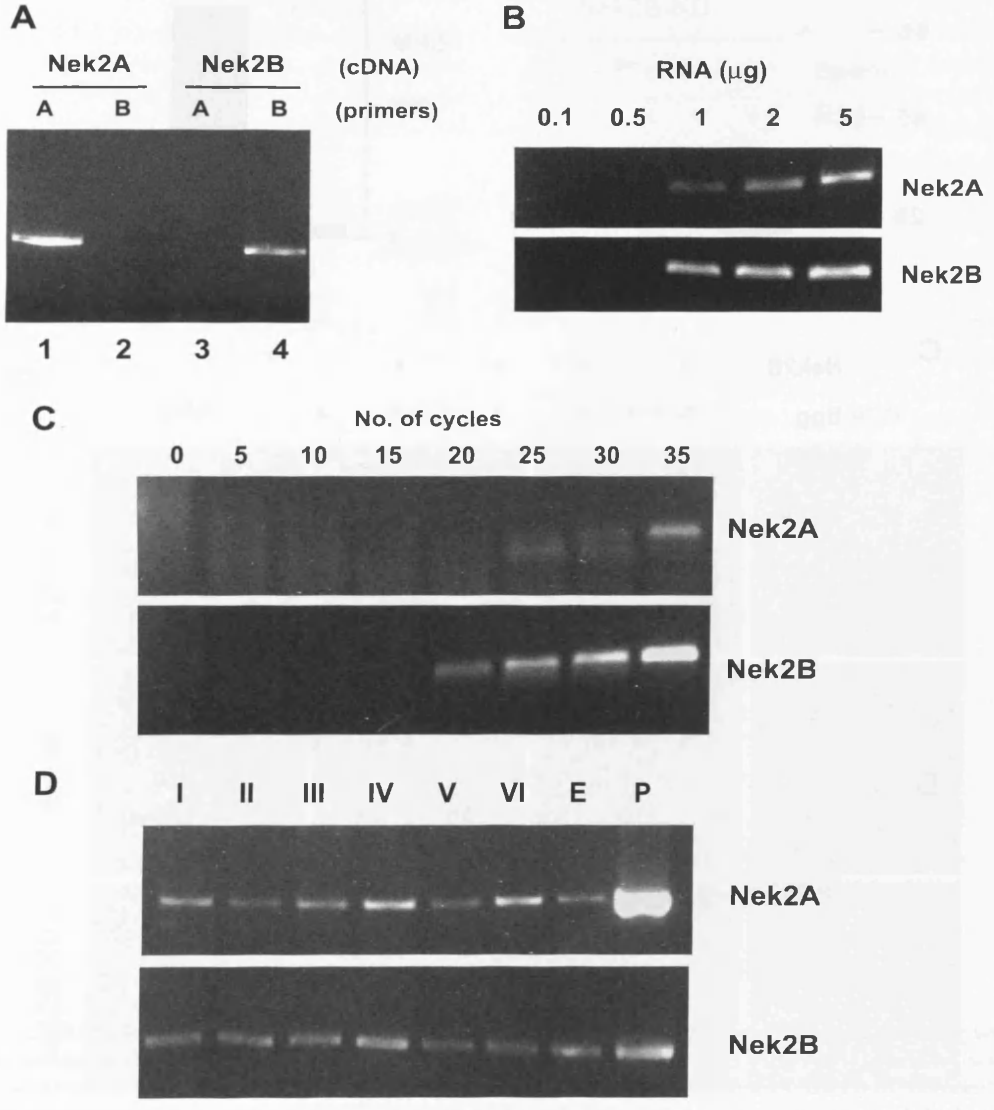

Fig. 2. Nek2A and Nek2B mRNAs are present in oocytes and eggs. (A) Primers specific for Nek2A (lanes 1 and 3) and Nek2B (lanes 2 and 4) were used in PCR reactions using a plasmid carrying either the Nek2A (lanes 1 and 2) or Nek2B (lanes 3 and 4) cDNA. (B) RT-PCR reactions were performed with Nek2A (upper panel) and Nek2B (lower panel) specific primers for 35 cycles using increasing amounts of total RNA as indicated. (C) RT-PCR reactions were performed with 5 μg total RNA with Nek2A (upper panel) and Nek2B (lower panel) specific primers. Aliquots were removed from the reaction after increasing numbers of cycles and visualized on ethidium bromide-stained agarose gels. (D) RNA was collected from stage I, II, III, IV, V and VI oocytes and eggs (E) and quantified by measuring the optical density at 260 nm. RT-PCR reactions were then performed with 2 μg total RNA for 35 cycles for Nek2A (upper panel) and with 1.5 μg total RNA and for 25 cycles for Nek2B (lower panel). As controls, PCR reactions were performed in parallel with plasmids (P) encoding the relevant cDNA.

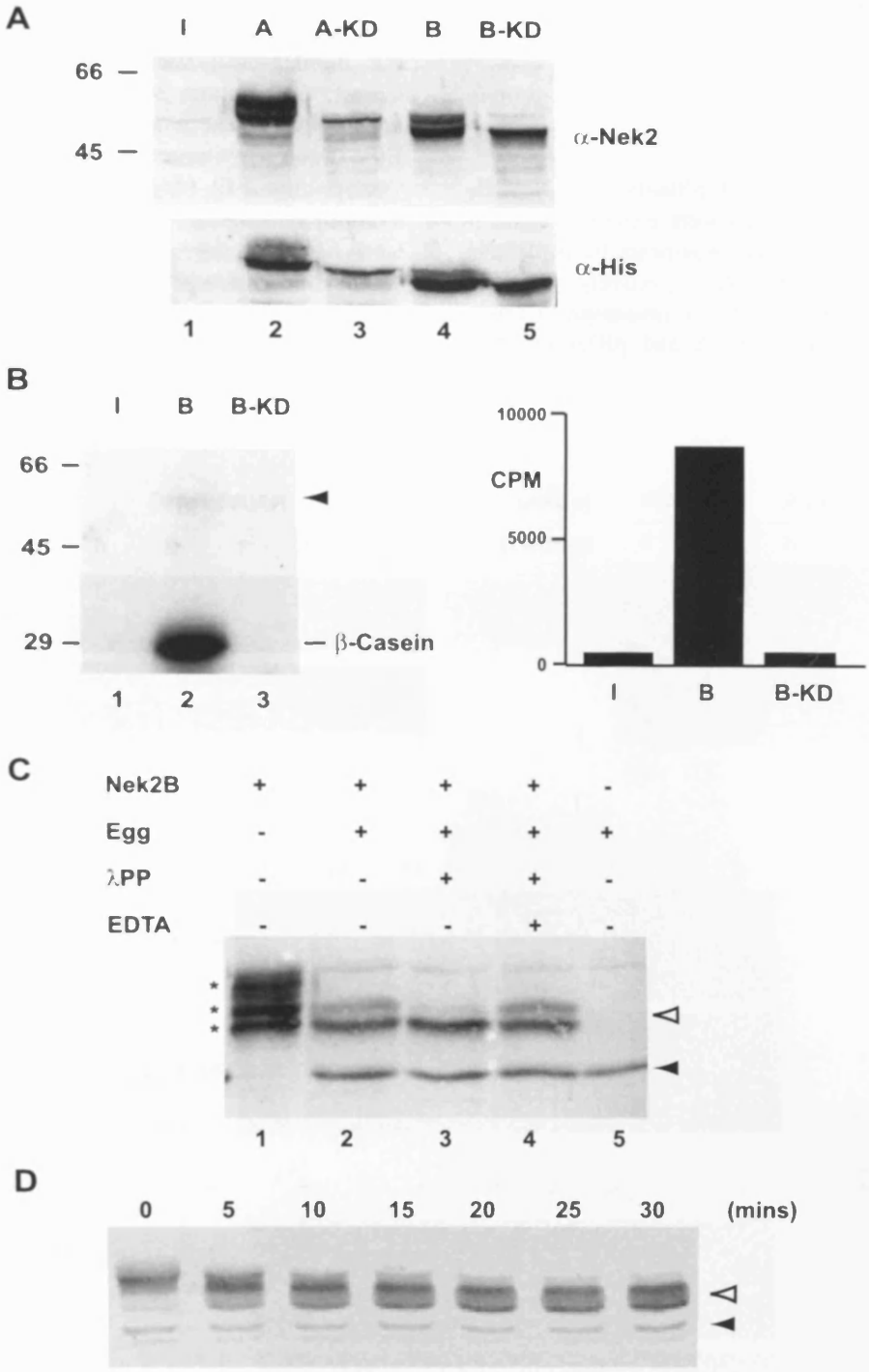

Fig. 3. Expression and phosphorylation of recombinant *Xenopus* Nek2A and Nek2B. (A) Immunoblot analysis with anti-Nek2 (top panel) and anti-His antibodies (bottom panel) of lysates of Sf9 insect cells that were uninfected (I, for insect lysate alone) or infected with recombinant baculoviruses expressing His-Nek2A (A), His-Nek2A-K37R (A-KD, for kinase-dead), His-Nek2B (B) or His-Nek2B-K37R (B-KD). Positions of molecular weight markers (kDa) are indicated on the top panel. (B) In vitro kinase assays were performed with Nek2 immunoprecipitates from insect cell lysates expressing no recombinant protein (lane 1), His-Nek2B (lane 2) or His-Nek2B-K37R (lane 3). β-casein was used as a substrate and the products analysed by SDS-PAGE and autoradiography (left panel). Weak autophosphorylation of the His-Nek2B protein in lane 2 is indicated by an arrowhead. The β-casein in each lane was excised and subjected to scintillation counting (right panel), confirming that the His-Nek2B-K37R protein is completely inactive. (C) Recombinant His-Nek2B was incubated for 30 min at 22 °C with CSF egg extract, λ protein phosphatase and EDTA as indicated before separation on 12% polyacrylamide gels and immunoblotting with R81 antibodies. Twice as much Nek2B protein was loaded in lane 1, as compared to lanes 2–4, to highlight the three major protein isoforms (asterisks). (D) Recombinant His-Nek2B was incubated at 22 °C with CSF egg extract for the time indicated and processed as in C. Open and closed arrowheads in C and D indicate migration of recombinant and endogenous Nek2B protein, respectively.

mycin). Recombinant proteins were obtained by infecting Sf9 cells with recombinant baculoviruses at m.o.i. of 5–10 for 67 h. Cells were harvested and protein extracted by the Nek2 extraction buffer (NEB) method described by Fry and Nigg (1997).

Glycerol gradient centrifugation

CSF extract (1 mg total protein, diluted to 1 ml with NEB) was loaded onto the top of a 10 ml 15–50% glycerol gradient (containing 20 mM HEPES, pH 7.4, 50 mM NaCl, 0.2 mM EDTA) and spun at 34 K rpm, 4°C for 72 h in a Sorvall TH641 ultracentrifuge rotor. Fractions (400 μl) were collected from the top of the gradient and precipitated by adding trichloroacetic acid to 20% and incubating on ice for 60 min. Samples were pelleted at 14 K rpm, 15 min, 4°C and pellets washed with 1 ml 70% EtOH (cold) and then 80% acetone (cold). Pellets were air-dried and resuspended in 20-μl protein sample buffer before SDS-PAGE and Western blotting. As size markers, 100 μg each of carbonic anhydrase (29 kDa), pepsinogen (35 kDa), bovine serum albumin (66 kDa), liver alcohol dehydrogenase (80 kDa), yeast alcohol dehydrogenase (150 kDa), β-amylase (200 kDa), and apoferritin (450 kDa) were separated on an

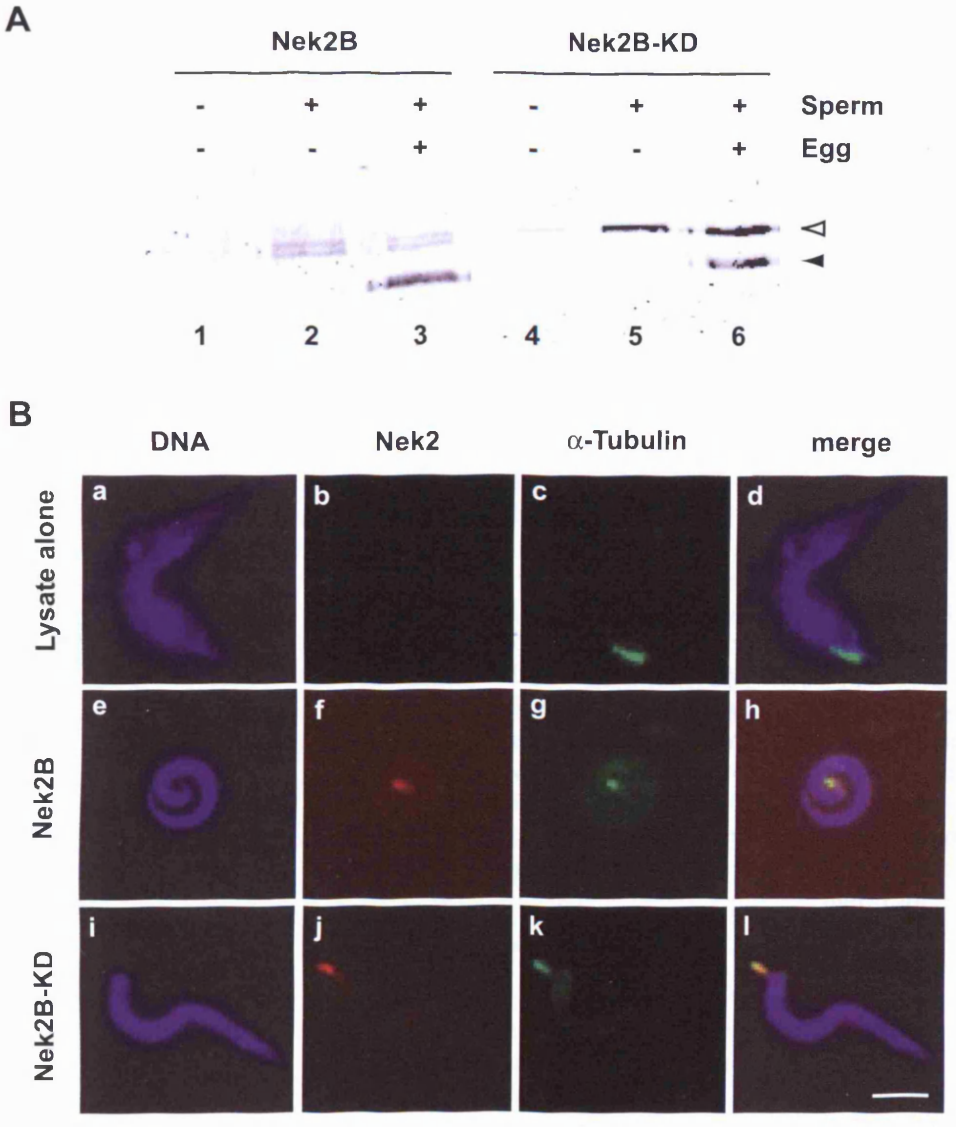

Fig. 4. Active and kinase-dead Nek2B are recruited to sperm centrosomes. (A) Sperm recruitment assays were performed by incubating insect cell lysates containing recombinant histidine-tagged Nek2B (lanes 1–3) and Nek2B-KD (lanes 4–6) with demembranated sperm and CSF egg extracts as indicated. Recombinant protein (open arrowhead) and endogenous egg Nek2B (closed arrowhead) are sedimented in the presence of sperm. Note that wild-type Nek2B shows the doublet characteristic of phosphorylated protein. (B) Immunoflourescence microscopy images of *Xenopus* sperm sedimented through a glycerol cushion onto coverslips following incubation with insect cell lysates containing no recombinant protein (a–d), recombinant Nek2B (e–h) or Nek2B-KD (i–l). DNA is stained with Hoechst 33258 (blue), recombinant protein revealed with anti-Nek2 antibodies (red) and the position of basal bodies revealed with α-tubulin antibodies (green). Scale bar = 10 μm.

identical gradient in parallel. Fractions were collected, resolved by SDS-PAGE and stained for marker proteins with Coomassie Blue.

Sperm recruitment assays

For Western blotting, 5×10^5 demembranated sperm heads were incubated in a 1.5-ml eppendorf with either 10 μl of egg extract (CSF or interphase) or 5 μl of insect cell lysate containing recombinant protein and 5 μl of spindle buffer (SB; 10 mM K.Pipes, pH 6.8, 0.3 M Sucrose, 0.1 M NaCl, 3 mM $MgCl_2$). By immunoblotting, it had been determined that 5 μl of insect cell lysate contained an equivalent amount of recombinant Nek2 protein to the amount of endogenous Nek2B present in 10 μl of egg extract (data not shown). Each reaction was supplemented with 1 μg/ml nocodazole to prevent microtubule polymerization and incubated at 22°C, except where otherwise indicated. Following incubation, the samples were diluted with 500 μl of ice-cold SB and layered onto a 1-ml cushion of 25% glycerol in SB and centrifuged at 3300 rpm, 20 min, 4°C. After removing 500 μl from the top of the cushion, the interface was gently washed three times with 100 μl of 1% Triton X-100. The cushion was then removed completely and the pellet washed twice in 1× PBS before being resuspended in 15 μl of protein sample buffer. Sperm were omitted from control experiments to assess the background precipitation of Nek2 proteins. Microscopy of isolated *Xenopus* sperm was based on published methods (Evans et al., 1985; Merdes et al., 1996; Stearns and Kirschner, 1994). In brief, a coverslip adaptor, a round 13-mm coverslip, and a 5-ml cushion of 25% glycerol in SB were placed in a 15-ml Corex tube (Corning Glass Works). Sperm (3000 in 1 μl) were incubated at 22°C for 0 or 30 min in 5 μl of recombinant protein preparation and 5 μl of SB with 1 μg/ml nocodazole. Samples were diluted with 500 μl of ice-cold SB and layered onto the glycerol cushion. Tubes were spun at 3000 rpm, 20 min, 4°C in a HB4 rotor. The top 1 ml of cushion was removed by aspiration and the interface washed with 0.5 ml of 1% Triton X-100. All but the last 1 ml of cushion was removed by aspiration and the coverslip lifted out and fixed with methanol at −20°C for 6 min.

Immunofluorescence microscopy

Immunofluorescence microscopy was performed as described (Fry et al., 1998a). Primary antibodies used were R81 α-X-Nek2 purified IgGs (5μg/ml). These were detected using biotinylated anti-rabbit antibodies (1:50; Amersham) followed by Texas Red-conjugated steptavidin (1:200; Amersham). DNA was stained with Hoechst 33258 (0.2 μg/ml in PBS). Coverslips were mounted in 80% glycerol, 3% *n*-propyl gallate in PBS. Images were captured using an Orca ER cooled CCD camera (Hamamatsu) and Openlab software (Improvision) on a Nikon TE300 inverted microscope and processed using Adobe Photoshop (San Jose, CA USA).

Microtubule aster assays

Recombinant proteins were recruited to sperm from crude insect cell lysates as described above except that nocodazole was not added. Following centrifugation, the sperm were subjected to a microtubule aster assay as described by Sawin and Mitchison (1991). Briefly, the sperm pellet was resuspended in 10 μl of CSF extract (untreated, Nek2 depleted or mock depleted) supplemented with rhodamine-labeled tubulin (20 μg/ml final concentration) and incubated at 22°C. At time points indicated, 1.2 μl was spotted onto a microscope slide and overlaid with 3 μl of extract fix (Desai et al., 1999) before addition of a coverslip and microscopic inspection. Taxol aster assays were performed with 100 nM taxol as described (Wignall and Heald, 2001).

Miscellaneous techniques

For semiquantitative RT-PCR reactions, total RNA was collected from oocytes and eggs using TRI reagent (Sigma) according to manufacturer's instructions. RNA was then treated with DNase I (Gibco) before use in RT-PCR reactions as described by Hames and Fry (2002), with oligonucleotide primers specific for either *Xenopus* Nek2A or

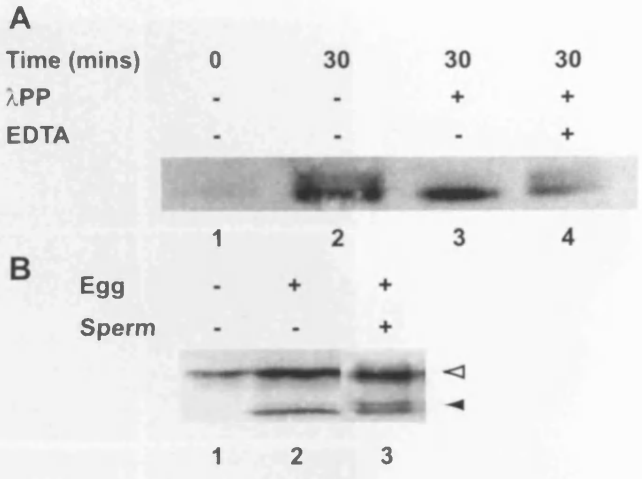

Fig. 5. Nek2B undergoes autophosphorylation upon recruitment to the sperm centrosome. (A) Recruitment of endogenous Nek2B to sperm was assayed by incubating sperm in CSF egg extract for the time indicated before treatment with or without λPP and EDTA. Sperm were then isolated through a glycerol cushion and Nek2B protein detected by SDS-PAGE using ProSieve acrylamide and immunoblotting with R81 antibodies. (B) Recombinant His-Nek2B-K37R protein was incubated with or without CSF egg extract and sperm as indicated using conditions for sperm recruitment assays. Where no sperm had been added (lanes 1 and 2), samples were loaded directly onto ProSieve gels and immunoblotted with R81 antibodies; where sperm had been added (lane 3), the sperm were isolated through a glycerol cushion and loaded on the gel. The positions of the recombinant (open arrowhead) and endogenous Nek2B (closed arrowhead) are indicated.

Nek2B. For in vitro translation, plasmids carrying Nek2 cDNAs were added to TnT-coupled transcription–translation reactions in the presence of [^{35}S] methionine–cysteine (NEN Life Science Products) according to the manufacturer's instructions (Promega Corp.). In vitro kinase assays were performed using immunoprecipitated Nek2 proteins as described by Fry and Nigg (1997).

Results

Expression of Nek2 splice variants in Xenopus sperm, eggs and oocytes

Previous studies in *X. laevis* revealed that the Nek2B splice variant is present in stage VI oocytes and eggs and that Nek2B is recruited to the sperm basal body upon incubation in the egg cytoplasm (Fry et al., 2000; Uto et al., 1999). Furthermore, removal of Nek2B from the cytoplasm retards the conversion of the sperm basal body into a functional centrosome competent for microtubule nucleation (Fry et al., 2000). However, although delayed, centrosome assembly was not blocked by Nek2 depletion, raising the possibility that either the depletion was incomplete or sperm basal bodies possess minor amounts of a Nek2 isoform that can contribute to centrosome assembly. To investigate this latter possibility, Western blot analysis was performed on concentrated preparations of demembranated sperm. In contrast to egg cytoplasm where only Nek2B is detected, both Nek2A and Nek2B were detected, albeit at low levels, in sperm preparations (Fig 1A). Nek2A is more highly expressed than Nek2B, as is seen in human adult cultured cells (Hames and Fry, 2002). Although sperm preparations can be contaminated with trace amounts of somatic tissue, our result falls in line with the faint detection of Nek2 on isolated *Xenopus* sperm by immunofluorescence staining (Uto and Sagata, 2000) and the observation that the majority of Nek2 in mouse testis is associated with spermatocytes (Rhee and Wolgemuth, 1997; Tanaka et al., 1997). Thus, it is possible that the incomplete block to centrosome assembly resulted from activity of the sperm-associated Nek2 proteins. A minor fraction of the sperm Nek2A protein appeared as a faint smear on the blot that disappeared upon treatment with lambda protein phosphatase (λPP), indicating that it is at least partially phosphorylated (Fig. 1B). The amount of Nek2B present in sperm was too low to detect possible phosphorylation. Similar analysis of Nek2B in egg cytoplasm revealed a protein smear that could also be removed by λPP treatment (Fig. 1C). Interestingly, we found that phosphorylation of Nek2B in the egg cytoplasm is more pronounced in the interphase than CSF-arrested extracts (Fig. 1D).

It has been estimated that a *Xenopus* egg contains sufficient stocks of maternal proteins to generate more than a thousand centrosomes before the need for further protein synthesis (Gard et al., 1990). As Nek2B is one of those maternally derived centrosomal components, we were interested to know when expression of the Nek2B protein is initiated. In line with a previous study (Uto et al., 1999), we found only a relatively small increase (approximately 2-fold) in the abundance of Nek2B protein during progesterone-induced oocyte maturation (Fig. 1E). We therefore analysed the amount of Nek2B protein expressed during oogenesis by sorting oocytes into their different stages (Smith et al., 1991). As oocytes of different stages vary tremendously in size, the amount of protein isolated from each stage was first equalized by spectrophotometry and then by Western blotting for the constitutively expressed Erk2 protein. Nek2B was only detected in oocytes from stage IV onwards (Fig. 1F). Hence, the major induction of Nek2B expression occurs during the process of oogenesis.

Regulation of Nek2 expression during oogenesis

To determine how Nek2 protein expression might be regulated during oogenesis, the abundance of Nek2A and Nek2B mRNA was measured using a semiquantitative RT-

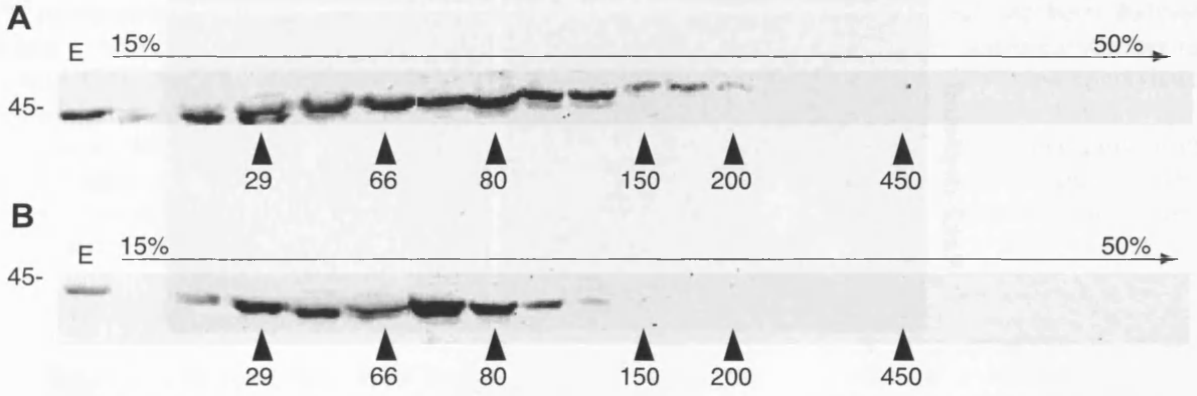

Fig. 6. Nek2B complex formation in CSF egg extracts. (A) High-speed supernatants of CSF egg extracts were subjected to fractionation over a 15–50% glycerol gradient prepared in CSF-XB buffer. Fractions collected from the gradient were precipitated with trichloroacetic acid, separated on 12% SDS-polyacrylamide gels and immunoblotted with R81 antibodies. Marker proteins were fractionated in parallel and identified by Coomassie Blue staining (not shown). The position of each marker protein (kDa) in the gradient is indicated. A sample of CSF egg extract (E) was also loaded directly onto the gel. (B) NaCl was added to the extract to a final concentration of 1 M before loading on the gradient.

PCR approach. Primers specific for each splice variant were synthesized that amplified a product from plasmids encoding only the appropriate cDNA (Fig. 2A). Moreover, sequencing of products generated by RT-PCR reactions from stage V oocytes confirmed their identity as the correct mRNA. To ensure that the amount of RT-PCR product reflected the abundance of the specific mRNA in the input sample, RT-PCR reactions were performed with different amounts of total RNA and numbers of cycles (Figs. 2B and C). Based upon these results, semiquantitative RT-PCR

A

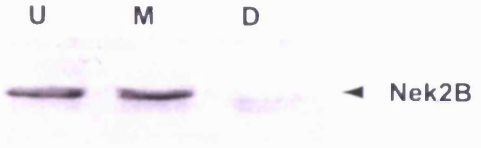

B

Mins	Untreated	Mock depleted	Nek2 depleted
0	0	0	0
5	0	0	0
10	10	20	35
15	>100	>100	>100
20	>100	>100	>100
30	>100	>100	>100

C

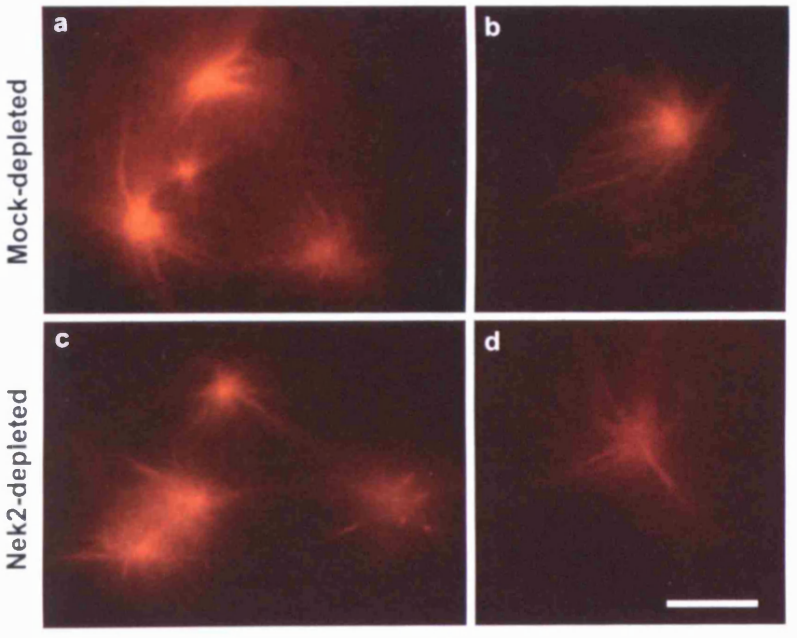

Fig. 7. Depletion of Nek2 does not interfere with taxol-induced aster formation. (A) CSF egg extracts were untreated (U), mock-depleted with rabbit IgGs (M) or depleted of Nek2B protein using R81 α-Nek2 antibodies (D). Aliquots of each extract were analysed by Western blotting for Nek2B with R81 antibodies (arrowhead). (B) Extracts (25 μl) were supplemented with 100 nM taxol and 0.15 mg/ml rhodamine-tubulin and incubated at 22 °C. At given times (mins), 1-μl samples were spotted onto glass slides, overlaid with spindle fix and the number of asters present in the 1 μl sample counted by fluorescence microscopy. The table shows results of a single experiment and the experiment was repeated three times. (C) Examples of asters present at 20 min in mock (a and b)- and Nek2B (c and d)-depleted extracts are shown. Scale bar = 10 μm.

reactions were carried out for Nek2A and Nek2B on eggs and oocytes of different stages (Fig. 2D). In contrast to the absence of Nek2A protein, Nek2A mRNA was detected in all oocyte stages, as well as eggs, suggesting that its translation is actively repressed in these cells. Nek2B mRNA was also detected in all oocyte stages and eggs with equal abundance, implying that its translation is repressed in early stage oocytes when Nek2B protein is not detected and that the increase in protein expression during oogenesis and oocyte maturation is due to derepression. Cytoplasmic polyadenylation elements, known to be involved in developmental control of translation (Richter, 1999), are present in the 3′ UTRs of both the human and the *Xenopus* Nek2B sequence. Moreover, it is highly unlikely that these results are due to changes in protein stability as previous studies indicate that Nek2A should be stable in G2-arrested oocytes and that Nek2B should be stable both in G2 oocytes and M-phase arrested eggs (Hames et al., 2001).

Generation of recombinant Nek2 proteins

To enable us to do the important reconstitution experiments, wild-type and catalytically inactive *Xenopus* Nek2A and Nek2B with C-terminal hexahistidine tags were expressed in Sf9 insect cells from recombinant baculoviruses. Western blotting of insect cell lysates with α-Nek2 or α-His antibodies revealed a major band of the expected size for each recombinant protein and, in the case of the wild-type kinases only, higher molecular weight forms indicative of autophosphorylation (Fig. 3A). IP-kinase assays using β-casein as the substrate confirmed that only the wild-type, and not the catalytically inactive, proteins were expressed in an active conformation (Fig. 3B, and data not shown). Interestingly, on highly resolving protein gels, recombinant wild-type Nek2B migrates as at least three clear isoforms (Fig. 3C, lane 1), but upon incubation in CSF egg extract, the uppermost band is lost, suggesting that it has been partially dephosphorylated (Fig. 3C, lane 2). The second retarded band is then removed by treatment with λPP presumably leaving a completely dephosphorylated protein (Fig. 3C, lanes 3 and 4). A time course of incubation in CSF extract confirms that the slowest migrating band is rapidly lost, leaving two stable isoforms (Fig. 3D). Thus, Nek2 undergoes autophosphorylation on multiple sites upon expression in insect cells but at least one of these sites is rapidly dephosphorylated by a Nek2 phosphatase active in the CSF egg cytoplasm.

Assembly of Nek2 into the zygotic centrosome

Recruitment of Nek2B is an early event in centrosome formation as it is evident immediately upon addition of sperm to egg extracts (Fry et al., 2000). However, whether Nek2 interacts directly with basal body components or indirectly via other proteins recruited from egg cytoplasm is unknown. We therefore used the recombinant proteins to investigate whether Nek2 recruitment could occur in the absence of egg cytoplasm. Unfortunately, attempts to purify the recombinant Nek2 proteins on nickel-agarose did not lead to significant protein enrichment, most likely due to masking of the histidine tag (data not shown). Therefore, crude insect cell lysates containing an equivalent concentration of Nek2 protein to that present in cytoplasmic egg extracts were incubated with sperm basal bodies before being separated from unbound protein by centrifugation through a glycerol cushion and detection by Western blotting (Fig 4A) or immunofluorescence microscopy (Fig. 4B). Western blotting indicated that both active and inactive Nek2B kinase sedimented with sperm in the absence of egg extract. Furthermore, the amount of recombinant Nek2B recruited was similar in the absence or presence of egg extract, and roughly equal to the amount of endogenous protein recruited (Fig. 4A, compare lanes 2 and 3, and 5 and 6). A small amount of recombinant protein was detected in the absence of sperm indicating minor contamination of the pellet with the starting material (Fig. 4A, lanes 1 and 4). Microscopy confirmed that recombinant Nek2B proteins associated with sperm were not randomly distributed, but specifically localized to one end of the chromatin overlying the basal body (Fig. 4B). Thus, the Nek2B protein can be recruited independently of other egg proteins and irrespective of whether it possesses kinase activity or not. Recombinant Nek2A was also recruited to sperm basal bodies to a similar extent as seen for either recombinant or endogenous Nek2B (data not shown).

We previously reported that the gel mobility of endogenous Nek2B is retarded upon recruitment to sperm basal bodies (Fry et al., 2000). To determine whether this was the result of phosphorylation, Nek2B was treated with λPP following recruitment to sperm. This treatment led to loss of any gel retardation, indicating that Nek2B was indeed being hyperphosphorylated upon recruitment (Fig. 5A and B). Furthermore, this mobility shift was detected after recruitment at 22 °C, but not 4 °C, and was dependent upon the presence of small molecules (i.e., ATP) as it did not occur with egg extracts that had been dialysed (data not shown). We also sought to determine whether recombinant, catalytically inactive Nek2B was phosphorylated following recruitment to sperm basal bodies. A hint of gel retardation was associated with the recombinant protein after, but not before, recruitment to sperm (Fig. 5B, compare lanes 2 and 3). These data strongly support a model in which the phosphorylation of Nek2B is stimulated by concentration at the zygotic centrosome.

Nek2B exists in the egg cytoplasm in small and large complexes

During our previous immunodepletion experiments, it was possible that other proteins bound to Nek2B were also removed from the extract and that this contributed to the delay in centrosome assembly. We therefore first investigat-

ed whether endogenous Nek2B in the egg cytoplasm exists in a complex. For this purpose, high-speed supernatants of CSF egg extracts were subjected to glycerol gradient centrifugation in the presence or absence of high salt (Fig. 6). Nek2B was found to exist predominantly in a salt-insensitive broad peak that extends between the 29- and 80-kDa marker. Due to the presence of the leucine zipper domain, *Xenopus* Nek2B (44 kDa), like human Nek2A and NekB, is expected to dimerise (Fry et al., 1999; Hames and Fry, 2002). Hence, this peak is almost certainly mostly Nek2B dimers. It was noticeable, however, that fractions containing Nek2 extended to the 200-kDa marker in the absence, but not presence, of high salt. Based on this observation, we propose that a small fraction of Nek2 molecules in the egg cytoplasm are in salt-sensitive complexes that could be higher-order oligomers or involve other proteins. Recombinant active and inactive His-tagged Nek2B proteins, which migrate at 50–60 kDa on gels (see Fig. 3A), were solely detected in fractions of 100–150 kDa, suggesting that the vast bulk of recombinant protein is present simply as a dimeric complex (data not shown). This indicates that other insect cell proteins are unlikely to be involved in the recruitment of Nek2 to sperm.

Nek2B is not required for acentrosomal microtubule asters

We next investigated whether depletion of Nek2B would delay the formation of noncentrosomally organized microtubule asters. For this purpose, we induced formation of asters in untreated or Nek2-depleted mitotic egg extracts (Fig. 7A) with the microtubule stabilizing poison taxol (Verde et al., 1991). Taxol-induced asters were abundant in untreated, mock-depleted and Nek2B-depleted extracts after 15 min of incubation at 22°C (Fig. 7B) and there was no obvious alteration in either the rate or morphology of aster formation (Fig. 7C). Hence, Nek2B is not required for the organization of noncentrosomally derived asters. This result also demonstrates that depletion of Nek2B does not diminish the availability of factors in the extract required for microtubule aster formation.

Nek2B protein, but not activity, is required for centrosome assembly

Finally, we examined the ability of recombinant Nek2B to rescue the delay in aster formation in Nek2-depleted CSF extracts. Nek2A was not tested in this assay as it is unstable in mitotic extracts. As it had not been possible to purify the recombinant proteins, sperm were first preincubated with crude insect cell lysates to allow Nek2B recruitment to the basal body. Sperm were then recovered

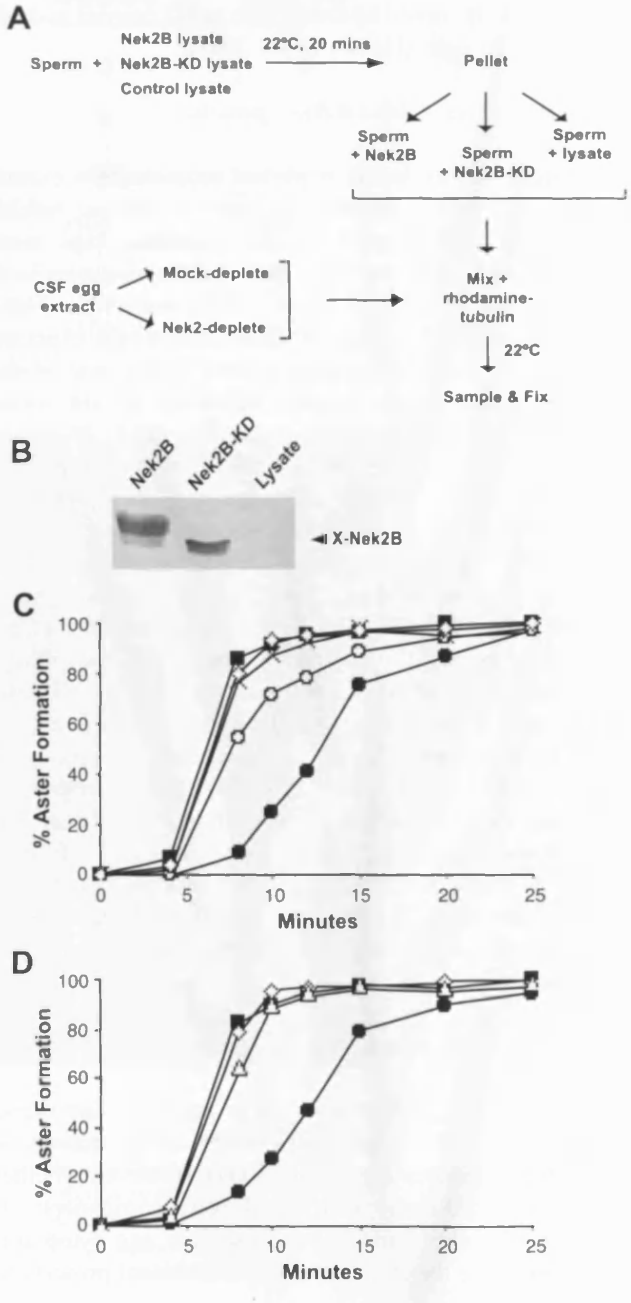

Fig. 8. Functional centrosome assembly requires Nek2 protein but not activity. (A) Outline of immunodepletion-reconstitution experiment indicating that sperm were pre-incubated in crude insect cell lysates expressing recombinant proteins, pelleted by centrifugation and then incubated in either mock- or Nek2-depleted CSF extract with rhodamine-tubulin. Samples were fixed for analysis at times indicated in graphs C and D. (B) Western blot with anti-Nek2 antibodies of insect cell lysates used in the reconstitution experiments. (C) The percentage of sperm with associated microtubule asters was counted following incubation in mock-depleted CSF extracts (closed squares) or in Nek2-depleted extracts with sperm pre-incubated with insect cell lysate alone (closed circles), or 1 μl (open circles), 3 μl (crosses) or 5 μl (open diamonds) of Nek2B-containing lysate. The graph indicates that Nek2B restores the timing of aster formation in a dose-dependent manner. (D) The percentage of sperm with associated microtubule asters was counted following incubation in mock-depleted CSF extracts (closed squares) or in Nek2-depleted extracts with sperm pre-treated with insect cell lysate alone (closed circles), or insect cell lysates containing recombinant Nek2B (open diamonds) or Nek2B-K37R (open triangles). The graph indicates that rescue is not dependent upon Nek2B kinase activity. The graphs in C and D are representative examples of three independent assays.

by centrifugation before being incubated in mock- or Nek2-depleted CSF extract in the presence of rhodamine-tubulin. At given time points, samples were fixed and the percentage of sperm with associated asters counted by fluorescence microscopy (Fig. 8A). Lysates from either uninfected insect cells or cells infected with wild-type or kinase-dead Nek2B were used (Fig. 8B). In these experiments, 5 μl of insect cell lysate contained an equivalent amount of Nek2B protein to that present in 10 μl of egg extract. In line with previous experiments, aster formation was reproducibly delayed in Nek2-depleted extracts as compared to mock-depleted extracts (Fig. 8C). Addition of recombinant wild-type Nek2B, but not insect cell lysate alone, led to complete recovery in the time of aster formation in Nek2-depleted extracts in a dose-dependent manner providing convincing evidence that the delay was due to removal of Nek2B and not any other protein (Fig. 8C). Strikingly, addition of kinase-dead Nek2B also led to complete recovery in the timing of aster formation (Fig. 8D), indicating that it is Nek2B protein, and not kinase activity, that is critical in the assembly pathway of the zygotic centrosome.

Discussion

Assembly of the first zygotic centrosome requires both maternal and paternal contributions (Schatten, 1994; Wu and Palazzo, 1999). In most animals, with the notable exception of rodents, the centrioles are paternally derived in the form of basal bodies that subtend the axonemal microtubules of the flagellum. However, for proteins that make up the pericentriolar matrix, some may be brought along with the centrioles whereas others may be recruited from the egg cytoplasm. Defining whether centrosomal proteins are maternally or paternally derived is of medical importance as incorrectly assembled zygotic centrosomes can contribute to both male and female infertility (Navara et al., 1997). Furthermore, defective centrosome organization has been invoked as one cause of aneuploidy in cancer cells and unraveling the pathway of zygotic centrosome assembly is likely to yield important information on how the centrosomes of adult cells are organized (Pihan and Doxsey, 1999). Here we show that the Nek2 protein is both paternally derived, in that it is present on sperm alone, and maternally derived in being significantly recruited to the centrosome from egg cytoplasm. The maternally derived protein, which is solely the Nek2B splice variant, is phosphorylated upon recruitment and its recruitment stimulates the rate at which a functional centrosome is assembled in a kinase-independent manner.

Centrosome assembly can almost certainly be achieved in many different ways depending on the particular circumstance. In adult cells, centrosomes are duplicated in a semiconservative manner once per cell cycle (Hinchcliffe and Sluder, 2001). During this process, new proteins are assimilated into what is an already highly ordered, functional centrosome either by passive diffusion or by motor-protein delivery along microtubules (Zimmerman and Doxsey, 2000). The most prominent reorganization of the PCM in the adult cell cycle occurs at the G2/M transition when mitosis-specific centrosomal proteins are recruited and assembled into the developing spindle pole (Blagden and Glover, 2003). This is in part dependent on Plk1 and Aurora-A kinase function. Experimentally, centrosomes can also assemble de novo in S-phase arrested adult cells though the mechanism of assembly is unclear as PCM clouds appear first within which centrioles are detected later (Khojakov et al., 2002). De novo centrosome formation appears to occur naturally during the first embryonic cell cycles in rodents with PCM foci again appearing first to organize the mitotic spindle (Maro et al., 1985; Schatten et al., 1986). However, following fertilization in most animal cells, zygotic centrosomes are assembled by recruitment of maternally contributed components onto paternally derived basal bodies (Archer and Solomon, 1994; Schatten, 1994). The addition of demembranated *Xenopus* sperm, which retain the basal body, to *Xenopus* cytoplasmic egg extracts provides an excellent cell-free experimental system for the study of this pathway of centrosome assembly (Felix et al., 1994). Using this assay, it was first shown that γ-tubulin must be recruited to the basal body from egg cytoplasm for microtubule aster assembly to occur (Felix et al., 1994; Stearns and Kirschner, 1994). Meanwhile, experimental analysis of zygotic centrosome assembly in fertilized *Drosophila* eggs indicated that another centrosomal protein CP190 was also recruited from the egg cytoplasm (Riparbelli et al., 1997). Centrin, a centriolar protein, and pericentrin, on the other hand, are present at the basal body before incubation in the egg cytoplasm (Doxsey et al., 1994; Stearns and Kirschner, 1994).

Basal bodies are structurally and functionally related to centrioles (Preble et al., 2000). Hence, one might predict that proteins tightly associated with centrioles are more likely to be paternally derived with the basal bodies than proteins that make up the pericentriolar material. Nek2 associates with proximal ends of centrioles (Fry et al., 1998b) and is generally referred to in the literature as a centriolar protein. In line with this, we were able to detect both Nek2A and, more weakly, Nek2B in concentrated sperm preparations by Western blot. Uto and Sagata (2000) also reported weak staining by fluorescence microscopy of sperm basal bodies with Nek2 antibodies before incubation in egg extracts. In a separate report, the same authors showed that *Xenopus* testis contains high levels of Nek2A and low levels of Nek2B (Uto et al., 1999). Thus, it would appear that Nek2 is a component of both basal bodies and centrioles. Nevertheless, considerably more Nek2B is recruited to the assembling centrosome upon incubation of sperm in the egg cytoplasm, indicating that the Nek2 protein in the zygotic centrosome has both paternal and maternal origins. The same appears to be true in fact of γ-tubulin,

which localizes both in the lumen of centrioles and in the pericentriolar material, and which has been detected at low levels in sperm before the significant increase that occurs upon incubation in the extract (Fuller et al., 1995; Moudjou et al., 1996; Simerly et al., 1999).

Eggs and early embryos express only the Nek2B splice variant. The purpose behind this may relate to the fact that Nek2B lacks destruction motifs present in Nek2A. Indeed, exogenous Nek2A protein is highly labile in early embryonic extracts (Hames et al., 2001; Uto and Sagata, 2000). During the rapid divisions that take place in the early embryo, repeated turnover of Nek2 protein may be detrimental. Nek2B protein expression is first clearly detected in stage IV oocytes before a further two-fold increase in protein expression upon oocyte maturation. A similar increase in Nek2B expression during *Xenopus* oocyte maturation was reported by Uto et al. (1999), although no such change was detected during porcine oocyte maturation (Fujioka et al., 2000). Upregulated expression of many centrosomal proteins during oogenesis may be vital to the stockpiling of centrosomal precursors in the egg. Interestingly, our results indicate that the change in Nek2B protein abundance is primarily regulated at a translational level as the amount of its mRNA remains unchanged throughout oogenesis and oocyte maturation. Nek2A mRNA is also present during these stages. We speculate that both mRNAs are subject to translational repression during early oogenesis but that, whilst Nek2A mRNA continues to be repressed throughout early embryogenesis, Nek2B mRNA is derepressed around stage III–IV of oogenesis. Human and *Xenopus* Nek2B share a potential cytoplasmic polyadenylation element close to the hexanucleotide polyadenylation sequence in the 3′UTR of their mRNAs. The sudden translation of Nek2B mRNA may therefore be stimulated through extension of its poly (A) tail. In this respect, Nek2B may represent another important cell cycle regulator whose expression during embryonic development is regulated by cytoplasmic polyadenylation (Richter, 1999).

Endogenous Nek2B in the egg cytoplasm and recombinant Nek2B expressed in insect cells exist predominantly in small complexes highly reminiscent of dimers, although a small fraction of Nek2B in the egg cytoplasm is incorporated into a salt-sensitive 150–200-kDa complex. However, the avid recruitment to sperm of recombinant Nek2B in the absence of egg cytoplasm demonstrates that Nek2B can bind directly to basal bodies and is not dependent upon the prior recruitment of other egg proteins. Both Nek2A in sperm and Nek2B in egg are weakly phosphorylated, but upon recruitment to the basal body, there is a significant increase in Nek2B phosphorylation. Following expression in insect cells, wild-type recombinant Nek2B migrates as at least three isoforms by SDS-PAGE, whereas catalytically inactive Nek2B migrates as a single band at the same position as the highest mobility form of wild-type Nek2B. This strongly supports the idea of at least two separate autophosphorylation events. Of course, there may be additional phosphorylation that does not cause gel migration shifts. Interestingly, incubation in CSF extract removes the slowest migrating form indicating the presence of a phosphatase that can remove some but not all Nek2 phosphorylation. As endogenous Nek2B is less phosphorylated in CSF than interphase extracts, it is possible that this is a cell cycle-regulated phosphatase and important for regulating endogenous as well as recombinant Nek2. We hypothesize that recruitment to the sperm acts both to concentrate Nek2B and to sequester it away from the phosphatase, thus allowing autophosphorylation to increase. Human Nek2A can bind and be dephosphorylated by PP1c (Helps et al., 2000). However, Nek2B lacks the PP1c binding site so the relevant phosphatase in CSF extracts is unknown.

A number of factors implicate Nek2B as a specific regulator of centrosome assembly, rather than of microtubule nucleation or organization. First, Nek2B recruitment is an early event in the centrosome assembly pathway with Nek2B perhaps interacting directly with the basal bodies. Second, recruitment of Nek2B promotes γ-tubulin recruitment (Fry et al., 2000), which is absolutely required for assembly of functional centrosomes (Felix et al., 1994; Stearns and Kirschner, 1994). Third, injection of inactive Nek2B gives rise to centrosome fragmentation and impaired spindle formation in *Xenopus* embryos, indicating that Nek2B is required for maintenance as well as assembly of centrosomes (Uto and Sagata, 2000). Finally, depletion of Nek2B does not interfere with formation of taxol-induced microtubule asters, implying that Nek2B is required only for centrosome assembly itself. Indeed, Nek2B inhibition did not prevent formation of meiotic spindles in *Xenopus* oocytes which lack centrosomes (Uto and Sagata, 2000).

The delay in aster formation in Nek2B-depleted extracts suggests that paternally derived Nek2 protein is not sufficient to allow a functional centrosome to form at the normal rate. It is possible that the Nek2 protein is absolutely essential for zygotic centrosome assembly but that the low levels of Nek2A and Nek2B present in sperm preparations allow assembly to occur, albeit more slowly. Unfortunately, attempts to impose a more complete block to aster formation by pre-incubating sperm with Nek2 antibodies were not successful (data not shown). Most importantly, though, the normal timing of aster formation was restored when sperm were pre-incubated with recombinant Nek2B protein before addition of the depleted extract. Moreover, this rescue was dependent upon the amount of Nek2B with which the sperm were pre-incubated. As the recruitment of Nek2 to sperm was done in crude insect cell lysates, it is possible that other insect cell proteins involved in centrosome assembly may have been recruited in parallel. However, incubation of sperm in insect cell lysates that lacked Nek2 did not rescue aster formation emphasizing the central importance of Nek2. The depletion–reconstitution approach also allowed us to ask the critical question of whether it is the kinase activity of Nek2 that is important in this context. Our results reveal that Nek2 kinase activity is, in fact, not required, as the catalyt-

ically inactive Nek2B protein rescued to the same extent as the active protein. This surprising result points strongly to a structural role for Nek2B in centrosome assembly and maintenance, which may not be restricted to embryonic cells as adult cells also express Nek2B. Indeed, Nek2B may be required for spindle pole integrity in adult cells as Nek2A is destroyed in early mitosis. As centrioles are essential for maintenance of the pericentriolar material (Bobinnec et al., 1998), Nek2B may contribute to centrosome assembly by stabilizing the centriole structure itself. Alternatively, it might provide docking sites for components of the pericentriolar material that anchor the microtubule–nucleation complexes. A full understanding of the mechanism by which Nek2B promotes centrosome assembly and the reason for its hyperphosphorylation at the centrosome will require further identification and characterization of its centrosomal partners.

Acknowledgments

We thank all members of the lab for useful discussion. This work was primarily supported by a grant to A.M.F. from The Wellcome Trust (056335). J.E.B. is sponsored by a studentship from Millennium Pharmaceuticals Limited. A.M.F. is a Lister Institute Research Fellow.

References

Andersen, C.W., Baum, P.R., Geseland, R.F., 1973. Processing of adenovirus 2-induced proteins. J. Virol. 12, 241–252.

Archer, J., Solomon, F., 1994. Deconstructing the microtubule-organizing center. Cell 76, 589–591.

Blagden, S.P., Glover, D.M., 2003. Polar expeditions—Provisioning the centrosome for mitosis. Nat. Cell Biol. 5, 505–511.

Bobinnec, Y., Khodjakov, A., Mir, L.M., Rieder, C.L., Eddé, B., Bornens, M., 1998. Centriole disassembly in vivo and its effect on centrosome structure and function in vertebrate cells. J. Cell Biol. 143, 1575–1589.

Dasso, M., 2001. Running on Ran: nuclear transport and the mitotic spindle. Cell 104, 321–324.

Desai, A., Murray, A., Mitchison, T.J., Walczak, C.E., 1999. The use of *Xenopus* egg extracts to study mitotic spindle assembly and function in vitro. In: Rieder, C.L. (Ed.), Mitosis and Meiosis, vol. 61. Academic Press, San Diego, pp. 385–412.

Doxsey, S., 2001. Re-evaluating centrosome function. Nat. Rev., Mol. Cell Biol. 2, 688–698.

Doxsey, S., Stein, P., Evans, L., Calarco, P.D., Kirschner, M., 1994. Pericentrin, a highly conserved centrosome protein involved in microtubule organization. Cell 76, 639–650.

Evans, L., Mitchison, T., Kirschner, M., 1985. Influence of the centrosome on the structure of nucleated microtubules. J. Cell Biol. 100, 1185–1191.

Felix, M.-A., Antony, C., Wright, M., Maro, B., 1994. Centrosome assembly in vitro: role of γ-tubulin recruitment in Xenopus sperm aster formation. J. Cell Biol. 124, 19–31.

Fry, A.M., 2002. The Nek2 protein kinase: a novel regulator of centrosome structure. Oncogene 21, 6184–6194.

Fry, A.M., Nigg, E.A., 1997. Characterization of mammalian NIMA-related kinases. Methods Enzymol. 283, 270–282.

Fry, A.M., Meraldi, P., Nigg, E.A., 1998a. A centrosomal function for the human Nek2 protein kinase, a member of the NIMA-family of cell cycle regulators. EMBO J. 17, 470–481.

Fry, A.M., Mayor, T., Meraldi, P., Stierhof, Y.-D., Tanaka, K., Nigg, E.A., 1998b. C-Nap1, a novel centrosomal coiled-coil protein and candidate substrate of the cell cycle-regulated protein kinase Nek2. J. Cell Biol. 141, 1563–1574.

Fry, A.M., Arnaud, L., Nigg, E.A., 1999. Activity of the human centrosomal kinase, Nek2, depends upon an unusual leucine zipper dimerization motif. J. Biol. Chem. 274, 16304–16310.

Fry, A.M., Descombes, P., Twomey, C., Bacchieri, R., Nigg, E.A., 2000. The NIMA-related kinase X-Nek2B is required for efficient assembly of the zygotic centrosome in *Xenopus laevis*. J. Cell. Sci. 113, 1973–1984.

Fujioka, T., Takebayashi, Y., Ito, M., Uchida, T., 2000. Nek2 expression and localization in porcine oocyte during maturation. Biochem. Biophys. Res. Commun. 279, 799–802.

Fuller, S.D., Gowen, B.E., Reinsch, S., Sawyer, A., Buendia, B., Wepf, R., Karsenti, E., 1995. The core of the mammalian centriole contains γ-tubulin. Curr. Biol. 5, 1384–1393.

Gaffal, K.P., 1988. The basal body–root complex of *Chlamydomonas reinhardtii* during mitosis. Protoplasma 143, 118–129.

Gard, D.L., Hafezi, S., Zhang, T., Doxsey, S.J., 1990. Centrosome duplication continues in cycloheximide-treated *Xenopus* blastulae in the absence of a detectable cell cycle. J. Cell Biol. 110, 2033–2042.

Gerhart, J., Wu, M., Kirschner, M., 1984. Cell cycle dynamics of an M-phase-specific cytoplasmic factor in *Xenopus laevis* oocytes and eggs. J. Cell Biol. 98, 1247–1255.

Hames, R.S., Fry, A.M., 2002. Alternative splice variants of the human centrosomal kinase Nek2 exhibit distinct patterns of expression in mitosis. Biochem. J. 361, 77–85.

Hames, R.S., Wattam, S.L., Yamano, H., Bacchieri, R., Fry, A.M., 2001. APC/C-mediated destruction of the centrosomal kinase Nek2A occurs in early mitosis and depends upon a cyclin A-type D-box. EMBO J. 20, 7117–7127.

Heald, R., Tournebize, R., Habermann, A., Karsenti, E., Hyman, A., 1997. Spindle assembly in *Xenopus* egg extracts: respective roles of centrosomes and microtubule self-organization. J. Cell Biol. 138, 615–628.

Helps, N.R., Luo, X., Barker, H.M., Cohen, P.T.W., 2000. NIMA-related kinase 2 (Nek2), a cell cycle-regulated protein kinase localized to centrosomes, is complexed to protein phosphatase 1. Biochem. J. 349, 509–518.

Hinchcliffe, E.H., Sluder, G., 2001. "It takes two to tango": understanding how centrosome duplication is regulated throughout the cell cycle. Genes Dev. 15, 1167–1181.

Hinchcliffe, E.H., Miller, F.J., Cham, M., Khodjakov, A., Sluder, G., 2001. Requirement of a centrosomal activity for cell cycle progression through G1 into S phase. Science 291, 1547–1550.

Johnson, U.G., Porter, K.R., 1968. Fine structure of cell division in *Chlamydomonas reinhardtii*. J. Cell Biol. 38, 403–425.

Khodjakov, A., Rieder, C.L., 2001. Centrosomes enhance the fidelity of cytokinesis in vertebrates and are required for cell cycle progression. J. Cell Biol. 153, 237–242.

Khodjakov, A., Cole, R.W., Oakley, B.R., Rieder, C.L., 2000. Centrosome-independent mitotic spindle formation in vertebrates. Curr. Biol. 10, 59–67.

Khojakov, A., Rieder, C.L., Sluder, G., Cassels, G., Sibon, O., Wang, C.-L., 2002. De novo formation of centrosomes in vertebrate cells arrested during S-phase. J. Cell Biol. 158, 1171–1181.

Maller, J., Poccia, D., Nishioka, D., Kido, P., Gerhart, J., Hartman, H., 1976. Spindle formation and cleavage in *Xenopus* eggs injected with centriole containing fractions from sperm. Exp. Cell Res. 99, 285–294.

Maro, B., Howlett, S.K., Webb, M., 1985. Non-spindle microtubule organizing centers in metaphase II-arrested mouse oocytes. J. Cell Biol. 101, 1665–1672.

Marshall, W.F., 2001. Centrioles take center stage. Curr. Biol. 11, R487–R496.

Merdes, A., Ramyar, K., Vechio, J.D., Cleveland, D.W., 1996. A complex

of NuMA and cytoplasmic dynein is essential for mitotic spindle assembly. Cell 87, 447–458.

Moudjou, M., Bordes, N., Paintrand, M., Bornens, M., 1996. γ-Tubulin in mammalian cells: the centrosomal and the cytosolic forms. J. Cell. Sci. 109, 875–887.

Murray, A.W., 1991. Cell cycle extracts. Methods Cell Biol. 36, 581–605.

Navara, C.S., Hewitson, L.C., Simerly, C.R., Sutovsky, P., Schatten, G., 1997. The implications of a paternally derived centrosome during human fertilization: consequences for reproduction and the treatment of male factor infertility. Am. J. Repro. Immunol. 37, 39–49.

Paintrand, M., Moudjou, M., Delacroix, H., Bornens, M., 1992. Centrosome organization and centriole architecture: their sensitivity to divalent cations. J. Struct. Biol. 108, 107–128.

Piel, M., Nordberg, J., Euteneuer, U., Bornens, M., 2001. Centrosome-dependent exit of cytokinesis in animal cells. Science 291, 1550–1553.

Pihan, G.A., Doxsey, S., 1999. The mitotic machinery as a source of genetic instability in cancer. Semin. Cancer Biol. 9, 289–302.

Preble, A.M., Giddings, T.M., Dutcher, S.K., 2000. Basal bodies and centrioles: their function and structure. Curr. Top. Dev. Biol. 49, 207–233.

Rhee, K., Wolgemuth, D.J., 1997. The NIMA-related kinase 2, Nek2, is expressed in specific stages of the meiotic cell cycle and associates with meiotic chromosomes. Development 124, 2167–2177.

Richter, J.D., 1999. Cytoplasmic polyadenylation in development and beyond. Microbiol. Mol. Biol. Rev. 63, 446–456.

Riparbelli, M.G., Whitfield, W.G.F., Dallai, R., Callaini, G., 1997. Assembly of the zygotic centrosome in the fertilized Drosophila egg. Mech. Dev. 65, 135–144.

Sawin, K.E., Mitchison, T.J., 1991. Mitotic spindle assembly by two different pathways in vitro. J. Cell Biol. 112, 925–940.

Schatten, G., 1994. The centrosome and its mode of inheritance: the reduction of the centrosome during gametogenesis and its restoration during fertilization. Dev. Biol. 165, 299–335.

Schatten, H., Schatten, G., Mazia, D., Balczon, R., Simerly, C., 1986. Behavior of centrosomes during fertilization and cell division in mouse oocytes and in sea urchin eggs. Proc. Natl. Acad. Sci. U. S. A. 83, 105–109.

Sharp-Baker, H., Chen, R.-H., 2001. Spindle checkpoint protein Bub1 is required for kinetochore localization of Mad1, Mad2, Bub3 and CENP-E, independently of its kinase activity. J. Cell Biol. 153, 1239–1249.

Simerly, C., Zoran, S.S., Payne, C., Dominko, T., Sutovsky, P., Navara, C.S., Salisbury, J.L., Schatten, G., 1999. Biparental inheritance of γ-tubulin during human fertilization: molecular reconstitution of functional zygotic centrosomes in inseminated human oocytes and in cell-free extracts nucleated by human sperm. Mol. Biol. Cell 10, 2955–2969.

Smith, L.D., Xu, W., Varnold, R.L., 1991. Oogenesis and oocyte isolation. Methods Cell Biol. 36, 45–60.

Stearns, T., Kirschner, M., 1994. In vitro reconstitution of centrosome assembly and function: the central role of γ-tubulin. Cell 76, 623–637.

Tanaka, K., Parvinen, M., Nigg, E.A., 1997. The in vivo expression pattern of mouse Nek2, a NIMA-related kinase, indicates a role in both mitosis and meiosis. Exp. Cell Res. 237, 264–274.

Uto, K., Sagata, N., 2000. Nek2B, a novel maternal form of Nek2 kinase, is essential for the assembly or maintenance of centrosomes in early *Xenopus* embryos. EMBO J. 19, 1816–1826.

Uto, K., Nakajo, N., Sagata, N., 1999. Two structural variants of Nek2 kinase, termed Nek2A and Nek2B, are differentially expressed in *Xenopus* tissues and development. Dev. Biol. 208, 456–464.

Verde, F., Berrez, J.-M., Antony, C., Karsenti, E., 1991. Taxol-induced microtubule asters in mitotic extracts of *Xenopus* eggs: requirement for phosphorylated factors and cytoplasmic dynein. J. Cell Biol. 112, 1177–1187.

Wignall, S.M., Heald, R., 2001. Methods for the study of centrosome-independent spindle assembly in *Xenopus* extracts. Methods Cell Biol. 67, 241–256.

Wittmann, T., Hyman, A., Desai, A., 2001. The spindle: a dynamic assembly of microtubules and motors. Nat. Cell Biol. 3, E28–E34.

Wu, X., Palazzo, R.E., 1999. Differential regulation of maternal vs. paternal centrosomes. Proc. Natl. Acad. Sci. U. S. A. 96, 1397–1402.

Zimmerman, W., Doxsey, S.J., 2000. Construction of centrosomes and spindle poles by molecular motor-driven assembly of protein particles. Traffic 1, 927–934.